NASA CR-134816
GESP-695

(NASA-CR-134816-Vol-1) T-111 RANKINE SYSTEM CORROSION TEST LOOP, VOLUME 1 Final Report (General Electric Co.) 276 p HC $9.25 CSCL 11F
N76-18258
Unclas
G3/26 14284

T-111 RANKINE SYSTEM CORROSION TEST LOOP

Volume I

by R. W. Harrison, E. E. Hoffman, and J. P. Smith

Nuclear Systems Programs Missile and Space Division
GENERAL ELECTRIC COMPANY

prepared for

NATIONAL AERONAUTICS AND SPACE ADMINISTRATION

Lewis Research Center
Contract NAS 3-6474

FOREWORD

The work described herein was performed by the General Electric Company, Nuclear Systems Programs (NSP), under the sponsorship of the National Aeronautics and Space Administration under Contract NAS 3-6474. The primary purpose of the Advanced Refractory Alloy Corrosion Loop Program was to evaluate the compatibility of candidate refractory alloys in contact with alkali metal working fluids under conditions simulating those anticipated in projected space electric power systems. This program which was initiated in 1965 consisted of four principal investigations, namely the T-111 Rankine System Corrosion Test Loop, 1900°F Lithium Loop, Advanced Tantalum Alloy Capsule Tests, and the 2500°F Lithium Thermal Convection Loop Test. This report describes the T-111 Rankine System Corrosion Test Loop, which shall be referred to as the T-111 Corrosion Loop in this report.

The basic design of the Corrosion Test Loop was developed and proven on a prior program,* also sponsored by NASA - Lewis Research Center, and only a limited number of minor design modifications were required for the T-111 alloy system. J. Holowach was responsible for making these design modifications.

Preparation of the specifications for the purchase of the refractory alloy materials and the performance of the quality assurance testing required prior to the release of the material for fabrication were the responsibility of R. G. Frank.

W. R. Young, P. A. Blanz, and H. Mann were responsible for the fabrication of the test loop. Dr. R. B. Hand, H. Bradley, L. E. Dotson, J. Reeves, and L. A. Paian were responsible for the purification, handling, and sampling of the alkali metals used in the loop test. W. H. Bennethum made noteworthy contributions in the various phases of loop instrumentation, particularly in the areas of thermocouple calibration and installation. Dr. T. F. Lyon was responsible for the calibration of the partial pressure analyzer and the

---

* NASA Contract NAS 3-2547.

interpretation of the spectra obtained during test operation. T. P. Irwin and A. C. Losekamp instrumented the loop and together with D. E. Field, S. Roof, and M. Hamilton monitored the operation of the loop during the 10,000-hour endurance test. T. Irwin and A. C. Losekamp were also responsible for the disassembly of the loop following test and the preparation of specimens for chemical, metallographic, and mechanical property evaluation and the compilation of the results of these investigations. J. P. Smith led the rather extensive posttest evaluation effort and was assisted in this work by A. Losekamp, I. Miller, and G. Anderson. The authors also wish to acknowledge the efforts of Ms. Carol Kiefel in the preparation of this report.

This program was administered for the General Electric Company by E. E. Hoffman and Dr. J. W. Semmel. R. W. Harrison acted as the Program Manager of the Advanced Refractory Alloy Corrosion Loop Program.

R. L. Davies and T. A. Moss acted as the Technical Managers for the National Aeronautics and Space Administration.

TABLE OF CONTENTS

Section		Page
	Volume I	
	SUMMARY	1
I.	INTRODUCTION	2
II.	LOOP DESIGN	6
III.	MATERIAL PROCUREMENT	13
	A. MATERIAL SPECIFICATIONS	13
	B. VENDOR SELECTION	16
	C. PROCESSING OF REFRACTORY ALLOY MILL PRODUCTS	17
	D. QUALITY ASSURANCE FOR REFRACTORY METAL MILL PRODUCTS	22
IV.	LOOP FABRICATION	51
	A. GENERAL WELDING PROCEDURES	51
	B. SLACK DIAPHRAGM TRANSDUCERS	55
	C. VALVES	55
	D. LITHIUM AND POTASSIUM EM PUMP DUCTS	57
	E. STRESSED DIAPHRAGM PRESSURE TRANSDUCER	57
	F. POTASSIUM AND LITHIUM SURGE TANKS	61
	G. BOILER	66
	H. POTASSIUM PREHEATER AND LITHIUM HEATER	68
	I. TURBINE SIMULATOR	74
	J. CONDENSER	74
	K. ASSEMBLY OF THE LOOP	79
V.	ALKALI METAL PURIFICATION AND HANDLING	93
	A. LITHIUM PURIFICATION	94
	B. POTASSIUM PURIFICATION	102
	C. REFILLING OF LOOP CIRCUITS FOLLOWING BOILER REPAIR	104
VI.	TEST FACILITY	107
	A. VACUUM SYSTEM	107
	B. CHAMBER PRESSURE AND PARTIAL PRESSURE MEASUREMENT	109
	C. HEATER POWER SUPPLIES	110

TABLE OF CONTENTS (CONT.)

Section		Page
VII.	INSTRUMENTATION AND INSTALLATION OF THE LOOP	114
	A. INSTALLATION OF THERMOCOUPLES AND THERMAL INSULATION	114
	B. TRANSFER OF LOOP AND CHAMBER SPOOL PIECE TO THE TEST FACILITY	119
VIII.	PRETEST OPERATION	128
	A. PUMPDOWN AND BAKEOUT OF THE VACUUM CHAMBER	128
	B. FINAL HELIUM LEAK CHECK OF THE TEST LOOP	129
	C. CHECKOUT AND CALIBRATION OF THE LOOP INSTRUMENTATION	131
	D. BOILING AND CONDENSING OPERATION	137
	E. DRAINING OF LOOPS AND DISCOVERY OF THE BOILER LEAK	139
IX.	TEST STARTUP AFTER REPAIR OF BOILER	142
X.	LOOP OPERATION	146
	A. LOOP OPERATION DURING THE 10,000-HOUR TEST	146
	B. TERMINATION OF THE TEST	164
	C. TOTAL PRESSURE AND PARTIAL PRESSURES IN THE CHAMBER DURING THE 10,000-HOUR TEST	164
XI.	DRAINING, DISASSEMBLY, AND CLEANING OF LOOP COMPONENTS	169
	A. ALKALI METAL SAMPLING, DRAINING, AND ANALYSIS	169
	B. INITIAL PREPARATION FOR POSTTEST EVALUATION	173
	C. REMOVAL OF RESIDUAL ALKALI METAL	179
	D. FINAL PREPARATION FOR POSTTEST EVALUATION	184
XII.	CHEMICAL AND METALLURGICAL EVALUATION OF LOOP COMPONENTS	194
	A. CHEMICAL ANALYSIS OF LOOP COMPONENTS	194
	B. WEIGHT CHANGE AND DIMENSIONAL ANALYSIS OF NOZZLES AND BLADES	206
	C. RESULTS OF METALLOGRAPHIC AND MICROPROBE EVALUATIONS	206
	D. TENSILE TEST RESULTS ON T-111 TUBING	239
XIII.	SUMMARY AND CONCLUSIONS	249
XIV.	PUBLISHED REPORTS	252

Volume II

XV.	APPENDICES	
	A. LIST OF DRAWINGS OF THE T-111 CORROSION LOOP	255

TABLE OF CONTENTS (CONT.)

Section		Page
B.	MAJOR DRAWINGS OF THE T-111 RANKINE SYSTEM CORROSION TEST LOOP	263
C.	TYPICAL T-111 ALLOY SPECIFICATION: SPECIFICATION NO. B50YA325, "SEAMLESS TUBING AND PIPE: T-111 (Ta-8W-2Hf) ALLOY"	281
D.	PROCESSING OF T-111 ALLOY	309
E.	PROCESSING OF Mo-TZC ALLOY	333
F.	PROCESSING OF Cb-132M ALLOY	355
G.	T-111 BELLOWS FABRICATION	371
H.	CALIBRATION OF PARTIAL PRESSURE GAS ANALYZER	377
I.	CALIBRATION OF W-3Re/W-25Re THERMOCOUPLE WIRE	381
J.	FAILURE MODE AND EFFECT ANALYSIS	389
K.	REMOVAL, REPAIR, AND REPLACEMENT OF THE T-111 BOILER	423
L.	LITHIUM-POTASSIUM SOLUBILITY STUDY	485

LIST OF TABLES

Table Number		Page
I.	Comparison of Test Materials and Test Conditions in the Advanced Rankine System Compatibility Test Loops.....	4
II.	Turbine Simulator Nozzle Design Test Conditions and Throat Diameters.....	12
III.	Refractory Alloy Material Specifications.....	14
IV.	Refractory Alloy Requirements for T-111 Rankine System Corrosion Test Loop.....	18
V.	Results of Quality Assurance Test Program.....	24
VI.	Chemical Analysis of Refractory Alloy Mill Products.....	29
VII.	Mechanical Properties and Grain Size of Refractory Alloy Mill Products.....	36
VIII.	Results of Nondestructive Quality Assurance Tests of Refractory Alloy Mill Products.....	41
IX.	Summary of Overall Quality Assurance Test Results.....	44
X.	Summary of Bend and Hardness Data of Aged T-111 to Cb-1Zr Weld Specimens.....	62
XI.	Results of Chemical Analysis of T-111 Specimens From 1 Hour - 2400°F (1316°C) Vacuum Anneal of T-111 Corrosion Loop Boiler Assembly at Stellite.....	86
XII.	Analytical Data for Lithium From Lithium Corporation of America.....	96
XIII.	Comparison of Results on Oxygen Concentration in Lithium as Determined by the Fast Neutron Activation and Vacuum Distillation Methods - Concentration in ppm.....	103
XIV.	Analytical Data for Potassium.....	105
XV.	Analytical Data for the Lithium and Potassium Used in the T-111 Corrosion Loop.....	106
XVI.	Chamber Bakeout Pressure Log.....	130
XVII.	Results of Calibration of W-3Re/W-25Re Thermocouples in the Boiler Section of the T-111 Corrosion Loop.....	134
XVIII.	T-111 Rankine System Corrosion Test Loop Performance....	152
XIX.	T-111 Rankine System Corrosion Test Loop Performance....	157
XX.	T-111 Rankine System Corrosion Test Loop Turbine Simulator Performance at 5000 Hours.....	158
XXI.	T-111 Rankine System Corrosion Test Loop Performance....	162
XXII.	T-111 Rankine System Corrosion Test Loop Turbine Simulator Performance at 10,000 Hours.....	163

PRECEDING PAGE BLANK NOT FILMED

LIST OF TABLES (CONT.)

Table Number		Page
XXIII.	Analyses of Potassium and Lithium Before and After the 10,000-Hour Test and the Analysis of a Residue Recovered From the Potassium by Distillation Following the Test	171
XXIV.	Results of Chemical Analysis of Specimens of T-111 Alloy Lithium Containment Tube From the Boiler	196
XXV.	Results of Chemical Analysis of Specimens of T-111 Alloy Potassium Containment Tube From the Boiler	197
XXVI.	Results of Chemical Analysis of Miscellaneous Specimens of T-111 Alloy Exposed to Potassium or Lithium During the 10,000-Hour Test	198
XXVII.	Oxygen Concentration of Potassium Boiler Tube as a Function of Distance From Potassium Inlet	200
XXVIII.	Results of Chemical Analysis of Turbine Simulator Blade Specimens Following the 10,000-Hour Test	204
XXIX.	Results of Chemical Analysis of Cb-1Zr Foil Taken From the Vapor Carryover Tube Following the 10,000-Hour Test.	205
XXX.	Weights of Turbine Simulator Nozzles and Blades Before and After 10,000 Hours Exposure in the T-111 Rankine System Corrosion Test Loop	207
XXXI.	Turbine Simulator Nozzle Throat Diameters Before and After 10,000 Hours Exposure in the T-111 Rankine System Corrosion Test Loop	208
XXXII.	Tensile Test Results on Specimens of T-111 Pipe Exposed for 10,000 Hours in the T-111 Rankine System Corrosion Test Loop	247

APPENDICES

D-I.	Extrusion Parameters for T-111 Alloy Ingots	310
D-II.	Chemical Analyses of Cracked T-111 Alloy Extrusion - Fansteel Ingot No. 111-D1632	316
D-III.	Microhardness and Grain Size of Unannealed and Annealed T-111 Alloy Heat Number 111-D-1670 Extruded Base Tube	322
D-IV.	Microhardness and Grain Size of Unannealed and Annealed T-111 Alloy Heat Number 111-D-1670 After First Reduction	328

LIST OF TABLES (CONT.)

Table Number		Page
E-I.	Extrusion Parameters for the 5.85-Inch (14.9-cm)-Diameter Machined Mo-TZC Alloy Ingot	335
E-II.	Recrystallization of 3.125-Inch (8.0-cm)-Diameter Mo-TZC Alloy Extrusion	336
E-III.	Chemical Analyses of Mo-TZC Alloy (Heat No. TAC-4431) Produced by Climax Molybdenum Company	338
E-IV.	Mechanical Properties of Mo-TZC Alloy (Heat No. TAC-441) Produced by Climax Molybdenum Company	339
E-V.	Extrusion Parameters for Mo-TZC Alloy Ingots	340
E-VI.	Chemical Analyses of Mo-TZC Alloy Produced by General Electric - LMCD	341
E-VII.	Mechanical Properties of Mo-TZC Alloy Produced by General Electric - LMCD	342
E-VIII.	Tensile Properties for Mo-TZC Alloy Plate and Rod	351
F-I.	Extrusion Parameters for the 5.36-Inch (13.62-cm)-Diameter Machined Cb-132M Alloy Ingot	356
F-II.	Extrusion Parameters for the 3.75-Inch (9.5-cm)-Diameter Extruded Cb-132M Alloy Billets	357
F-III.	Extrusion Parameters for the 2.0-Inch (5.1-cm)-Diameter Extruded Cb-132M Alloy Billet	358
F-IV.	Chemical Analyses of Cb-132M Alloy (Heat No. 66-95119) Produced by Universal Cyclops Steel Corporation	359
F-V.	Mechanical Properties of Cb-132M Alloy (Heat No. 66-95119) Produced by Universal Cyclops Steel Corporation	360
F-VI.	Tensile Properties of 2-Inch (5.1-cm)-Diameter Cb-132M Alloy Rod	368
G-I.	Room Temperature Compressive Properties of T-111 Alloy and Cb-1Zr Alloy Valve Bellows	376
H-I.	Relative Sensitivity of Mass Spectrometer and Ionization Gauge	379

LIST OF TABLES (CONT.)

Table Number		Page
I-I.	Calibration Data for W-3Re/W-25Re Thermocouple Wire.....	386
I-II.	Comparison of W-3Re/W-25Re Thermocouple EMF With Values Obtained at Engelhard Industries, Inc.....	387
K-I.	Chemical Analysis of the Alkali Metals for T-111 Rankine System Corrosion Test Loop.....	427
K-II.	Interstitial Analysis of 0.375-Inch (0.95-cm)-OD T-111 Tube Specimens.....	458
K-III.	Spectrographic Analysis of 0.375-Inch (0.95-cm)-OD T-111 Tubing.....	459
K-IV.	Analysis of the Potassium Used in Flushing the T-111 Corrosion Test Loop.....	481
K-V.	Analysis of the Lithium Used in Flushing the T-111 Corrosion Test Loop.....	483
K-VI.	Analysis of the Alkali Metals Used in Operation of the T-111 Corrosion Test Loop.....	484
L-I.	Mutual Solubilities of Potassium and Lithium.....	488

LIST OF ILLUSTRATIONS

Figure Number		Page
1.	Schematic Diagram of T-111 Rankine System Corrosion Test Loop	7
2.	Estimated Temperature Distribution and Quality as a Function of Boiler Length for T-111 Rankine System Corrosion Test Loop	9
3.	Effect of Polishing and Pickling on the Surface Roughness of T-111 Tantalum Alloy Tubing	46
4.	Radial Cracks in 0.375-Inch-OD x 0.065-Inch-Wall (0.95-cm-OD x 0.16-cm-Wall) T-111 Alloy Tubing After Cutting With an Alumina Abrasive Wheel	48
5.	Samples of Flattened 0.375-Inch-OD x 0.065-Inch-Wall (0.95-cm-OD x 0.16-cm-Wall) T-111 Alloy Tubing After Cutting With an Alumina Abrasive Wheel Showing the Beneficial Effect on Tube Ductility of Removing the Surface Layer After Cutting	49
6.	Flattened 0.375-Inch-OD x 0.065-Inch-Wall (0.95-cm-OD x 0.16-cm-Wall) T-111 Alloy Tube After Cutting With an Allison C120KRA Silicon Carbide Abrasive Wheel. The Cut Surface Was Not Ground Back Prior to Flattening	50
7.	Fabrication Sequence for the T-111 Corrosion Test Loop	52
8.	Vacuum-Purge Inert Gas Welding Chamber, 3-Foot (0.9-m) Diameter x 6-Foot (1.8-mm) Long, With Helium Supply and Purity Control System Showing the Pipe Welding Extension Tube Attached to the Chamber Door	53
9.	Vacuum-Purge Inert Gas Welding Chamber and Helium Purity Control System With Welding Chamber Extension Tank Attached to 3-Foot (0.9-m)-Diameter x 6-Foot (1.8-m)-Long Welding Chamber	54
10.	Modified Hoke Valve and Assocated Drive Components for the Cb-1Zr Corrosion Loop	56
11.	Double-Race Ball Bearing Used in Metering and Isolation Valves of the T-111 Corrosion Test Loop. Casing is Tool Steel and Balls are Tungsten Carbide	58
12.	EM Pump Ducts for T-111 Corrosion Loop	59
13.	Stressed Diaphragm Pressure Transducer for the T-111 Corrosion Test Loop at Various Stages During Fabrication	60
14.	Microstructures of Automatic Weldments of Cb-1Zr to T-111 Prepared Without Filler Additions Following Various Post-weld Heat Treatments	64

Figure Number		Page
15.	Microstructures of Manual Weldments of Cb-1Zr to T-111 Prepared With Cb-1Zr and T-111 Filler Material Following Various Postweld Heat Treatments.....	65
16.	Cb-1Zr-to-T-111 Weldments Prepared With T-111 Filler Showing T-111 Particle Which Was Washed into the Fusion Zone. Specimen Was Heat-Treated at 1500°F (816°C) for 50 Hours Following Welding.....	67
17.	Effect of Polishing and Pickling on the Surface Roughness of T-111 Tantalum Alloy Tubing. Polishing to Remove 0.001 Inch (0.002 cm) of the Tube Wall Performed With 120- and 600-Grit Alumina Cloth. Specimens Pickled for Five Minutes in $HF-HNO_3-H_2SO_4-H_2O$ (1-4-1-2, Parts by Volume)...	69
18.	Tube-in-Tube Boiler of T-111 Corrosion Loop Prior to Insertion of the Boiler Plug.....	70
19.	Lithium Heater Assembly of T-111 Corrosion Loop.....	71
20.	Potassium Preheater of T-111 Corrosion Loop.....	72
21.	T-111 Alloy Preheater Coil Electrodes for the T-111 Corrosion Test Loop.....	73
22.	Test Nozzles for Turbine Simulator (Stages 2 to 10) of the T-111 Corrosion Test Loop Prior to Assembly.....	75
23.	Entrance and Exit Side of the Nozzle and the Blade Assembly of the Second Stage (Mo-TZC) of the Turbine Simulator.....	76
24.	Entrance and Exit Side of the Nozzle and the Blade Assembly of Sixth Stage (Cb-132M) of the Turbine Simulator	77
25.	Turbine Simulator (Stages 2 to 10) of the T-111 Corrosion Loop Prior to Assembly.....	78
26.	T-111 Corrosion Loop Condenser Prior to Coating of Tantalum Fins With Iron Titanate.....	80
27.	Condenser - Turbine Simulator Assembly Following Application of Iron Titanate Coating on Tantalum Fins.....	81
28.	Nine-Stage Turbine Simulator and Top of Condenser.....	82
29.	Potassium Preheater - Boiler - First-Stage Turbine Simulator Assembly Following Postweld Anneal.....	83
30.	Potassium Surge Tank and EM Pump Subassembly of the T-111 Corrosion Test Loop Mounted on the Welding Fixture.....	84
31.	Lithium Surge Tank and EM Pump Subassembly of the T-111 Corrosion Test Loop Mounted on the Welding Fixture.....	85

Figure Number		Page
32.	T-111 Corrosion Test Loop and Chamber Spool Piece During the Transfer of the Loop From the Support Structure to the Welding Fixture.....	89
33.	T-111 Corrosion Test Loop Mounted on the Welding Fixture Prior to Final Welding and Weld Heat-Treatment Operations.	90
34.	T-111 Corrosion Test Loop and the Vacuum Chamber Spool Piece Following Completion of Loop Fabrication.....	91
35.	Lower Portion of the T-111 Corrosion Test Loop Following Completion of Fabrication.....	92
36.	Thirty-Five-Pound (16-kg)-Capacity Lithium Shipping Container.....	95
37.	Hot Trap for Purifying Alkali Metals - Before Assembly....	97
38.	Hot Trap for Purifying Alkali Metals - After Assembly.....	98
39.	Distillation for Purifying Alkali Metal for the T-111 Corrosion Loop Test. Components of System Shown Prior to Assembly.....	99
40.	Alkali Metal Still - After Assembly.....	100
41.	Alkali Metal Purification Facility.....	101
42.	Test Facility for Operation of T-111 Corrosion Test Loop..	108
43.	Ion Gauge, Partial Pressure Analyzer Tube, and Variable Leak Valve Mounted on Chamber Sump.....	111
44.	Electronic Control Unit and X-Y Recorder for the Partial Pressure Analyzer.....	112
45.	Instrumentation of T-111 Rankine System Corrosion Test Loop Showing Typical Test Conditions.....	116
46.	Thermocouple Installation on the Tube-in-Tube Helical Boiler of the T-111 Corrosion Test Loop.....	117
47.	Typical Cb-1Zr Dimpled Foil Thermal Insulation of Various Loop Components.....	118
48.	Thermocouple Wire Terminals (192 Total) Located in the Sump of the Test Chamber for the T-111 Corrosion Test Loop	120
49.	Six Thermocouple Lead Wire Feedthrough Flanges With 32 Wires in Each Flange. An Enlarged View of One of the Flanges is Shown on the Right.....	121
50.	T-111 Rankine System Corrosion Test Loop. Following Instrumentation Before Installation on the Vacuum Chamber Sump.....	122

Figure Number		Page
51.	Metering Valve and Isolation Valves of the T-111 Corrosion Test Loop	124
52.	Auxiliary Quartz Lamp Heater Used on the Lithium Surge Tank	125
53.	Adjustable Condenser Shield and Drive Mechanism	126
54.	Lower Portion of the T-111 Corrosion Test Loop	127
55.	Calibration of Slack Diaphragm Pressure Transducer No. 1 for the T-111 Corrosion Test Loop	132
56.	Calibration of Fast-Response Stressed Diaphragm Pressure Transducer for the T-111 Corrosion Test Loop	133
57.	Potassium Flowmeter Calibration for T-111 Corrosion Test Loop	135
58.	Lithium Flowmeter Calibration for the T-111 Corrosion Test Loop	136
59.	The Effect of Plugging the Metering Valve on Potassium Flow Rate and Pressure Drop Across the Metering Valve During Operation of the T-111 Rankine System Corrosion Test Loop	140
60.	Test Chamber Environment During Startup and Early Operation Testing of the T-111 Corrosion Loop	143
61.	The Effect of Boiling Instabilities on the Potassium Pressure and Flow During Startup of the T-111 Rankine System Corrosion Test Loop	145
62.	Temperatures of Interest Recorded During Operation of the T-111 Corrosion Test Loop on the Daytime Shift Only With Unattended Operation Between 1600 Hours and 0800 Hours	147
63.	Temperatures of Interest Recorded During Operation of the T-111 Corrosion Test Loop on the Daytime Shift Only With Unattended Operation Between 1600 Hours and 0800 Hours	148
64.	T-111 Corrosion Test Loop Temperatures at 2000 Hours	150
65.	T-111 Corrosion Test Loop Operating Temperatures - 2000 Hours	151
66.	T-111 Corrosion Test Loop Boiler Conditions After 1000 Hours Operation	153
67.	Potassium and Lithium Flow Traces Recorded on April 19, 1969, After 2000 Hours of Operation of the T-111 Rankine System Corrosion Test Loop	154

Figure Number		Page
68.	T-111 Corrosion Test Loop Operating Temperatures - 5000 Hours	156
69.	T-111 Rankine System Corrosion Test Loop Thermocouple Instrumentation Layout	160
70.	T-111 Corrosion Test Loop Operating Temperatures - 10,000 Hours	161
71.	Potassium Pressure on Either Side of the Metering Valve During the Shutdown Completing the 10,000 Hours of Testing of the T-111 Rankine System Corrosion Test Loop	165
72.	Test Chamber Environment During Testing of the T-111 Rankine System Corrosion Test Loop	167
73.	T-111 Corrosion Test Loop Potassium Draining and Sampling Schematic	170
74.	T-111 Corrosion Test Loop Lithium Draining and Sampling Schematic	172
75.	Top Portion of T-111 Corrosion Test Loop After Completion of 10,000 Hours of Testing	174
76.	T-111 Corrosion Test Loop After Completion of 10,000 Hours of Testing	175
77.	Lower Portion of T-111 Corrosion Test Loop After Completion of 10,000 Hours of Testing	176
78.	T-111 Corrosion Test Loop Boiler and Turbine Simulator Following Removal of the Thermal Insulation	177
79.	Components of T-111 Corrosion Loop After Removal of Thermal Insulation From Areas to Undergo Posttest Evaluation	178
80.	Vinyl Chamber Used for Cutting Operations on T-111 Corrosion Test Loop	180
81.	T-111 Corrosion Test Loop Showing Location of Cuts Necessary to Remove Boiler and Turbine Simulators for Evaluation at the Completion of 10,000 Hours of Testing	181
82.	Boiler, Crossover Line, and Turbine Simulators After Removal From T-111 Corrosion Test Loop	182
83.	Setup for the Removal of Residual Alkali Metals From T-111 Rankine System Corrosion Test Loop Components by Reaction With Liquid Ammonia	183

Figure Number		Page
84.	Components of Boiler Plug Section of T-111 Rankine System Corrosion Test Loop Following 10,000 Hours of Continuous Operation	185
85.	Components of Plug Section of Boiler From T-111 Rankine System Corrosion Test Loop Following 10,000 Hours Operation Showing the HfN Deposit Observed on the Potassium Boiler Tube	186
86.	Boiler From T-111 Rankine System Corrosion Test Loop Following 10,000 Hours of Operation Illustrating Location of Cut Providing Removal and Inspection of Individual Coils	188
87.	Repair Welds in Boiler Tubes of T-111 Rankine System Corrosion Test Loop Following 10,000 Hours of Operation	189
88.	Turbine Simulator Nozzles, Blades, and Support Pads Following 10,000 Hours of Exposure to Potassium Vapor in the T-111 Rankine System Corrosion Test Loop	190
89.	Concave and Convex Side of Turbine Simulator Blades Following 10,000 Hours Exposure to Potassium Vapor in the T-111 Rankine System Corrosion Test Loop	191
90.	Longitudinal Cross Section of Turbine Simulator Nozzles Following 10,000 Hours of Exposure to Potassium Vapor in the T-111 Rankine System Corrosion Test Loop	193
91.	Location of Specimens Used for Chemical Analyses of Loop Components From the T-111 Corrosion Test Loop Following 10,000 Hours of Continuous Operation	195
92.	Results of Oxygen Analysis of Loop Components	199
93.	Flow Pattern at End of Swirler Wire Plug Insert in Water Test	202
94.	Location of Specimens for Metallographic Examination From the T-111 Corrosion Test Loop	209
95.	Pretest Microstructure of the T-111 Tubing	210
96.	Hafnium Nitride Deposit Near Bottom of 3/8-Inch (0.95-cm)-OD T-111 Tube in Plug Section of Boiler	212
97.	Base Metal - Weld Interface at Bottom of the 3/8-Inch (0.95-cm)-OD T-111 Potassium Containment Tube in the Plug Section of the Boiler Before and After Etching	213
98.	Microprobe Scans of the Base Metal - Weld Interface at the Bottom of the 3/8-Inch (0.95-cm)-OD T-111 Potassium Containment Tube in the Plug Section of the Boiler. Same Area as Figure 97	214

Figure Number		Page
99.	T-111 Potassium Containment Tube to the Plug Section Approximately 6 Inches (15 cm) Above Lithium Exit From Boiler	216
100.	T-111 Potassium Containment Tube in the Plug Section of the Boiler Adjacent to the Top of the Swirler Wire Insert.	217
101.	Potassium Boiler Containment Tube Approximately 1/2 Inch (1.2 cm) Above Top of Swirler Wire Insert	219
102.	T-111 Potassium Containment Tube 1/2 Inch (1.2 cm) Above the Top of the Swirler Wire Insert. Same Area as Figure 101	220
103.	T-111 Swirler Wire From Plug Section of Boiler	221
104.	T-111 Swirler Wire From Plug Section of the Boiler Approximately 6 Inches (15 cm) From the Lithium Exit	222
105.	Lithium Containment Tube (1-Inch, 2.5-cm OD) From Top of Plug Section	224
106.	Repair Welds in Top Coil of the 3/8-Inch (0.95-cm) and 1-Inch (2.5-cm) T-111 Tubing From the Boiler	225
107.	Lithium Containment Tube From Top of Boiler Following 10,000 Hours of Continuous Operation at Approximately 2240°F (1227°C) Illustrating Effect of Strain From Pretest Forming Operation on Grain Growth	227
108.	3/8-Inch (0.95-cm) Potassium Containment Tube From Top of Boiler Illustrating Effect of Strain From Pretest Forming on Grain Growth During the 10,000-Hour Test. Adjacent to Sample in Figure 107	228
109.	Repair Socket Weld in 3/8-Inch (0.95-cm) Lithium Inlet to the Boiler	229
110.	Repair Socket Weld in 3/8-Inch (0.95-cm)-OD Lithium Exit Line From Boiler	230
111.	Repair Socket Weld in Lithium Exit Line From Boiler. Same Area as Figure 110	232
112.	Heat-Affected Zone of Field Weld Joining Top of Boiler to Bottom of First-Stage Turbine Simulator	233
113.	Lithium Line Connecting Heater Exit to the Boiler Inlet	235
114.	Specimens of 1-Inch (2.5-cm)-OD x 0.1-Inch (0.25-cm)-Wall T-111 Pipe Following 10,000 Hours Exposure in the T-111 Rankine System Corrosion Test Loop. Ring Specimens Deformed at Room Temperature	236

Figure Number		Page
115.	1-Inch (2.5-cm)-OD Potassium Vapor Crossover Line Following 10,000 Hours of Continuous Operation at Approximately 1880°F (1027°C)	237
116.	Scanning Electron Micrographs of Various Components of T-111 Rankine System Corrosion Test Loop. All Are Fractures From Compression Tests on Rings From 1-Inch (2.5-cm)-OD Tubing	238
117.	Pretest Microstructure of Materials Used for the Turbine Simulator	240
118.	Mo-TZC Alloy First-Stage Nozzle and Blade Turbine Simulator Following 10,000 Hours of Continuous Exposure to Flowing Potassium Vapor in the Corrosion Test Loop	241
119.	Mo-TZC Alloy Second-Stage Nozzle and Blade Turbine Simulator Following 10,000 Hours of Continuous Exposure to Flowing Potassium Vapor in the T-111 Corrosion Test Loop	242
120.	Cb-132M Alloy Sixth-Stage Nozzle and Blade Turbine Simulator Following 10,000 Hours of Continuous Exposure to Potassium Vapor in the T-111 Corrosion Test Loop	243
121.	Mo-TZC Alloy Tenth-Stage Nozzle and Blade Turbine Simulator Following 10,000 Hours of Continuous Exposure to Potassium Vapor in the T-111 Corrosion Test Loop	244
122.	Tensile Specimens Used for Posttest Evaluation of 1-Inch (2.5-cm)-OD Pipe	246
123.	Fractured Tensile Test Specimens Cut From 1-Inch (2.5-cm) T-111 Pipe of the 10,000-Hour T-111 Corrosion Test Loop. Tensile Tests Performed at 80°F (27°C)	248

APPENDICES

B-1.	T-111 Rankine System Corrosion Test Loop Assembly (Drawing No. 246R897)	264
B-2.	Lithium Surge Tank Assembly (Drawing No. 263E807, Rev. A)	267
B-3.	Lithium EM Pump Duct Assembly (Drawing No. 941D881)	268
B-4.	Lithium Heater Line (Drawing No. 263E829, Rev. A)	269
B-5.	Heater Assembly (Drawing No. 941D883)	270
B-6.	Potassium Boiler Assembly (Drawing No. 263E828)	271
B-7.	Preheater Assembly (Drawing No. 941D884)	272

Figure Number		Page
B-8.	Single-Stage Turbine Simulator (Drawing No. 119C2979).....	273
B-9.	Nozzle Assembly (Drawing No. 119C2977).....	274
B-10.	Turbine Simulator Blade Assembly (Drawing No. 119C2976, Rev. A).....	275
B-11.	Turbine Simulator Nozzle (Drawing No. 119C2975).....	276
B-12.	High-Temperature Liquid Metal, Modified, Hoke Valve (Drawing No. 263E827, Rev. A).....	277
B-13.	Potassium Surge Tank Assembly (Drawing No. 263E808, Rev. A).....	278
B-14.	Turbine Simulator and Condenser Assembly (Drawing No. 941D897, Rev. A).....	279
B-15.	Nine-Stage Turbine Simulator (Drawing No. 941D874, Rev. A).....	280
D-1.	Macrographs of the T-111 Alloy Extrusion From Heat 111D1632 Showing Intergranular Cracks at Surface at Approximately 120° Intervals.....	312
D-2.	Sectioning of Transverse Slice From Extrusion of Fansteel Ingot No. 111D1632.....	313
D-3.	The Microstructure of the Center of the Transverse Slice From the T-111 Alloy Extrusion - Fansteel Heat No. 111D1632.....	314
D-4.	Microstructures of Transverse Sections From the T-111 Extrusion - Fansteel Heat No. 111D1632.....	315
D-5.	Transverse Microstructure of T-111 Alloy Extruded Base Tube.....	318
D-6.	Transverse Microstructure of T-111 Alloy Extruded Base Tube.....	319
D-7.	Transverse Microstructure of T-111 Alloy Extruded Base Tube.....	320
D-8.	Transverse Microstructure of T-111 Alloy Extruded Base Tube After Annealing at 3000°F (1649°C) for One Hour in Vacuum.....	321
D-9.	Longitudinal Microstructure of T-111 Alloy Tubing After First Reduction.....	324
D-10.	Longitudinal Microstructure of T-111 Alloy Tubing After First Reduction.....	325

Figure Number		Page
D-11.	Longitudinal Microstructure of T-111 Alloy Tubing After First Reduction.....	326
D-12.	Longitudinal Microstructure of T-111 Alloy Tubing After First Reduction.....	327
D-13.	Photomicrographs of Typical Defects on the ID Surface and Inner Wall of 0.375-Inch (0.95-cm)-OD x 0.065-Inch (0.16-cm)-Wall T-111 Alloy Tubing.....	329
E-1.	Microhardness and Microstructure of Longitudinal Specimens Cut From 0.75-Inch (1.9-cm)-Thick Mo-TZC Alloy Plate as a Function of Heat-Treatment Temperature.....	344
E-2.	Microhardness and Microstructure of Longitudinal Specimens Cut From 1.375-Inch (3.49-cm)-Thick Mo-TZC Alloy Plate as a Function of Heat-Treatment Temperature.....	346
E-3.	Microhardness and Microstructure of Longitudinal Specimens Cut From 1.0-Inch (2.5-cm)-Diameter Mo-TZC Alloy Rod as a Function of Heat-Treatment Temperature.....	348
E-4.	Design of Buttonhead Tensile Specimens Machined From Cb-132M Alloy and Mo-TZC Alloy Materials.....	350
F-1.	Microhardness and Microstructure of Longitudinal Specimens Cut From 2.0-Inch (5.1-cm)-Diameter Cb-132M Alloy Rod....	362
F-2.	Longitudinal Microstructure of 2.0-Inch (5.1-cm)-Diameter Cb-132M Alloy Rod.....	363
F-3.	Longitudinal Microstructure of 2.0-Inch (5.1-cm)-Diameter Cb-132M Alloy Rod.....	364
F-4.	Longitudinal Microstructure of 2.0-Inch (5.1-cm)-Diameter Cb-132M Alloy Rod.....	365
F-5.	Longitudinal Microstructure of 2.0-Inch (5.1-cm)-Diameter Cb-132M Alloy Rod Annealed 50 Hours at 2500°F (1371°C).....	367
G-1.	Stages in the Formation of T-111 Alloy Bellows.....	373
G-2.	T-111 Alloy Valve Bellows.....	374
G-3.	(a) A Transverse Section of T-111 Alloy Bellows Convolutions Showing the Uniformity of the Wall Thickness. (b) A Transverse Section at the Apex of a Convolution Indicating an ASTM Grain Size 7-8.....	375

Figure Number		Page
I-1.	Thermocouple Calibration Furnace Attached to the 24-Inch (61 cm)-Diameter Getter-Ion Pumped Vacuum Chamber.....	382
I-2.	Thermocouple Bundle Used in Calibration of W-3Re/W-25Re Thermocouple Wire.....	383
I-3.	Difference Parameter vs Temperature Obtained in Calibration of Two W-3Re/W-25Re Thermocouples Made From Wire Used to Instrument the T-111 Rankine System Corrosion Test Loop.....	385
K-1.	Distillation and Sampling System Used in Isolating Particulate Matter in the Potassium Drained From the T-111 Corrosion Test Loop.....	424
K-2.	Lithium Purification and Transfer System Schematic.....	429
K-3.	Schematic of System Used for Draining Lithium From the Primary Circuit of the Loop.....	433
K-4.	Effect of Heating Localized Sections of the T-111 Boiler on Helium Level in Evacuated Potassium Circuit Measured With a General Electric M-60 Helium Leak Detector.....	436
K-5.	Vinyl Chamber Used for Cutting Operations on the Boiler..	438
K-6.	Vacuum Equipment and Instrumentation Used for Evacuation and Backfilling of Vinyl Chamber and Analysis of Exiting Inert Gas.....	439
K-7.	Welds in 0.375-Inch (0.95-cm)-OD T-111 Alloy Tubing in the Boiler Which Separates the Potassium and Lithium Circuits.....	440
K-8.	T-111 Boiler Following Initial Cut. The Potassium Circuit Was Sealed From Atmosphere With Expandable Plugs.	441
K-9.	Expandable Plugs Used to Seal the Loop Tubing After Cutting.....	443
K-10.	Location of Tubing Cuts Made to Remove Boiler From Loop as Indicated on the Boiler Assembly Before Final Loop Assembly.....	444
K-11.	Top of Boiler After Cutting and Sealing Lithium Inlet and Potassium Exit Lines.....	445
K-12.	Schematic of Apparatus Used to Remove Residual Alkali Metal From Boiler by Dissolution in Liquid Ammonia.....	447
K-13.	Location of Leak in Weld Nugget of 0.375-Inch (0.95-cm)-Diameter T-111 Tube Removed From Boiler. The Bubbles Were Produced by Air Pressurization of Tube With a Soap Film Coating on OD.....	450

Figure Number		Page
K-14.	Grain Boundary Crack in Weld Nugget of the Potassium Containment Tube Responsible for Leak in the Boiler of the T-111 Loop.....	451
K-15.	Intergranular Crack in the Weld Nugget of the Potassium Boiler Tube Removed From the T-111 Loop.....	453
K-16.	Intergranular Crack in the Weld Nugget of the Boiler Tube	454
K-17.	Intergranular Crack in the Weld Nugget of the Boiler Tube	456
K-18.	Schematic of the Boiler Repair.....	461
K-19.	Socket Weld Fitting Specimen to Qualify This Joint Design for the Boiler Repair and Reinstallation.....	462
K-20.	Joint Design at the Ends of the Boiler.....	463
K-21.	Top of the Boiler Following Initial Repair Welds.....	465
K-22.	Top of the Boiler Following Final Repair Welding.....	466
K-23.	Bottom of the Boiler Following Repair Welding.....	467
K-24.	T-111 Corrosion Loop Boiler.....	468
K-25.	Repaired T-111 Corrosion Loop Boiler Wrapped With Cb-1Zr Foil in Preparation for Postweld Annealing.....	469
K-26.	Installation of the Welding Chamber Around the T-111 Corrosion Loop. Lower Spool Piece in Position.....	471
K-27.	Welding Chamber Installed Around the T-111 Corrosion Loop. The Chamber Consists of Two Spools Which Can Be Rotated Independently for Improved Access to Weld Locations.....	472
K-28.	Welding Chamber and Ancillary Instrumentation Installed on the Test Facility.....	473
K-29.	Gas Chromatographs Used to Analyze the Helium Atmosphere in the Welding Chamber for the Repair of the T-111 Corrosion Loop.....	474
K-30.	Repaired Boiler Installed into the T-111 Corrosion Loop. Arrows Indicate Installation Welds.....	475
K-31.	Top of Repaired Boiler After Installation in the T-111 Corrosion Loop.....	477
K-32.	Bottom of Repaired Boiler After Installation in the T-111 Corrosion Loop.....	478
K-33.	Potassium Transfer System for Filling and Flushing the T-111 Corrosion Test Loop.....	480

LIST OF ILLUSTRATIONS (CONT.)

Figure Number		Page
L-1.	Lithium-Potassium Solubility Apparatus.....	486
L-2.	Lithium-Potassium Solubility Study Sampler.....	487

SUMMARY

A 10,000-hour test was conducted on a two-loop T-111 alloy system, in which lithium was circulated in the heater circuit and potassium was boiled and circulated in a two-phase secondary loop, which contained turbine simulator test specimens of Mo-TZC and Cb-132M alloy. Maximum and minimum temperatures in the lithium circuit were 2250°F (1232°C) and 2078°F (1137°C), respectively, while temperatures in the two-phase potassium circuit ranged from 2140°F (1171°C) (superheated vapor) at the boiler outlet to a minimum of 920°F (493°C) in the coolest portion of the loop.

During test startup, a leak developed in a butt weld of the potassium containment tube of the boiler. A detailed repair plan was developed and carried out successfully with no significant contamination of the test components or the working fluids.

The test was performed in a 4-foot-diameter x 11-foot-high getter-ion pumped vacuum chamber. Total pressure of the test chamber environment was maintained at less than 2×10^{-8} torr (3.3×10^{-6} N/m^2) for most of the test period. Posttest evaluation of test components indicated no significant contamination of the loop components by the vacuum chamber environment.

Extensive chemical and metallurgical evaluation of the T-111 alloy containment material and the Mo-TZC and Cb-132M turbine simulator materials indicated that these candidate materials have suitable compatibility with these energy transfer fluids for application in future rankine system electric power systems.

I. INTRODUCTION

This report describes the design, fabrication, instrumentation, operation, and evaluation of a T-111 Rankine System Corrosion Test Loop which was operated for 10,000 hours. The primary purpose of the test was to determine the compatibility of an advanced refractory metal with potassium under conditions representative of those anticipated in future space electric power systems. An ancillary purpose included the evaluation of the compatibility of candidate turbine blade and nozzle materials in contact with potassium vapor and the compatibility of the T-111 alloy with lithium in the primary or heater circuit of the test system.

The statement of work in the contract stated that the containment alloy for the test system would be selected by NASA from the list of four candidate materials given below:

T-111* (Ta-8W-2Hf)
T-222 (Ta-9.6W-2.4Hf-0.1C)
D-43 (Cb-10W-1Zr-0.1C)
FS-85 (Cb-28Ta-10.5W-0.9Zr)

The tantalum alloy, T-111, was subsequently selected as the loop material.

The turbine simulator alloys under consideration included the following:

Mo-TZC (Mo-1.25Ti-0.15Zr-0.15C)
Mo-TZM (Mo-0.5Ti-0.8Zr)
Cb-132M (Cb-20Ta-15W-5Mo-1Zr-0.1C)
AS-30 (Cb-20W-1Zr-0.1C)

Both Mo-TZC and Cb-132M were selected for evaluation in the turbine simulator section of the T-111 Corrosion Loop.

---

* Nominal compositions in weight percent.

The basic design of the test system was developed and proven in a prior program,** the results of which have been described in a recent report.(1) The purpose of this earlier program was to develop a prototype corrosion test loop system for use in the evaluation of refractory alloys in boiling and condensing potassium environments which simulate projected Rankine systems. The prototype test system consisted of a two-loop Cb-1Zr facility; sodium being heated by direct resistance in the primary loop and used in a heat exchanger (boiler) to boil potassium in the secondary test loop. The method chosen to heat the boiler of the Cb-1Zr Rankine System Corrosion Test Loop was the use of a primary of heater loop in which I^2R-heated sodium was to be pumped through the outer annulus of a tube-in-tube counterflow boiler where the required heat was to be transferred to the potassium in the secondary, two-phase circuit. One of the principal goals of this prior test program was to incorporate as many components in the Cb-1Zr Corrosion Test Loop as required to assure an accurate determination of the test conditions and, thereby, minimize the possibility of undetected test variations; e.g., high-frequency boiling instabilities, which might compromise loop operation or the posttest compatibility evaluation. All the goals of this program were successfully accomplished, and only minor design changes were required prior to the fabrication of the T-111 Corrosion Loop.

The test materials and test conditions for the Cb-1Zr alloy system and the T-111 alloy system are listed in Table I. The major differences in materials and operating conditions in the two test loops are as follows:

1. T-111 was designated as the containment material in place of Cb-1Zr.

2. Lithium was selected as the heat transfer fluid in the primary circuit in place of sodium.

** NASA Contract NAS 3-2547.

(1) Hoffman, E. E. and Holowach, J., Cb-1Zr Rankine System Corrosion Test Loop, NASA CR-1509, June 1970.

TABLE I

COMPARISON OF TEST MATERIALS AND TEST CONDITIONS
IN THE ADVANCED RANKINE SYSTEM COMPATIBILITY TEST LOOPS

	Cb-1Zr Corrosion Loop	T-111 Corrosion Loop
Loop Material	Cb-1Zr Alloy	T-111 Alloy (Ta-8W-2Hf)
Turbine Simulator Materials	Mo-TZM Alloy	Mo-TZC and Cb-132M Alloys
Primary Heater Circuit	Sodium	Lithium
Primary Heater Temperature	2150°F (1177°C)	2250°F (1232°C)
Secondary Two-Phase Circuit	Potassium	Potassium
Boiling Temperature	1900°F (1038°C)	2050°F (1121°C)
Superheat Temperature	2000°F (1093°C)	2150°F (1177°C)
Condensing Temperature	1350°F (732°C)	1400°F (760°C)
Potassium Mass Flow Rate	40 lb/hr (96 kg/hr)	40 lb/hr (96 kg/hr)
Boiler Exit Vapor Velocity	150 ft/sec (46 m/sec)	50 ft/sec (15 m/sec)
Vapor Velocity, Nozzle Exit	1250 ft/sec (381 m/sec)	1000 ft/sec (305 m/sec)
Potassium Vapor Quality, Nozzle Exit	88%	88%
Average Heat Flux in Boiler	24,000 Btu/hr-ft^2 75,600 W/m^2	23,000 Btu/hr-ft^2 72,450 W/m^2
Test Duration	5000 hours	10,000 hours

3. Substitution of the advanced turbine simulator materials, Mo-TZC and Cb-132M, for the Mo-TZM nozzle and blade specimens used in the earlier experiment.

4. The potassium boiler outlet temperature was increased from 2000°F (1093°C) to 2150°F (1177°C).

5. Test duration was increased from 5000 to 10,000 hours.

At the time of the selection of T-111 as the containment alloy, only limited data was available in the literature regarding the compatibility of T-111 with potassium and essentially no data on the compatibility of T-111 with flowing lithium. Refluxing potassium capsule tests performed at Oak Ridge National Laboratory[2] indicated that both T-111 and T-222 were unattacked in 4000-hour tests at a temperature of approximately 2300°F (1260°C). Although no data existed on the compatibility of T-111 with lithium at elevated temperatures, the inhibition of lithium attack in niobium alloys by getter-element additions such as zirconium was clearly established,[3] and extrapolation of this result to tantalum alloys containing the strong oxide former, hafnium, appeared to be entirely justified. The results of the 10,000-hour loop test to be described in this report confirmed the rationale used in selecting the T-111 alloy.

(2) DeVan, J. H., et al., Lithium and Potassium Corrosion Studies With Refractory Metals, ORNL-TM-1673, 1966.

(3) DiStefano, J. R. and Hoffman, E. E., "Corrosion Mechanisms in Refractory Metal - Alkali Metal Systems," The Science and Technology of Tungsten, Tantalum, Molybdenum, Niobium, and Their Alloys, Edited by N. E. Promisel, Pergamon Press, London, 1964, p. 257.

II. LOOP DESIGN

The design of the T-111 Rankine System Corrosion Test Loop was very similar to that of the Cb-1Zr Rankine System Corrosion Test Loop.[4] A schematic drawing of the loop reflecting the location of various components and the design conditions is shown in Figure 1. The Cb-1Zr Loop configuration was modified to reflect the experience gained in the fabrication and operation of that loop. In addition to the design changes in selected components, regrouping of several subassemblies was made to facilitate the welding and heat treating of the completed assembly.

The changes which were made in the Cb-1Zr Corrosion Loop design are as follows:

1. Relocation of Primary EM Pump - During the installation of the Cb-1Zr Loop, some difficulty was experienced in inserting the primary and secondary EM pump ducts in their respective vacuum tank ports because of the 90^{o} angle between them. Moving the primary EM pump from 90^{o} to 45^{o} from the secondary EM pump eliminated this installation problem for the T-111 Corrosion Loop.

2. Boiler Plug Length - During the startup and early operation of the Cb-1Zr Corrosion Loop, it was observed that two features of the test system which were most responsible for the boiling stability were the pressure drop across the metering valve and the 12-inch-long (30.5-cm) plug section located in the boiler entrance region. The boiler plug is a flow-swirling device formed by wrapping and tack welding a 1/16-inch-diameter (1.6-mm) wire on a 1/8-inch-diameter (3.2-mm) rod using a 1-inch (2.54-cm) pitch. This plug is located in the first 12 inches (30.5 cm) of the 1/4-inch-ID (6.4-mm) boiler tube.

---

(4) Hoffman, E. E. and Holowach, J., Cb-1Zr Rankine System Corrosion Test Loop, NASA CR-1509, June 1970.

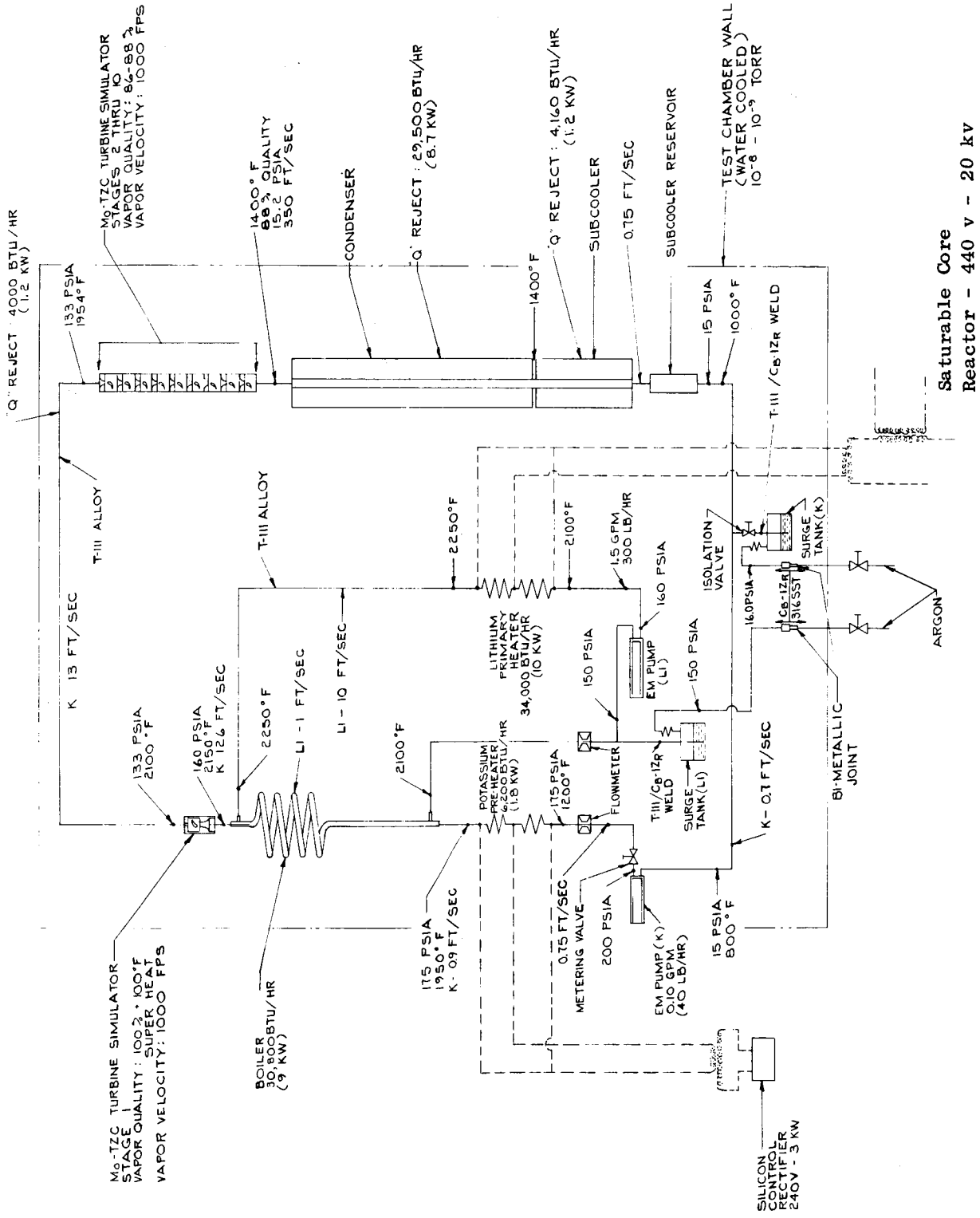


Figure 1. Schematic Diagram of T-111 Rankine System Corrosion Test Loop.

ORIGINAL PAGE IS
OF POOR QUALITY

Although the Cb-1Zr Loop was observed to operate in a stable manner with the bulk of the boiling occurring in various locations along the boiler length, operation was most stable when the nucleate boiling was occurring principally in the plug section. Movement of the nucleate boiling region along the boiler length was observed during test startup due to changes in the test conditions and during routine operation as a result of momentary power fluctuations. Periods of substantial operational instability were associated with the movement of the boiling location to a new region of the boiler. More substantial perturbations of the system conditions; sodium flow, sodium temperature, potassium flow, etc.; were required to dislodge the nucleate boiling region from the plug section than to cause movement of this region from other portions of the boiler.

The observations cited above indicated that lengthening of the plug portion of the boiler would result in more stable loop operation during startup and during periods when loop test conditions may change as a result of changes in loop performance or power fluctuations. For this reason, the plug section length was increased from 12 inches (30.5 cm) to 18 inches (45.7 cm) for the T-111 Corrosion Loop.

A review of the heat transfer characteristics of the plug section of the Cb-1Zr boiler indicated that lengthening the plug from 12 to 18 inches (30.5 to 45.7 cm) would not significantly change the overall performance of the boiler. Calculations indicated that the vapor quality at the exit of the plug would only increase from 72 to 77 percent as shown in Figure 2.

Although the addition of the 6 inches (15.2 cm) to the plug length would increase the heat flux in this section compared to the comparable length with no plug, calculations indicated the

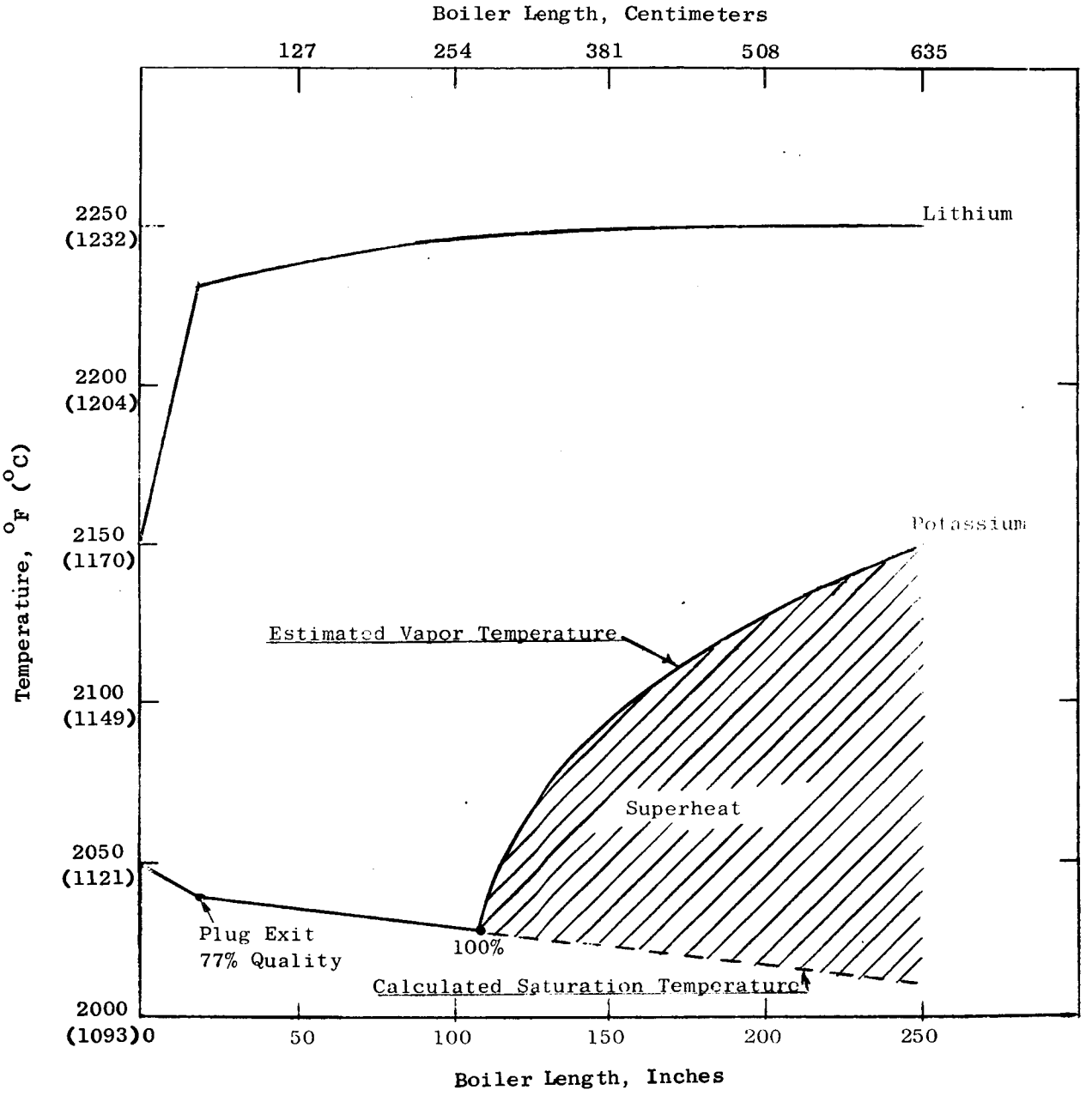


Figure 2. Estimated Temperature Distribution and Quality as a Function of Boiler Length for T-111 Rankine System Corrosion Test Loop.

average heat flux in the boiler plug would decrease from 295,000 Btu/hr ft^2 (92,900 W/m^2) for the 12-inch (30.5-cm) plug to 240,000 Btu/hr ft^2 (75,600 W/m^2) for the 18-inch (45.7-cm) plug.

3. Lithium Heater Length - There were indications of possible induction heating of the insulating foil on the Cb-1Zr sodium heater. To minimize this minor problem, the number of turns in each coil of the lithium heater was increased from 2 1/2 to 3 1/2 to increase the overall electrical resistance and reduce the current required for the design power input. The increased length and the higher electrical resistivity of the T-111 alloy with respect to Cb-1Zr would increase the overall resistance of the heater by 25 percent. The lithium heater electrodes made of tantalum were lengthened by 2 inches (5.1 cm) and clamped to the ORHC copper bus bars with Cb-1Zr bolts threaded on both ends. The longer length lowered the tantalum/copper bus bar interface temperature. The lower coefficient of thermal expansion of the Cb-1Zr bolts, as compared to the stainless steel bolts employed in the Cb-1Zr Loop, would limit the possibility of an open circuit resulting from thermal cycling during startup and shutdown.

4. Pressure Transducer - An additional slack diaphragm pressure transducer was added downstream of the metering valve and adjacent to the original stress-diaphragm pressure transducer. The slack-diaphragm pressure transducer is less sensitive to zero shift and would provide a better indication of changes in the pressure drop across the boiler and the metering valve. The fast-response pressure transducer had proven to be useful in detecting minor instabilities and was therefore retained.

5. Subcooler Reservoir - The reservoir was redesigned in an effort to remove particles that might be present in the flow circuit by diverting the potassium through a double-reversed, low-velocity flow path. An increase in the pressure drop as a function of time during one period of the Cb-1Zr Loop operation indicated that small solid particles may have been partially restricting

the 0.004-inch-wide (0.10-mm) annulus of the metering valve, and the change was made to eliminate the probability of this occurring.

6. Metering Valve - A redesign of the plug to provide better flow control at a flow rate of 40 pounds per hour (5 gm per sec) of potassium was made by reducing the included angle of the plug control surface from 75^{o} to 10^{o}. The pinion gear of the valve drive was changed from a 6- to 10-tooth gear for smoother operation at the higher torque level. A change was made in valve gear material from stainless steel to hardened steel on cemented carbides to reduce the galling tendency.

7. Condenser - Distortion and out-of-roundness were observed in the Cb-1Zr Corrosion Loop condenser tube after GTA welding of the fins to the tube wall. For the T-111 Corrosion Loop, the distortion was eliminated by replacing the tube with a 1- x 2-inch (2.5- x 5.1-cm) diamond-shaped bar which was center gun-drilled to form a 0.42-inch-diameter (1.06-cm) hole through the full 60-inch (152-cm) length of the condenser.

8. Turbine Simulator - The higher boiler temperatures and higher potassium boiler exit pressures in this loop test necessitate changes in the nozzle throat diameters in order to achieve the desired potassium vapor velocities and quality. The turbine simulator test conditions and required nozzle throat diameters for the T-111 Corrosion Loop Test are listed in Table II.

TABLE II

TURBINE SIMULATOR NOZZLE DESIGN TEST CONDITIONS AND THROAT DIAMETERS

Nozzle Number	Material	Design Throat Velocity ft/sec	Design Throat Velocity m/sec	Quality %	Inlet Pressure psia	Inlet Pressure $N/m^2 \times 10^{-3}$	Pressure Drop psi	Pressure Drop $N/m^2 \times 10^{-3}$	Throat Diameter inch	Throat Diameter cm
1	Mo-TZC	1000	305	100°F S. H.	175	1206	-	-	0.089	0.226
2	Mo-TZC	1000	305	86	144	990	31	214	0.088	0.224
3	Mo-TZC	1000	305	to	117	805	27	186	0.096	0.244
4	Mo-TZC	1000	305	88	95	655	22	152	0.108	0.274
5	Mo-TZC	1000	305		77	530	18	124	0.118	0.299
6	Cb-132M	1000	305		62	427	15	103	0.129	0.327
7	Mo-TZC	1000	305		50	344	12	82	0.146	0.371
8	Mo-TZC	1000	305		40	276	10	69	0.160	0.406
9	Cb-132M	1000	305		32	220	8	55	0.178	0.452
10	Mo-TZC	1000	305		25	172	7	48	0.199	0.505

Inlet Temperature - 2150°F (1177°C)
Exit Temperature - 1400°F (760°C)
Flow Rate - 40 lb/hr (18.1 kg/hr)

Heat Rejection - Between stages 1 and 2, 4000 Btu/hr (1.2 kw) radiantly rejected from 14.5 inches (36.8 cm) of uninsulated, 1-inch (2.5-cm)-OD Cb-1Zr crossover tube.

Between stages 2 to 10, 1300 Btu/hr (0.28 kw) radiantly rejected from turbine simulator shell with one layer of Cb-1Zr foil.

III. MATERIAL PROCUREMENT

A. MATERIAL SPECIFICATIONS

The material specifications that were prepared and utilized for the procurement of refractory metals and alloys used in the fabrication of the T-111 Corrosion Test Loop are listed in Table III. By far the greatest bulk of material required for the construction of the loop was bar and rod, sheet, plate and foil, and seamless tubing and pipe of the tantalum alloy, T-111 (Ta-8W-2Hf). Smaller quantities of Mo-TZC (Mo-1.25Ti-0.15Zr-0.15C) and Cb-132M (Cb-20Ta-15W-5Mo-2Zr-0.13C) bar for the turbine simulator, Mo-TZM (Mo-0.5Ti-0.08Zr) bar for the valves, T-222 (Ta-10.4W-2.4Hf-0.01C) sheet for the fast-response pressure transducer, and various other mill products of Cb-1Zr and unalloyed tantalum for miscellaneous loop components were required.

Preliminary material specifications were prepared for this program under NASA Contract NAS 3-2547.[5] The preparation of the tentative specifications for the candidate containment alloys was based primarily on information gained from the past experience of the material producers; preparation of the tentative specifications for the two turbine alloys was based primarily on experience at General Electric. The following material producers and laboratories were visited by GE personnel prior to the preparation of the tentative specifications for the containment alloys:

E. I. duPont de Nemours and Company, Inc.;
Fansteel Metallurgical Corporation;
Metals Division, Norton Company;
Stellite Division, Cabot Corporation;
Westinghouse Electric Corp., Astronuclear Laboratory;
Wah Chang Albany Corporation (Teledyne).

---

(5) Miketta, D. N. and Frank, R. G., Materials Specifications for Advanced Refractory Alloys, NASA-CR-54761, NASA Contract NAS 3-2547, October 1965.

TABLE III

REFRACTORY ALLOY MATERIAL SPECIFICATIONS

Title	Specification Number Used for NAS 3-6474	Current Specification Number
A. T-111 (Ta-8W-2Hf) Tantalum Alloy		
Bar and Rod	01-0015-00-B	B50YA323
Sheet, Plate and Strip	01-0040-00-B	B50YA324
Seamless Tubing and Pipe	01-0035-00-D	B50YA325-S1
	01-0035-01-D	
Foil	01-0043-00-A	B50YA322
Wire	01-0048-00-A	B50YA320-S2
B. T-222 (Ta-10.4W-2.4Hf-0.01C) Tantalum Alloy		
Sheet, Plate and Strip	01-0044-00-C(a)	
C. Tantalum		
Ingots and Flat Mill Products	ASTM B 364-61T; 62T(a)	
Rod and Wire	ASTM B 365-61T(a)	
D. Cb-132M (Cb-20Ta-15W-5Mo-2Zr-0.13C) Columbium Alloy		
Bar and Rod	01-0010-01-A	
E. Cb-1Zr Columbium Alloy		
Bar and Rod	01-0003-04B	B50YA328
	01-0052-01-D	
Sheet, Plate and Strip	01-0003-04-B	B50YA329
Seamless Tubing and Pipe	01-0004-01-C, D	B50YA327
	01-0004-03-B	
Foil	01-0003-03-B	B50YA330
Wire	01-0003-03-B	B50YA333
F. Mo-TZC (Mo-1.25Ti-0.15Zr-0.15C) Molybdenum Alloy		
Bar and Rod	01-0011-01-C(a)	
G. Mo-TZM (Mo-0.5Ti-0.08Zr)		
Wrought Bar	CMX-WB-TZM-2	

(a) Modified by Purchase Order.

Upon completion of the specifications, inquiries were forwarded to the material producers requesting comments and recommendations with respect to the tentative specifications. Generally, the response from the material producers was most gratifying, and it was apparent that the majority of the producers invested considerable time and effort in attempting to establish mutually acceptable specifications. Suggested changes that were made by the material producers can be categorized in the following sections of the specifications:

- Chemical Composition
- Mechanical Properties
  - Tensile
  - Stress-Rupture
- Grain Size
- Dimensional Tolerances
- Ultrasonic Inspection Procedures and Requirements

A comparison of the specification requirements established in the tentative specification with the recommended revisions made by the material producers and the final revisions incorporated in the specifications were made and reported in detail in the previously referenced report.[5]

In making the final revisions to the specifications, considerable emphasis was placed on recommendations received from the originators of the alloy. Limits for stress-rupture properties were based on data supplied by NASA. Also, an attempt was made to arrive at specifications that were amenable to at least two suppliers for each alloy.

No changes were made from the tentative specifications in the dimensional tolerances or ultrasonic inspection procedures and requirements. The majority of the producers requested changes in dimensional tolerances that were convenient for their own equipment and the tolerances established for the tentative specifications appeared to be as suitable as any that were proposed. Suggested changes in ultrasonic procedures generally were unacceptable for technical reasons. It should be noted that the material specifications are continually updated and revised; a listing of the current specification numbers, as of July 1971, is given in Table III. A typical current T-111 specification, "Seamless Tubing and Pipe: T-111 (Ta-8W-2Hf) Alloy," is reproduced in Appendix C.

It can be concluded that the existence of fairly stringent specifications contributed significantly to the successful procurement of generally high-quality mill products.

B. VENDOR SELECTION

Notification was received on August 6, 1965, from the NASA Program Manager that the T-111 alloy had been selected as the containment alloy for this program. Mo-TZC alloy and Cb-132M were selected for nozzles and blade specimens of the turbine simulator for the T-111 alloy loop. Subsequently, the procurement of the refractory alloy mill products for the program was initiated by personal visits by General Electric personnel to vendors representative of the industry, and considered capable of supplying the program's material needs. The purpose of these visits was: (1) to review vendor facilities and previous experience in producing the desired mill products of the alloys of interest, i.e., primarily T-111 alloy; (2) to present the program's technical requirements and material delivery schedules; and (3) to review the NASA-Lewis quality assurance program provisions for research, test, and development programs (QA-2a).

After the final revisions were made to the specifications, inquiries were sent to the material producers for final price and delivery quotations. The quotations were carefully reviewed, and composite tabulations were prepared for purposes of comparison, with emphasis of the final vendor selection being placed on adherence to the specification, price, delivery, and previous experience with that vendor on past programs. In general, adherence to the requirements of the specification was satisfactory. The greatest and most repeated areas of concern on the part of the vendors arose from the number of tests required, the stress-rupture requirements, and the defect level and techniques specified in the ultrasonic inspection section of the specifications. Mutual agreements on minor modifications to the specifications were reached in all cases. Several vendors who could not fulfill the ultrasonic inspection requirements of the specifications were persuaded to enlist the services of outside testing sources specializing in that type of inspection. In the case of T-111 alloy, a minimum of two major producers quoted to the specifications with no exceptions. No quotations were received without exceptions to the specifications for the turbine alloys, Cb-132M and Mo-TZC.

A summary of the responses received from the material producers for the containment alloy, T-111, and the turbine alloys, Mo-TZC and Cb-132M, is given in tabular form in the previously referenced report.[5] Purchase orders were placed with the following producers:

	Alloy	Producer	Exceptions to Specifications
1.	T-111	Fansteel Metallurgical Corp.	No exceptions.
2.	T-111	Wah Chang Albany Corp.	No exceptions.
3.	Cb-132M	Universal Cyclops Steel Corporation	Hydrogen to be 10 ppm maximum instead of 5 ppm maximum.
4.	Mo-TZC	Climax Molybdenum Company of Michigan	No guarantee of mechanical properties.
5.	Mo-TZC	GE-Lamp Metals and Components Department	Single-vacuum arc melt, no guarantee of properties, C range 0.10-0.15%, Ti range 1.15-1.55%, Zr range 0.13-0.23%.

Table IV summarizes all the refractory alloy mill products purchased for the T-111 Corrosion Loop.

C. PROCESSING OF REFRACTORY ALLOY MILL PRODUCTS

1. T-111 Alloy. All mill products of T-111 alloy were produced from electron-beam-purified and vacuum-arc-cast ingots. Purification and alloying of the tungsten to form the Ta-8W matrix were accomplished by a minimum of two electron beam melts with the final melt forming a 4- to 5-inch (10- to 12.5-cm)-diameter electrode for consolidation of the T-111 alloy by the consumable-electrode vacuum-arc-melting process. Hafnium in the form of reactor-grade strip, crystal bar, or electron-beam-melted strip, was added to the electrode surface by GTA or EB welding. Final consolidation was accomplished by a single vacuum-arc-cast melt in the case of six ingots ranging in size from 7 1/2 to 9 1/2 inches (19 to 24 cm) in diameter (Fansteel) and by a double vacuum-arc-cast melt for three ingots of 6 1/2 to 7 inches (16.5 to 17.8 cm) in diameter (Wah Chang).

The ingots produced by Fansteel Metallurgical Corporation were converted by extrusion at temperatures of 2200°-2300°F (1204°-1260°C) using reduction ratios of 2.71/1 to 3.25/1. Subsequent reduction was successfully accomplished by rod rolling at about 800°-1700°F (427°-927°C). Other attempts to reduce the extrusion by hammer or press forging were unsuccessful probably because of

TABLE IV

REFRACTORY ALLOY REQUIREMENTS FOR T-111 RANKINE SYSTEM CORROSION TEST LOOP

	Weight	
	lbs	kg
A. Containment Test Alloy (T-111)		
1. Rod		
0.250 inch diameter	1	2.2
0.500 inch diameter	11	24.2
0.625 inch diameter	5	11.0
1.000 inch diameter	40	88.0
1.125 inch diameter	10	22.0
1.500 inch diameter	13	28.6
2.000 inch diameter	85	187.0
2.500 inch diameter	93	204.2
3.125 inch diameter	74	162.8
	332	730.0
2. Bar		
1.0 inch x 1.0 inch	30	66.0
1.0 inch x 2.0 inch	115	253.0
	145	319.0
3. Wire		
0.062 inch diameter	13	28.6
0.094 inch diameter	8	17.6
0.125 inch diameter	31	68.2
	52	114.4
4. Sheet/Foil/Plate		
0.005 inch x 3.5 inch	2	4.4
0.009 inch x 3.5 inch	1	2.2
0.035 inch x 1.0 inch	1	2.2
0.040 inch x 12.0 inch	29	63.8
0.125 inch x 6.0 inch	5	11.0
0.500 inch x 6.125 inch	41	90.2
	79	173.8
5. Tube/Pipe		
2.25 inch OD x 0.375 inch wall	40	88.0
2.50 inch OD x 0.450 inch wall	46	102.0
3.00 inch OD x 0.375 inch wall	50	110.0
3.25 inch OD x 0.250 inch wall	40	88.0
3.25 inch OD x 0.500 inch wall	73	161.0
1.00 inch OD x 0.100 inch wall	104	229.0
0.375 inch OD x 0.065 inch wall	66	145.2
0.375 inch OD x 0.008 inch wall	3	6.6
	422	929.8
Total T-111 Alloy	1030	2266.0

TABLE IV (Cont.)

B. Turbine Alloy (Mo-TZC)

1. Rod

2.0 inch diameter
1.0 inch diameter

2. Bar

1.375 inch x 2.0 inch
0.750 inch x 0.750 inch

C. Turbine Alloy (Cb-132M)

1. Rod

2.0 inch diameter
1.0 inch diameter

D. Mo-TZM Alloy

1. Rod

0.125 inch diameter
0.500 inch diameter
0.875 inch diameter
2.000 inch diameter
2.125 inch diameter

E. Cb-1Zr Alloy

1. Rod

0.250 inch diameter
0.5 inch diameter
0.625 inch diameter x 12 inch
1.25 inch diameter x 24 inch

2. Wire

0.062 inch diameter x 2 lbs
0.094 inch diameter x 3 lbs

3. Foil/Sheet

0.002 inch x 0.5 inch
0.002 inch x 3.5 inch
0.005 inch x 8.0 inch
0.0175 inch x 12 inch
0.030 inch x 24 inch
0.125 inch x 4 inch
0.250 inch x 6 inch

4. Tube

0.250 inch OD x 0.062 inch wall
0.5 inch OD x 0.040 inch wall
2.75 inch OD x 0.125 inch wall

F. Tantalum

1. Rod

0.250 inch diameter
0.625 inch diameter
1.250 inch diameter

2. Bar

0.250 inch x 4.0 inch
0.5 inch x 0.5 inch
0.500 inch x 1.00 inch
1.00 inch x 1.00 inch

3. Wire

0.020 inch diameter

4. Foil/Sheet

0.002 inch x 0.5 inch
0.032 inch x 0.75 inch
0.062 inch x 2.125 inch

G. T-222 Alloy

1. Sheet

0.009 inch x 3.5 inch

ORIGINAL PAGE IS
OF POOR QUALITY

the small reduction in the prior extrusion process. Conversion of the arc-cast ingots melted by Wah Chang was accomplished by forging at temperatures of about 2400°F (1316°C). Seamless tubing was produced by reextrusion of rolled billets at 1600°-1700°F (871°-927°C) to form tube hollows which subsequently were reduced by conventional tube reducing and drawing operations.* Details of the processing history of the T-111 alloy mill products are reported in Appendix D.

In processing T-111 alloy for the program requirements, the metal producers encountered cracking during extrusion, forging, rolling, and tube reduction. It is a policy and contractural requirement at GE-NSP to maintain traceability back to the ingot for all T-111 alloy components. This capability enabled GE-NSP to review the quality and processing history of the as-received material used for each item that cracked, to determine if a common material property and/or processing history might be responsible for the observed cracking. The properties and processing histories of the cracked material were also compared with T-111 alloy mill products that had no history of cracks. No property variation was found that was clearly associated with T-111 alloy that eventually cracked. Evaluating the contribution of processing history to cracking proved to be difficult. Some of the processing information was incomplete because the vendor supplying the T-111 alloy considered the information proprietary. Within the limits of available information, fair comparison of processing procedures was further complicated by the following processing differences among the vendors; number of heats melted, melting practice, size of ingots, primary conversion techniques, and secondary fabrication techniques.

During fabrication at GE-NSP, some type of cracking was observed on T-111 supplied by each vendor. No conclusive evidence could be found that showed that one processing approach was clearly superior to another. However,

---

* All T-111 alloy mill products used to fabricate the Corrosion Loop were given a final anneal of 1 hour at 3000°F (1649°C) at pressures of 10^{-5} torr (10^{-3} N/m^2) or lower.

based on overall experience with T-111 alloy vendors, some general suggestions for improving the compositional control and the chances of successful ingot coversion are: (1) Hf additions should be made by the vacuum-arc-melting process (two melts are preferred with the ingot being inverted between melts to improve Hf homogenization); (2) Hf content should be on the low side (< 2.0 percent) of the specification; (3) initial conversion temperatures around 2000°F (1093°C) should be avoided because of possible low ductility; (4) reduction limits should be observed in extrusion (> 3:1) and primary forging to avoid cracking; (5) proper cutting and grinding procedures should be used to avoid crack initiation and subsequent propagation; and (6) contact between T-111 alloy and copper or copper alloys should be avoided whenever possible.

2. Mo-TZC Alloy. The Mo-TZC alloy rod required for the fabrication of the turbine simulator components was produced from consumable-electrode, single-melt vacuum-arc-melted ingots. Because of the development nature of the alloy, two vendors were selected in order to avoid a program delay in the event of processing difficulties. Climax Molybdenum Company melted one 9-inch (22.9-cm)-diameter ingot by their continuous press-sinter-melt (PSM) process producing three 7-inch (17.8-cm)-diameter billets for extrusion. GE-LMCD melted four 6-inch (15.2-cm)-diameter ingots which produced 5-inch (12.7-cm)-diameter extrusion billets. Primary conversion of the billets was accomplished by extrusion at temperatures of 3100°-3200°F (1704°-1760°C) and at reduction ratios of 3.25/1 to 3.8/1. Extrusions produced by Climax Molybdenum were vacuum annealed for 1 hour at 3000°F (1649°C), and subsequent reductions were made by rod rolling at temperatures of 2400°F (1316°C). Sheet bar extrusions produced by GE-LMCD were cross rolled at temperatures starting at 2910°F (1600°C) and finish rolled at 2390°F (1300°C).

Initial processing problems in extrusion were encountered by both vendors resulting in incomplete extrusions and loss of two billets by Climax. However, minor adjustments in the process variables, primarily die design, lubrication and reduction ratio, were made, and good extrusions were obtained.

Complete details of the process history of material from both vendors, including selection of the final annealing temperature, were reported in Appendix E.

3. Cb-132M Alloy. The Cb-132M alloy rod used for the fabrication of turbine simulator components was produced from a triple-melted, consumable-electrode, vacuum-arc-cast ingot. The electrode was formed by double electron beam melting a Cb-20Ta-15W-5Mo alloy ingot to which zirconium was added to the surface by welding. The approximately 6 1/2-inch (16.5-cm)-diameter, arc-cast ingot was cleaned up at 5 3/8-inch (13.6-cm) diameter and extruded to rod at a temperature of 3120°F (1716°C) and a reduction ratio of 2.56/1. Material for the 2-inch (5-cm)-diameter finished rod was re-extruded to final size using a reduction ratio of 2.4/1 at 2400°F (1316°C); the material scheduled for the 1-inch (2.5-cm)-diameter finished rod was recrystallized at 3100°F (1704°C)/1 hour and reextruded at 2900°F (1593°C) to 2.25-inch (5.7-cm)-diameter (2.4/1 reduction ratio), stress relieved at 2300°F (1260°C), and reextruded for a third time at 2400°F (1316°C) through a 1.75-inch (4.4-cm)-diameter die using a reduction ratio of 3.0/1.

The processing temperatures, reductions, and intermediate recrystallization/solutioning anneals were designed to achieve a combination of good elevated temperature creep strength with low-temperature ductility through proper control of the microstructure, i.e., grain size of the matrix along with the desired dispersion and morphology of the second-phase monocarbide (Cb,Zr)C. Details of the processing history of the Cb-132M alloy rod, including selection of the final annealing temperatures, are reported in Appendix F.

D. QUALITY ASSURANCE FOR REFRACTORY METAL MILL PRODUCTS

The quality assurance program was established and approved by the NASA Program Manager, to provide adequate identification and documentation of the quality of the refractory metals and alloys used in the construction of the T-111 Corrosion Loop. In addition, the information acquired in the quality assurance program would help to fulfill the material documentation required for the test history of the loop components. The majority of the

quality assurance measures were performed and certified to be within specification by the materials producers; check tests performed by the General Electric Company generally were limited to chemical analyses of the interstitial elements, metallographic examination, hardness measurements, and visual inspection of the incoming products.

Upon receipt of material from the materials producers, a Material Control Number (MCN) was assigned to each homogeneous lot of material. A homogeneous lot includes all material of the same size, shape, condition, and finish from one heat of material and which has received the same processing, has been annealed in the same vacuum-annealing charge, and has been processed in the same manner in all operations in which the processing temperatures exceeded 500°F (260°C).

A listing of the refractory metal and alloy mill products procured for the program, the specifications to which they were procured, and the results of the quality assurance tests are presented in Tables V through VIII. A summary of the quality assurance test results with respect to meeting the requirements of the specification is shown in Table IX.

The failure of numerous pieces of T-111 alloy to meet the stress-rupture life requirements is attributed to the 2687°F (1475°C)/1-hour heat treatment given this material. Samples of these pieces which were annealed a second time for one hour at 3000°F (1649°C) and all specimens from T-111 alloy material which was originally heat treated for one hour at 3000°F (1649°C) passed the stress-rupture life requirements. All of the T-111 alloy that was used in the T-111 Corrosion Loop was given a final anneal of one hour at 3000°F (1649°C).

All of the various ultrasonic defects found in the refractory metal products were removed prior to use with only three exceptions. The ultrasonic defects reported in the 1-inch x 2-inch x 32-inch-long (2.5-cm x 5.1-cm x 81.3-cm-long) T-111 alloy bar (MCN 02A-047), which was utilized in the construction of the loop condenser, were surface defects which were removed in

ORIGINAL PAGE IS
OF POOR QUALITY

TABLE V. RESULTS OF QUALITY ASSURANCE TEST PROGRAM

Alloy	MCN Number	Mill Product Form	Mill Product Size	Vendor	Heat Number	Specifications Number	Specifications Major Exceptions	Meets All Specification Requirements	Remarks
T-111	02B-011	Foil	0.005" x 3.5" x 52"	Fansteel	111-D-1632	01-0043-00-A	None	Yes	
	02A-042	Foil	0.005" x 3.5" x 52"	Fansteel	111-D-1670	01-0043-00-A	None	Yes	
	02A-064	Foil	0.005" x 3.5" x 52"	Wah Chang	65076	01-0043-00-A	None	Yes	
	02B-012	Foil	0.009" x 3.5" x 12"	Fansteel	111-D-1632	01-0043-00-A	None	No	High oxygen (238 ppm).
	02A-043	Foil	0.009" x 3.5" x 12"	Fansteel	111-D-1670	01-0043-00-A	None	Yes	
	02A-063-(1-2)	Foil	0.009" x 3.5" x 12"	Wah Chang	65076	01-0043-00-A	None	No	Surface imperfections.
	02A-065-(1-3)	Sheet	0.035" x 1" x 14"	Wah Chang	65076	01-0040-00-B	None	Yes	
	02B-010-(1-2)	Sheet	0.040" x 12" x 50"	Fansteel	111-D-1632	01-0040-00-B	None	No	Stress-rupture life below minimum.(1)
	02A-057	Sheet	0.125" x 6" x 10"	Wah Chang	65076	01-0040-00-B	None	No	High carbon (80 ppm).
	02B-009	Plate	0.500" x 6.125" x 11"	Fansteel	111-D-1632	01-0040-00-B	None	No	Stress-rupture life below minimum.(1)
	02A-056	Plate	0.500" x 6.125" x 11"	Wah Chang	65076	01-0040-00-B	None	Yes	
	02A-066-(1-3)	Tube	0.375" OD x 0.065"wall x 144"	Fansteel	111-D-1670	01-0035-00-B	None	Yes	Failed visual, ultrasonic & penetrant inspection; all defects removed.
	02A-067-(1-18)	Tube	0.375" OD x 0.065" wall x 72"	Fansteel	111-D-1670	01-0035-00-B	None	Yes	
	02A-068-(1-2)	Tube	1.0" OD x 0.100" wall x 140"	Fansteel	111-D-1670	01-0035-00-B	None	Yes	
	02A-074	Tube	1.0" OD x 0.100" wall x 112"	Fansteel	111-D-1670	01-0035-00-B	None	Yes	
	02A-075-(1-2)	Tube	1.0" OD x 0.100" wall x 9'	Fansteel	111-D-1670	01-0035-00-B	None	Yes	
	02A-079-(1-2)	Tube	2.250" OD x 0.375" wall x 15"	Fansteel	111-D-1765	01-0035-00-B	None	Yes	
	02A-085	Tube	2.50"OD x 1.610" ID x 13"	Fansteel	111-D-1829	01-0035-01-D	None	Yes	
	02A-080	Tube	2.50" OD x 1.610" ID x 13"	Fansteel	111-D-1765	01-0035-00-B	None	Yes	
	02A-046-(1-2)	Tube	3.0" OD x 0.375" wall x 13"	Fansteel	111-D-1102	01-0035-00-B	None	Yes	
	02A-048	Tube	3.25" OD x 0.250" wall x 14"	Fansteel	111-D-1102	01-0035-00-B	None	Yes	
	02A-045	Tube	3.25" OD x 0.500" wall x 14"	Fansteel	111-D-1102	01-0035-00-B	None	Yes	
	02A-086	Tube	3.25" OD x 0.25" wall x 14"	Fansteel	111-D-1829	01-0035-01-D	None	Yes	
	02A-087	Tube	3.25" OD x 0.50" wall x 14"	Fansteel	111-D-1829	01-0035-01-D	None	Yes	

C1238-5

TABLE V. (Cont.)

Alloy	MCN Number	Mill Product Form	Mill Product Size	Vendor	Heat Number	Specifications Number	Specifications Major Exceptions	Meets All Specification Requirements	Remarks
T-111	02B-001	Wire	0.062" diameter x 6 lbs	Fansteel	111-D-1633	01-0048-00-A	None	Yes	
	02A-039-(1-2)	Wire	0.062" diameter x 6.47 lbs	Wah Chang	70616	01-0048-00-A	None	Yes	
	02B-002	Wire	0.094" diameter x 8 lbs	Fansteel	111-D-1633	01-0048-00-A	None	Yes	
	02B-003	Wire	0.125" diameter x 168'	Fansteel	111-D-1633	01-0048-00-A	None	Yes	
	02A-059	Wire	0.125" diameter x 40'	Wah Chang	70616	01-0048-00-A	None	Yes	
	02A-060	Wire	0.125" diameter x 7.9 lbs	Wah Chang	65076	01-0048-00-A	None	Yes	
	02A-073	Wire	0.125" diameter x 4.4 lbs	Wah Chang	65077	01-0048-00-A	None	Yes	
	02B-004	Rod	0.250" diameter x 24"	Fansteel	111-D-1633	01-0015-00-B	None	No	Stress-rupture life below min.(2)
	02A-054	Rod	0.250" diameter x 24"	Wah Chang	65076	01-0015-00-B	None	Yes	Failed penetrant inspection; defects removed.
	02B-005	Rod	0.500" diameter x 48"	Fansteel	111-D-1633	01-0015-00-B	None	No	Stress-rupture life below min.(2)
	02A-052	Rod	0.500" diameter x 48"	Wah Chang	65076	01-0015-00-B	None	Yes	
	02B-006	Rod	0.625" diameter x 14"	Fansteel	111-D-1633	01-0015-00-B	None	No	Stress-rupture life below min.(2)
	02A-053	Rod	0.625" diameter x 14"	Wah Chang	65076	01-0015-00-B	None	Yes	
	02B-007-(1-2)	Rod	1.0" diameter x 42"	Fansteel	111-D-1633	01-0015-00-B	None	No	Stress-rupture life below min.(2)
	02A-062	Rod	1.0" diameter x 42"	Wah Chang	65076	01-0015-00-B	None	Yes	
	02B-008	Rod	1.125 "diameter x 8"	Fansteel	111-D-1633	01-0015-00-B	None	No	Stress-rupture life below min.(2)
	02A-061	Rod	1.125" diameter x 8"	Wah Chang	65076	01-0015-00-B	None	Yes	
	02B-014	Rod	1.50"diameter x 6"	Fansteel	111-D-1633	01-0015-00-B	None	No	Failed grain size requirement.
	02A-058	Rod	1.50" diameter x 6"	Wah Chang	65076	01-0015-00-B	None	Yes	
	02A-044-(1-3)	Rod	2.0" diameter x 21"	Fansteel	111-D-1102	01-0015-00-B	None	Yes	
	02A-082	Rod	2.0" diameter x 24"	Fansteel	111-D-1829	01-0015-00-B	None	Yes	
	02A-038	Rod	2.5" diameter x 21 1/16"	Fansteel	111-D-1670	01-0015-00-B	None	Yes	
	02A-077	Rod	2.5" diameter x 5.188"	Fansteel	111-D-1765	01-0015-00-B	None	Yes	
	02A-083	Rod	2.5" diameter x 5"	Fansteel	111-D-1829	01-0015-00-B	None	Yes	
	02A-076	Rod	3.125" diameter x 16"	Fansteel	111-D-1765	01-0015-00-B	None	Yes	Failed ultrasonic inspection; defect removed.

ORIGINAL PAGE IS OF POOR QUALITY

TABLE V. (Cont.)

Alloy	MCN Number	Mill Product Form	Mill Product Size	Vendor	Heat Number	Specifications Number	Specifications Major Exceptions	Meets All Specification Requirements	Remarks
T-111	02B-013-(1-3)	Bar	1" x 1" x 12.5"	Fansteel	111-D-1633	01-0015-00-B	None	No	Failed grain size requirement.
	02A-051	Bar	1" x 1" x 12.5"	Wah Chang	65076	01-0015-00-B	None	Yes	
	02A-047	Bar	1" x 2" x 32"	Fansteel	111-D-1102	01-0015-00-B	None	No	Failed ultrasonic inspection.
	02A-078	Bar	1" x 2" x 63"	Fansteel	111-D-1765	01-0015-00-B	None	Yes	
Mo-TZC	02A-037-(1-3)	Rod	1.0" diameter x 14.75"	Climax	4331	01-0011-01-C	Tensile & stress rupture tests for information only - no radiographic inspection.	Yes	
	02A-036-(1-3)	Rod	2.0" diameter x 16.187"	Climax	4331	01-0011-01-C		Yes	
	02A-035-(1-5)	Bar	0.750" x 0.750" x 7"	GE-LMCD	M96	01-0011-01-C	Tensile & stress rupture tests for information only - no radiographic inspection. Start-ingots Ti 1.15-1.55%, Zr 0.13-0.23%, C 0.10-0.15%, W 0.15% max.	No	High tungsten (118 ppm)
	02A-032-(1-6)	Bar	1.375" x 2" x 5"	GE-LMCD	M97	01-0011-01-C		Yes	
	02A-033	Bar	1.375" x 2" x 5"	GE-LMCD	M92	01-0011-01-C		Yes	
Mo-TZM	02A-004	Rod	0.125" diameter x 36"	Climax	5960	CMX-WB-TZM-2	None	Yes	
	02A-005	Rod	0.500" diameter x 36"	Climax	7468	CMX-WB-TZM-2	None	Yes	
	02A-072	Rod	0.500" diameter x 18"	Climax	7498	CMX-WB-TZM-2	None	Yes	
	02A-006	Rod	0.875" diameter x 16"	Climax	7473	CMX-WB-TZM-2	None	Yes	
	02A-071	Rod	0.875" diameter x 24"	Climax	7876	CMX-WB-TZM-2	None	Yes	
	02A-081	Rod	0.875" diameter x 12'	Climax	7876	CMX-WB-TZM-2	None	Yes	
	02A-007	Rod	2.0" diameter x 24"	Climax	7555	CMX-WB-TZM-2	None	Yes	
	02A-070	Rod	2.125" diameter x 12"	Climax	7893	CMX-WB-TZM-2	None	Yes	
Cb-132M	02A-055-(1-3)	Rod	1.0" diameter x 22"	Universal Cyclops	66-95119	01-0010-01-A	None	Yes	
	02A-041-(1-2)	Rod	2.0" diameter x 24"	Universal Cyclops	66-95119	01-0010-01-A	None	No	Elongation & ultimate tensile strength below minimum.
Cb-1Zr	02A-001	Foil	0.002" x 0.5" x 30 lbs	Kawecki	5818	01-0003-03-B	None	Yes	
	02A-002	Foil	0.002" x 3.5" x 10 lbs	Kawecki	5818	01-0003-03-B	None	Yes	

TABLE V. (Cont.)

Alloy	Number	Mill Product Form	Mill Product Size	Vendor	Heat Number	Specifications Number	Specifications Major Exceptions	Meets All Specification Requirements	Remarks
Cb-1Zr	02A-003	Foil	0.005" x 8.0" x 15 lbs	Kawecki	5818	01-0003-03-B	None	Yes	
	02A-022-(1-6)	Sheet	0.0175" x 12" x 24"	Wah Chang	912-70112	01-0003-04-B	Calibration notch of 0.001" deep	Yes	
	02A-034-(1-2)	Sheet	0.030" x 24" x 32"	Wah Chang	912-70112	01-0003-04-B	None	Yes	
	02A-023	Sheet	0.125" x 4" x 12"	Wah Chang	912-70112	01-0003-04-B	None	Yes	
	02A-019	Sheet	0.250" x 6" x 36"	Wah Chang	912-70112	01-0003-04-B	None	Yes	
	02A-050	Tube	0.250" OD x 0.062" wall x 60"	Wah Chang	70303	01-0004-01-D	None	No	Failed ultrasonic inspection.
	02A-040-(1-2)	Tube	0.5" OD x 0.040" wall x 3'-5'	Kawecki	5886	01-0004-01-C	None	No	Failed ultrasonic inspection.
	02A-029	Tube	2.75" OD x 0.125" wall x 48"	Kawecki	5886	01-0004-03-B	None	No	Failed ultrasonic inspection; High Fe (90 ppm).
	02A-030	Wire	0.062" diameter x 2 lbs	Kawecki	5868	01-0003-03-B	None	No	High Ta(1340 ppm), High Fe(60 ppm)
	02A-031	Wire	0.094" diameter x 3 lbs	Kawecki	5868	01-0003-03-B	None	No	High Ta(1340 ppm), High Fe(60 ppm)
	02A-069	Rod	0.250" diameter x 60"	Kawecki	6075	01-0052-01-D	None	Yes	
	02A-020-(1-2)	Rod	0.5" diameter x 120"	Wah Chang	911-53002	01-0003-04-B	None	Yes	
	02A-024	Rod	0.5" diameter x 120"	Wah Chang	911-70559	01-0003-04-B	None	Yes	
	02A-026	Rod	0.625" diameter x 12"	Wah Chang	911-70559	01-0003-04-B	None	Yes	
	02A-025	Rod	1.25" diameter x 24"	Wah Chang	912-900	01-0003-04-B	None	Yes	
	02A-049-(1-8)	Foil	0.002" x 0.5" x 4 lbs	Fansteel	CG-117	B364-62T	H - 10 ppm Max.	Yes	
	02A-012	Sheet	0.032" x 0.75" x 12"	Un.Carbide	81274	B364-61T	H - 15 ppm Max.	Yes	
	02A-011	Sheet	0.062" x 2.125" x 36"	Un.Carbide	81310	B364-61T	H - 15 ppm Max.	Yes	
	02A-013-(1-2)	Bar	0.250" x 4.0" x 72"	Un.Carbide	81371	B364-61T	H - 15 ppm Max.	Yes	
	02A-021	Bar	0.5" x 0.5" x 3'	Un.Carbide	81303	B365-62T	H - 10 ppm max.	Yes	
	02A-016	Bar	0.500" x 1.00" x 28"	Un.Carbide	81259	B364-61T	H - 15 ppm Max.	Yes	
	02A-015	Bar	1.00" x 1.00" x 15"	Un.Carbide	81259	B364-61T	H - 15 ppm Max.	Yes	
	02A-008	Wire	0.020" diameter x 600'	Un.Carbide	81259	B365-61T	H - 15 ppm Max.	Yes	

ORIGINAL PAGE IS OF POOR QUALITY

TABLE V. (Cont.)

Alloy	Number	Mill Product Form	Mill Product Size	Vendor	Heat Number	Specifications Number	Specifications Major Exceptions	Meets All Specification Requirements	Remarks
Ta	02A-009	Rod	0.250" diameter x 24"	Un.Carbide	81303	B365-61T	H - 15 ppm Max.	Yes	
	02A-010	Rod	0.625" diameter x 12"	Un.Carbide	81341	B365-61T	H - 15 ppm Max	Yes	
	02A-014	Rod	1.250" diameter x 8"	Un.Carbide	81259	B365-61T	None	Yes	
T-222	02A-027	Sheet	0.009" x 3.5" x 6.5"	Westinghouse	Ta-39-3	Best Effort			

(1) Material not used in loop fabrication.

(2) After an additional 3000°F/1-hour anneal material passed stress rupture requirements.

ORIGINAL PAGE IS
OF POOR QUALITY

TABLE VI. CHEMICAL ANALYSIS OF REFRACTORY ALLOY MILL PRODUCTS

Alloy	MCN Number	Mill Product Form	Size	Heat Number	Sample Source	Analyzed By	Chemical Analyses, ppm C	O	N	H	Other (%) W	Hf
T-111	SPECIFICATION 01-0043-00-A						Max 75	Max 300	Max 100	Max 10	Max 9.0	Max 2.4
	02B-011	Foil	0.005" x 3.5" x 52"	111-D-1632	Ingot	Vendor	10[2]	25[2]	20[2]	5[2]	7.79[1]	2.38[1]
					Extruded Bar	Vendor	11[2]	15[2]	21[2]	4[2]	7.73[2]	2.21[2]
					Final Product	Vendor	12	41	20	5.2	---	---
	02A-042	Foil	0.005" x 3.5 "x 52"	111-D-1670	Ingot	Vendor	10[2]	72[2]	20[2]	5[2]	7.70[3]	2.17[3]
					Extruded Bar	Vendor	29[2]	30[2]	16[2]	7[2]	7.64[2]	2.37[2]
					Final Product	Vendor	40[1]	62	21	1	---	---
					Final Product	GE	55[1]	114[1]	7[3]	1[1]	---	---
	02A-064	Foil	0.005" x 3.5" x 52"	65076	Ingot	Vendor	<40[3]	50[1]	14[3]	2.8[1]	8.60[3]	1.93[3]
					Final Product	Vendor	<40[1]	110[1]	9[1]	2.6[1]	---	---
					Final Product	GE	60[1]	150[1]	10[1]	1.5[1]	---	---
	02B-012	Foil	0.009" x 3.5" x 12"	111-D-1632	Ingot	Vendor	10[2]	25[2]	20[2]	5[2]	7.79[1]	2.38[1]
					Extruded Bar	Vendor	11[2]	15[2]	21[2]	4[2]	7.73[2]	2.21[2]
					Final Product	Vendor	---	---	---	---	---	---
					Final Product	GE	45[1]	238	12	3	---	---
	02A-043	Foil	0.009" x 3.5" x 12"	111-D-1670	Ingot	Vendor	10[2]	72[2]	20[2]	5[2]	---	---
					Extruded Bar	Vendor	29[2]	30[2]	16[2]	7[2]	---	---
					Final Product	Vendor	40[1]	61	15	1	---	---
					Final Product	GE	35[1]	141[1]	7[1]	2[1]	---	---
	02A-063-(1-2)	Foil	0.009" x 3.5" x 12"	65076	Ingot	Vendor	<40[3]	50[1]	14[1]	2.8[1]	8.60[3]	1.93[3]
					Final Product	Vendor	40[1]	<50[1]	32[1]	2.7[1]	---	---
					Final Product	GE	52[1]	249[1]	8[1]	1[1]	---	---
	SPECIFICATION 01-0040-00-B						Max 50	Max 150	Max 75	Max 10	Max 9.0	Max 2.4
	02A-065-(1-3)	Sheet	0.035" x 1" x 14"	65076	Ingot	Vendor	<40[3]	50[1]	14[3]	2.8[1]	8.60[3]	1.93[3]
					Final Product	Vendor	<40[1]	100	20	2.6	---	---
					Final Product	GE	41[1]	79	4	1	---	---
	02B-010-(1-2)	Sheet	0.040" x 12" x 50"	111-D-1632	Ingot	Vendor	10[2]	25[2]	20[2]	5[2]	7.79[1]	2.38[1]
					Extruded Bar	Vendor	11[2]	15[2]	21[2]	4[2]	7.73[2]	2.21[2]
					Final Product	Vendor	14[1]	34	17	5	---	---
					Final Product	GE	10[1]	89[1]	9[3]	1[1]	---	---
	02A-057	Sheet	0.125" x 6" x 10"	65076	Ingot	Vendor	<40[3]	50[1]	14[3]	2.8[1]	8.60[3]	1.93[3]
					Final Product	Vendor	80	60	12	2.6	---	---
	02B-009	Plate	0.500" x 6.125" x 11"	111-D-1632	Ingot	Vendor	10[2]	25[2]	20[2]	5[2]	7.79[1]	2.38[1]
					Extruded Bar	Vendor	11[2]	15[2]	21[2]	4[2]	7.73	2.21
					Final Product	Vendor	10[3]	10[1]	20[3]	9.3[1]	---	---
	02A-056	Plate	0.500" x 6.125" x 11"	65076	Ingot	Vendor	<40[3]	50[1]	14[3]	2.8[1]	8.60[3]	1.93[3]
					Final Product	Vendor	<40[1]	<50[1]	20[1]	2.2[1]	---	---
					Final Product	GE	24[1]	9[1]	3[1]	8[1]	---	---
	SPECIFICATION 01-0035-00-B						Max 50	Max 150	Max 75	Max 10	Max 9.0	Max 2.4
	02A-066-(1-3)	Tube	0.375" OD x 0.065" wall x 144"	111-D-1670	Ingot	Vendor	10[2]	72[2]	20[2]	5[2]	7.70[3]	2.17[3]
					Extruded Bar	Vendor	29[2]	20[2]	16[2]	7[2]	7.65[2]	2.37[2]
					Final Product	Vendor	43	43	16	2	---	---
	02A-067-(1-18)	Tube	0.375" OD x 0.065" wall x 72"	111-D-1670	Ingot	Vendor	10[2]	72[2]	20[2]	5[2]	7.70[3]	2.17[3]
					Extruded Bar	Vendor	29[2]	20[2]	16[2]	7[2]	7.65[2]	2.37[2]
					Final Product	Vendor	43	43	16	2	---	---
					Final Product	GE	25[2]	46[2]	5[2]	3[2]	---	---

C1238-6

TABLE VI. (Cont.)

Alloy	MCN Number	Mill Product Form	Mill Product Size	Heat Number	Sample Source	Analyzed By	Chemical Analyses, ppm C	O	N	H	Other (%) W	Hf
							Max 50	Max 150	Max 75	Max 10	Max 9.0	2.4
T-111	02A-068-(1-2)	Tube	1.0" OD x 0.100" wall x 140"	111-D-1670	Ingot	Vendor	10[2]	72[2]	20[2]	5[2]	7.70[2]	2.17[2]
					Extruded Bar	Vendor	29[2]	20[2]	16[2]	7[2]	7.65[2]	2.37[2]
					Final Product	Vendor	40[2]	37[2]	22[2]	2[2]	---	---
					Final Product	GE	51[2]	50[2]	4[2]	2[2]	---	---
	02A-074	Tube	1.0" OD x 0.100" wall x 112"	111-D-1670	Ingot	Vendor	10[2]	72[2]	20[2]	5[2]	7.70[3]	2.17[3]
					Extruded Bar	Vendor	29[2]	20[2]	16[2]	7[2]	7.65[2]	2.37[2]
					Final Product	Vendor	23[1]	24[1]	45[1]	5[1]	---	---
					Final Product	GE	22[1]	26[1]	< 1[1]	6[1]	---	---
	02A-075-(1-2)	Tube	1.0" OD x 0.100" wall x 9'	111-D-1670	Ingot	Vendor	10[2]	72[2]	20[2]	5[2]	7.70[3]	2.17[3]
					Extruded Bar	Vendor	29[2]	20[2]	16[2]	7[2]	7.65[2]	2.37[2]
					Final Product	Vendor	23	24	45	5	---	---
					Final Product	GE	27[2]	26[2]	5[2]	6[2]	---	---
	02A-079-(1-2)	Tube	2.250" OD x 0.375" wall x 15"	111-D-1765	Ingot	Vendor	10[2]	44[2]	23[2]	5[2]	8.44[2]	1.93[2]
					Final Product	Vendor	22[1]	25[1]	22[1]	5[1]	---	---
					Final Product	GE	15[1]	41[1]	9[1]	5[1]	---	---
	02A-085	Tube	2.5" OD x 1.610" ID x 13"	111-D-1829	Ingot	Vendor	34	32	19	5	5.75	2.31
					Final Product	Vendor	10	20	33	5	---	---
					Final Product	GE	20[2]	15[2]	2[2]	2[2]	---	---
	02A-080	Tube	2.50" OD x 1.610" ID x 13"	111-D-1765	Ingot	Vendor	10[2]	44[2]	23[2]	5[2]	8.44[2]	1.93[2]
					Final Product	Vendor	22	25	22	5	---	---
	02A-046-(1-2)	Tube	3.0" OD x 0.375" wall x 13"	111-D-1102	Ingot	Vendor	10	53	20	5	7.97[1]	2.40[1]
					Finished Product	GE	22	58	8	6	---	---
	02A-048	Tube	3.25" OD x 0.250" wall x 14"	111-D-1102	Ingot	Vendor	10[2]	53[2]	20[2]	5[2]	7.97[2]	2.40[2]
					Extruded Bar	Vendor	20[2]	51[2]	21[2]	3[2]	7.94[2]	2.28[2]
					Final Product	Vendor	34[1]	20[1]	13[1]	3.3[1]	---	---
					Final Product	GE	20[1]	58[1]	9[1]	6[1]	---	---
	02A-045	Tube	3.25" OD x 0.500" wall x 14"	111-D-1102	Ingot	Vendor	10[2]	53[2]	20[2]	5[2]	7.97[1]	2.40[1]
					Extruded Bar	Vendor	20[2]	51[2]	21[2]	3[2]	7.94[2]	2.28[2]
					Final Product	Vendor	34[1]	20[1]	13[1]	3.3[1]	---	---
					Final Product	GE	20[1]	58[1]	9[1]	6[1]	---	---
	02A-086	Tube	3.25" OD x 0.25" wall x 14"	111-D-1829	Ingot	Vendor	34	32	19	5	5.75	2.31
					Final Product	Vendor	10	20	29	5	---	---
	02A-087	Tube	3.25" OD x 0.50" wall x 14"	111-D-1829	Ingot	Vendor	34	32	19	5	5.75	2.31
					Final Product	Vendor	10	20	29	5	---	---
					Final Product	GE	29	10	1	2	---	---
	SPECIFICATION 01-0048-00-A						Max 50	Max 150	Max 75	Max 10	Max 9.0	Max 2.4
	02B-001	Wire	0.062" diameter x 6 lbs	111-D-1633	Ingot	Vendor	10	25	10	10	7.74[1]	2.23[1]
					Extruded Bar	Vendor	17	19	16	6	7.80[2]	2.24[2]
					Finished Product	Vendor	42[1]	110	22	1	---	---
					Finished Product	GE	23[1]	126[1]	6[1]	1[1]	8.16[1]	2.53[1]
	02A-039-(1-2)	Wire	0.062" diameter x 6.47 lbs	70616	Ingot	Vendor	20[1]	<50[1]	14[1]	2.8[1]	8.0[1]	1.83[1]
					Finished Product	Vendor	60	<50	< 5	1.2	---	---

TABLE VI. (Cont.)

Alloy	MCN Number	Mill Product Form	Mill Product Size	Heat Number	Sample Source	Analyzed By	Chemical Analyses, ppm C	O	N	H	Other (%) W	Hf
							Max	Max	Max	Max	Max	Max
T-111	02B-002	Wire	0.094" diameter x 8 lbs	111-D-1633	Ingot	Vendor	50	150	75	10	9.0	2.4
					Extruded Bar	Vendor	10	25	10	10	7.74[1]	2.23[1]
					Finished Product	Vendor	17	19	16	6	7.80[2]	2.24[2]
					Finished Product	GE	43	111	20	< 1	---	---
	02B-003	Wire	0.125" diameter x 168'	111-D-1633	Ingot	Vendor	16[1]	57	3	1	8.49[1]	2.60[1]
					Extruded Bar	Vendor	10	25	10	10	7.74[2]	2.23[2]
					Finished Product	Vendor	17	19	16	6	7.80[2]	2.24[2]
					Finished Product	GE	33	69	21	< 1	---	---
	02A-059	Wire	0.125" diameter x 40'	70616	Ingot	Vendor	18[1]	68	5	1	8.41	2.73
					Finished Product	Vendor	20[1]	<50[1]	14[1]	2.8[1]	8.00[1]	1.83[1]
					Finished Product	GE	<40[1]	<50[1]	20[1]	1.3[1]	---	---
	02A-060	Wire	0.125" diameter x 7.9 lbs	65076	Ingot	Vendor	29[1]	6[1]	1[1]	1[1]	---	---
					Finished Product	Vendor	<40[3]	50[1]	14[3]	2.8[1]	8.60[3]	1.93[3]
					Finished Product	GE	60	<50	15	2.6	---	---
	02A-073	Wire	0.125" diameter x 4.4 lbs	65076	Ingot	Vendor	36[1]	46[1]	5[1]	1[1]	---	---
					Finished Product	Vendor	<40[3]	50[1]	14[3]	2.8[1]	8.60[3]	1.93[3]
	SPECIFICATION 01-0015-00-B						60	<50	15	2.6	---	---
							Max	Max	Max	Max	Max	Max
	02B-004	Rod	0.250" diameter x 24"	111-D-1633	Ingot	Vendor	50	150	75	10	9.0	2.4
					Extruded Bar	Vendor	10	25	10	10	7.74[1]	2.23[1]
					Finished Product	Vendor	17	19	16	6	7.80[2]	2.24[2]
					Finished Product	GE	13[1]	15	23	< 1	---	---
	02A-054	Rod	0.250" diameter x 24"	65076	Ingot	Vendor	25[1]	77[1]	11[3]	2[1]	---	---
					Final Product	Vendor	<40[3]	50[1]	14[3]	2.8[1]	8.60[3]	1.93[3]
					Final Product	GE	40	<50[1]	12[1]	2.7[1]	---	---
	02B-005	Rod	0.500" diameter x 48"	111-D-1633	Ingot	Vendor	NP	21[1]	3[1]	1[1]	---	---
					Extruded Bar	Vendor	10	25	10	10	7.74[1]	2.23[1]
					Finished Product	Vendor	17	19	16	6	7.80[2]	2.24[2]
	02A-052	Rod	0.500" diameter x 48"	65076	Ingot	Vendor	17[3]	30[1]	20[3]	< 1[1]	---	---
					Final Product	Vendor	<40[3]	50[1]	14[3]	2.8[1]	8.60[3]	1.93[3]
					Final Product	GE	<40[1]	130[1]	12[1]	1.8	---	---
	02B-006	Rod	0.625" diameter x 14"	111-D-1633	Ingot	Vendor	27[1]	14[1]	3[1]	< 1	---	---
					Extruded Bar	Vendor	10	25	10	10	7.74[1]	2.23[1]
					Finished Product	Vendor	17	19	16	6	7.80[2]	2.24[2]
	02A-053	Rod	0.625" diameter x 14"	65076	Ingot	Vendor	17[3]	30[1]	20[3]	< 1[1]	---	---
					Final Product	Vendor	<40[3]	50[1]	14[3]	2.8[1]	8.60[3]	1.93[3]
					Final Product	GE	<40[1]	130[1]	12[1]	1.8	---	---
	02B-007-(1-2)	Rod	1.0" diameter x 42"	111-D-1633	Ingot	Vendor	23[1]	13[1]	5[1]	< 1	---	---
					Extruded Bar	Vendor	10	25	10	10	7.74[1]	2.23[1]
					Finished Product	Vendor	17	19	16	6	7.80[2]	2.24[2]
	02A-062	Rod	1.0" diameter x 42"	65076	Ingot	Vendor	9	11	24	1	---	---
					Final Product	Vendor	<40[3]	50[1]	14[3]	2.8[1]	8.60[3]	1.93[3]
					Final Product	GE	<40[1]	<50[1]	17[1]	3.7[1]	---	---
							24[1]	17[1]	5[1]	9[1]	---	---

TABLE VI. (Cont.)

Alloy	MCN Number	Mill Product Form	Mill Product Size	Heat Number	Sample Source	Analyzed By	Chemical Analyses, ppm C	O	N	H	Other (%) W	Hf
							Max	Max	Max	Max	Max	Max
							50	150	75	10	9.0	2.4
T-111	02B-008	Rod	1.125" diameter x 8"	111-D-1633	Ingot	Vendor	10	25	10	10	7.74[1] 2	2.23[1] 2
					Extruded Bar	Vendor	17	19	16	6	7.80[2]	2.24[2]
					Finished Product	Vendor	9[3]	11[1]	24[3]	1[1]	---[3]	---[3]
	02A-061	Rod	1.125" diameter x 8"	65076	Ingot	Vendor	<40[3]	50[1]	14[3]	2.8[1]	8.60[3]	1.93[3]
					Final Product	Vendor	<40[1]	<50[1]	17[1]	3.7[1]	---	---
					Final Product	GE	26[1]	19[1]	5[1]	11[1]	---	---
	02B-014	Rod	1.5" diameter x 6"	111-D-1633	Ingot	Vendor	10	25	10	10	7.74[1] 2	2.23[1] 2
					Extruded Bar	Vendor	17	19	16	6	7.80[2]	2.24[2]
					Final Product	Vendor	25[1]	28	48	1	---	---
					Final Product	GE	15[1]	48[1]	10[3]	3[1]	---	---
	02A-058	Rod	1.50" diameter x 6"	65076	Ingot	Vendor	<40[3]	50[1]	14[3]	2.8[1]	8.60[3]	1.93[3]
					Final Product	Vendor	<40[1]	120[1]	15[1]	3.4[1]	---	---
					Final Product	GE	8[1]	14[1]	3[1]	15[1]	6.91[1]	2.06[1]
	02A-044-(1-3)	Rod	2.0" diameter x 21"	111-D-1102	Ingot	Vendor	10[2]	53[2]	20[2]	5[2]	7.97[2]	2.4[2]
					Extruded Bar	Vendor	20[2]	51[2]	21[2]	3[2]	7.94[2]	2.28[2]
					Final Product	Vendor	20[1]	73[1]	26[1]	3.7[1]	---	---
					Final Product	GE	26[2]	43[2]	7[2]	4[2]	---	---
	02A-082	Rod	2.0" diameter x 24"	111-D-1829	Ingot	Vendor	34[2]	33[2]	19[2]	5[2]	7.50[2]	2.31[2]
					Final Product	Vendor	10[1]	20[1]	33[1]	5[1]	---	---
					Final Product	GE	25[1]	17[1]	3[1]	5[1]	---	---
	02A-038	Rod	2.5" diameter x 21 1/16"	111-D-1670	Ingot	Vendor	10[2]	72[2]	20[2]	5[2]	7.70[3]	2.17[3]
					Extruded Bar	Vendor	29[2]	20[2]	16[2]	7[2]	7.05[2]	2.37[2]
					Final Product	Vendor	26[1]	30[1]	31[1]	2[1]	---	---
					Final Product	GE	23[1]	33[1]	4[1]	8[1]	---	---
	02A-077	Rod	2.5" diameter x 5.188"	111-D-1765	Ingot	Vendor	10[2]	44[2]	23[2]	6[2]	8.44[2]	1.93[2]
					Final Product	Vendor	22	25	22	5	---	---
					Final Product	GE	14[2]	23[2]	19[2]	2[2]	---[2]	---[2]
	02A-083	Rod	2.5" diameter x 5"	111-D-1829	Ingot	Vendor	34[2]	33[2]	19[2]	5[2]	7.5[2]	2.3[2]
					Final Product	Vendor	10[2]	20[2]	33[2]	5[2]	---	---
	02A-076	Rod	3.125" diameter x 16"	111-D-1765	Ingot	Vendor	10[2]	44[2]	23[2]	6[2]	8.44[2]	1.93[2]
					Final Product	Vendor	40[1]	10[1]	19[1]	5[1]	---	---
					Final Product	GE	15[1]	55[1]	21[1]	6[1]	---	---
	02B-013-(1-3)	Bar	1" x 1" x 12.5"	111-D-1633	Ingot	Vendor	10	25	10	10	7.74[1] 2	2.23[1] 2
					Extruded Bar	Vendor	17	19	16	6	7.80[2]	2.24[2]
					Final Product	Vendor	25[1]	28	48	1	---	---
					Final Product	GE	15[1]	53[1]	6[3]	3[1]	---	---
	02A-051	Bar	1" x 1" x 12.5"	65076	Ingot	Vendor	<40[3]	50[1]	14[3]	2.8[1]	8.60[3]	1.93[3]
					Final Product	Vendor	<40	120[1]	15[1]	3.4	---	---
					Final Product	GE	NP	148[1]	8[1]	< 1	---	---
	02A-047	Bar	1" x 2" x 32"	111-D-1102	Ingot	Vendor	10[2]	53[2]	20[2]	5[2]	7.97[2]	2.40[1] 2
					Extruded Bar	Vendor	20[2]	51[2]	21[2]	3[2]	7.94[2]	2.30[2]
					Final Product	Vendor	42[1]	55	18	4.7	---	---
					Final Product	GE	40[1]	58[1]	12[2]	2[2]	---[2]	---[2]
	02A-078	Bar	1" x 2" x 63"	111-D-1765	Ingot	Vendor	10[2]	44[1]	23[2]	6[2]	8.44[2]	1.65[2]
					Final Product	Vendor	40[1]	28[1]	34[1]	5[1]	---	---
					Final Product	GE	18[1]	36[1]	15[1]	6[1]	---	---

ORIGINAL PAGE IS
OF POOR QUALITY

TABLE VI. (Cont.)

Alloy	MCN Number	Mill Product Form	Mill Product Size	Heat Number	Sample Source	Analyzed By	Chemical Analyses, ppm C	O	N	H	Other (%) Ti	Other (%) Zr
Mo-TZC	SPECIFICATION 01-0011-00-C						Max 1400	Max 20	Max 10	Max 5	Max 1.3	Max 0.18
	02A-037-(1-3)	Rod	1.0" diameter x 14.75"	4331	Final Product	Vendor	1300[2]	4	< 1	< 1	1.20[2]	0.17[2]
					Final Product	GE	1350[1]	15	8	3	---	---
	02A-036-(1-3)	Rod	2.0" diameter x 16.187"	4331	Final Product	Vendor	1300[2]	4	2	< 1	1.20[2]	0.17[2]
					Final Product	GE	1220[1]	11[1]	4[1]	2[1]	---	---
	02A-035-(1-5)	Bar	0.750" x 0.750" x 7"	M96	Final Product	Vendor	1309[1]	6[1]	3[1]	2[1]	1.40[1]	0.21[1]
					Final Product	GE	1140[1]	20[1]	4[1]	3[1]	---	---
	02A-032-(1-6)	Bar	1.375" x 2" x 5"	M97	Final Product	Vendor	1163[1]	5[1]	2[1]	2[1]	1.35[1]	0.19[1]
					Final Product	GE	1140[1]	24[1]	2[1]	1[1]	---	---
	02A-033	Bar	1.375" x 2" x 5"	M92	Final Product	Vendor	1171[1]	3[1]	3[1]	2[1]	1.35[1]	0.20[1]
					Final Product	GE	700[1]	98	4	< 1	---	---
Mo-TZM	SPECIFICATION CMX-WB-TZM-2						Max 300	Max 25	Max 20	Max 5	Max 0.55	Max 0.12
	02A-004	Rod	0.125" diameter x 36"	5960	Final Product	Vendor	140[1]	<10	< 3	< 1	0.55	0.08
	02A-005	Rod	0.500" diameter x 36"	7468	Final Product	GE	108[1]	11	2	< 1	---	---
					Final Product	Vendor	220	< 4	1	< 1	0.50	0.09
	02A-072	Rod	0.500" diameter x 18"	7498	Final Product	Vendor	160	4	1	< 1	0.54	0.09
	02A-006	Rod	0.875" diameter x 16"	7473	Final Product	Vendor	160	2[1]	< 1	< 1	0.50	0.09
					Final Product	GE	104[1]	9[1]	3[1]	< 1	---	---
	02A-071	Rod	0.875" diameter x 24"	7876	Final Product	Vendor	160	< 4	1	< 1	0.49	0.105
	02A-081	Rod	0.875" diameter x 12"	7876	Final Product	Vendor	160	< 4[1]	1[1]	< 1[1]	0.49	0.105
					Final Product	GE	176[1]	5[1]	7[1]	< 1[1]	---	---
	02A-007	Rod	2.0" diameter x 24"	7555	Final Product	Vendor	210[1]	< 4[1]	< 1[1]	< 1	0.49	0.10
					Final Product	GE	184[1]	5[1]	1[1]	1	---	---
	02A-070	Rod	2.125" diameter x 12"	7893	Final Product	Vendor	180	14	2	1	0.44	0.11
Cb-132M	SPECIFICATION 01-0010-01-A						Max 1500	Max 200	Max 100	Max 10	Max Mo-5.5 Ta-21.5	Max W-16.5 Zr-2.25[2]
	02A-055-(1-3)	Rod	1.0" diameter x 22"	66-95119	Ingot	Vendor	1375[2]	55[2]	33[2]	2.3[2]	Mo-4.95[2] Ta-19.79[2]	W-14.5[2] Zr-2.0[2]
					Final Product	Vendor	1300[1]	24[1]	34[1]	4[1]	---	---
					Final Product	GE	1350[1]	14[1]	6[1]	1[1]	---	---
	02A-041-(1-2)	Rod	2.0" diameter x 24"	66-95119	Ingot	Vendor	1375[2]	55[2]	33[2]	2.3[2]	Mo-4.95[2] Ta-19.79[2]	W-14.5[2] Zr-2.0[2]
					Final Product	Vendor	1220[1]	27[1]	79	3.7[1]	---	---
					Final Product	GE	1300[1]	28[3]	18[3]	17[3]	---	---
Cb-1Zr	SPECIFICATION 01-0003-03-B						Max 100	Max 300	Max 300	Max 10	Zr 0.8-1.2	
	02A-001	Foil	0.002" x 0.5" x 30 lbs	5818	Ingot	Vendor	40	70	30	2.1	1.1	
					Final Product	Vendor	50	60	30	2.3	---	
	02A-002	Foil	0.002" x 3.5" x 10 lbs	5818	Ingot	Vendor	40	70	30	2.1	1.1	
					Final Product	Vendor	50	60	30	2.3	---	
	02A-003	Foil	0.005" x 8.0" x 15 lbs	5818	Ingot	Vendor	40	70	30	2.1	1.1	
					Final Product	Vendor	50	60	30	2.3	---	
	SPECIFICATION 01-0003-04-B						Max 100	Max 300	Max 300	Max 10	Zr 0.8-1.2	
	02A-022-(1-6)	Sheet	0.0175" x 12" x 24"	912-70112	Ingot	Vendor	42	210	63[2]	3.7[1]	1.02[2]	
					Final Product	Vendor	70	180	50	7	---	
					Final Product	GE	48[1]	110[1]	28[1]	3	---	

TABLE VI. (Cont.)

Alloy	MCN Number	Mill Product Form	Mill Product Size	Heat Number	Sample Source	Analyzed By	Chemical Analyses, ppm C	O	N	H	Other (%)
							Max	Max	Max	Max	Zr
Cb-1Zr	02A-034-(1-2)	Sheet	0.030" x 24" x 32"	912-70112	Ingot	Vendor	100 [2] 32	300 130	300 [2] 65	10 [1] 4.5	0.8-1.2 [2] 1.03
					Final Product	Vendor	<30 [1]	130 [1]	35 [1]	6	---
					Final Product	GE	25 [2]	121 [1]	60 [2]	< 1 [1]	---
	02A-023	Sheet	0.125" x 4" x 12"	912-70112	Ingot	Vendor	42	210	63	3.7 [1]	1.02 [2]
					Final Product	Vendor	30 [1]	130 [1]	52 [1]	3.1 [1]	---
					Final Product	GE	45 [2]	132 [1]	27 [1]	< 1 [1]	---
	02A-019	Sheet	0.250" x 6" x 36"	912-70112	Ingot	Vendor	42	210	63 [2]	3.7 [1]	1.02 [2]
					Final Product	Vendor	<30 [1]	<50 [1]	50 [1]	4.1	---
					Final Product	GE	30 [1]	71 [1]	22 [1]	< 1	---
	SPECIFICATION 01-0004-01-D										
							Max	Max	Max	Max	Zr
	02A-050	Tube	0.250" OD x 0.062" wall x 60"	70303	Ingot	Vendor	200 [1] 42	300 [1] 260	100 [1] 55	10 [1] 3.5	0.8-1.2 0.97
					Final Product	Vendor	<40 [1]	140	65	5.1	---
					Final Product	GE	75 [1]	211	63	3	---
	SPECIFICATION 01-0004-01-C										
							Max	Max	Max	Max	Zr
	02A-040-(1-2)	Tube	0.5" OD x 0.040" wall x 3'-5'	5886	Ingot	Vendor	200 [2] 40	300 [2] 70	100 [2] 30	10 [2] 2.1	0.8-1.2 [2] 1.1
					Final Product	Vendor	35 [1]	60	40	2.4	---
					Final Product	GE	87 [1]	84	13	4	---
	SPECIFICATION 01-0004-03-B										
							Max	Max	Max	Max	Zr
	02A-029	Tube	2.75" OD x 0.125" wall x 48"	5886	Final Product	Vendor	100 40 [1]	300 70 [1]	300 40 [1]	10 2	0.8-1.2 1.1
					Final Product	GE	43 [1]	97 [1]	6 [1]	1	---
	SPECIFICATION 01-0003-03-B										
							Max	Max	Max	Max	Zr
	02A-030	Wire	0.062" diameter x 2 lbs	5868	Ingot	Vendor	100 <100	300 60	300 50	10 5	0.8-1.2 1.08
					Final Product	Vendor	80	50	40	5	---
	02A-031	Wire	0.094" diameter x 3 lbs	5868	Ingot	Vendor	<100	60	50	5	1.08
					Final Product	Vendor	80	50	40	5	---
	SPECIFICATION 01-0052-01-C										
							Max	Max	Max	Max	Zr
	02A-069	Rod	0.250" diameter x 60"	6075	Final Product	Vendor	200 40	300 70	100 <10	10 1.8	0.8-1.2 1.1
	SPECIFICATION 01-0003-04-B										
							Max	Max	Max	Max	Zr
	02A-020-(1-2)	Rod	0.5" diameter x 120"	911-53002	Ingot	Vendor	100 [2] 54	300 [1] 125	300 [2] 42	10 [1] 3.9	0.8-1.2 [2] 0.93
					Final Product	Vendor	40 [1]	130 [1]	50 [1]	2.7	---
					Final Product	GE	20 [1]	122 [1]	27 [1]	< 1 [1]	---
	02A-024	Rod	0.5" diameter x 120"	911-70559	Ingot	Vendor	30 [1]	165 [1]	55 [1]	4.9 [1]	0.91 [1]
					Final Product	Vendor	<30 [1]	148 [1]	30 [1]	1.9	---
					Final Product	GE	32 [1]	156 [1]	35 [1]	< 1 [1]	---
	02A-026	Rod	0.625" diameter x 12"	911-70559	Ingot	Vendor	33 [3]	165 [1]	60 [3]	4.9 [1]	0.95 [2]
					Final Product	Vendor	40 [1]	120 [1]	45 [1]	2.6	---
					Final Product	GE	42 [1]	145 [1]	31 [1]	< 1 [1]	---
	02A-025	Rod	1.25" diameter x 24"	912-900	Ingot	Vendor	31 [2]	285 [1]	97 [2]	2.2 [1]	1.08 [2]
					Final Product	Vendor	50	200	45	4.3	---
					Final Product	GE	114	248	61	7	---

TABLE VI. (Cont.)

Alloy	MCN Number	Mill Product Form	Size	Heat Number	Sample Source	Analyzed By	Chemical Analyses, ppm C	O	N	H	Other (%)
Ta	SPECIFICATION ASTM-B364-62T						Max 300	Max 300	Max 150	Max 10	
	02A-049-(1-8)	Foil	0.002" x 0.5" x 4 lbs	CG-117	Final Product	Vendor	10	28	28	5	Zr-5
	SPECIFICATION ASTM-B364-61T						Max 300	Max 300	Max 150	Max 15	
	02A-012	Sheet	0.032" x 0.75" x 12"	81274	Final Product	Vendor	10	12	5	3	---
					Final Product	GE	4[1]	8[1]	5[1]	< 1	---
	02A-011	Sheet	0.062" x 2.125" x 36"	81310	Final Product	Vendor	50	22	17	8	---
					Final Product	GE	6[1]	16[1]	11[1]	< 1	---
	02A-013-(1-2)	Bar	0.250" x 4.0" x 72"	81371	Final Product	Vendor	29[1]	45[1]	10[1]	1[1]	---
					Final Product	GE	12[1]	12[1]	2[1]	1[1]	---
	SPECIFICATION ASTM-B-365-62T						Max 300	Max 300	Max 150	Max 10	
	02A-021	Bar	0.5" x 0.5" x 3'	81303	Final Product	Vendor	<10	24	12	3	---
	SPECIFICATION ASTM-B-364-61T						Max 300	Max 300	Max 150	Max 15	
	02A-016	Bar	0.500" x 1.00" x 28"	81259	Final Product	Vendor	<10	6	10	3	---
					Final Product	GE	10[1]	37[1]	10[1]	< 1	---
	02A-015	Bar	1.00" x 1.00" x 15"	81259	Final Product	Vendor	10	6	10	3	---
					Final Product	GE	3[1]	12[1]	5[1]	< 1	---
	SPECIFICATION ASTM-B-365-62T						Max 300	Max 300	Max 150	Max 15	
	02A-008	Wire	0.020" diameter x 600'	81259	Final Product	Vendor	<10	6	10	3	---
	02A-009	Rod	0.250" diameter x 24"	81303	Final Product	Vendor	<10[1]	24[1]	12	3[1]	---
					Final Product	GE	17[1]	52[1]	20[1]	< 1[1]	---
	02A-010	Rod	0.625" diameter x 12"	81341	Final Product	Vendor	<10	6	2	3	---
					Final Product	GE	18[1]	19[1]	12[1]	1[1]	---
	02A-014	Rod	1.250" diameter x 8"	81259	Final Product	Vendor	<10[1]	6	10	3	---
					Final Product	GE	21[1]	20	18	< 1	---
T-222	SPECIFICATION						Best Effort				
	02A-027	Sheet	0.009" x 3.5" x 6.5"	Ta-39-	Final Product	Vendor	130	18	41	---	W-8.9 Hf-2.2
					Final Product	GE	290	162	28	< 1	---

[1] Average of 2 analyses.

[2] Average of 4 analyses or more.

[3] Average of 3 analyses.

TABLE VII. MECHANICAL PROPERTIES & GRAIN SIZE OF REFRACTORY ALLOY MILL PRODUCTS

Alloy	MCN Number	Mill Product Form	Mill Product Size	Heat Number	Final Heat Treatment	Room Temperature Tensile Properties Ult. Ksi	0.2%Y.S. Ksi	Elong. %	2400°F Stress-Rupture Life at 19,000 psi Hours	Elong,%	Bend or Flare	Hardness Bulk	Hardness Micro (DPH) Surface	Hardness Micro (DPH) Center	Grain Size Vendor ASTM No.	Grain Size GE ASTM No.	Recrystallization (%) Vendor	Recrystallization (%) GE
T-111	SPECIFICATION	Foil	01-0043-00-A								180°w/No Fail.						100%	
	02B-011	Foil	0.005" x 3.5" x 52"	111-D-1632	1475°C/1 hr.*	-	-	-	-	-	180° Passed	-	-	-	-	-	100	-
	02A-042	Foil	0.005" x 3.5" x 52"	111-D-1670	1475°C/1 hr.	-	-	-	-	-	180° Passed	-	-	-	-	8	95	100
	02A-064	Foil	0.009" x 3.5" x 52"	65076	3000°F/1 hr.	-	-	-	-	-	180° Passed	215BHN	-	-	-	6-7	100	100
	02B-012	Foil	0.009" x 3.5" x 12"	111-D-1632	1475°C/1 hr.	-	-	-	-	-	180° Passed	-	-	-	-	8	100	100
	02A-043	Foil	0.009" x 3.5" x 12"	111-D-1670	1475°C/1 hr.	-	-	-	-	-	180° Passed	-	-	-	-	8	95	100
	02A-063-(1-2)	Foil	0.009" x 3.5" x 12"	65076	3000°F/1 hr.	-	-	-	-	-	180° Passed	215BHN	-	-	-	7	100	100
	SPECIFICATION	Sheet, Plate, and Strip - 01-0040-00-B				Max. 110	Max. 100	Min. 20	Min. 20		105°w/No Fail.		Max. 50 Variance		6		100	
	02A-065-(1-3)	Sheet	0.035" x 1" x 14"	65076	3000°F/1 hr.	79.9[1]	93.2[1]	31[1]	>20[1]	-	180° Passed	215BHN	275	249	7½	6	100	100
	02B-010-(1-2)	Sheet	0.040" x 12" x 50"	111-D-1632	1475°C/1 hr.	91.6[1]	82.6[1]	30.5[1]	15.9[1]	-	135° Passed	-	226	223	7½	8	100	100
	02A-057	Sheet	0.125" x 6" x 10"	65076	3000°F/1 hr.	92.9[1]	77.9[1]	36.5[1]	>20[1]	-	105° Passed	215BHN	257	226	7-7½	-	100	-
	02B-009	Plate	0.500" x 6.125" x 11"	111-D-1632	1475°C/1 hr.	91.5[1]	77.7[1]	42.5[1]	12.6[1]	-	-	-	245	213	6½	-	100	-
	02A-056	Plate	0.500" x 6.125" x 11"	65076	3000°F/1 hr.	90.7[1]	73.1[1]	37.5[1]	>20[1]	-	-	215BHN	251	227	6-6½	4-6	100	100
	SPECIFICATION	Seamless Tubing and Pipe - 01-0035-00-B				Max. 110	Max. 100	Min. 20	Min. 20		Flare - 15% OD Increase		Max. 50 Variance		Min. 5		Min. 100	
	02A-066-(1-3)	Tube	0.375" OD x 0.065" W x 144"	111-D-1670	3000°F/1 hr.	88.3[1]	75.9[1]	32.5[1]	>43[1]	-	-	-	226	219	5½	5	100	100
	02A-067-(1-18)	Tube	0.375" OD x 0.065" W x 72"	111-D-1670	3000°F/1 hr.	88.3[1]	75.9[1]	32.5[1]	>43[1]	-	-	-	226	219	5½	5	100	100
	02A-068-(1-2)	Tube	1.0" OD x 0.100" W x 140"	111-D-1670	3000°F/1 hr.	91.8[1]	74.6[1]	27[1]	>43[1]	-	-	-	226	219	5½	5	100	100
	02A-074	Tube	1.0" OD x 0.100" W x 112"	111-D-1670	3000°F/1 hr.	91.4	74.5	33	38.9[1]	-	-	-	224	217	5	5	100	100
	02A-075-(1-2)	Tube	1.0" OD x 0.100" W x 9'	111-D-1670	3000°F/1 hr.	91.4	74.5	33	38.9[1]	-	-	-	224	217	5	5	100	100
															Min. 3		Min. 90	
	02A-079-(1-2)	Tube	2.250" OD x 0.375" W x 15"	111-D-1765	3000°F/1 hr.	91.5[1]	73.4[1]	34.5[1]	43.5[1]	-	-	-	230	226	5	4	100	100
	02A-085	Tube	2.5" OD x 1.610 ID x 13"	111-D-1829	3000°F/1 hr.	88.5[1]	69.4[1]	42.5[1]	26.6[1]	-	-	-	213	219	5½	6	100	100
	02A-080	Tube	2.50" OD x 1.610" ID x 13"	111-D-1765	3000°F/1 hr.	91.5[1]	73.4[1]	34.5[1]	43.5[1]	-	-	-	230	226	5	-	100	-
	02A-046-(1-2)	Tube	3.0" OD x 0.375" W x 13"	111-D-1102	1475°C/2 hrs.**	86.6[1]	74.1[1]	42[1]	>21[1]	-	-	-	216	213	4-6	3	100	100

C1238-7

ORIGINAL PAGE IS
OF POOR QUALITY

TABLE VII. (Cont.)

Alloy	MCN Number	Mill Product Form	Mill Product Size	Heat Number	Final Heat Treatment	Room Temperature Tensile Properties Ult. Ksi	Room Temperature Tensile Properties 0.2%Y.S. Ksi	Room Temperature Tensile Properties Elong. %	2400°F Stress-Rupture Life at 19,000 psi Hours	2400°F Stress-Rupture Life at 19,000 psi Elong.,%	Bend or Flare	Hardness Bulk	Hardness Micro (DPH) Surface	Hardness Micro (DPH) Center	Grain Size Vendor ASTM No.	Grain Size GE ASTM No.	Recrystallization (%) Vendor	Recrystallization (%) GE
T-111	02A-048	Tube	3.25" OD x 0.250" W x 14"	111-D-1102	1475°C/2 hrs.**	86.6[1]	74.1[1]	42[1]	>21[1]	-	-	-	216	213	4-6	4	100	100
	02A-045	Tube	3.25" OD x 0.500" W x 14"	111-D-1102	1475°C/2 hrs.**	86.6[1]	74.1[1]	42[1]	>21[1]	-	-	-	216	213	4-6	4	100	100
	02A-086	Tube	3.25" OD x 0.25" W x 14"	111-D-1829	3000°F/1 hr.	87.6[1]	69.1[1]	32.5[1]	28.1[1]	-	-	-	213	213	4	-	100	-
	02A -087	Tube	3.25" OD x 0.500" W x 14"	111-D-1829	3000°F/1 hr.	87.6[1]	69.1[1]	32.5[1]	28.1[1]	-	-	-	213	213	4	-	100	-
	SPECIFICATION	Wire	01-0048-00-A														100	
	02B-001	Wire	0.062" Ø x 6#	111-D-1633	1475°C/1 hr.	-	-	-	-	-	-	-	-	-	-	6-7	100	100
	02A-039-(1-2)	Wire	0.062" Ø x coil	70616	-	-	-	-	-	-	-	-	-	-	-	-	-	-
	02B-002	Wire	0.094" Ø x 8#	111-D-1633	1475°C/1 hr.	-	-	-	-	-	-	-	-	-	-	6	100	100
	02B-003	Wire	0.125" Ø x 168'	111-D-1633	1475°C/1 hr.	-	-	-	-	-	-	-	-	-	-	6	100	100
	02A-059	Wire	0.125" Ø x 40' (3.1#)	70616	3000°F/1 hr.	-	-	-	-	-	-	215BHN	-	-	-	7	-	100
	02A-060	Wire	0.125" Ø x 7.9#	65076	3000°F/1 hr.	-	-	-	-	-	-	215BHN	-	-	-	5	100	100
	SPECIFICATION	Bar and Rod - 01-0015-00-B				Max. 110	Max. 100	Min. 20	Min. 20				Max. 50 Variance		2		2	
	02B-004	Rod	0.250" Ø x 24"	111-D-1633	1475°C/1 hr.	89.8[1]	76.5[1]	34[1]	13.6[1]	-	-	-	237	234	6½	6	100	100
	02A-054	Rod	0.250" Ø x 24"	65076	3000°F/1 hr.	91.2[1]	76.4[1]	28.5[1]	>20.1[1]	-	-	215BHN	260	238	7½	7	100	100
	02B-005	Rod	0.500" Ø x 48"	111-D-1633	1475°C/1 hr.	89.6[1]	72.7[1]	42.5[1]	16.7[1]	-	-	-	226	216	6½	7	100	100
	02A-052	Rod	0.500" Ø x 48"	65076	3000°F/1 hr.	90.5[1]	72.9[1]	32.5[1]	>20.1[1]	-	-	215BHN	264	237	7½	7	100	100
	02B-006	Rod	0.625" Ø x 14"	111-D-1633	1475°C/1 hr.	89.6[1]	72.7[1]	42.5[1]	16.7[1]	-	-	-	226	216	6½	7	100	100
	02A-053	Rod	0.625" Ø x 14"	65076	3000°F/1 hr.	90.5[1]	72.9[1]	32.5[1]	>20.1[1]	-	-	215BHN	264	237	7½	7	100	100
	02B-007-(1-2)	Rod	1.0" Ø x 42"	111-D-1633	1475°C/1 hr.	83.3[1]	69.7[1]	46.5[1]	14.3[1]	-	-	-	226	207	4-5½	5-6	100	100
	02A-062	Rod	1.0" Ø x 42"	65076	3000°F/1 hr.	92.0[1]	74.0[1]	35[1]	>20.1[1]	-	-	215BHN	252	230	7	5-6	100	100
	02B-008	Rod	1.125" Ø x 8"	111-D-1633	1475°C/1 hr.	83.3[1]	69.7[1]	46.5[1]	14.3[1]	-	-	-	-	-	4-5½	5	100	100
	02A-061	Rod	1.125" Ø x 8"	65076	3000°F/1 hr.	92.0[1]	74.0[1]	35[1]	>20.1[1]	-	-	215BHN	252	230	7	4-6	100	100
	02B-014	Rod	1.5" Ø x 6"	111-D-1633	1475°C/2 hrs.	86.5[1]	75.5[1]	42.5[1]	21.0+[3] 25.0+[3]	-	-	-	201	204	3-7	-	95	0
	02A-058	Rod	1.50"Ø x 6"	65076	3000°F/1 hr.	87.4[1]	71.0[1]	32.5[1]	>20.0[1]	-	-	215BHN	263	226	7	4-6	100	100

TABLE VII. (Cont.)

Alloy	MCN Number	Mill Product Form	Mill Product Size	Heat Number	Final Heat Treatment	Room Temperature Tensile Properties Ult. Ksi	0.2%Y.S. Ksi	Elong. %	2400°F Stress Rupture Life at 19,000 psi Hours	Elong,%	Bend or Flare	Hardness Bulk	Micro (DPH) Surface	Micro (DPH) Center	Grain Size Vendor ASTM No.	Grain Size GE ASTM No.	Recrystallization (%) Vendor	Recrystallization (%) GE
T-111	02A-044-(1-3)	Rod	2.0" Ø x 21"	111-D-1102	1475°C/2 hrs.** +3000°F/1 hr.	86.4[1]	75.4[1]	42.5[1]	16.6[3] 21.5[3]	-	-	-	225	209	4-6	5	100	100
	02A-082	Rod	2.0" Ø x 24"	111-D-1829	3000°F/1 hr.	88.5[1]	69.4[1]	42.5[1]	-	-	-	-	213	219	5½	4½	100	100
	02A-038	Rod	2.5" Ø x 21-1/16"	111-D-1670	1475°C/2 hrs.** 3000°F/1 hr.	84.2[1]	69.9[1]	39.5[1]	9.4[3] 22.8[3]	-	-	-	219	213	5-7	5	100	100
	02A-077	Rod	2.5" Ø x 5.188"	111-D-1765	3000°F/1 hr.	91.5[1]	73.4[1]	34.5[1]	43.5[1]	-	-	-	230	226	5	3½	100	100
	02A-083	Rod	2.5" Ø x 5"	111-D-1829	3000°F/1 hr.	88.5[1]	69.4[1]	42.5	-	-	-	-	213	219	5½	4½	100	100
	02A-076	Rod	3.125" Ø x 16"	111-D-1765	3000°F/1 hr.	93.4[1]	74.8[1]	34[1]	43+[1]	-	-	-	230	226	3-5	4	100	100
	02B-013-(1-3)	Bar	1" x 1" x 12.5"	111-D-1633	1475°C/1 hr.	86.5[1]	75.5[1]	42.5[1]	21.0+[3] 25.0+[3]	-	-	-	201	204	3-7	5	100	100
	02A-051	Bar	1" x 1" x 12.5"	65076	3000°F/1 hr.	87.4[1]	71.0[1]	32.5[1]	>20.0[1]	-	-	215BHN	263	226	7	5	100	100
	02A-047	Bar	1" x 2" x 32"	111-D-1102	1475°C/2 hrs.** 3000°F/1 hr.	89.8[1]	78.0[1]	37.5[1]	>21.5[1]	-	-	-	219	212	6	6	100	100
	02A-078	Bar	1" x 2" x 63"	111-D-1765	3000°F/1 hr.	92.8[1]	75.8[1]	37[1]	43[1]	-	-	-	224	234	4½	5	100	100
	SPECIFICATION	Bar and Rod - 01-0011-00-C				Max. 175	Max. 140	Min. 15	Min. 20								Max. 5	
Mo-TZC	02A-037-(1-3)	Rod	1.0" Ø x 14.75"	4331	2400°F/1 hr.	118.2[1]	107.5[1]	24.5[1]	32.8[1]	-	-	-	-	-	-	-	0	0
	02A-036-(1-3)	Rod	2.0" Ø x 16.187"	4331	2400°F/1 hr.	105.1[1]	96.6[1]	1.8[1]	87.5[4]	31[1]	-	-	-	-	-	-	0	0
	02A-035-(1-5)	Bar	0.750" x 0.750" x 7"	M96	1300°C/1 hr.	103.6[1]	98.2[1]	1.2[1]	12.8[4]	1.26	-	-	-	-	-	-	0	0
	02A-032-(1-6)	Bar	1.375" x 2" x 5"	M97	1300°C/1 hr.	95.7[1]	94.0[1]	0.36[1]	25.3[4]	2.8	-	-	-	-	-	-	0	0
	02A-033	Bar	1.375" x 2" x 5"	M92	1300°C/1 hr.	130.5[1]	105.4[1]	1.3[1]	29.4[4]	12.8	-	-	-	-	-	-	0	0
Mo-TZM	SPECIFICATION	Rod	CMX-WB-TZM-2			Min. 115	Min. 100	Min. 18	No Requirement				Mid-Radius Min. 260	Mid-Radius Max. 320			Stress Relieved	
	02A-004	Rod	0.125" Ø x 36"	5960	2200°F/¼ hr.	117.8[1]	103.6[1]	32[1]	-	-	-	-	268	293	-	-	-	-
	02A-005	Rod	0.500" Ø x 36"	7468	2250°F/½ hr.	133.7[1]	131.6[1]	28[1]	-	-	-	-	292	306	-	-	-	0
	02A-072	Rod	0.500" Ø x 18"	7498	2250°F/½ hr.	135.3[1]	124.3[1]	27[1]	-	-	-	-	281	299	-	-	-	-
	02A-006	Rod	0.875" Ø x 16"	7473	2300°F/3/4 hr.	125.2[1]	107.8[1]	29[1]	-	-	-	-	276	287	-	-	-	0
	02A-071	Rod	0.875" Ø x 24"	7876	2300°F/3/4 hr.	122.9[1]	104.1[1]	30[1]	-	-	-	-	279	289	-	-	-	-
	02A-081	Rod	0.875" Ø x 12"	7876	2300°F/3/4 hr.	122.9[1]	104.1[1]	30[1]	-	-	-	-	279	289	-	-	-	0

TABLE VII. (Cont.)

Alloy	MCN Number	Mill Product Form	Mill Product Size	Heat Number	Final Heat Treatment	Room Temperature Tensile Properties Ult. Ksi	0.2%Y.S. Ksi	Elong. %	2400°F Stress-Rupture Life at 19,000 psi Hours	Elong.%	Bend or Flare	Hardness Bulk	Micro (DPH) Surface	Micro (DPH) Center	Grain Size Vendor ASTM No.	Grain Size GE ASTM No.	Recrystallization (%) Vendor	Recrystallization (%) GE
Mo-TZM	02A-007	Rod	2.0" Ø x 24"	7555	2350°F/1 hr.	104.9[1]	89.1[1]	16.5[1]	-	-	-	-	268	272	-	-	-	
	02A-070	Rod	2.125" Ø x 12"	7893	2350°F/1 hr.	103.9[1]	87.9[1]	18[1]	-	-	-	-	262	280	-	-	-	-
Cb-132M	SPECIFICATION	Rod	01-0010-01-A			Max. 190	Max. 160	Min. 20	Min. 20				Max. 50 Variance		Min. 4		Max. 5	
	02A-055-(1-3)	Rod	1.0" Ø x 22"	66-95119	2400°F/1 hr.	138.8[1]	115.8[1]	11[1]	10.3[1]	26[1]	-	-	281	310	-	9-10	0	50
	02A-041-(1-2)	Rod	2.0" Ø x 24"	66-95119	2400°F/1 hr.	136.1[5]	120.2[5]	3.8[5]	>87[5]	>15[5]	-	-	292	300	-	-	0	0
Cb-1Zr	SPECIFICATION	Bar, Rod, Sheet, Plate, and Strip - 01-0003-04-B				Max. 75	Max. 60	Min. 10			(60°) 1.15 x Diameter	$90R_b$ Max.	Max. 50 Variance		Min. 3			
	02A-022-(1-6)	Sheet	0.0175" x 12" x 24"	912-70112	2200°F/1 hr.	40.7[1]	26.6[1]	29.7[1]	-	-	-	$90R_b$	89	98	8.5	-	-	-
	02A-034-(1-2)	Sheet	0.030" x 24" x 32"	912-70112	2200°F/1 hr.	44.1[1]	32.3[1]	28.7[1]	-	-	-	$97R_b$	95	110	7.5	-	-	-
	02A-023	Sheet	0.125" x 4" x 12"	70112	2200°F/1 hr.	60.6[1]	52.0[1]	13.3[1]	-	-	-	$90R_b$	151	139	7.5	-	-	-
	02A-019	Sheet	0.250" x 6" x 36"	912-70112	2200°F/1 hr.	60.6[1]	52.0[1]	13.3[1]	-	-	-	$90R_b$	151	139	7.5	-	-	-
	SPECIFICATION	Seamless Tubing - 01-0004-01-D				Max. 75	Max. 60	Min. 10			(60°) 1.15 x Diameter	$90R_b$	Max. 50 Variance		Min. 6		100	
	02A-050	Tube	0.250" OD x 0.062" W x 60"	70303	2200°F/1 hr.	61.4[1]	45.8[1]	23[1]	-	-	To 60%	-	116	96	6.5	-	80-90	-
	SPECIFICATION	Seamless Tubing and Pipe - 01-0004-01-C				Max. 75	Max. 60	Min. 20				$90R_b$	Max. 50 Variance					
	02A-040-(1-2)	Tube	0.5" OD x 0.040" W x 3-5'	5886	2200°F/1 hr.	49.2	32.6	42	-	-	To 15%	-	129	141	8	-	100	-
	SPECIFICATION	Seamless Tubing - 01-0004-03-B				Max. 75	Max. 60	Min. 20				$90R_b$	Max. 50 Variance		Min. 3		100	
	02A-029	Tube	2.75" OD x 0.125" W x 48"	5886	2200°F/1 hr.	39.4	22.2	48	-	-	To 3.16"	-	22 Variance		6	6	-	25
	SPECIFICATION	Bar and Rod - 01-0052-01-C				Max. 75	Max. 60	Min. 20				$90R_b$			Min. 4		100	
	02A-069	Rod	0.250" Ø x 60"	6075	2200°F/1 hr.	40.0[1]	24.2[1]	46.5[1]	-	-	-	-	92	86	8.5	-	-	-
	SPECIFICATION	Bar, Rod, Sheet, Plate, and Strip - 01-0003-04-B				Max. 75	Max. 60	Min. 10			(60°) 1.15 x Diameter	Max. $90R_b$			Min. 3			
	02A-020-(1-2)	Rod	0.5" Ø x 120"	911-53002	2200°F/1 hr.	42.2[1]	23.2[1]	43.5[1]	-	-	-	$75R_b$	80	85	1-9	-	-	-
	02A-024	Rod	0.5" Ø x 120"	911-70559	2200°F/1 hr.	41.8[1]	26.2[1]	41.5[1]	-	-	-	$86R_b$	86	85	7	-	-	-
	02A-026	Rod	0.625" Ø x 12"	911-70559	2200°F/1 hr.	43.5[1]	24.2[1]	44[1]	-	-	-	$86R_b$	100	102	7.5	-	-	-

ORIGINAL PAGE IS OF POOR QUALITY

TABLE VII. (Cont.)

Alloy	MCN Number	Mill Product Form	Mill Product Size	Heat Number	Final Heat Treatment	Room Temperature Tensile Properties Ult. Ksi	0.2%Y.S. Ksi	Elong. %	2400°F Stress-Rupture Life at 19,000 psi Hours	Elong,%	Bend or Flare	Hardness Bulk	Micro (DPH) Surface	Micro (DPH) Center	Grain Size Vendor ASTM No.	Grain Size GE ASTM No.	Recrystallization (%) Vendor	Recrystallization (%) GE
Cb-1Zr	02A-025	Rod	1.25" Ø x 24"	912-900	2000°F/1 hr.	41.6[1]	32.1[1]	29[1]	-	-	-	98R_b	108	136	4-4.5	-	-	-

* Fansteel heat treatment 1475°C or 2685°F.

**Material given an additional 3000°F/1-hr. anneal before usage in loop fabrication.

[1] Average of two tests.

[2]

Product Diameter or Thickness, Inches	Minimum Allowable ASTM Grain Size Number	% R_x Minimum
0.125 to 0.250	4	100
0.250 to 0.500	4	100
0.500 to 1.0	4	100
1.0 to 2.0	4	95
Greater than 2.0	3	90

[3] Heat treated at General Electric at 3000°F/ 1 hour which is a thermal treatment superimposed on materials present thermal condition.

[4] 2400°F @ 30,000 psi., 2 specimens

[5] 2200°F @ 30,000 psi., 3 specimens

ORIGINAL PAGE IS
OF POOR QUALITY

TABLE VIII. RESULTS OF NONDESTRUCTIVE QUALITY ASSURANCE TESTS OF REFRACTORY ALLOY MILL PRODUCTS

Alloy	MCN Number	Mill Product Form	Mill Product Size	Heat Number	Nondestructive Tests Penetrant	Nondestructive Tests Ultrasonic	Nondestructive Tests Hydrostatic
T-111	02A-065-(1-3)	Sheet	0.035" x 1" x 14"	65076	100% Passed	100% Passed	-
	02B-010-(1-2)	Sheet	0.040" x 12" x 50"	111-D-1632	100% Passed	100% Passed-Numerous small indications <60% amp.	-
	02A-057	Sheet	0.125" x 6" x 10"	65076	100% Passed	100% Passed	-
	02B-009	Plate	0.500" x 6.125" x 11"	111-D-1632	100% Passed	100% Passed	-
	02A-056	Plate	0.500" x 6.125" x 11"	65076	100% Passed	100% Passed	-
	02A-066-(1-3)	Tube	0.375" OD x 0.065" W x 144"	111-D-1670	Failed-Defects Removed	Failed-Defects Removed	Passed
	02A-067-(1-18)	Tube	0.375" OD x 0.065" W x 72"	111-D-1670	Failed-Defects Removed	Failed-Defects Removed	Passed
	02A-068-(1-2)	Tube	1.0" OD x 0.100" W x 140"	111-D-1670	Failed-Defects Removed	Failed-Defects Removed	Passed
	02A-074	Tube	1.0" OD x 0.100" W x 112"	111-D-1670	100% Passed	100% Passed	Passed
	02A-075-(1-2)	Tube	1.0" OD x 0.100" W x 9'	111-D-1670	100% Passed	100% Passed	Passed
	02A-079-(1-2)	Tube	2.250" OD x 0.375" W x 15"	111-D-1765	100% Passed	100% Passed-1 piece with small groove running around end 0-75% amp. (Visual)	-
	02A-085	Tube	2.5" OD x 1.610 ID x 13"	111-D-1102	100% Passed	100% Passed	-
	02A-080	Tube	2.50" OD x 1.610" ID x 13"	111-D-1765	100% Passed	100% Passed	-
	02A-046-(1-2)	Tube	3.0" OD x 0.375" W x 13"	111-D-1102	100% Passed	100% Passed	-
	02A-048	Tube	3.25" OD x 0.250" W x 14"	111-D-1102	100% Passed	100% Passed	-
	02A-015	Tube	3.25" OD x 0.500" W x 14"	111-D-1102	100% Passed	100% Passed	-
	02A-086	Tube	3.25" OD x 0.25" W x 14"	111-D-1829	100% Passed	100% Passed	-
	02A-087	Tube	3.25" OD x 0.500" W x 14"	111-D-1829	100% Passed	100% Passed	-
	02B-004	Rod	0.250" Ø x 24"	111-D-1633	100% Passed	100% Passed	-
	02A-054	Rod	0.250" Ø x 24"	65076	Failed-Defects Removed	100% Passed	-
	02B-005	Rod	0.500" Ø x 48"	111-D-1633	100% Passed	100% Passed	-
	02A-052	Rod	0.500" Ø x 48"	65076	100% Passed	100% Passed	-
	02B-006	Rod	0.625" Ø x 14"	111-D-1633	100% Passed	100% Passed	-
	02A-053	Rod	0.625" Ø x 14"	65076	100% Passed	100% Passed	-
	02B-007-(1-2)	Rod	1.0" Ø x 42"	111-D-1633	100% Passed	100% Passed	-

TABLE VIII. (Cont.)

Alloy	MCN Number	Mill Product Form	Mill Product Size	Heat Number	Nondestructive Tests Penetrant	Nondestructive Tests Ultrasonic	Hydrostatic
T-111	02A-062	Rod	1.0" Ø x 42"	65076	100% Passed	100% Passed	-
	02B-008	Rod	1.125" Ø x 8"	111-D-1633	100% Passed	100% Passed	-
	02A-061	Rod	1.125" Ø x 8"	65076	100% Passed	100% Passed	-
	02B-014	Rod	1.5" Ø x 6"	111-D-1633	100% Passed	100% Passed	-
	02A-058	Rod	1.50" Ø x 6"	65076	100% Passed	100% Passed	-
	02A-044-(1-3)	Rod	2.0" Ø x 21"	111-D-1102	100% Passed	100% Passed	-
	02A-082	Rod	2.0" Ø x 24"	111-D-1829	100% Passed	100% Passed	-
	02A-038	Rod	2.5" Ø x 21-1/16"	111-D-1670	100% Passed	100% Passed	-
	02A-077	Rod	2.5" Ø x 5.188"	111-D-1765	100% Passed	100% Passed	-
	02A-083	Rod	2.5" Ø x 5"	111-D-1829	100% Passed	100% Passed	-
	02A-076	Rod	3.125" Ø x 16"	111-D-1765	100% Passed	1 indication 100%, 6¼" from noted end (Removed)	-
	02B-013-(1-3)	Bar	1" x 1" x 12.5"	111-D-1633	100% Passed	100% Passed	-
	02A-051	Bar	1" x 1" x 12.5"	65076	100% Passed	100% Passed	-
	02A-047	Bar	1" x 2" x 32"	111-D-1102	100% Passed	2 indications of 90% and 100%, 5¼" from noted end bottom side, 2'5¼" from noted end, top side.	-
	02A-078	Bar	1" x 2" x 63"	111-D-1765	100% Passed	100% Passed	-
Mo-TZC	02A-037-(1-3)	Rod	1.0" x 14.75"	4331	100% Passed	100% Passed	-
	02A-036-(1-3)	Rod	2.0"Øx 16.187"	4331	100% Passed	100% Passed	-
	02A-035-(1-5)	Bar	0.750" x 0.750" x 7"	M96	100% Passed	100% Passed	-
	02A-032-(1-6)	Bar	1.375" x 2" x 5"	M97	100% Passed	100% Passed	-
	02A-033	Bar	1.375" x 2" x 5"	M92	100% Passed	100% Passed	-
Mo-TZM	02A-004	Rod	0.125" Ø x 36"	5960	100% Passed	-	-
	02A-005	Rod	0.500" Ø x 36"	7468	100% Passed	-	-
	02A-072	Rod	0.500" Ø x 18"	7498	100% Passed	100% Passed	-
	02A-006	Rod	0.875" Ø x 16"	7473	100% Passed	-	-
	02A-071	Rod	0.875" Ø x 24"	7876	100% Passed	-	-

ORIGINAL PAGE IS
OF POOR QUALITY

TABLE VIII. (Cont.)

Alloy	MCN Number	Mill Product Form	Mill Product Size	Heat Number	Nondestructive Tests Penetrant	Nondestructive Tests Ultrasonic	Nondestructive Tests Hydrostatic
Mo-TZM	02A-081	Rod	0.875" Ø x 12"	7876	100% Passed	100% Passed	-
	02A-007	Rod	2.0" Ø x 24"	7555	100% Passed	100% Passed	-
	02A-070	Rod	2.125" Ø x 12"	7893	100% Passed	100% Passed	-
Cb-132M	02A-055-(1-3)	Rod	1.0" Ø x 22"	66-95119	—	100% Passed	-
	02A-041-(1-2)	Rod	2.0" Ø x 24"	66-95119	—	100% Passed	-
Cb-1Zr	02A-022-(1-6)	Sheet	0.0175" x 12" x 24"	912-70112	100% Passed	100% Passed	-
	02A-034-(1-2)	Sheet	0.030" x 24" x 32"	912-70112	100% Passed	100% Passed	-
	02A-023	Sheet	0.125" x 4" x 12"	70112	100% Passed	100% Passed	-
	02A-019	Sheet	0.250" x 6" x 36"	912-70112	100% Passed	100% Passed	-
	02A-050	Tube	0.250" OD x 0.062" W x 60"	70303	100% Passed	Failed-8 indications >40%	-
	02A-040-(1-2)	Tube	0.5" OD x 0.040" W x 3-5'	5886	100% Passed	02A-040-1-Failed, 7 indications >80%	Satisfactory
	02A-029	Tube	2.75" OD x 0.125" W x 48"	5886	100% Passed	Failed-3 indications 1) 19-24" from ref. end 40-90% amp 2) 32.5-34.5" from ref. >40% amp 3) 42-44" from ref. end >40% amp	-
	02A-069	Rod	0.250" Ø x 60"	6075	100% Passed	100% Passed	-
	02A-020-(1-2)	Rod	0.5" Ø x 120"	911-53002	100% Passed	100% Passed	-
	02A-024	Rod	0.5" Ø x 120"	911-70559	100% Passed	100% Passed	-
	02A-026	Rod	0.625" Ø x 12"	911-70559	100% Passed	100% Passed	-
	02A-025	Rod	1.25" Ø x 24"	912-900	100% Passed	100% Passed	-

TABLE IX. SUMMARY OF OVERALL QUALITY ASSURANCE TEST RESULTS

Material	Form	Number of Lots	Chemistry		Tensile Properties		Stress-Rupture		Hardness		Grain Size		Penetrant*		Ultrasonic*		Hydrostatic*		Flare		Bend	
			Passed	Failed	Passed	Failed	Passed	Failed	Passed	Failed	Passed	Failed	Passed	Failed	Passed	Failed	Passed	Failed	Passed	Failed	Passed	Failed
T-111	Foil	6	5	1	-	-	-	-	-	-	-	-	-	-	-	-	-	-	-	-	6	0
	Sheet	3	2	1	3	0	2	1	3	0	3	0	6	0	6	0	-	-	-	-	3	0
	Plate	2	1	1	2	0	1	1	2	0	2	0	2	0	2	0	-	-	-	-	-	-
	Tube	13	13	0	13	0	13	0	13	0	13	0	12	23	12	23	35	0	-	-	-	-
	Wire	7	7	0	-	-	-	-	-	-	7	0	-	-	-	-	-	-	-	-	-	-
	Rod	18	18	0	18	0	13	5	18	0	17	1	20	1	20	1	-	-	-	-	-	-
	Bar	4	4	0	4	0	4	0	4	0	3	1	6	0	5	1	-	-	-	-	-	-
Mo-TZC	Rod	2	2	0	2	0	2	0	2	0	-	-	6	0	6	0	-	-	-	-	-	-
	Bar	3	2	1	3	0	3	0	3	0	-	-	7	0	7	0	-	-	-	-	-	-
Mo-TZM	Rod	8	8	0	8	0	-	-	8	0	-	-	8	0	4	0	-	-	-	-	-	-
Cb-132M	Rod	2	2	0	1	1	2	0	2	0	2	0	-	-	5	0	-	-	-	-	-	-
Cb-1Zr	Foil	3	3	0	-	-	-	-	-	-	-	-	-	-	-	-	-	-	-	-	-	-
	Sheet	4	4	0	4	0	-	-	4	0	4	0	10	0	10	0	-	-	-	-	-	-
	Tube	3	2	1	3	0	-	-	4	0	4	0	4	0	0	4	4	0	4	0	-	-
	Wire	2	0	2	-	-	-	-	-	-	-	-	-	-	-	-	-	-	-	-	-	-
	Rod	5	5	0	5	0	-	-	5	0	5	0	6	0	6	0	-	-	-	-	-	-
Ta	Foil	1	1	0	-	-	-	-	-	-	-	-	-	-	-	-	-	-	-	-	-	-
	Sheet	2	2	0	-	-	-	-	-	-	-	-	-	-	-	-	-	-	-	-	-	-
	Wire	1	1	0	-	-	-	-	-	-	-	-	-	-	-	-	-	-	-	-	-	-
	Rod	3	3	0	-	-	-	-	-	-	-	-	-	-	-	-	-	-	-	-	-	-
	Bar	4	4	0	-	-	-	-	-	-	-	-	-	-	-	-	-	-	-	-	-	-
T-222	Sheet	1	1	0	-	-	-	-	-	-	-	-	-	-	-	-	-	-	-	-	-	-

* Total Number of Pieces Tested.

subsequent machining of the bar. The ultrasonic defects in the 0.5-inch-OD x 0.040-inch-wall (1.72-cm-OD x 0.10-cm-wall) (MCN 02A-040) and 2.75-inch-OD x 0.125-inch-wall (7.0-cm-OD x 0.32-cm-wall) (MCN 02A-029) Cb-1Zr alloy tubes were not removed since the tubes were to be used in noncritical applications in the lithium distillation facility and were not an integral part of the T-111 Corrosion Loop.

It should be noted that the material specifications for the Mo-TZC and Cb-132M alloys were prepared from extremely limited data, and the apparent failure of the Mo-TZC and Cb-132M alloys to meet the specifications in certain areas does not imply that the material is inferior. The data obtained on these materials, both from the vendor and work done at GE-NSP, will make possible the preparation of improved specifications and aid in selecting processing parameters which will result in improved material properties.

In the posttest metallographic evaluation of loop components following long-time exposure to alkali metals, it is often difficult to determine if the surface irregularities observed on the inner surface of the tube wall are a result of corrosion. Quite often, the most that can be stated is that the before-test surface and after-test surface are similar in appearance. In order to permit a more precise determination of the extent of any attack, the smoothness of the ID surface of portions of the T-111 alloy loop tubing was improved by polishing with 120- and 600-grit alumina cloth followed by pickling in accordance with NSP Specification No. 03-0010-00-C,* "Chemical Cleaning of Columbium, Tantalum, and Their Alloys."

The smoothness of the ID surface of transverse tube specimens in the as-received, as-received and pickled, as-polished, and as-polished plus pickled conditions is shown in Figure 3. The inside surface of the tube specimens was polished by means of a portable drill with the alumina grit cloth inserted in a slotted rod. The ID of the tube was polished until 0.001 inch (0.0025 cm) was removed from the surface. Following polishing

---

* Current Designation, GE-NSP Specification No. P4AYA20-S1.

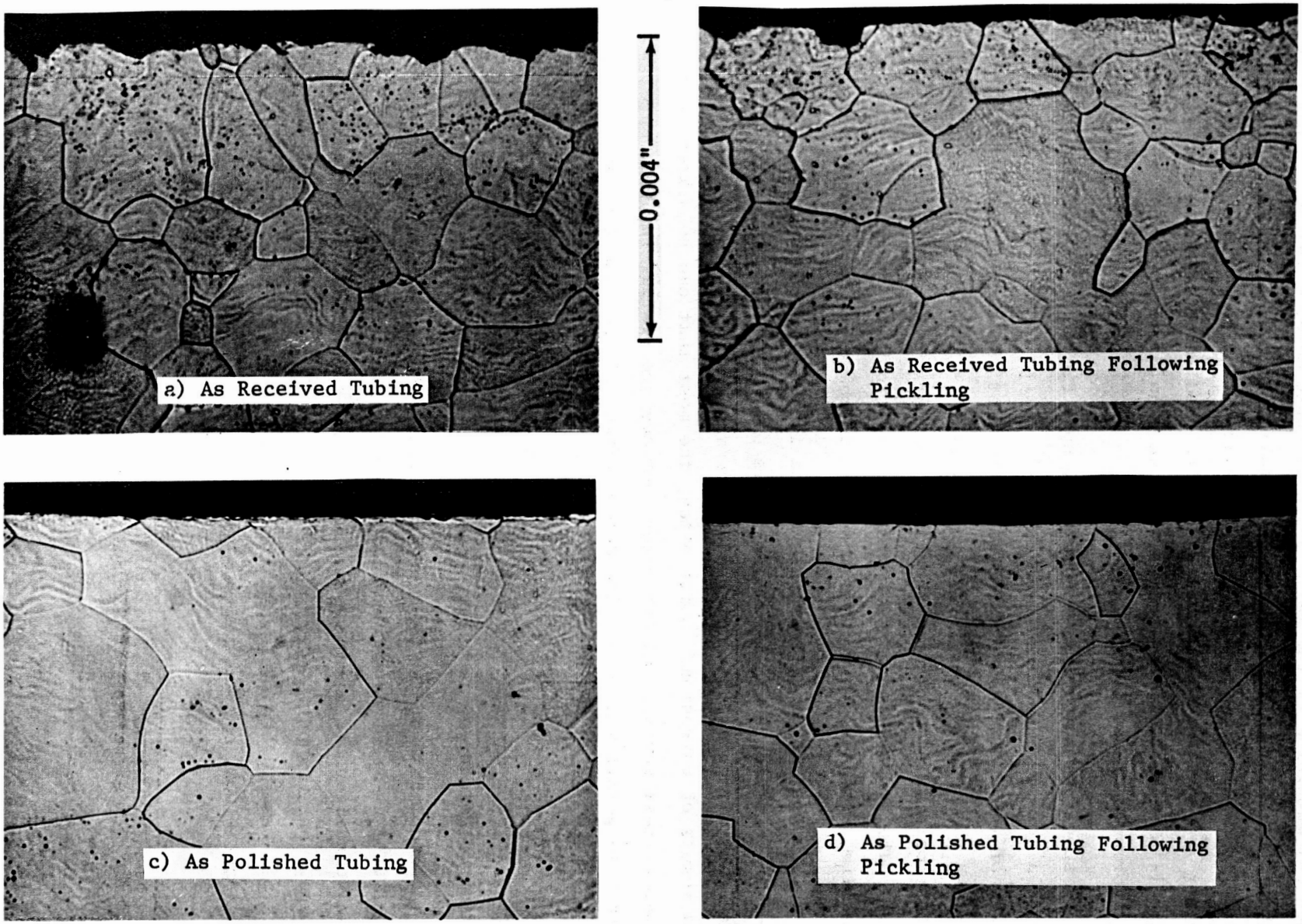


Figure 3. Effect of Polishing and Pickling on the Surface Roughness of T-111 Tantalum Alloy Tubing.

Metallographic Etchant: $30gNH_4F$-$50ml HNO_3$-$20ml H_2O$ Mag. 500X

of the tube ID, the specimens were pickled for five minutes in $HF-HNO_3-H_2SO_4-H_2O$ (1-4-2, parts by volume). As shown in Figure 3, the combination polishing and pickling treatment resulted in an essentially smooth surface free of flowed metal.

During the sampling of the T-111 alloy tubing for the quality assurance tests, severe radial cracking was observed on surfaces cut with an abrasive cutoff wheel as illustrated in Figure 4. The cracks were greatly accented by flattening the cut tube. After flattening, it was apparent that the cracks were concentrated on the side of the tube that made the initial contact with the abrasive cutoff wheel. The belief that the cracking was caused by the action of the abrasive cutoff wheel was substantiated by the fact that removal of the cut surface of the tube by grinding resulted in no cracking in the tube upon flattening, Figure 5. The abrasive wheel used for these cuts was an Allison* aluminum oxide wheel, designation VA1202MRA. Subsequently, an Allison silicon carbide abrasive wheel, C120KRA, was used to cut the T-111 alloy tubing with greatly improved results, Figure 6. Although cracking of the T-111 alloy tubing due to cutting with an abrasive wheel was essentially eliminated with the use of a silicon carbide wheel (C120KRA), a few very small cracks still were observed in portions of the cut tubes. As a result, it is necessary to exercise extreme care in using an abrasive wheel for cutting T-111 alloy mill products in order to avoid subsequent cracking. Under these conditions, the cut surfaces should be ground back, etched, and penetrant inspected in order to be sure that all cracks have been removed. (Studies conducted on T-111 subsequent to the fabrication and testing of the T-111 Corrosion Loop suggest that hydrogen pickup during the abrasive wheel-cutting operation was responsible for the embrittlement noted.)

* Allison-Campbell Division, American Chain and Cable Company, Bridgeport, Connecticut.

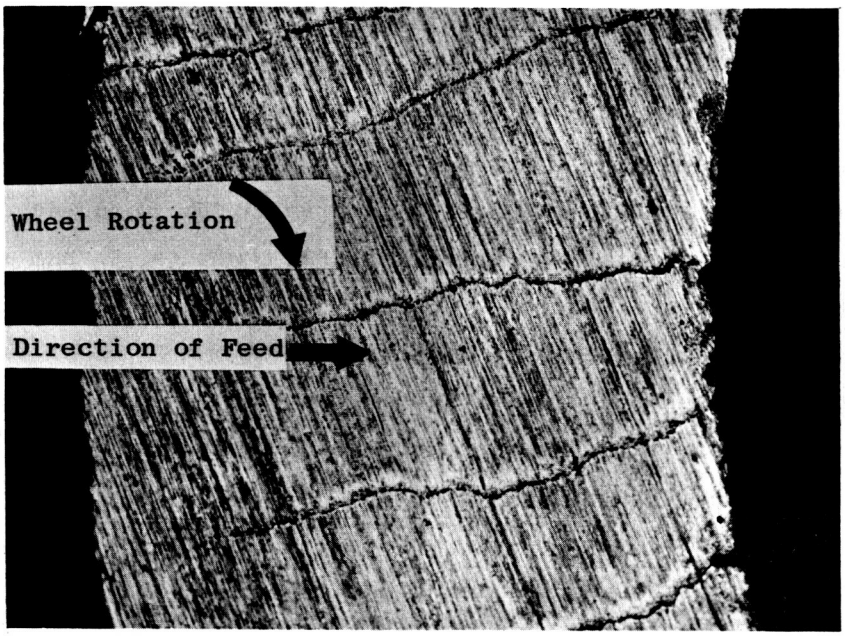
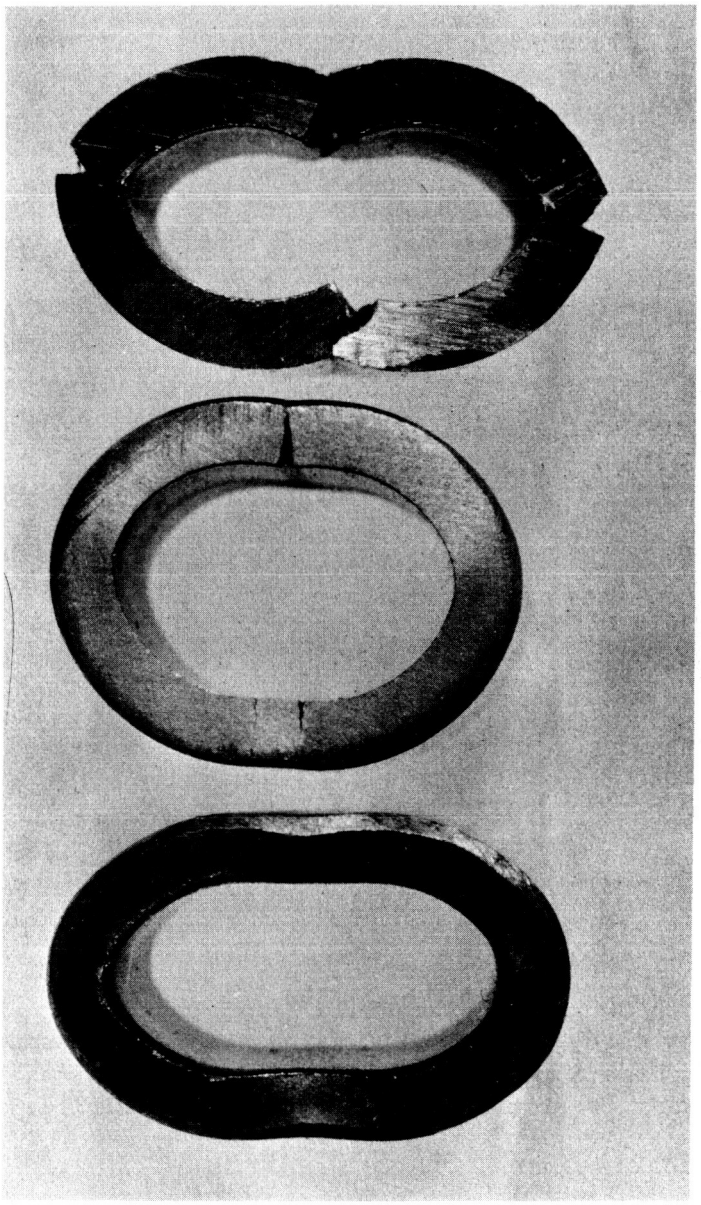


Figure 4. Radial Cracks in 0.375-Inch-OD x 0.065-Inch-Wall (0.95-cm-OD x 0.16-cm-Wall)T-111 Alloy Tubing After Cutting With an Alumina Abrasive Wheel.

(Orig. D160112) Mag.: 50X

C1238-2



a) Bent as Cut.

b) 0.040" Ground Off Cut Surfaces Prior to Bending

c) 0.10" Ground Off Cut Surfaces Prior to Bending

Figure 5. Samples of Flattened 0.375-Inch-OD x 0.065-Inch-Wall (0.95-cm-OD x 0.16-cm-Wall) T-111 Alloy Tubing After Cutting With an Alumina Abrasive Wheel Showing the Beneficial Effect on Tube Ductility of Removing the Surface Layer After Cutting. (Orig. C66122323)

C1238-3

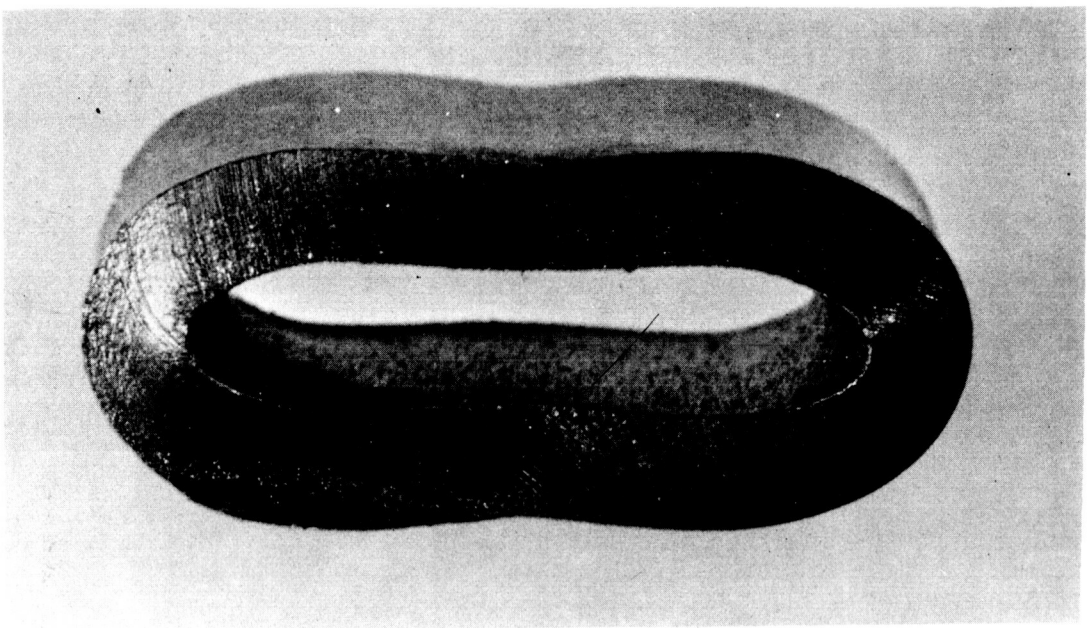


Figure 6. Flattened 0.375-Inch-OD x 0.065-Inch-Wall (0.95-cm-OD x 0.16-cm-Wall) T-111 Alloy Tube After Cutting With an Allison C120KRA Silicon Carbide Abrasive Wheel. The Cut Surface Was Not Ground Back Prior to Flattening. (Orig. C66121614)

C1238-4

IV. LOOP FABRICATION

The overall fabrication sequence for the T-111 Rankine System Corrosion Test Loop is illustrated in Figure 7.

The loop components, as delineated in Figure 7, were the boiler, condenser, lithium heater, turbine simulators, potassium preheater, two electromagnetic (EM) pump ducts, surge tanks, stressed diaphragm pressure transducer, slack diaphragm pressure transducers, and bellows-sealed valves. Each component and the welding procedures employed will be discussed individually below.

A. GENERAL WELDING PROCEDURES

Prior to the welding of the T-111 Corrosion Test Loop, a preliminary qualification test of the welding equipment was conducted according to requirements defined in GE-NSP Specification 03-0025-00-A. This specification requires that the inert gas be initially purified to contain less than 1 ppm each of oxygen and water vapor by volume and that no contamination of the weld metal, as determined by chemical analysis, occurs during the welding cycle.

The mass spectrometer helium analysis system described in an earlier report,[6] was used to monitor the welding chamber helium for oxygen and nitrogen. An electrolytic hygrometer was used to monitor the helium for moisture concentration. The welding chamber and gas analysis system is shown in Figure 8. To accommodate long, straight tubing sections such as the boiler, an extension tube is attached to the basic chamber, as shown in Figure 8. During final loop assembly, the 8-foot (2.4-m)-diameter extension tank, illustrated in Figure 9, was required to contain the large structure.

The general welding procedure consisted of an overnight vacuum pump-down with hot water bakeout (140°F, 60°C) on the chamber. After cooling

(6) Lyon, T. F., Purification and Analysis of Helium for the Welding Chamber, NASA-CR-54168, July 1, 1965, p. 35.

ORIGINAL PAGE IS
OF POOR QUALITY

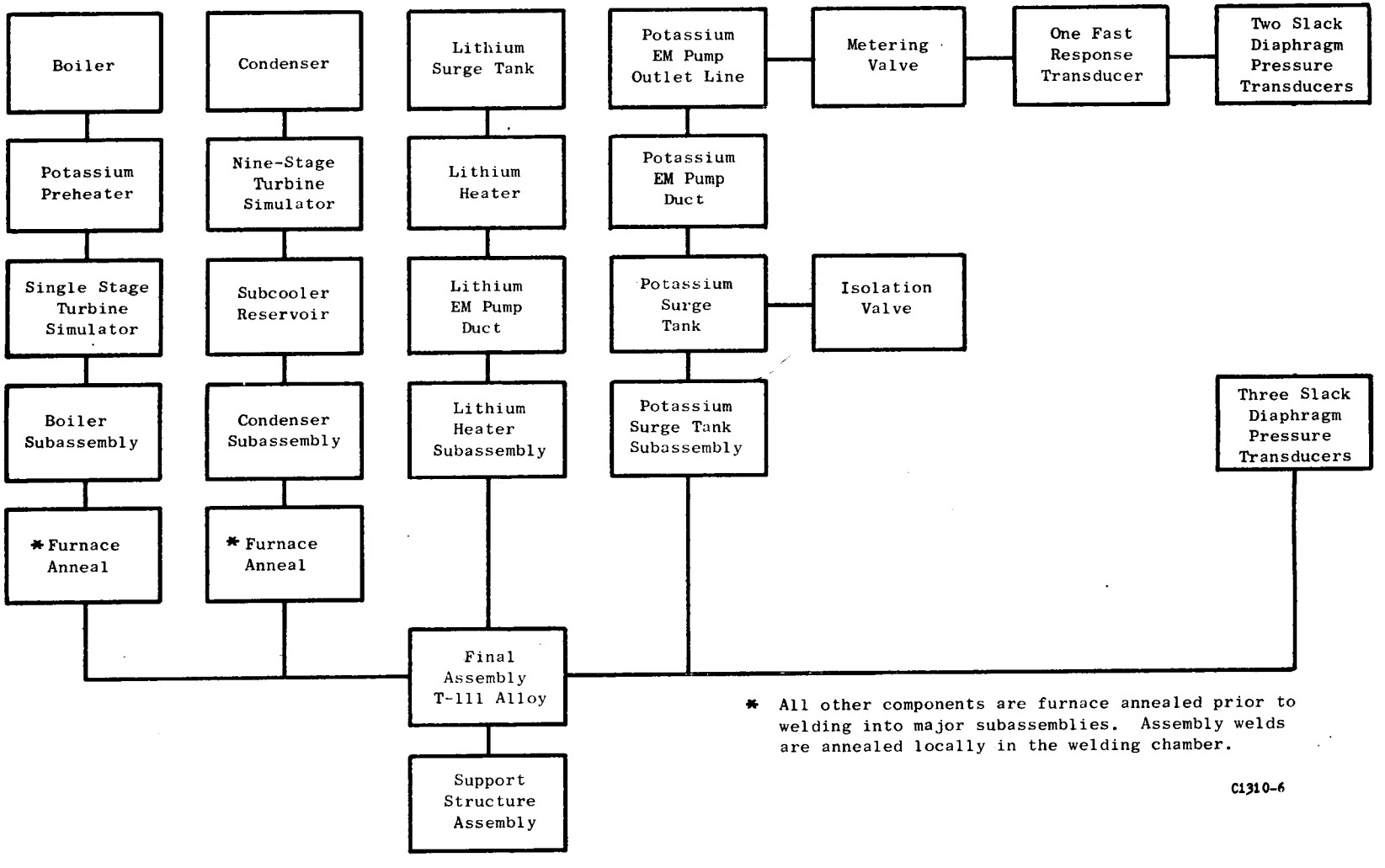


Figure 7. Fabrication Sequence for the T-111 Corrosion Test Loop.

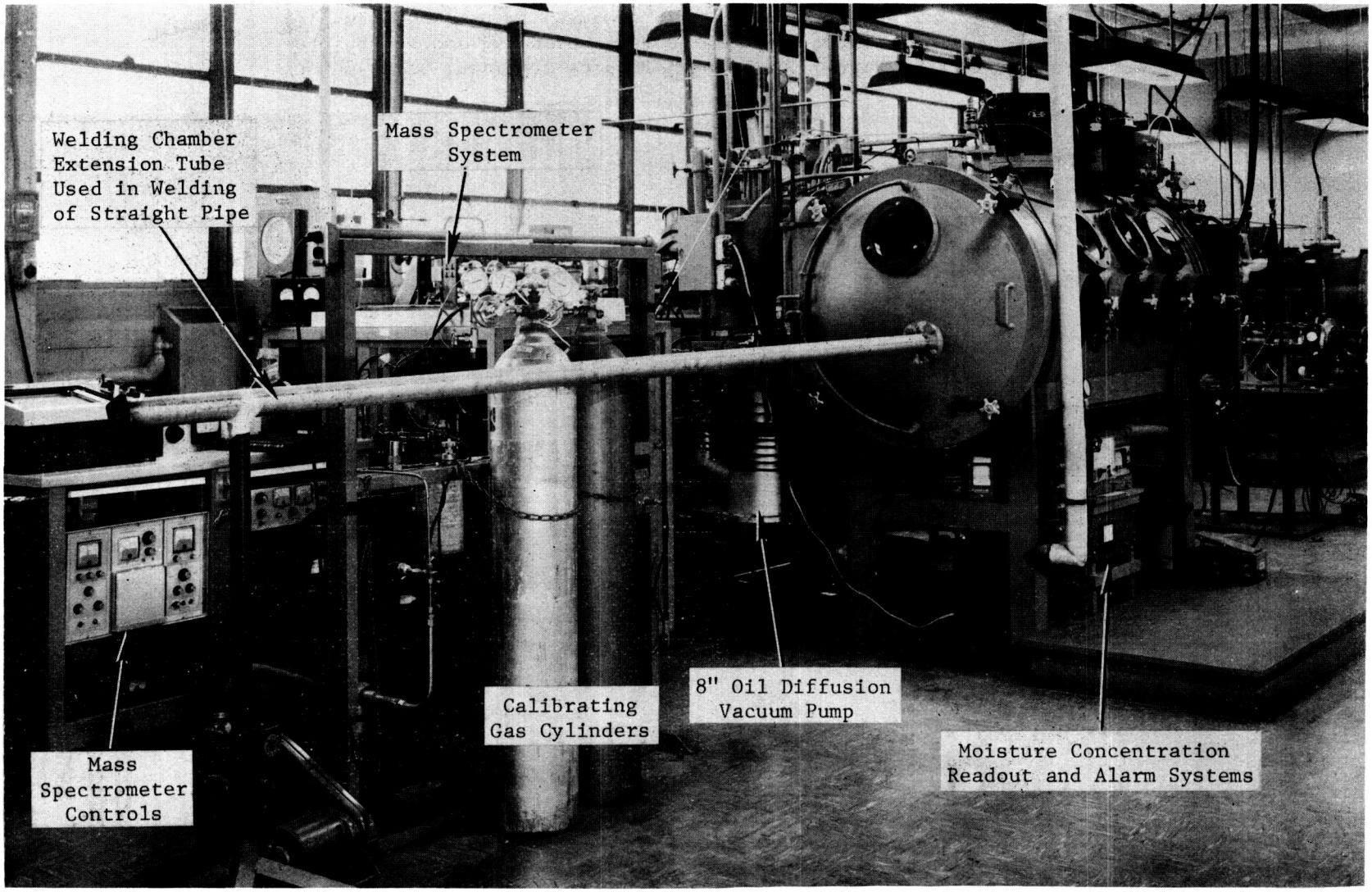


Figure 8. Vacuum-Purge Inert Gas Welding Chamber, 3-Foot (0.9-m) Diameter x 6-Foot (1.8-mm) Long, with Helium Supply and Purity Control System Showing the Pipe Welding Extension Tube Attached to the Chamber Door. (Orig. C67112001)

ORIGINAL PAGE IS
OF POOR QUALITY

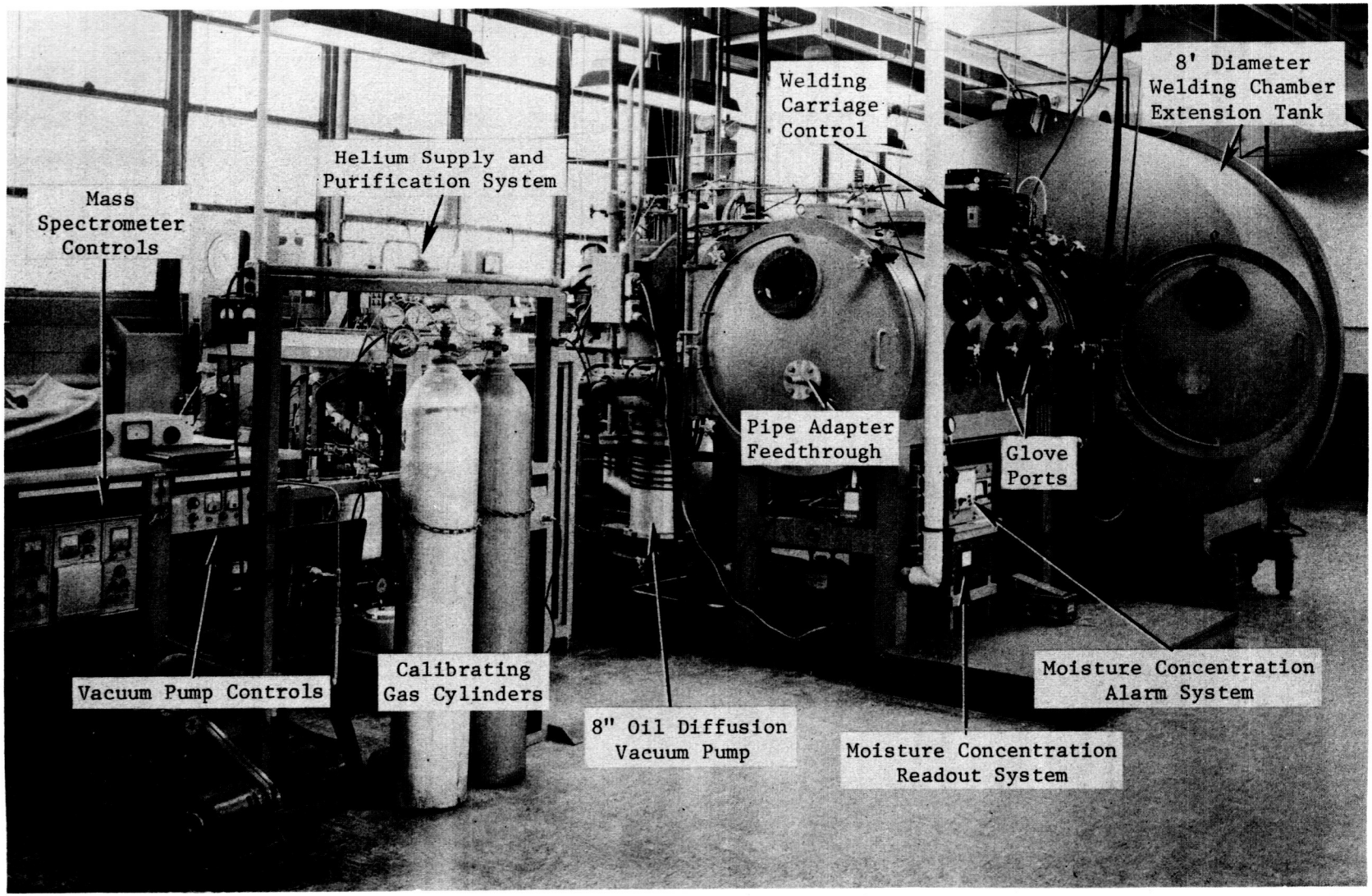


Figure 9. Vacuum-Purge Inert Gas Welding Chamber and Helium Purity Control System with Welding Chamber Extension Tank Attached to 3-Foot (0.9-m)-Diameter x 6-Foot (1.8-m)-Long Welding Chamber. (Orig. C6711228)

the chamber, a pressure of less than 1 x 10^{-5} torr (1.3 x 10^{-3} N/m^2) was attained. The pressure rise rate on the chamber was then taken prior to backfilling with purified helium gas. Welding operations were continued until completed or until gaseous contaminants reached the upper limits of GE-NSP Specification 03-0025-00-A; 5 ppm oxygen, 15 ppm nitrogen, and 20 ppm water vapor (10 ppm water vapor in the case of components to contain lithium).

B. SLACK DIAPHRAGM TRANSDUCERS

Six Taylor Instrument Companies' slack diaphragm transducers were fabricated for the T-111 Corrosion Test Loop. The manufacturing sequence was identical with the procedure described in an earlier report and will not be duplicated here.[7]

The NaK filling operation was performed by Taylor Instrument Companies. A sample of NaK taken by Taylor during the filling was analyzed by GE-NSP to contain less than 3 ppm oxygen.

C. VALVES

The metering and isolation valves were of the same design as those used on the Cb-1Zr Pumped Sodium Loop[7] and Cb-1Zr Rankine System Corrosion Test Loop,[8] and similar fabrication procedures were employed. The valve components for the Cb-1Zr loops are shown in Figure 10. For the T-111 Corrosion Loop, the valve body and piping were fabricated from T-111. T-111 bellows were considered for use in the T-111 Corrosion Loop, and a number of these bellows were successfully fabricated. Because these bellows were the first ones fabricated of this high-strength alloy, some of the detailed information associated with this development is included in Appendix G. Despite the excellent appearance and leak tightness of the T-111 bellows, the decision was made jointly by G. E. and the NASA Program Manager to take the more conservative and demonstrated approach of using Cb-1Zr bellows from the same

(7) Hoffman, E. E. and Holowach, J., Cb-1Zr Pumped Sodium Loop, NASA CR-1135, September 1968.

(8) Hoffman, E. E. and Holowach, J., Cb-1Zr Rankine System Corrosion Test Loop, NASA CR-1509, June 1970.

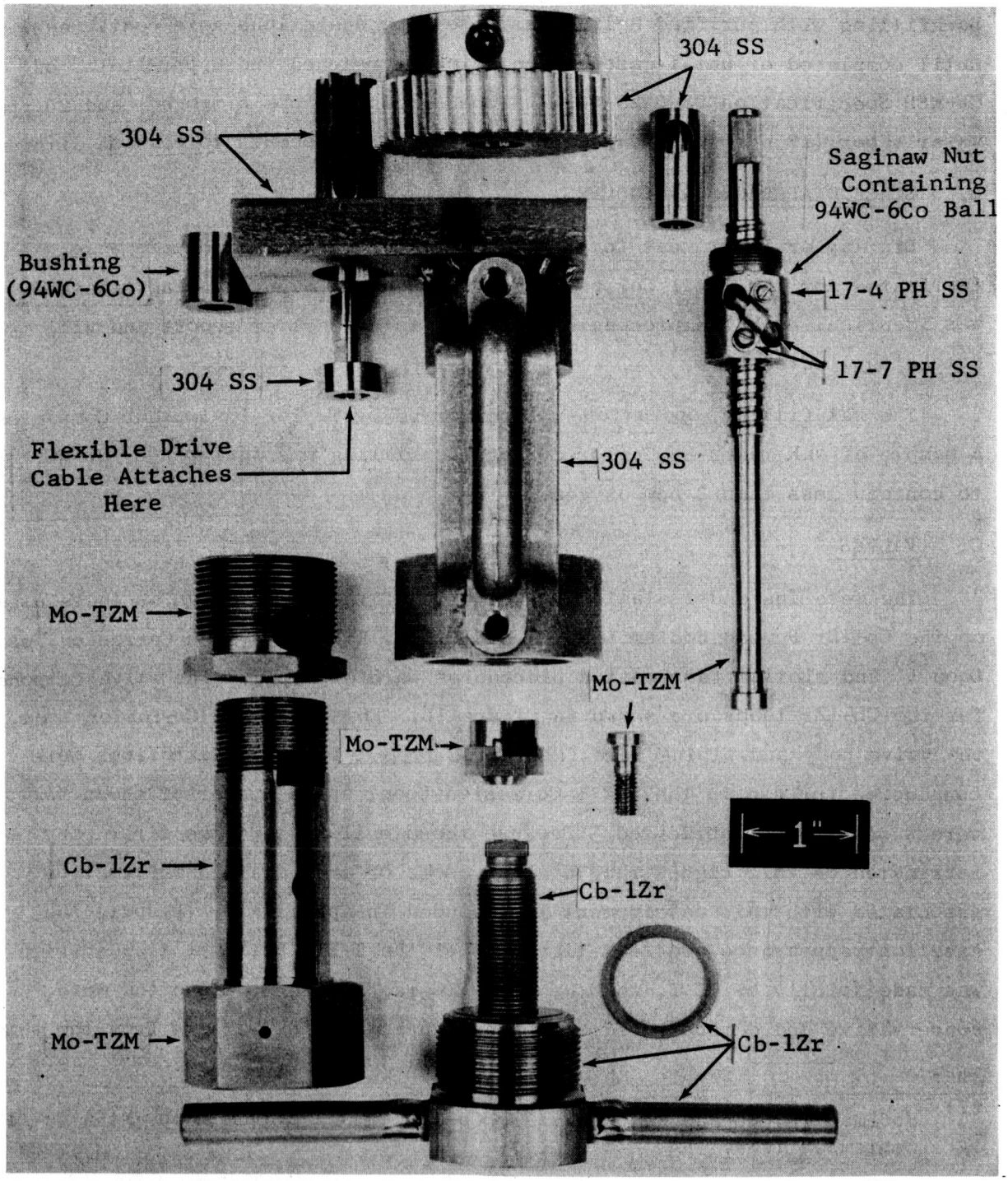


Figure 10. Modified Hoke Valve and Associated Drive Components for the Cb-1Zr Corrosion Loop. (Orig. C65032923)

ORIGINAL PAGE IS
OF POOR QUALITY

lot used in the valves of the successful 5000-hour Cb-1Zr Corrosion Loop Test. Because of the relatively low operating temperature and low stress in the bellows' wall, the higher strength T-111 alloy was not required.

Valve operation during testing of the Cb-1Zr Corrosion Test Loop indicated galling between the stainless steel pinion gear and the tungsten carbide bushing. Mo-TZM was selected as a replacement material for the pinion and spur gears to be used on the T-111 Corrosion Loop valves. At a later date, operation of these valves indicated similar galling problems and the tungsten carbide bushing was replaced with a double-race ball bearing shown in Figure 11. The ball bearing casing was tool steel and the balls were tungsten carbide.

D. LITHIUM AND POTASSIUM EM PUMP DUCTS

The electromagnetic (EM) pump duct principal component is a helical finned duct which is interference fit into an outer wrapper to provide the liquid metal flow channel. After machining and careful dimensional inspection, these interference fits were produced by immersing the finned duct in liquid nitrogen just prior to inserting the duct into the wrapper. The closure welds on the end caps and connectors were made, and each pump duct was final machined on the outside diameters. The complete EM pump ducts are shown in Figure 12.

E. STRESSED DIAPHRAGM PRESSURE TRANSDUCER

The design of stressed diaphragm pressure transducer was the same as that used in the Cb-1Zr Corrosion Loop. The transducer is shown in Figure 13 at various stages during the fabrication sequence.

The housing was first welded to the retainer body which was then welded to the reducer and process tube. This subassembly was then annealed at 2400°F (1316°C) for one hour per GE-NSP Specification 03-0037-00-A.

The diaphragm assembly shown in Figure 13b was produced by first electron beam welding the 0.020-inch (0.05-cm)-diameter W-25Re wire to the T-111 alloy probe mount. A second electron beam weld attached the probe mount to the T-222 alloy diaphragm. The diaphragm was then positioned between the housing and housing cap and electron beam welded. As an added precaution, an electron beam weld was made between the housing and

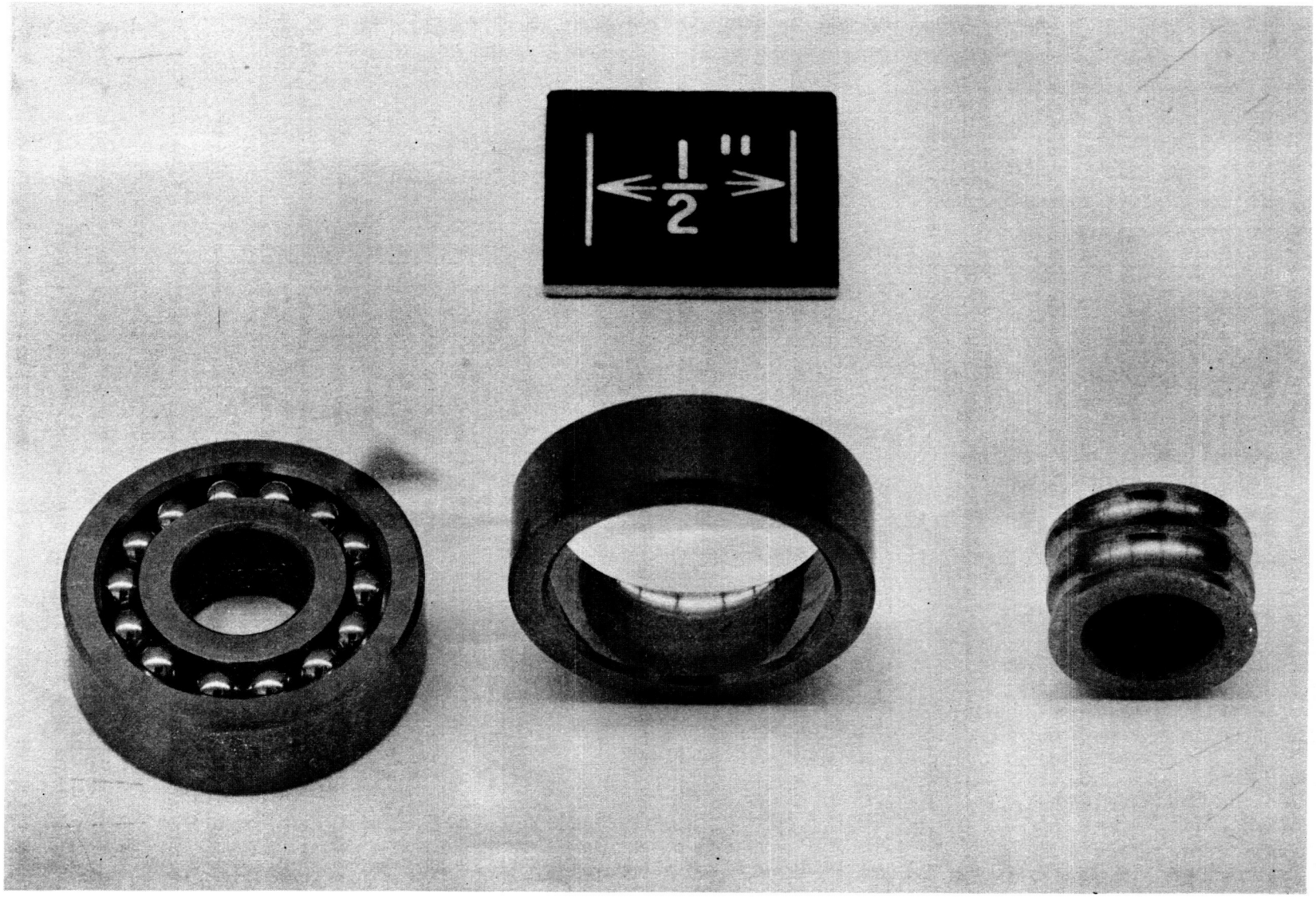


Figure 11. Double-Race Ball Bearing Used in Metering and Isolation Valves of the T-111 Corrosion Test Loop. Casing is Tool Steel and Balls are Tungsten Carbide. (Orig. P69-1-19C)

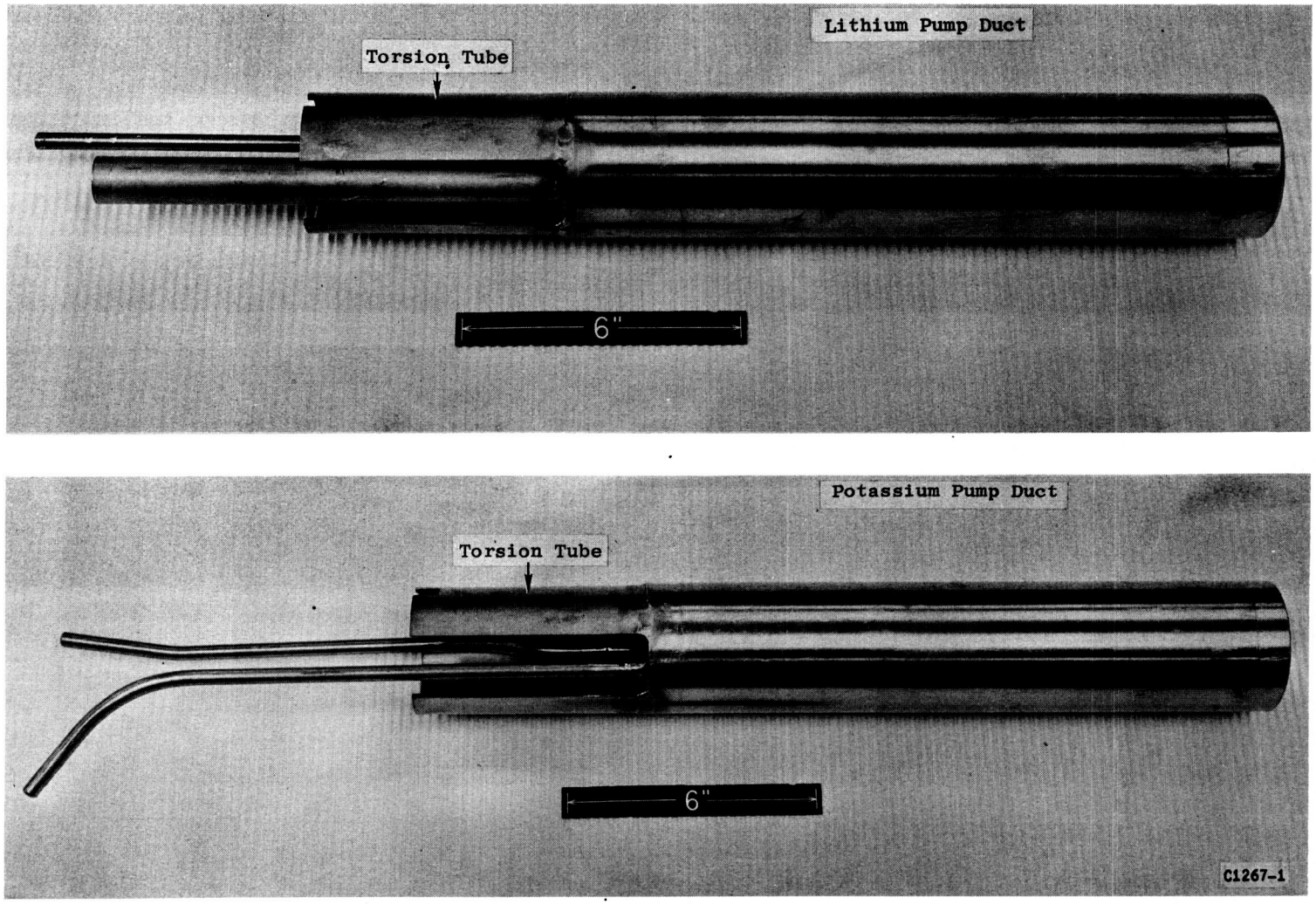
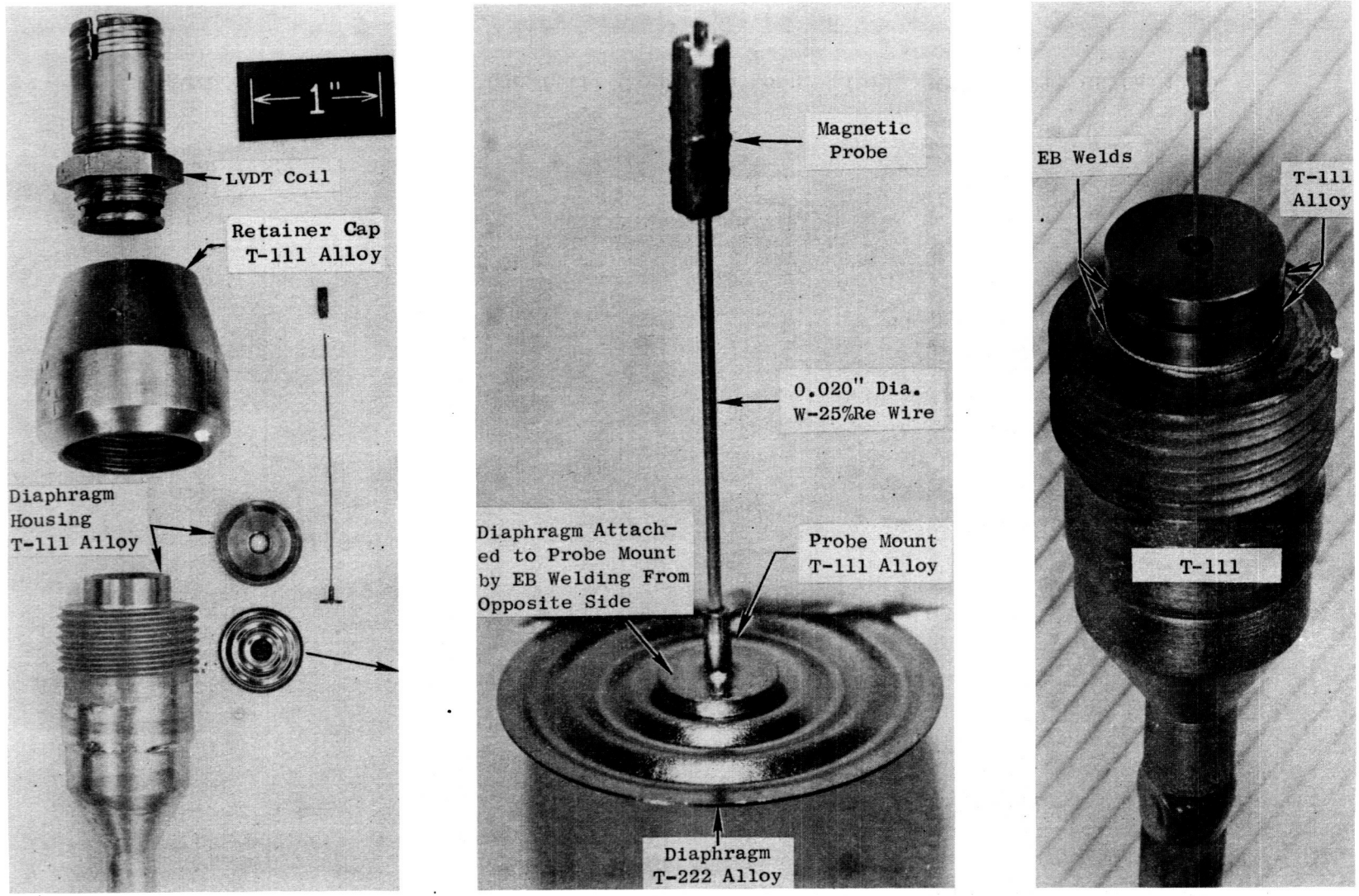


Figure 12. EM Pump Ducts for T-111 Corrosion Loop. (Orig. C67081421, C67081425)



a) b) c)

Figure 13. Stressed Diaphragm Pressure Transducer for the T-111 Corrosion Test Loop at Various Stages During Fabrication. (Orig. C65062193)

the retainer body on the outside diameter, which, in combination with the internal tungsten inert gas weld, effected a double seal between these components.

The final fabrication step was the brazing of the magnetic probe to the 0.020-inch (0.05-cm)-diameter W-25Re wire. Brazing was accomplished using localized heating with a graphite-tipped heater probe under high-purity argon in the welding chamber. The brazing alloy (72Ag-28Cu) was applied to the joint manually in wire form. The completed assembly, shown in Figure 13c, was mass spectrometer leak-tested successfully and submitted to instrumentation for room temperature calibration prior to installation in the loop.

F. POTASSIUM AND LITHIUM SURGE TANKS

The T-111 Corrosion Loop used the Cb-1Zr surge tanks which had been used previously on the Cb-1Zr Rankine System Corrosion Test Loop.[8]

1. T-111-to-Cb-1Zr Welding Study

The transition to T-111 alloy occurred between the T-111 alloy loop fill tubes and the Cb-1Zr alloy surge tanks. Although the welding requirements for the T-111 and Cb-1Zr alloys are quite similar, the selection of a weld filler wire and postweld annealing treatment required a brief welding study. Tungsten inert gas welds were made between both 0.040-inch (1.0-mm)- and 0.080-inch (2.0-mm)-thick sheets of T-111 and Cb-1Zr materials to provide samples required for the study of weldment bend characteristics after exposure to various postweld thermal cycles. Those welds between the 0.040-inch (1.0-mm)-thick sheet were made by the automatic weld process without filler additions, while those between the 0.080-inch (2.0-mm) stock were made by the manual process using either Cb-1Zr or T-111 filler material. One- and two-hour postweld annealing treatments at 2200°F (1204°C), 2300°F (1260°C), and 2400°F (1316°C) were performed on several automatic weld samples, while additional samples were aged at 1500°F (816°C) for 50 hours after welding. Other samples of these automatic welds were then exposed to both the various annealing treatments and the 1500°F (816°C) age treatment. Subsequent bend testing (1t bend radius) at room temperature and -100°F (-73°C) indicated that optimum weld stability was associated with the 2300°F and 2400°F (1260°C and 1316°C) treatments, as shown in Table X. Hence, these overaging

ORIGINAL PAGE IS
OF POOR QUALITY

TABLE X

SUMMARY OF BEND AND HARDNESS DATA OF AGED T-111 TO Cb-1Zr WELD SPECIMENS

	Filler Material	Heat Treat Condition[1]	Bend Test Results[2]		Hardness, Knoop (100-gram Test Load)		
			Room Temp.	-100°F	T-111 HAZ[3]	Weld	Cb-1Zr HAZ[3]
I.							
Automatic Welds (0.040-inch-thick sheet)	None	1500°F/50 hr	B(70°-90°) (Cb HAZ)		273	256	241
		2200°F/1 hr	D				
		2200°F/2 hr	D				
		2300°F/1 hr	D		250	142	123
		2300°F/2 hr	D				
		2400°F/1 hr	D		227	136	115
		2200°F/1 hr + 1500°F/50 hr	D	B(70°-90°) (Cb HAZ)			
		2200°F/2 hr + 1500°F/50 hr		D			
		2300°F/1 hr + 1500°F/50 hr	D	D	281	150	115
		2300°F/2 hr + 1500°F/50 hr	D	D			
		2400°F/1 hr + 1500°F/50 hr	D	D	277	153	129
II.							
Manual Welds (0.080-inch-thick sheet)	T-111	1500°F/50 hr	B(5°-10° weld)		265	320	230
	T-111	2300°F/1 hr	D				
	T-111	2400°F/1 hr	D				
	T-111	2300°F/1 hr + 1500°F/50 hr	B(10°-20° weld)		263	196	115
	T-111	2400°F/1 hr + 1500°F/50 hr	B(10°-20° weld)		235	250	121
	Cb-1Zr	1500°F/50 hr	B(30°-40°) (Cb HAZ)		240	218	224
	Cb-1Zr	2300°F/1 hr	D				
	Cb-1Zr	2400°F/1 hr	D				
	Cb-1Zr	2300°F/1 hr + 1500°F/50 hr	D		277	144	138
	Cb-1Zr	2400°F/1 hr + 1500°F/50 hr	D		219	139	136

(1) Temperatures: 1500°F (816°C); 2200°F (1204°C); 2300°F (1260°C); 2400°F (1316°C).

(2) All specimens bent over a 1T radius. D indicates ductile - full bend through 90° to 105° without fracture; B indicates brittle - numbers in parenthesis indicate approximate bend angle at failure.

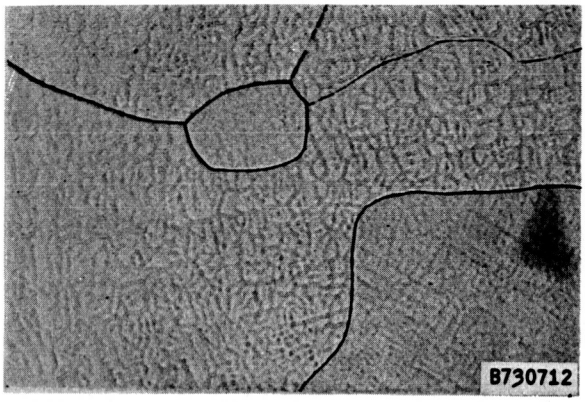
(3) HAZ = heat-affected zone.

temperatures were selected for postweld treatments on the manual weld samples. Samples of the manual welds were given one-hour heat treatments at 2300°F and 2400°F (1260°C and 1316°C), aging treatments of 1500°F (816°C) for 50 hours, while others were both overaged and reaged at these times and temperatures. The bend data (Table X) for these welds pointed out that the selected postweld annealing treatments successfully stabilized those welds prepared with Cb-1Zr filler; while samples made with T-111 filler were still subject to additional aging during the 1500°F (816°C)/50-hour reage cycle. Hardness testing was also performed on selected samples to provide additional clarification of the bend test results. The hardness data obtained are also summarized in Table X.

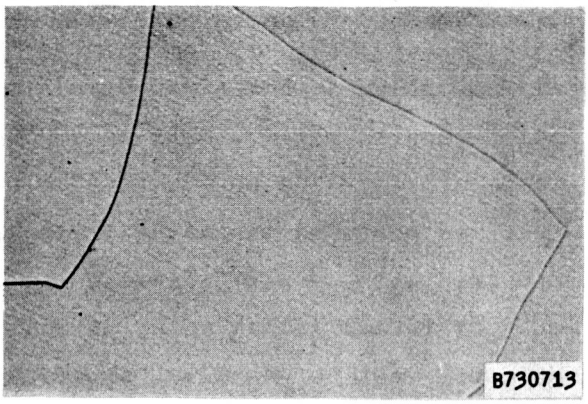
Metallographic examination of T-111-to-Cb-1Zr weld specimens provided a plausible explanation for the differences in hardness and bend ductility.

Representative photomicrographs (weld zone and Cb-1Zr heat-affected zone) of the T-111-to-Cb-1Zr automatic welds of 0.040-inch (0.1-cm)-thick sheet specimens in selected heat treat conditions are shown in Figure 14. The lower hardness of the overaged specimens was associated with significant homogenization in the fusion zone and random precipitation of second-phase particles in the Cb-1Zr heat-affected zone. No obvious microstructural changes were noted in the heat-affected zone of the T-111 alloy as a result of the different heat treatments.

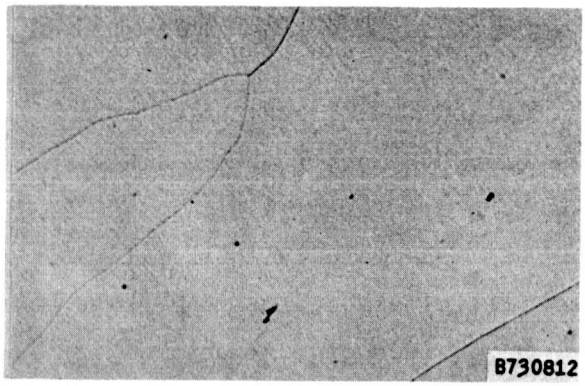
Microstructure comparisons of the manual weld samples of 0.080-inch (0.2-cm)-thick plate after the various heat treatments shown in Figure 15 revealed the probable cause for the superior stability of those welds prepared with Cb-1Zr filler. The 2300°F (1260°C) for one-hour and 2400°F (1316°C) for one-hour heat treatments were capable of significant homogenization of the fusion zones of these welds, while the same thermal cycles apparently had little effect on microstructures of the welds prepared with T-111 filler. Also, the higher welding temperatures associated with the use of T-111 filler may have caused more relative solutioning of the base Cb-1Zr into the fusion zone leading to depressed aging reaction rates and apparent lesser stability in that area.



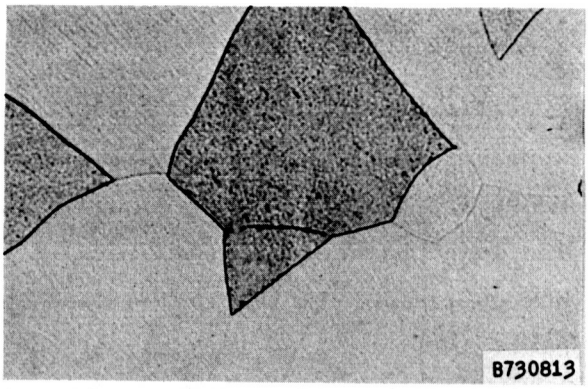
1500°F/50 Hr.



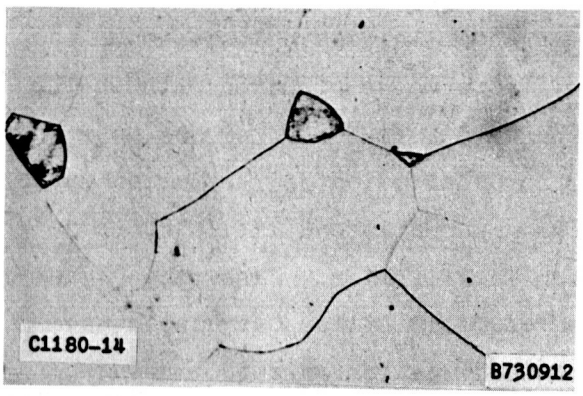
1500°F/50 Hr.



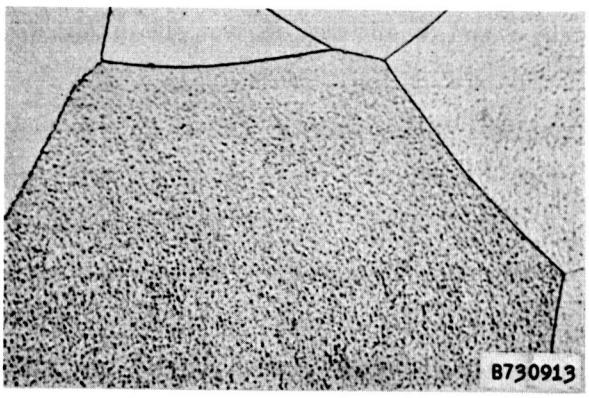
2300°F/1 Hr.



2300°F/1 Hr.



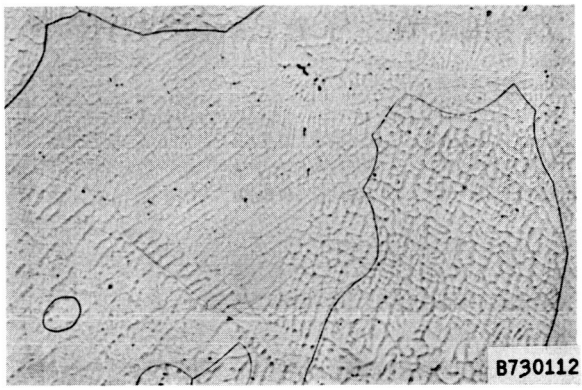
2400°F/1 Hr.



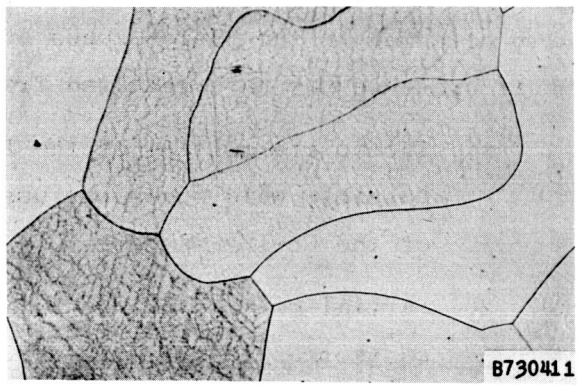
2400°F/1 Hr.

Figure 14. Microstructures of Automatic Weldments of Cb-1Zr to T-111 Prepared Without Filler Additions Following Various Postweld Heat Treatments.

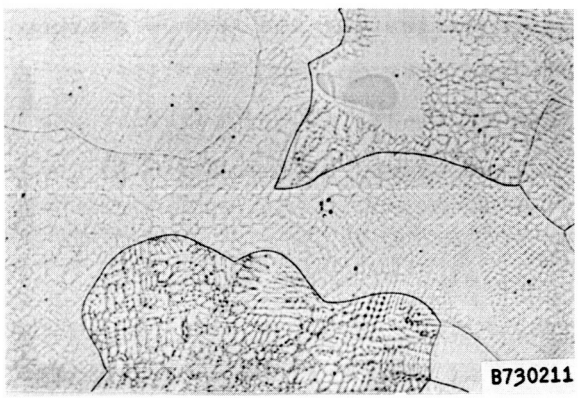
Etchant: 30gmNH_4F-50mlHNO_3-20mlH_2O Mag.: 250X



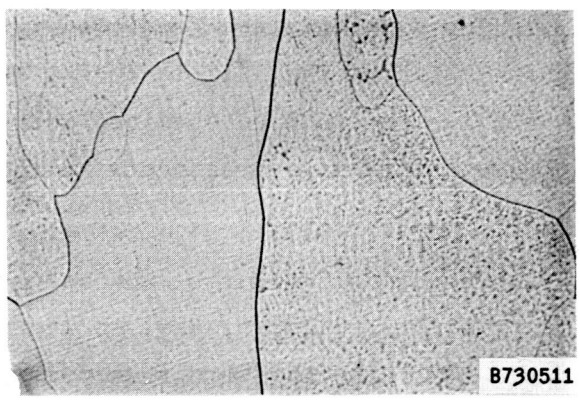
1500°F/50 Hr.



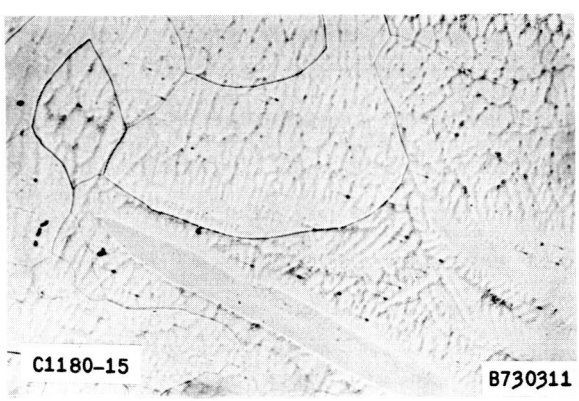
1500°F/50 Hr.



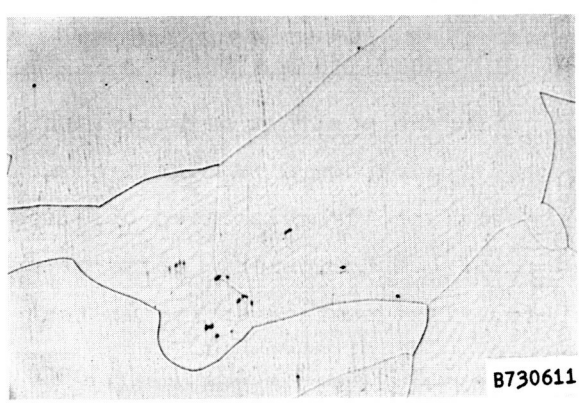
2300°F/1 Hr. + 1500°F/50 Hr.



2300°F/ 1 Hr. + 1500°F/50 Hr.



2400°F/1 Hr. + 1500°F/50 Hr.



2400°F/1 Hr. + 1500°F/50 Hr.

Figure 15. Microstructures of Manual Weldments of Cb-1Zr to T-111 Prepared With Cb-1Zr and T-111 Filler Material Following Various Postweld Heat Treatments.

Etchant: 30gmHN_4F-50mlHNO_3-20mlH_2O Mag.: 250X

Small particles of T-111 alloy, as exemplified in Figure 16, were also detected in the fusion zones of welds prepared with T-111 alloy filler. Their presence may have resulted from the following:

1. Incomplete melting of the filler metal because the lowest possible weld power was used to minimize melting distortion of the Cb-1Zr member;

2. Partial melting of the T-111 base metal caused by momentary contact of the welding arc.

These particles could act as stress concentrations during bending, thereby lowering the ductility of the weld.

The data obtained from bend testing, hardness testing and microstructural examination of the T-111-to-Cb-1Zr welds indicated that optimum stability of manual welds could be obtained through the use of Cb-1Zr filler material and postweld annealing treatments in the 2300°F (1260°C) and 2400°F (1316°C) temperature range.

The potassium surge tank assembly was completed with the welding of the T-111 alloy isolation valve to the Cb-1Zr tank. This assembly and the lithium surge tank assembly were then postweld annealed at 2200°F (1204°C) for one hour in the Union Carbide Company's ABAR furnace at Kokomo, Indiana, in accordance with GE-NSP Specification 03-0037-00-A.

G. BOILER

1. Polishing and Pickling of T-111 Tantalum Alloy Boiler Tubing

In the posttest metallographic evaluation of loop components following long-time exposure to alkali metals, it is often difficult to determine if the surface irregularities observed on the inner surface of tube wall are a result of corrosion. Quite often, the most that can be stated is that the before-test surface and after-test surface are similar in appearance. In order to permit a more precise determination of the extent of attack, the smoothness of the ID surface of portions of the T-111 alloy boiler tubing was improved by polishing with 120- and 600-grit alumina cloth followed by pickling in accordance with NSP Specification No. 03-0010-00-C, "Chemical Cleaning of Columbium, Tantalum, and Their Alloys."

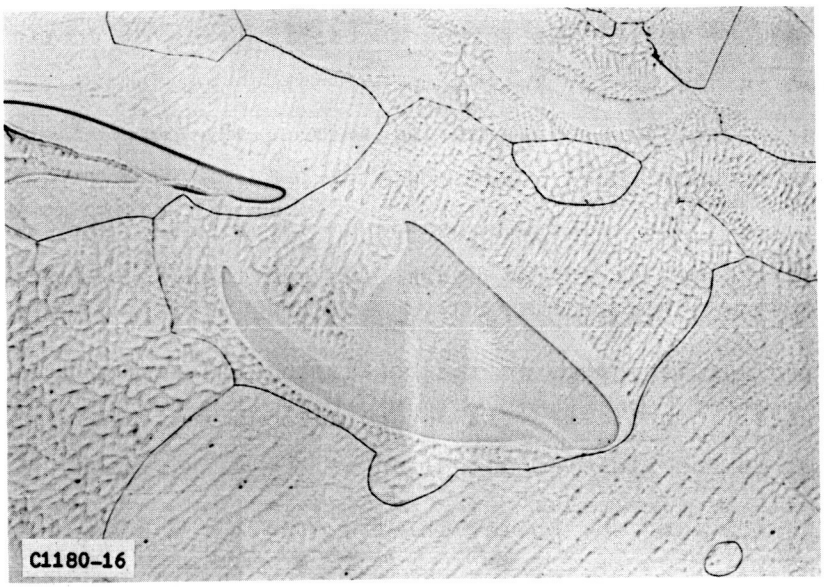


Figure 16. Cb-1Zr-to-T-111 Weldments Prepared With T-111 Filler Showing T-111 Particle Which Was Washed into the Fusion Zone. Specimen Was Heat-Treated at 1500°F (816°C) for 50 Hours Following Welding. (B730111)

Etchant: 30gm NH_4F-50ml HNO_3-20ml H_2O Mag.: 100X

The smoothness of the ID surface of transverse tube specimens in the as-received, as-received and pickled, as-polished, and as-polished plus pickled conditions is shown in Figure 17. The inside surface of the tube specimens was polished by means of a portable drill with the alumina grit cloth inserted in a slotted rod. The ID of the tube was polished until 0.001 inch (0.025 mm) was removed from the surface. As shown in Figure 17, the combination polishing and pickling treatment resulted in an essentially smooth surface free of flowed metal.

The tube-in-tube boiler was formed successfully using similar techniques to that employed in the Cb-1Zr Test Loop.[8] The sugar which was used to pack the internal tube and annulus during forming was removed by mechanical vibration. When no additional sugar could be removed, a deionized water flush was initiated. The water was heated to 150°F (66°C) and was allowed to flush through the boiler for 15 hours. An additional cold water flush for 30 minutes was used for the final rinse. At this time water samples were equilibrated for two hours in the boiler and tested for sugar using the Molisch[9] test. Duplicate test determinations indicated less than 50 ppm sugar, which is the limit of detection of the method used.

The final welding of the boiler inlet and outlet connectors was then completed. The assembled boiler and helical plug insert are shown in Figure 18. This component was subsequently incorporated into the boiler assembly, which included the potassium preheater and single-stage turbine simulator.

H. POTASSIUM PREHEATER AND LITHIUM HEATER

The heater configurations are shown after welding in Figures 19 and 20. The electrodes, as shown in Figure 21, illustrate the welding of the thermocouple wells and the joint between the electrode and electrode bar. Full penetration butt welds were then used to join the electrodes to the heater coil tubing.

---

(9) Cheronis, N. D., Techniques of Organic Chemistry, Interscience Publishers, Inc., New York, N. Y., 1954, p. 466-467.

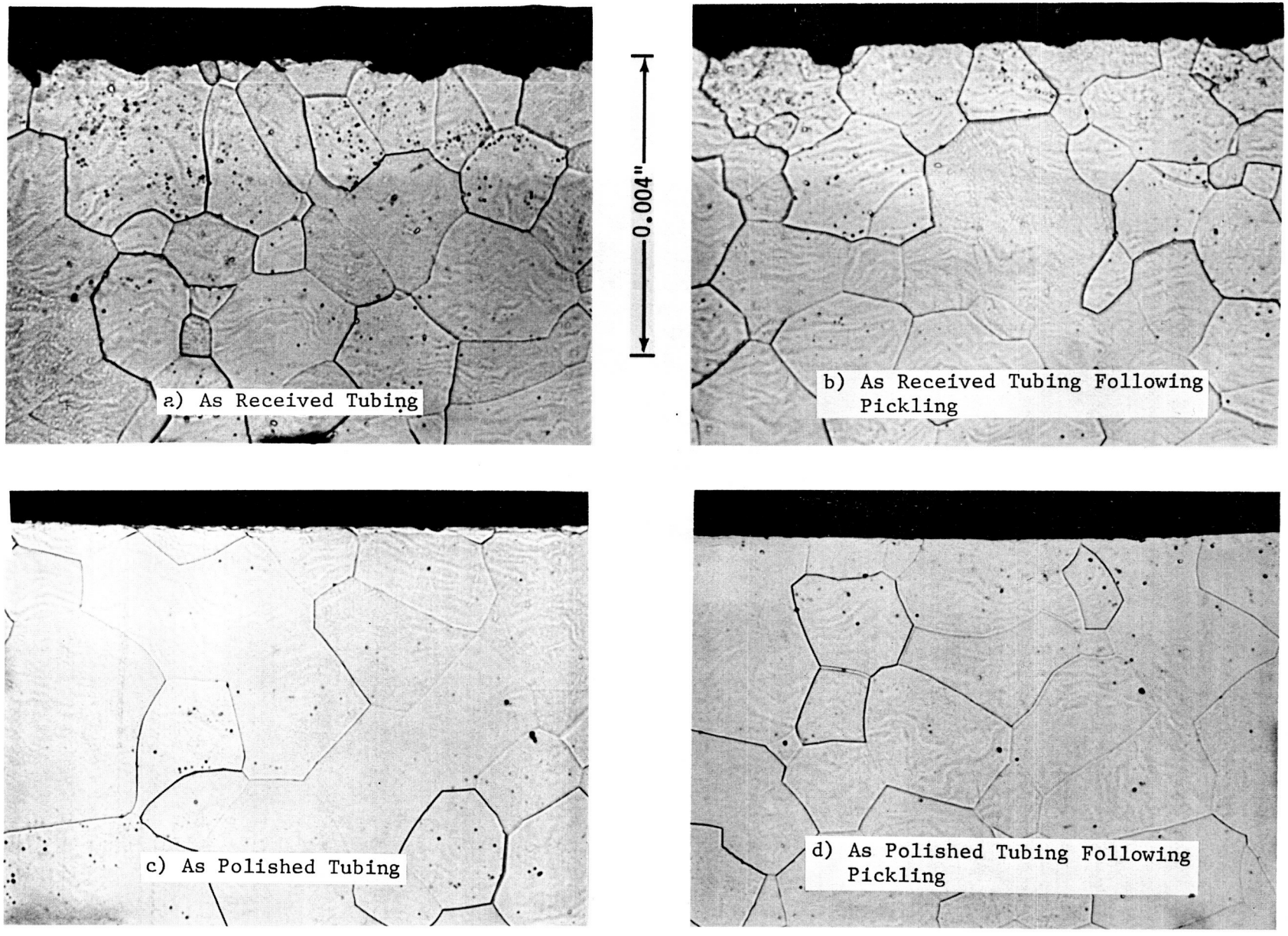


Figure 17. Effect of Polishing and Pickling on the Surface Roughness of T-111 Tantalum Alloy Tubing. Polishing to Remove 0.001 Inch (0.002 cm) of the Tube Wall Performed With 120- and 600-Grit Alumina Cloth. Specimens Pickled for Five Minutes in $HF-HNO_3-H_2SO_4-H_2O$ (1-4-1-2, Parts by Volume).

Metallographic Etchant: $30gNH_4F-50mlHNO_3-20mlH_2O$ Mag.: 500X

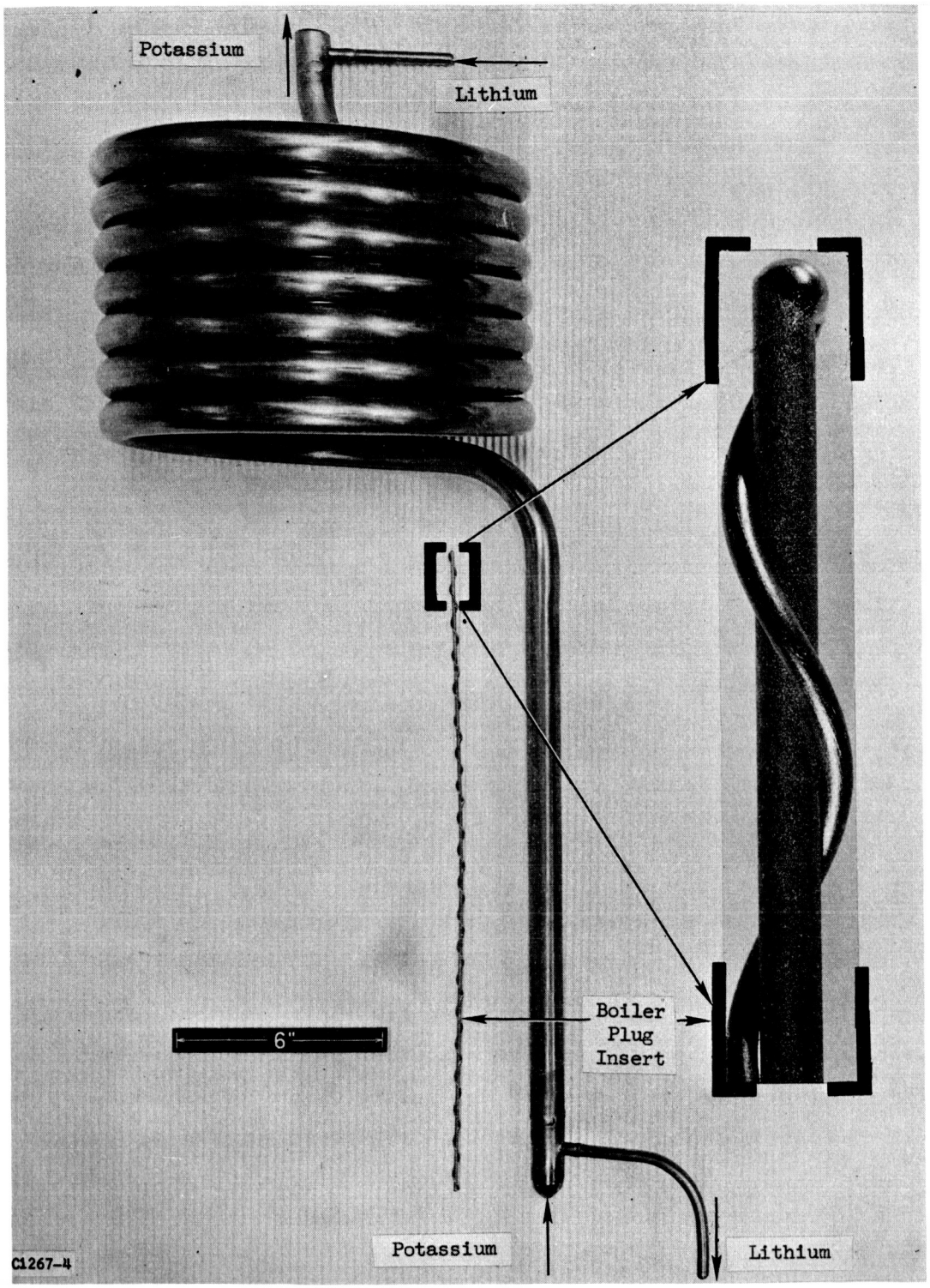


Figure 18. Tube-in-Tube Boiler of T-111 Corrosion Loop Prior to Insertion of the Boiler Plug. (Orig. C67071832, C67072436)

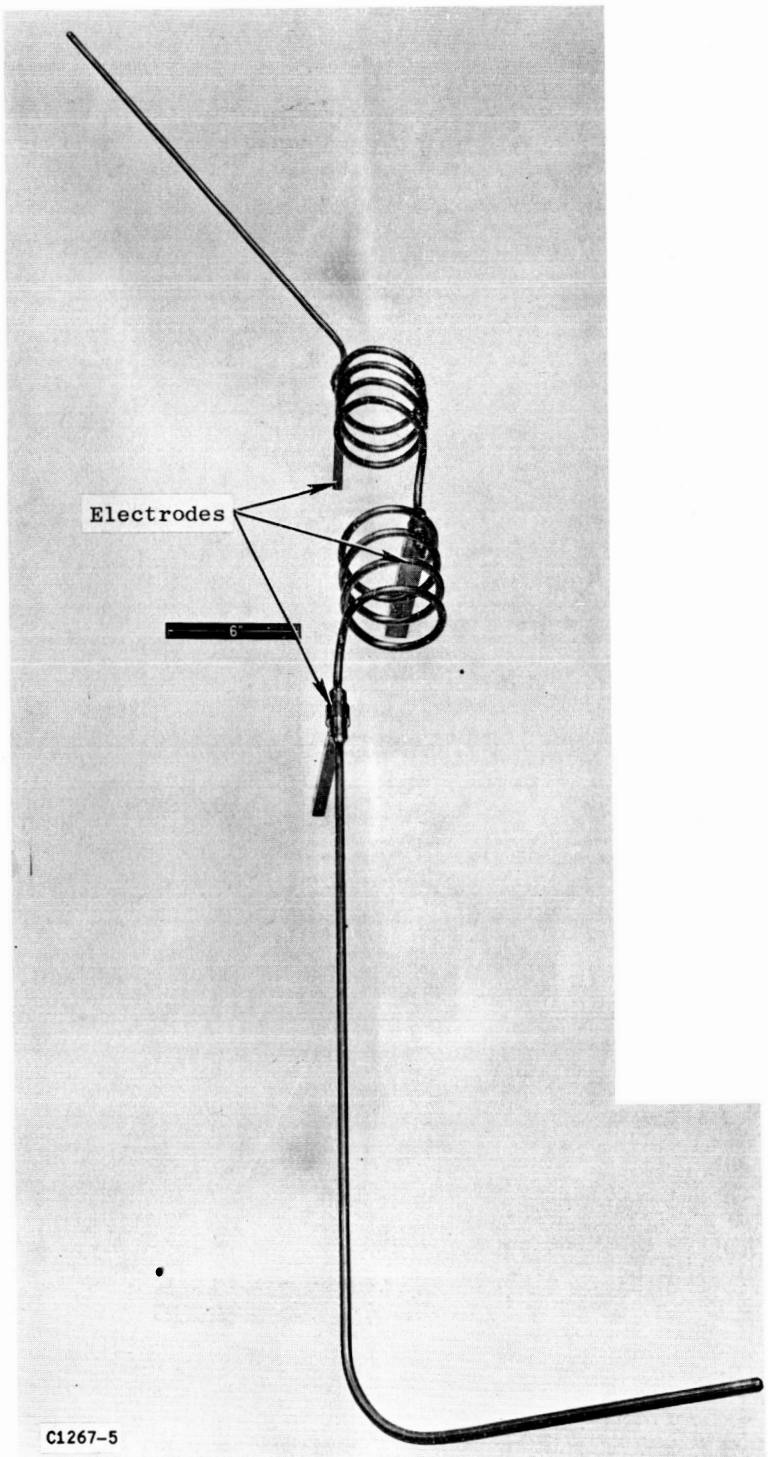


Figure 19. Lithium Heater Assembly of T-111 Corrosion Loop. (Orig. C67071830)

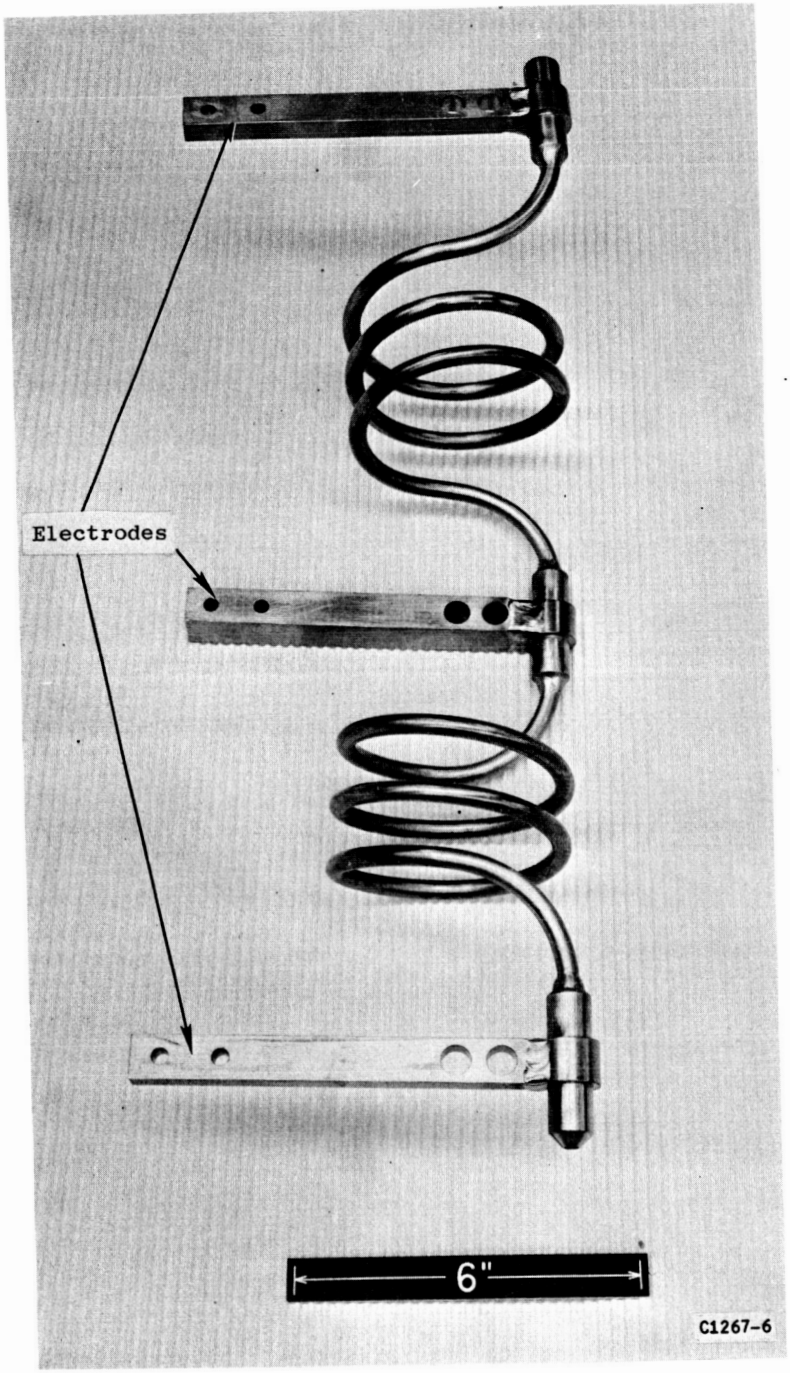
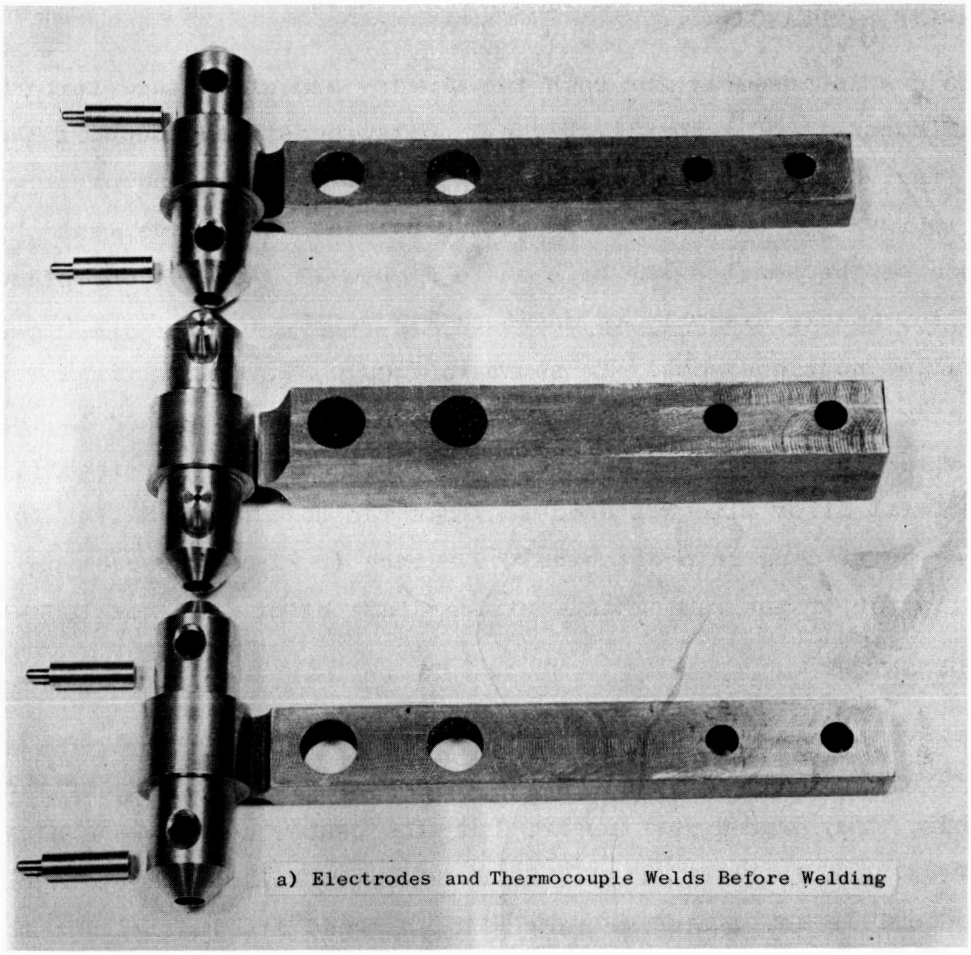


Figure 20. Potassium Preheater of T-111 Corrosion Loop. (Orig. C67052559)



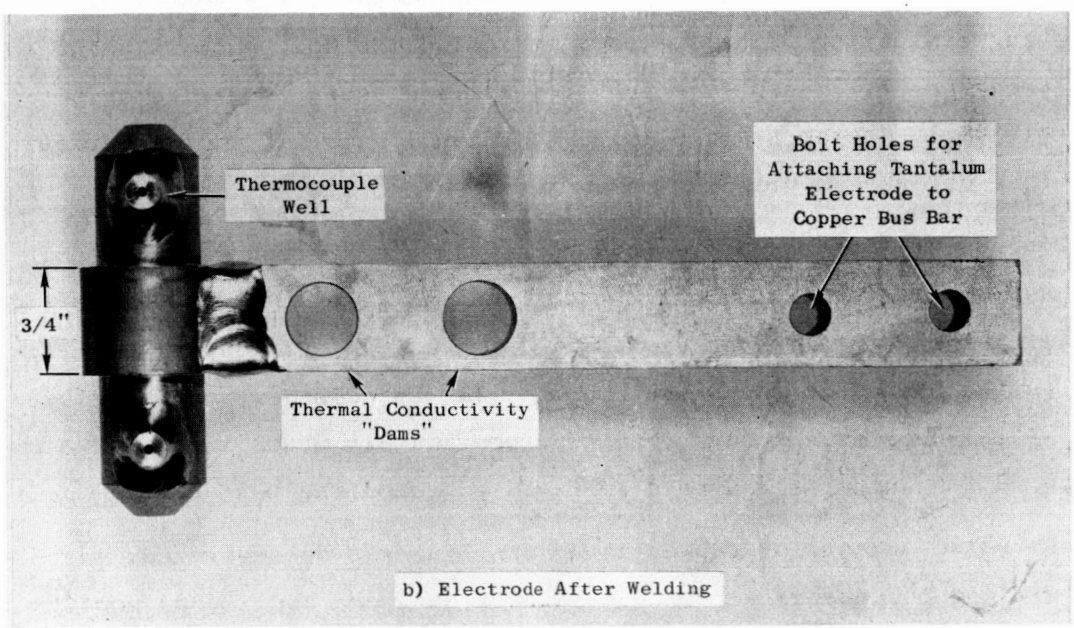


Figure 21. T-111 Alloy Preheater Coil Electrodes for the T-111 Corrosion Test Loop.

ORIGINAL PAGE IS
OF POOR QUALITY

I. TURBINE SIMULATOR

Each nozzle assembly for both the single- and nine-stage turbine simulator consists of a nozzle, blade, and two pads which support the blade. Final hand-polishing using 30- and 15-micron diamond paste was used to improve the surface finish of the nozzles. The excellent appearance of the nozzles may be seen in Figure 22. The second-stage, Mo-TZC alloy nozzle assembly is shown in Figure 23, and the sixth-stage, Cb-132M alloy nozzle assembly is shown in Figure 24. After final weighing and cleaning operations, the nozzle assemblies were positioned in the turbine simulator casings as depicted in Figure 25. A 0.062-inch (1.6-mm)-diameter T-111 alloy wire was used to align the nozzle assemblies inside the casing by sliding into matching 0.032-inch (0.81-mm) grooves on the inside diameter of the casing and outside diameter of each nozzle assembly.

J. CONDENSER

A 1-inch x 2-inch x 32-inch-long (2.5-cm x 5.0-cm x 81-cm-long), T-111 alloy bar was committed for evaluation of drilling procedures for the center hole. Two procedures for drilling the center hole were evaluated. Since initial gun drilling trials had resulted in failure due to a breakage of carbide drills and excessive wear of high-speed steel drills, a sample of T-111 alloy was supplied to Standard Tool Company, a producer of gun drills for evaluation. Their report indicated the most success using a high-speed gun drill head to which they applied a positive rake chip break along with a 10-degree stack point. Additional material would be required to further define gun drilling parameters.

Concurrent with the above investigation, one 32-inch (81-cm)-long condenser bar was committed for conventional drilling. A 0.406-inch (1.03-cm)-diameter hole was drilled successfully using a long, fluted twist drill with an extension brazed to the shank. The drill was ground with an included angle of 135 degrees. A hand feed of approximately 0.003 inch (0.076 mm) per revolution and a drill speed of 6 SFM produced the best cutting action.

After the success of conventional drilling was demonstrated, the 63-inch (160-cm)-long condenser bar was cut in half, and one additional section was

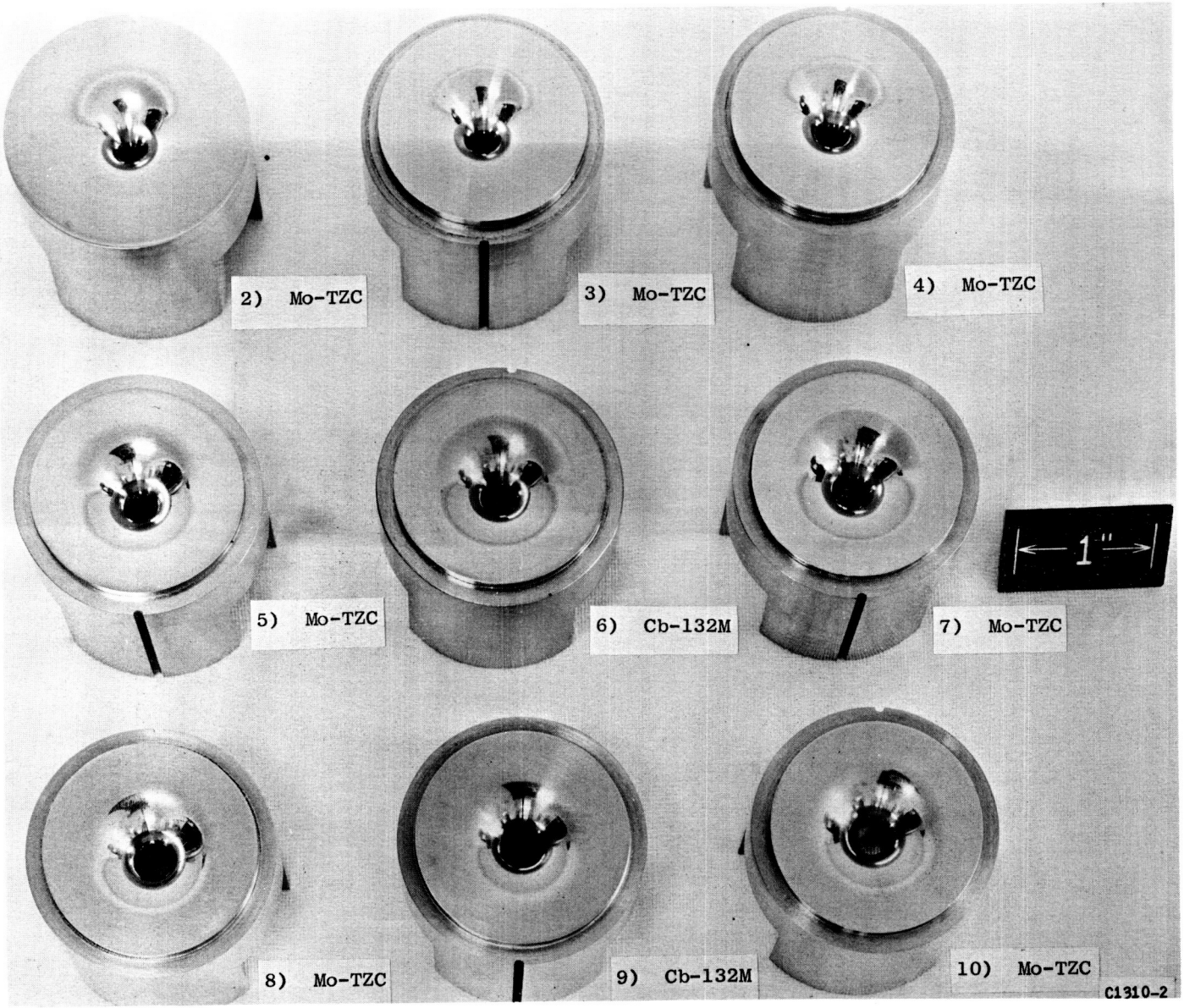
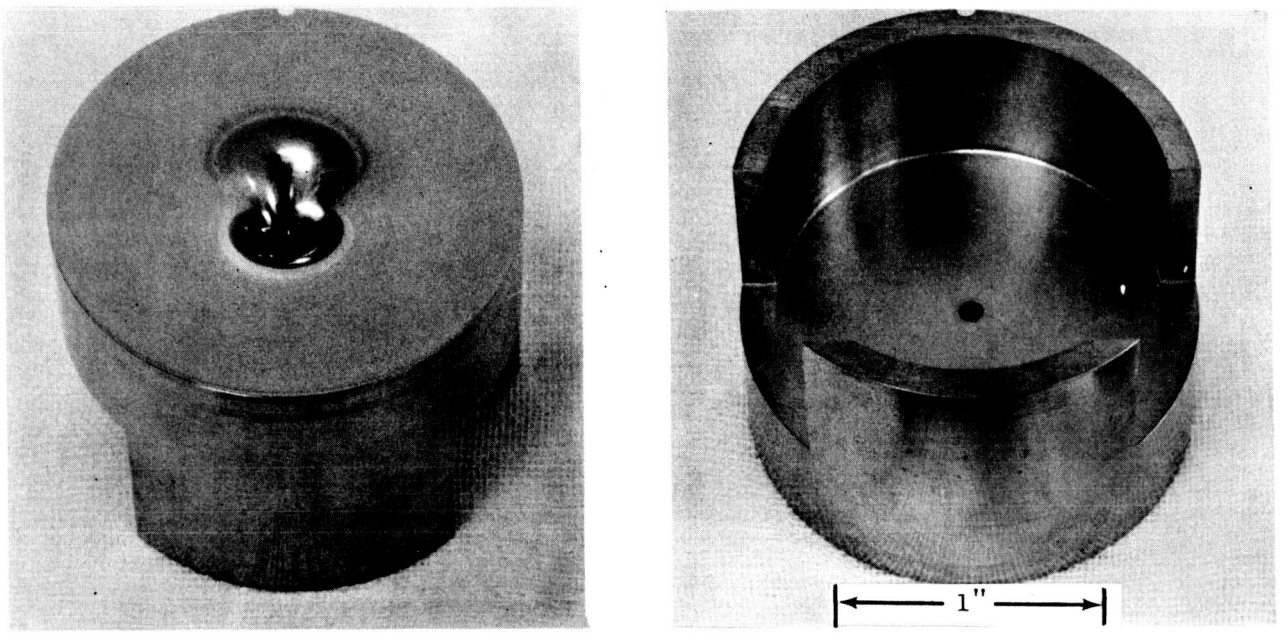


Figure 22. Test Nozzles for Turbine Simulator (Stages 2 to 10) of the T-111 Corrosion Test Loop Prior to Assembly. (Orig. 67090663)



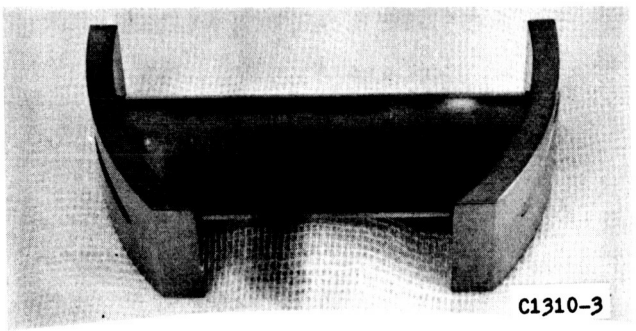


Figure 23. Entrance and Exit Side of the Nozzle and the Blade Assembly of Second Stage (Mo-TZC) of the Turbine Simulator.
(Orig. C67090666, C6709670)

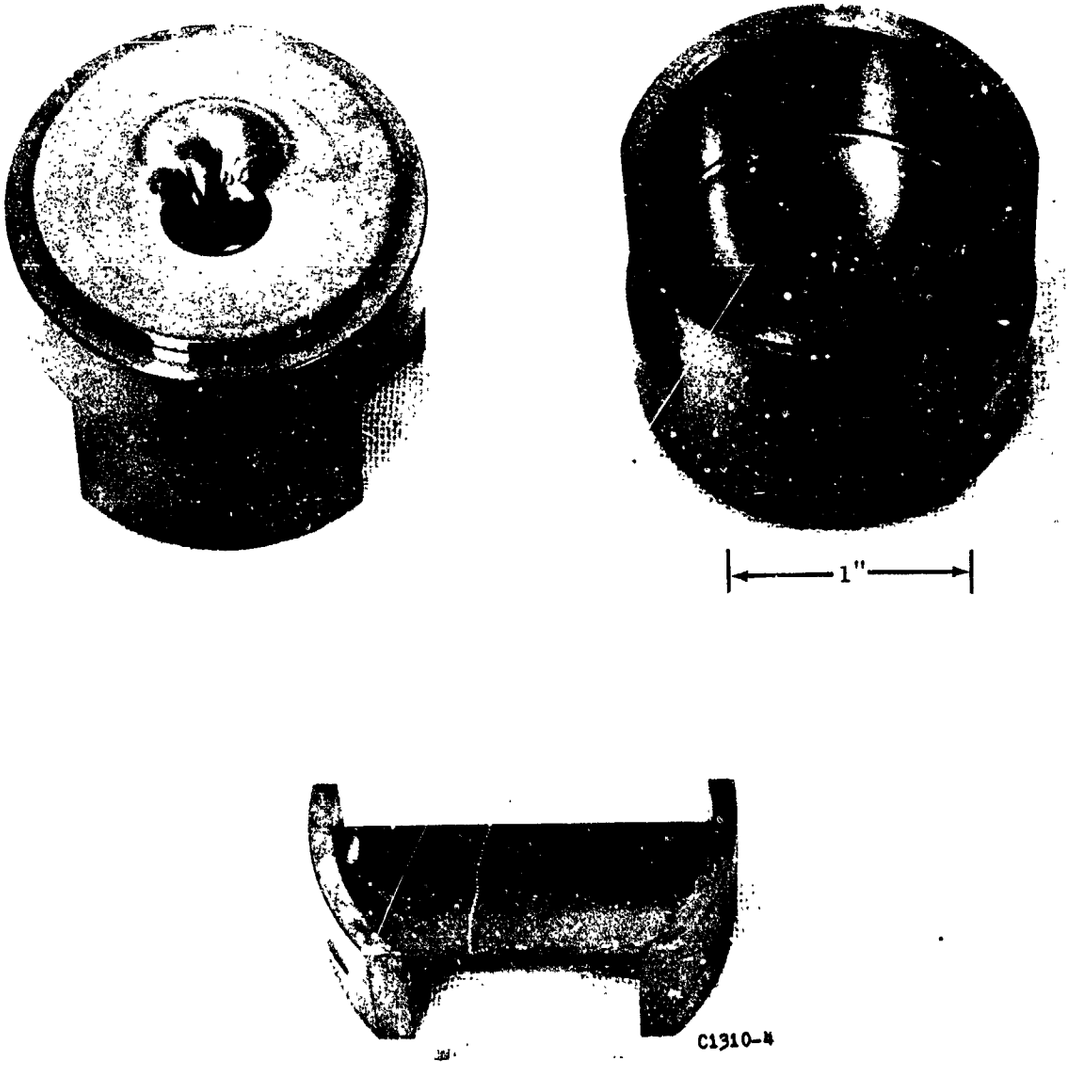


Figure 24. Entrance and Exit Side of the Nozzle and the Blade Assembly of Sixth Stage (Cb-132M) of the Turbine Simulator.
(Orig. C67090667, C67090669)

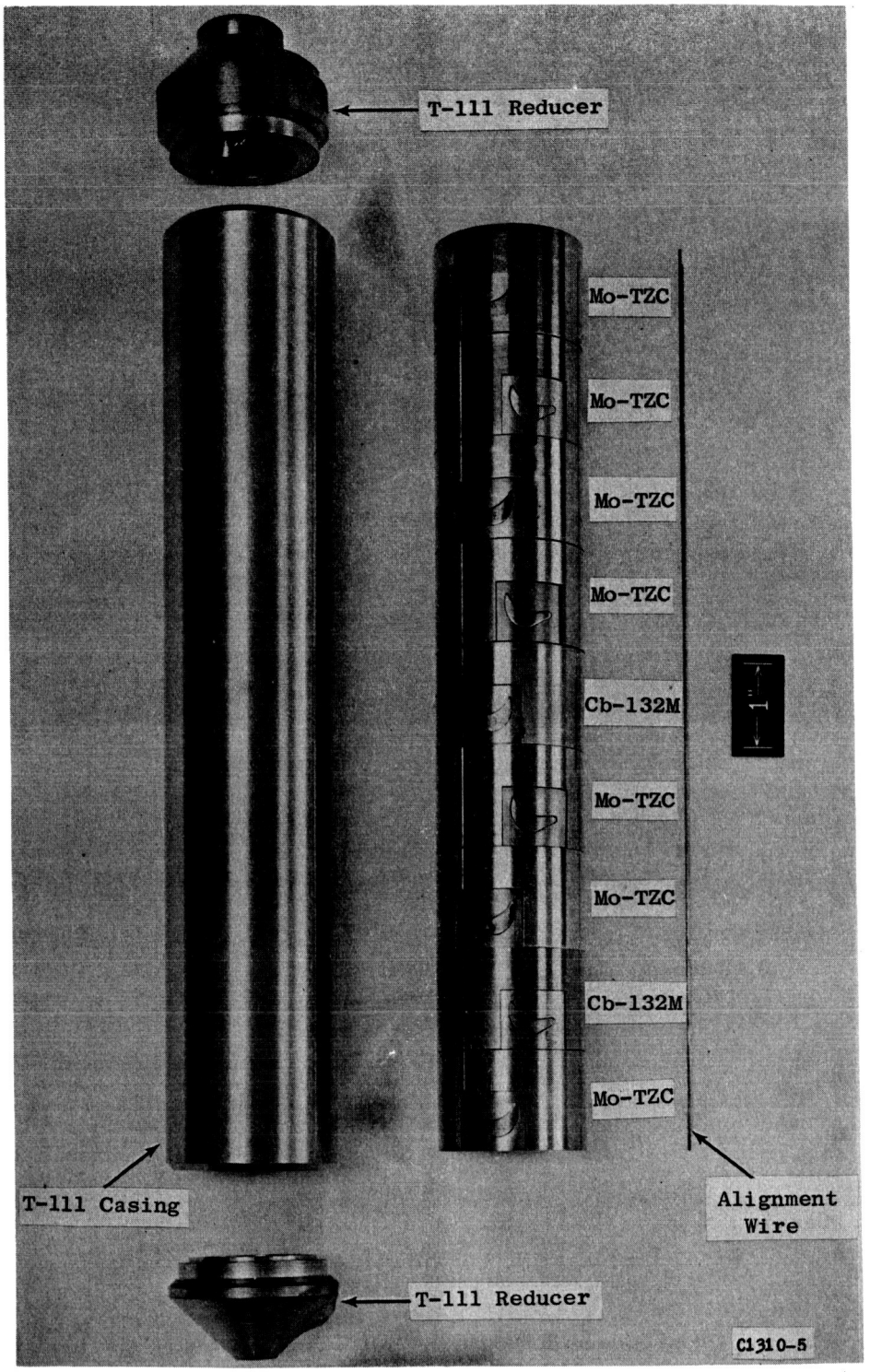


Figure 25. Turbine Simulator (Stages 2 to 10) of the T-111 Corrosion Loop Prior to Assembly. (Orig. C67090661)

drilled successfully to produce the two sections required for the 60-inch (152-cm)-long condenser. These two drilled components were then released for final machining and honing of the inside diameter.

The honing of the inside diameter of the two 30-inch (76-cm)-long condenser bars was completed. The welding of the condenser was then completed with the joining of the two condenser bars and tantalum fins as shown in Figure 26.

K. ASSEMBLY OF THE LOOP

The final assembly of the loop consisted of joining four major subassemblies; the condenser, boiler, potassium surge tank, and lithium heater.

The condenser assembly consisted of the condenser, nine-stage turbine simulator, subcooler reservoir, and associated piping as shown in Figure 27. A more detailed view of the turbine simulator and potassium vapor line is shown in Figure 28. The boiler assembly consists of the boiler, single-stage turbine simulator, and potassium preheater as shown in Figure 29. The potassium surge tank assembly consisted of the potassium surge tank, potassium EM pump duct, and potassium EM pump outlet line as shown in Figure 30. The outlet line contains the metering valve, two slack diaphragm pressure transducers and one fast-response pressure transducer. Three local postweld anneals at 2400°F (1316°C) for one hour were necessary for heat treatment of nine assembly welds. The lithium heater assembly consisted of the lithium heater, EM pump duct, and surge tank as shown in Figure 31.

The boiler and condenser major subassemblies and the lithium heater were wrapped with Cb-1Zr foil and postweld annealed at 2400°F (1316°C) for one hour in a Brew furnace, Model 966 (at Stellite Division of Cabot Corporation, Kokomo, Indiana). All other postweld anneals were performed locally at GE-NSP in the weld chamber. All anneals were performed in accordance with GE-NSP Specification 03-0037-00-A. The results of chemical analyses performed on the T-111 coupons, which were attached to the loop during the annealing operation, are given in Table XI and indicate no significant contamination occurred during the heat treatment.

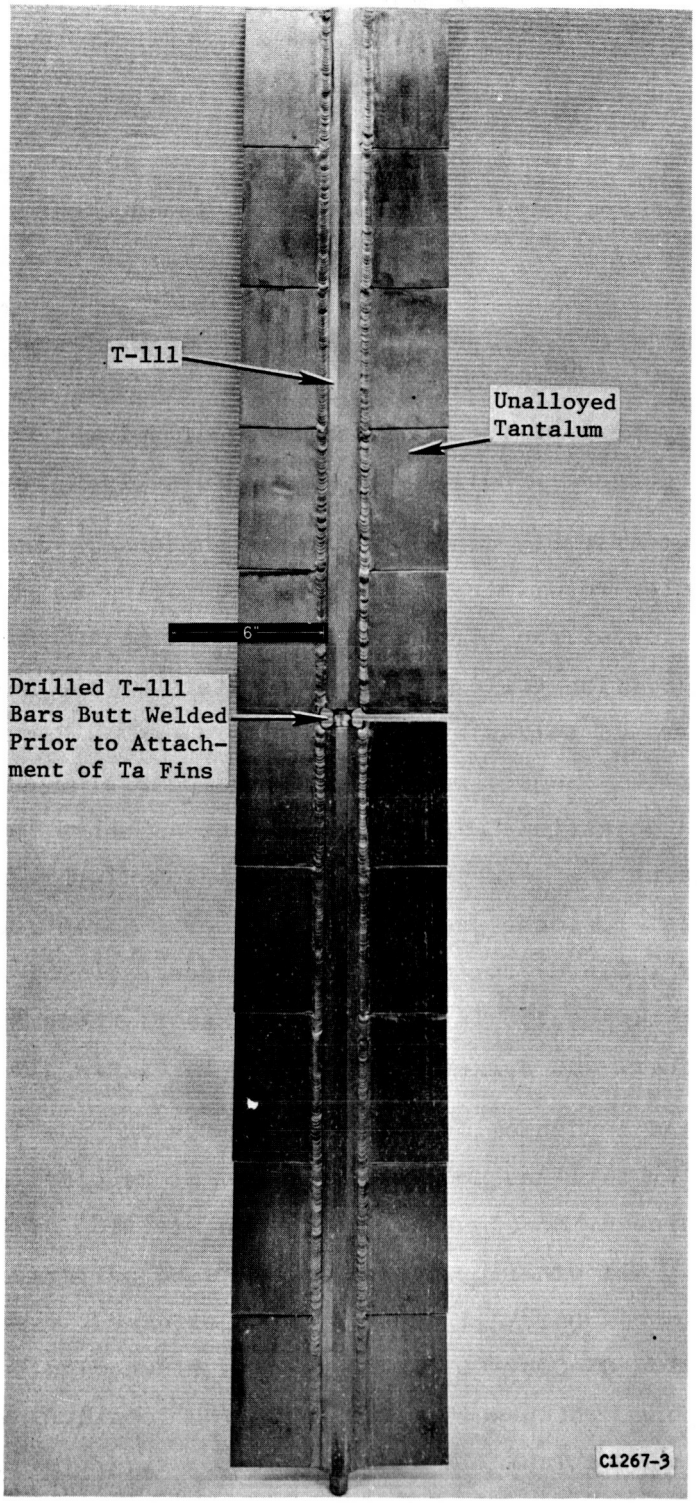


Figure 26. T-111 Corrosion Loop Condenser Prior to Coating of Tantalum Fins With Iron Titanate. (Orig. C67081423)

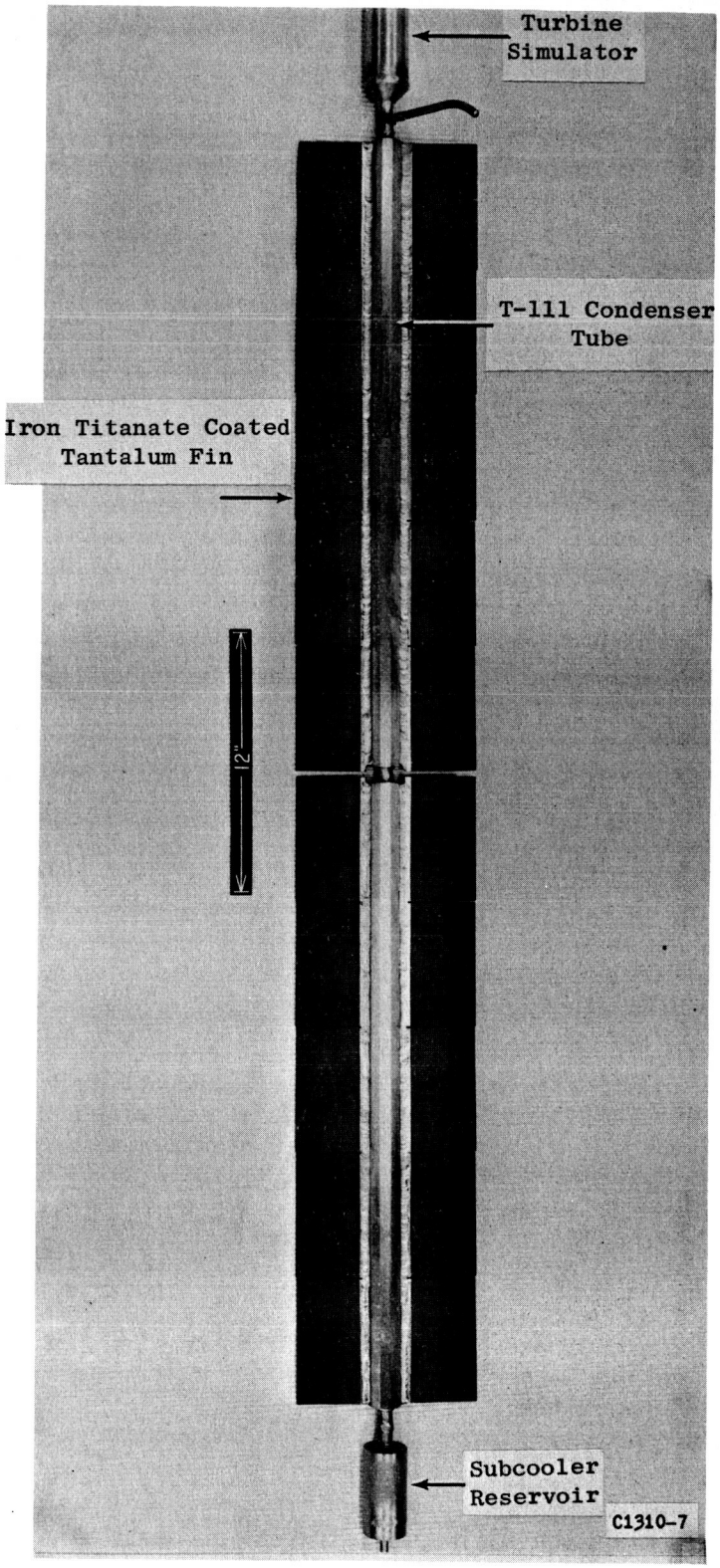


Figure 27. Condenser - Turbine Simulator Assembly Following Application of Iron Titanate Coating on Tantalum Fins. (Orig. C67100410)

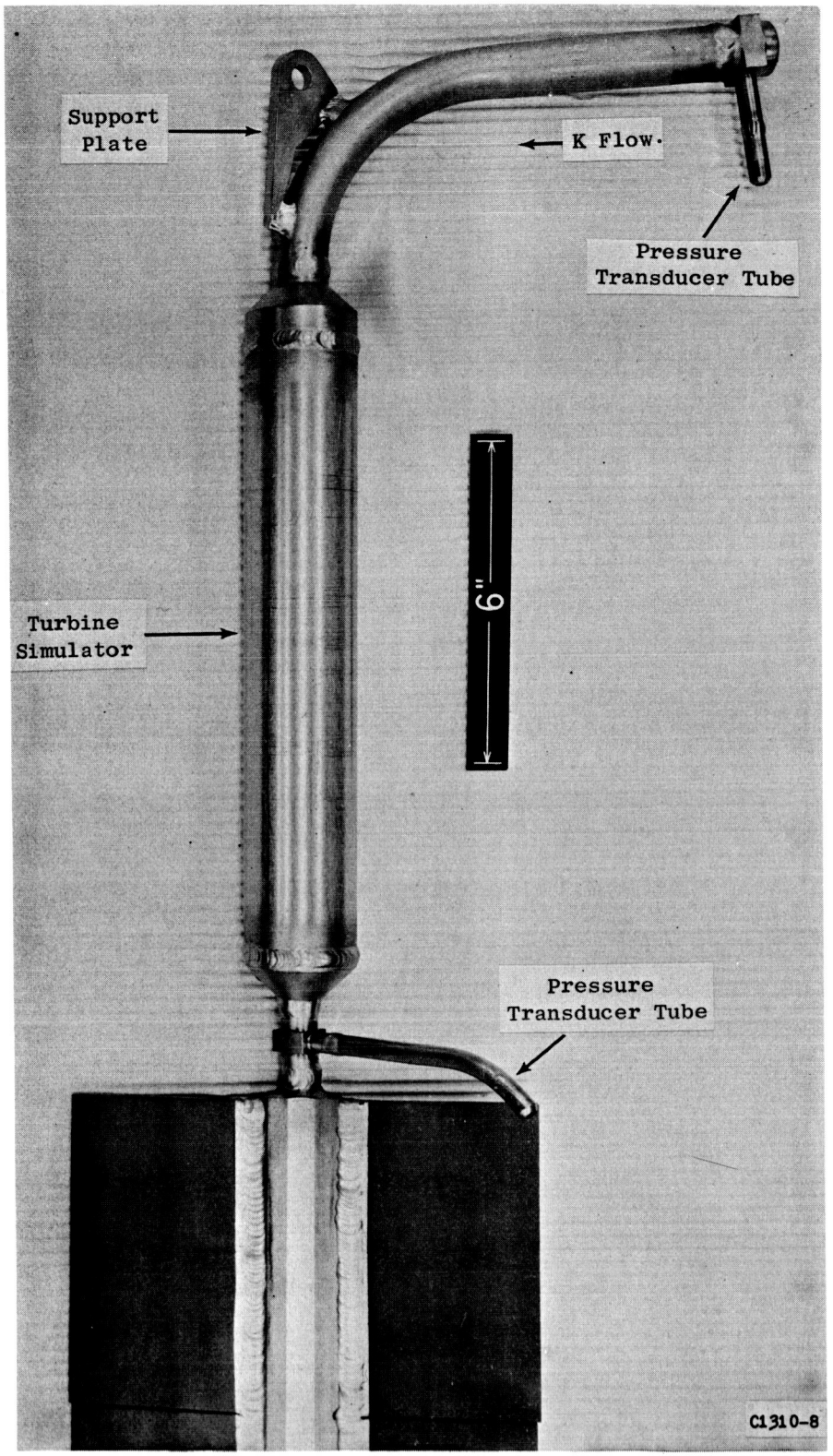


Figure 28. Nine-Stage Turbine Simulator and Top of Condenser.
(Orig. C67100409)

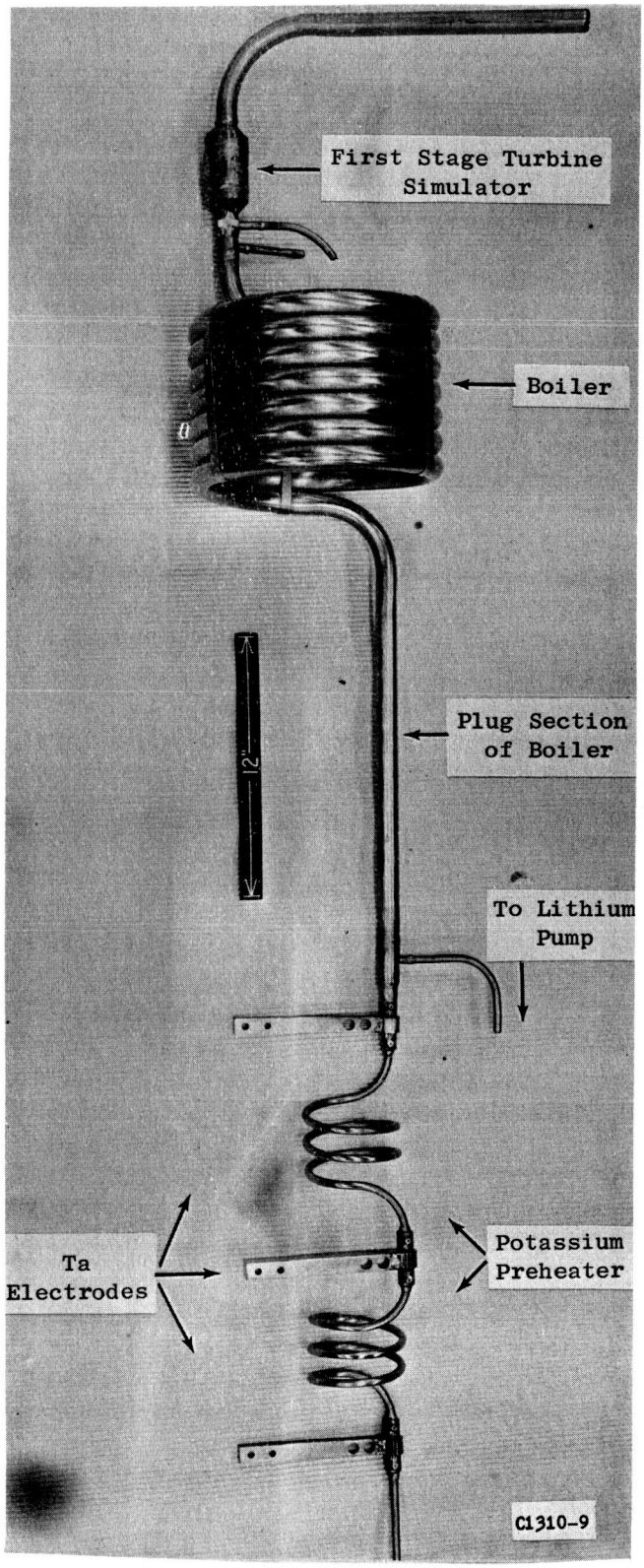


Figure 29. Potassium Preheater - Boiler - First-Stage Turbine Simulator Assembly Following Postweld Anneal. (Orig. C67100412)

ORIGINAL PAGE IS
OF POOR QUALITY

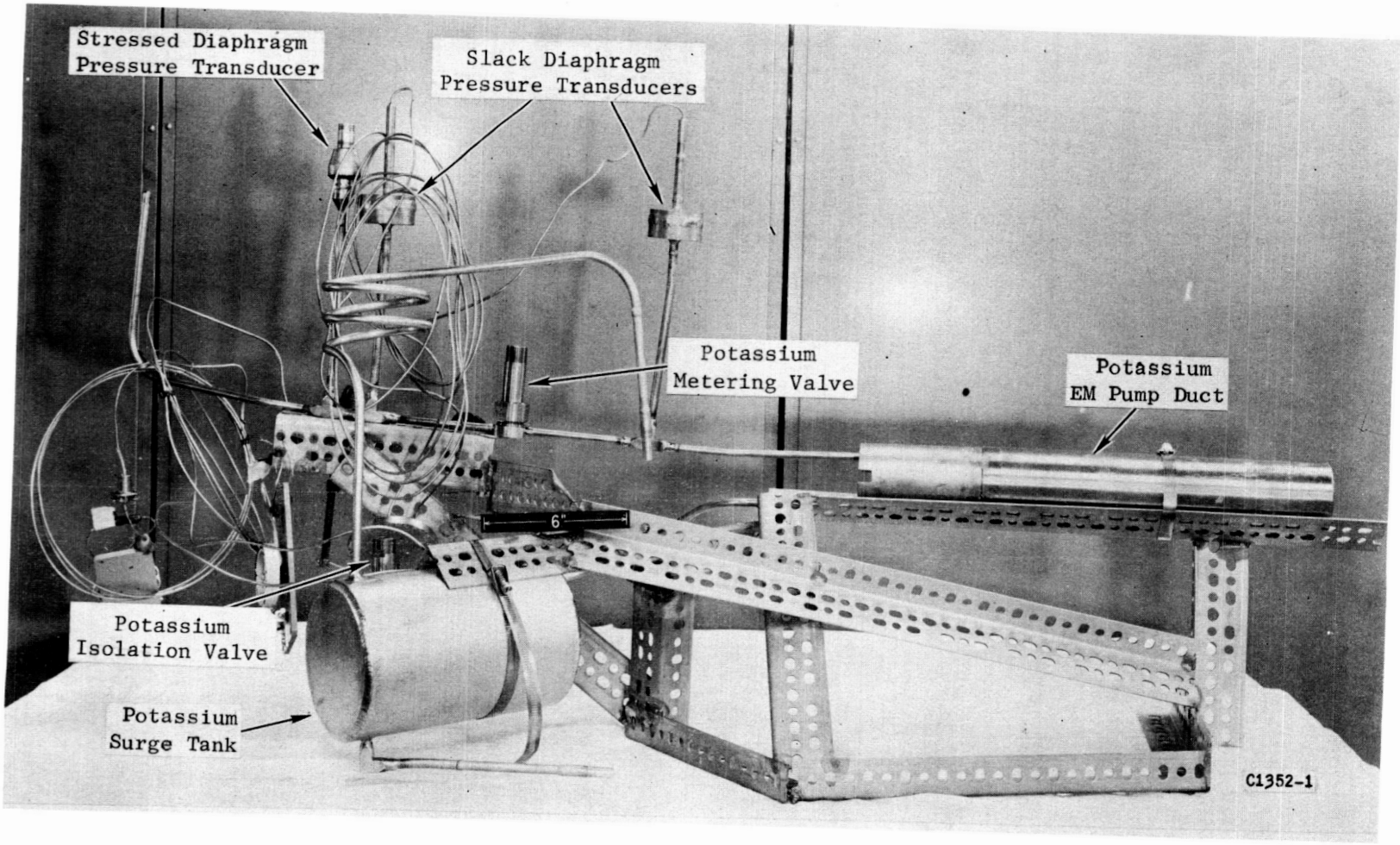


Figure 30. Potassium Surge Tank and EM Pump Subassembly of the T-111 Corrosion Test Loop Mounted on the Welding Fixture. (Orig. C67110669)

ORIGINAL PAGE IS
OF POOR QUALITY

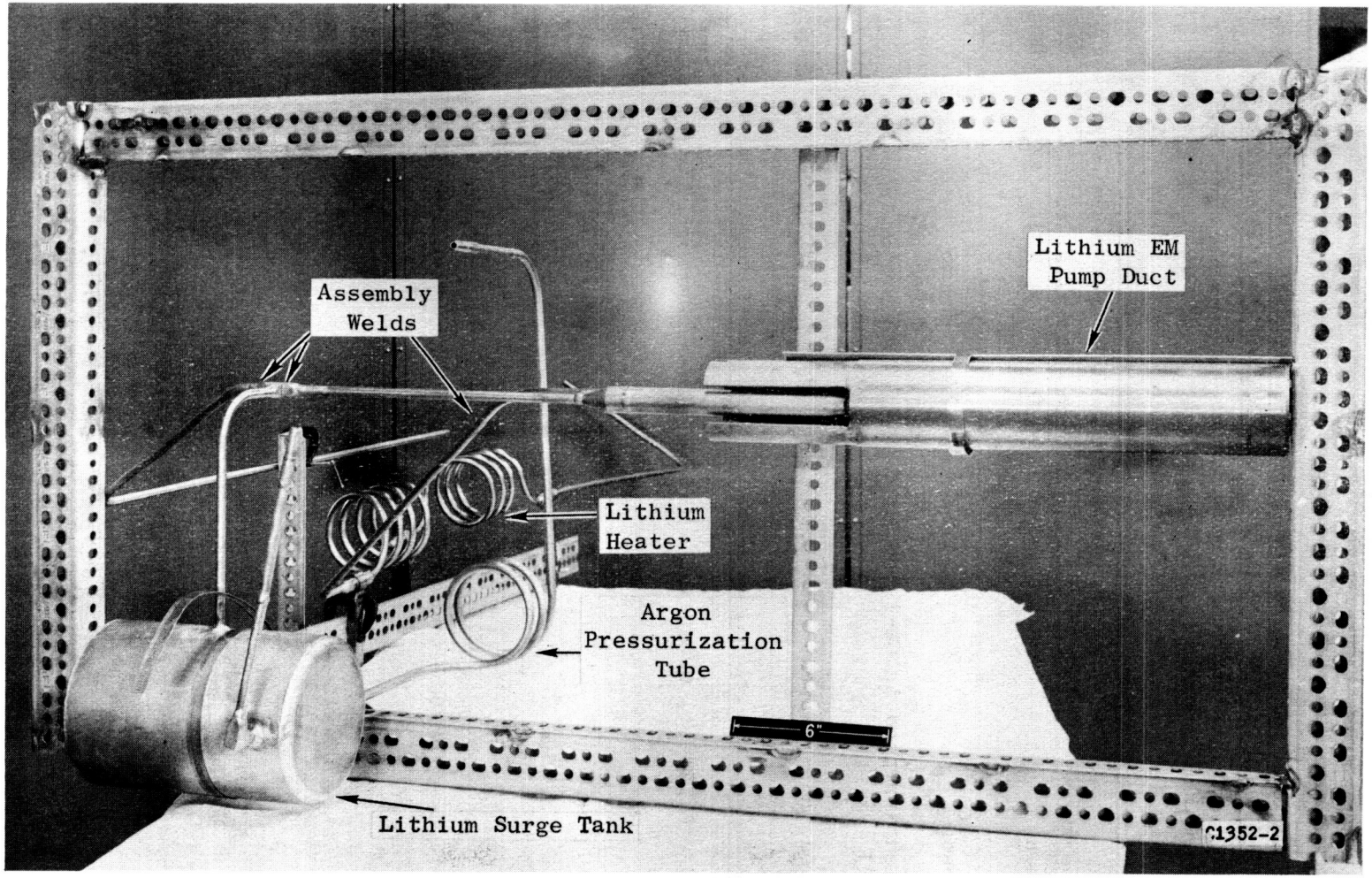


Figure 31. Lithium Surge Tank and EM Pump Subassembly of the T-111 Corrosion Test Loop Mounted on the Welding Fixture. (Orig. C67110668)

TABLE XI

RESULTS OF CHEMICAL ANALYSIS OF T-111 SPECIMENS FROM 1 HOUR - 2400°F (1316°C) VACUUM ANNEAL OF T-111 CORROSION LOOP BOILER ASSEMBLY AT STELLITE

Specimen	Chemical Analysis, ppm			
	C	O	N	H
Unexposed[a]	52	14	26	1
Annealed (wrapped in Cb-1Zr foil)	47	15	6	< 1
Annealed (not wrapped)	57	59	9	< 1

[a] MCN 04B-121-01, 0.040-inch (0.1-cm)-thick sheet.

The completed lithium heater, condenser, boiler, and potassium surge tank subassemblies were positioned in the stainless steel support structure attached to the vacuum chamber spool section for reference alignment. The tubing which joins the boiler and potassium surge tank subassemblies was match marked for alignment, and the two subassemblies were removed from the spool section for welding in the 8-foot (2.4-m)-diameter extension to the welding chamber. This assembly step was required because this particular weld could not be reached with the entire loop positioned in the welding chamber. After radiographic inspection of this weld, this unit was repositioned in the permanent support structure.

The lithium heater and condenser subassemblies were also positioned in the support structure. The final assembly weld fixture was attached to the loop (Figure 32) holding the subassemblies and three slack diaphragm pressure transducers (not shown) in alignment. The permanent support structure was disassembled, and the loop, now supported by the welding fixture, was removed from the vacuum chamber spool section and placed in the welding chamber as shown in Figure 33.

The seven welds required to join the subassemblies and attach the three pressure transducers were inspected radiographically and subsequently annealed in the welding chamber at 2400°F (1316°C) for 1 hour in accordance with GE-NSP Specification 03-0037-00-A.

The loop was removed from the welding chamber, and the electrode area of the lithium heater and the potassium preheater were grit-blasted to increase emittance per GE-NSP Specification 03-0011-00-A, "Grit Blasting of Columbium and Columbium Alloy Products." The loop was then positioned in the vacuum chamber spool section, and the permanent support structure was affixed. After the loop was supported properly, the final welding fixture was removed. An overall view of the loop spool piece is shown in Figure 34. A close-up photograph of the components in the lower portion of the loop is given in Figure 35.

The stainless steel tube attachments to the drain and gas pressurization lines were welded to the loop connections and vacuum chamber feedthroughs.

A final mass spectrometer helium leak test was then performed on the entire loop with no leak indication. The vacuum connections for the NaK-filled tubes from the slack diaphragm pressure transducer and the EM pump-duct, stainless steel, outer cans were welded to the appropriate vacuum spool section feedthroughs. The completed loop was then removed to the test site.

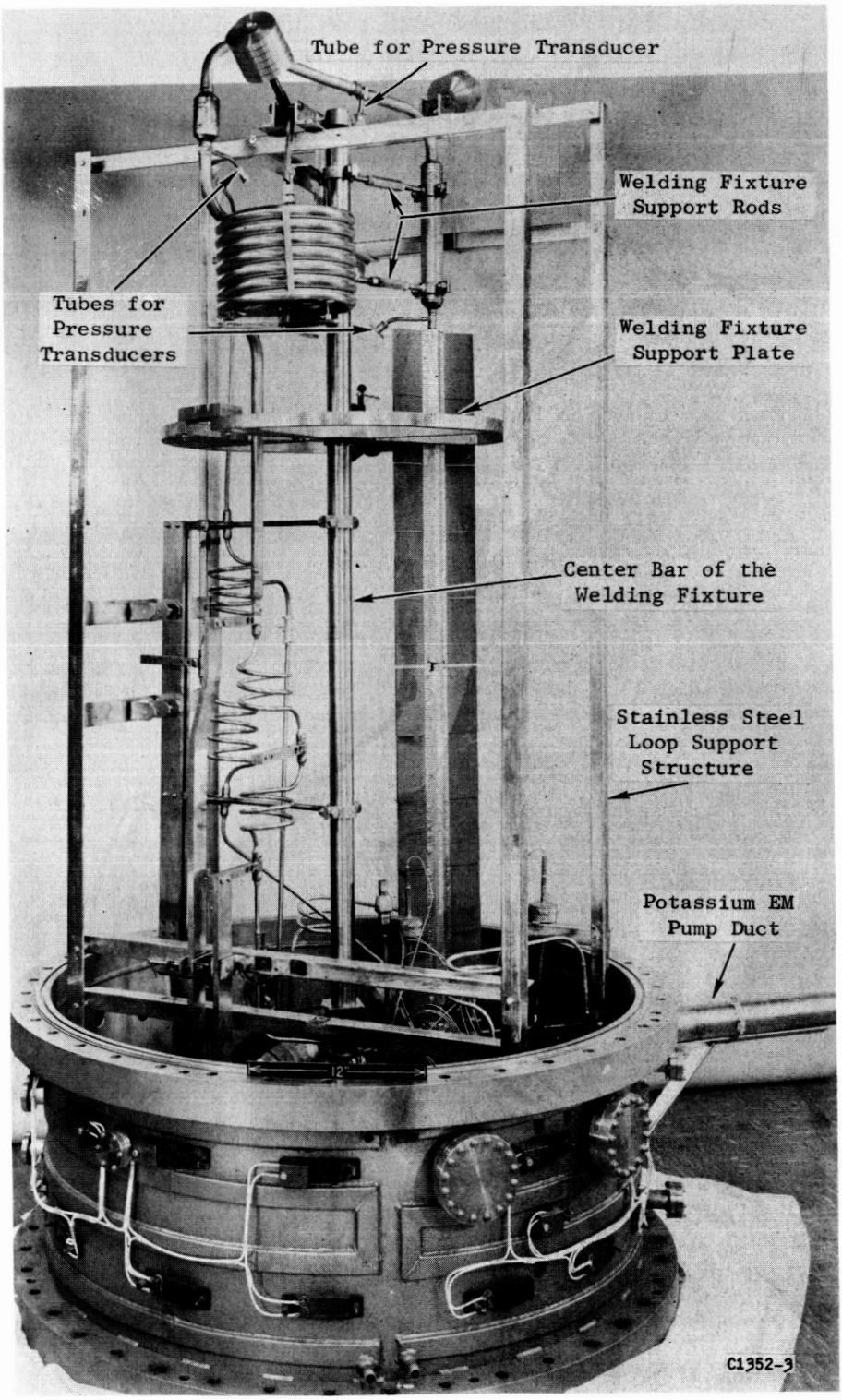


Figure 32. T-111 Corrosion Test Loop and Chamber Spool Piece During the Transfer of the Loop from the Support Structure to the Welding Fixture. (Orig. C67112232)

ORIGINAL PAGE IS
OF POOR QUALITY

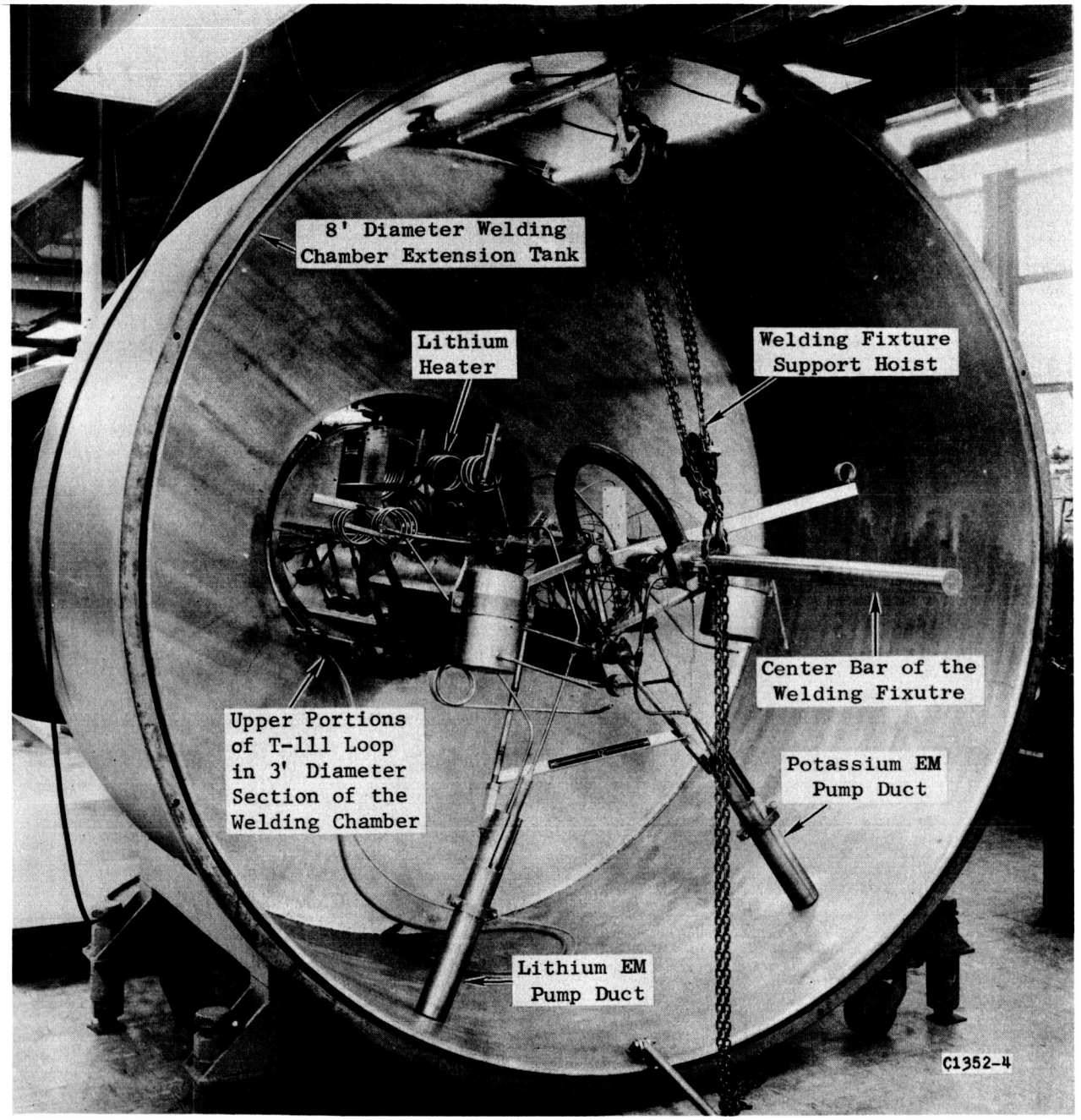


Figure 33. T-111 Corrosion Test Loop Mounted on the Welding Fixture Prior to Final Welding and Weld Heat Treatment Operations. (Orig. C67120714)

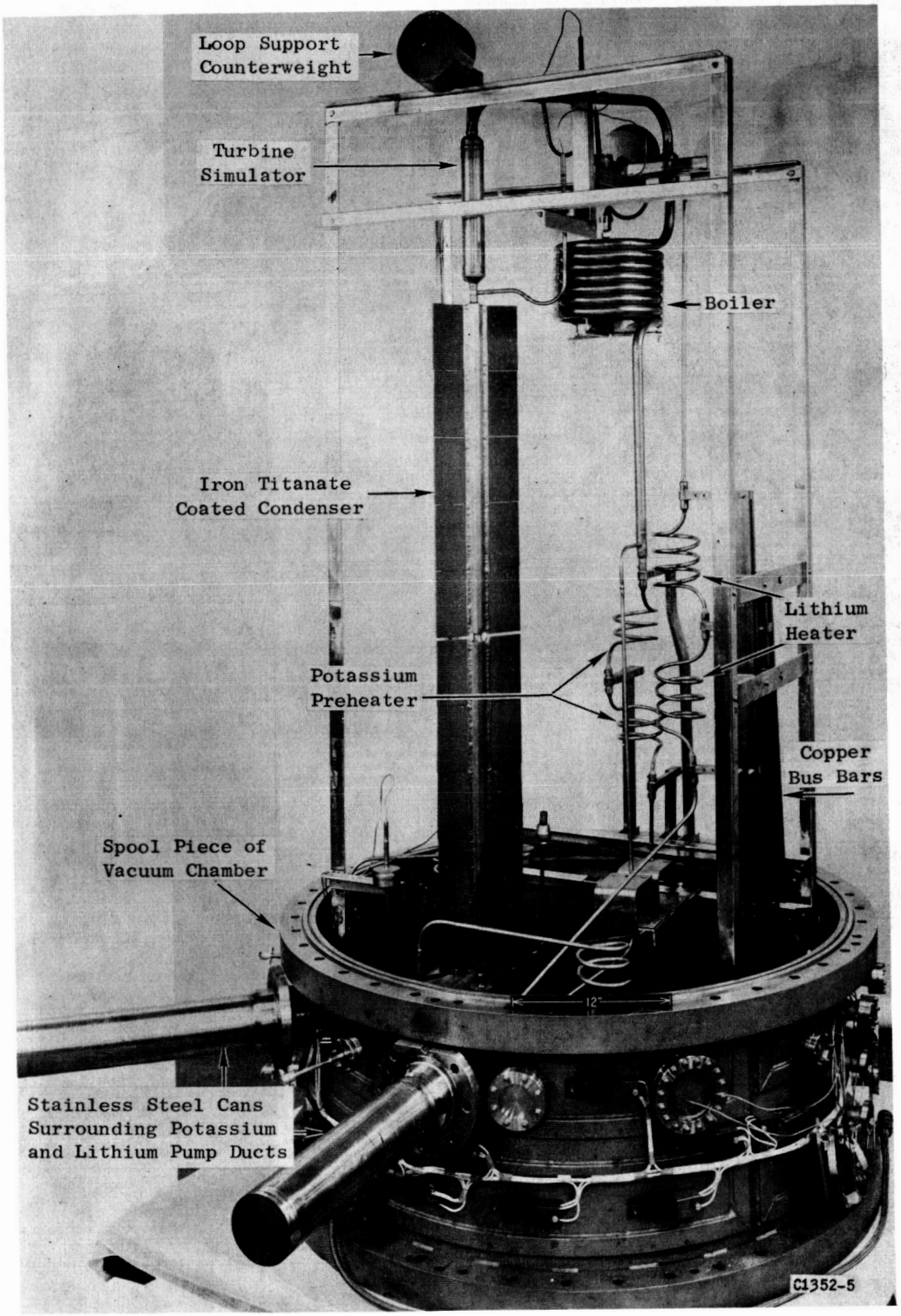


Figure 34. T-111 Corrosion Test Loop and the Vacuum Chamber Spool Piece Following Completion of Loop Fabrication. (Orig. C67122143)

ORIGINAL PAGE IS
OF POOR QUALITY

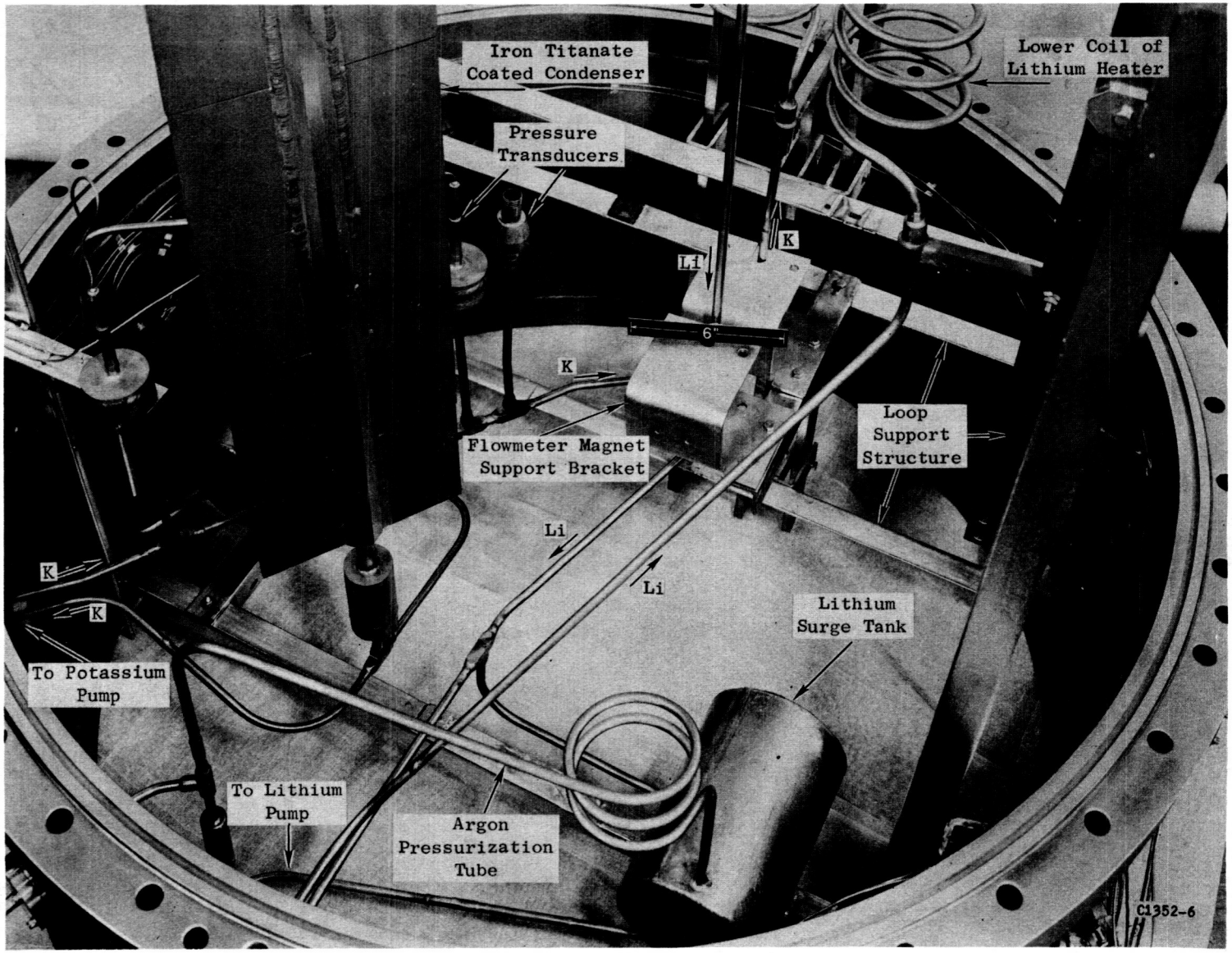


Figure 35. Lower Portion of the T-111 Corrosion Test Loop Following Completion of Fabrication. (Orig. C67122147)

V. ALKALI METAL PURIFICATION AND HANDLING

Most of the confusion and negative information regarding the limitations of various potential materials for use in liquid metals have resulted from inattention of the investigators to the problem of obtaining and maintaining the purity of the liquid metal under study. This is particularly true of the alkali metals because of their tendency to react readily with the atmosphere when exposed. Although the effects of some impurities in the alkali metals on various materials have been defined, there is much that is unknown. For example, it is known that small concentrations of oxygen, nitrogen, hydrogen, and carbon can lead to corrosion, embrittlement, and mass transfer.[10,11,12,13] However, the effects of most metallic impurities, nonmetals, and metalloids are unknown. Consequently, GE-NSP adopted the philosophy of using alkali metals of the highest obtainable purity in systems of exceptional cleanliness in order to circumvent the problem in so far as was practical. The purity of the liquid metals was monitored for the subject program from procurement until the end of testing in order to insure that adequate purity was maintained and that a complete chemical analytical history was available.

A detailed description of the procedures and equipment used to purchase, purify, transfer, sample, and analyze the sodium and potassium for the

---

(10) Hoffman, E. E. and Harrison, R. W., "The Compatibility of Refractory Metals With Liquid Metals," Symposium on Metallurgy and Technology of Refractory Metals Alloys, Sponsored by the Metallurgical Society of AIME and the National Aeronautics and Space Administration, Washington, D.C., April 25-26, 1968.

(11) Nezerov, B. A., et al., "Corrosion Resistance of Constructional Materials in Alkali Metals," Paper A/Conf. 28/F/343, Third U.N. International Conference on the Peaceful Uses of Atomic Energy, Geneva, Switzerland, 1964.

(12) Weeks, J. R., "Effects of Impurities," NASA-AEC Liquid Metals Corrosion Meeting, I, 59 National Aeronautics and Space Administration, Washington, D.C., October 1963.

(13) Leavenworth, H. W. and Cleary, R. E., "The Solubility of Ni, Cr, Fe, Ti, and Mo in Liquid Lithium," Acta Met., Vol. 9, 1961.

Cb-1Zr Corrosion Test Loop was presented in a topical report.[14] Since similar techniques were employed in the handling of lithium and potassium for the T-111 Corrosion Test Loop, only an abbreviated review of these techniques will be included in this report. Essentially the same techniques and duplicate purification systems were used for the purification of lithium and potassium.

A. LITHIUM PURIFICATION

High-purity lithium was obtained from Lithium Corporation of America, Bessemer City, North Carolina. A special shipping container was manufactured for this procurement, and it is shown in Figure 36. After fabrication, it was vacuum outgassed at 500°F (260°C) (maximum outgassing rate, 1 micron ℓ/min, helium leak checked (per NSP Specification No. P3CYA16), and backfilled with high-purity argon. On receipt, the lithium was sampled (No. 292) and analyzed. All analytical results for this lithium are given in Table XII.

The lithium was filtered through a 5-micron-pore-size, sintered, stainless steel filter at 400°F (204°C) into the 35-lb (16-kg)-capacity hot trap. This hot trap is shown in Figures 37 and 38. A sample (No. 293) was removed and analyzed. The lithium was then hot trapped at 1500°F (816°C) for 126 hours, sampled (No. 309), and analyzed. It was then vacuum distilled at 1235°F (668°C) and again sampled (No. 1355) and analyzed. The distillation rate was about 0.5 lb/hr (0.063 gm/sec). The components of the lithium distillation system are shown prior to assembly in Figure 39 and following assembly in Figure 40. The hot trap, distillation system, and other purification facility components are shown on the portable cart in Figure 41.

Just prior to filling the loop, the lithium transfer system was baked out at temperatures ranging from 250° to 700°F (120° to 370°C) until the outgassing rate was <1 micron ℓ/min. The transfer lines and charge pot were then flushed by filling them with lithium and then dumping the lithium into the disposal tank. They were then refilled, and a sample (No. 1488) was taken and analyzed. The charge pot was then emptied into the loop surge

(14) Dotson, L. E. and Hand, R. B., Purification, Analysis, and Handling of Sodium and Potassium, R66SD3012, General Electric Company, June 13, 1966, p. 15.

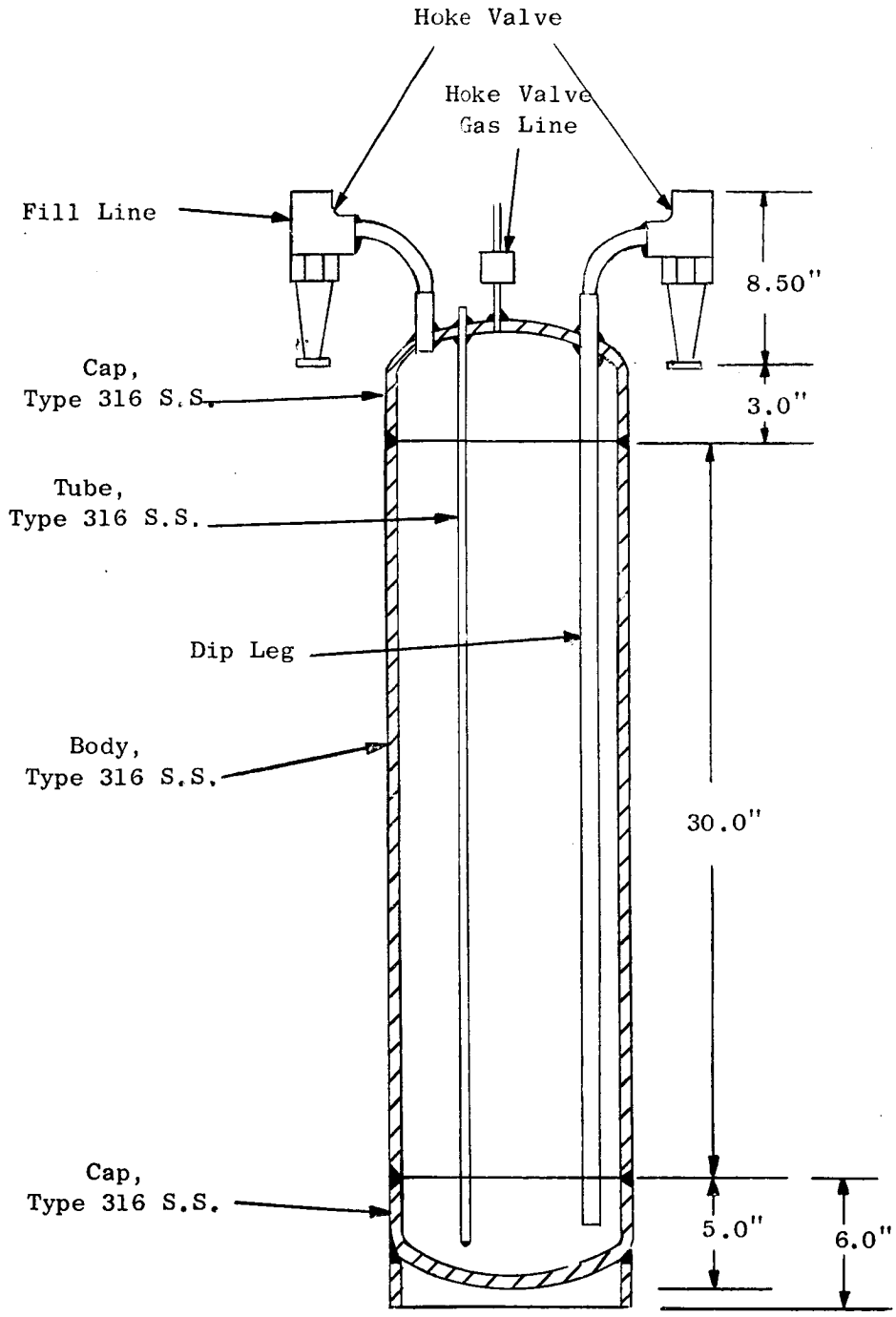


Figure 36. Thirty-Five-Pound (16-kg)-Capacity Lithium Shipping Container.

TABLE XII

ANALYTICAL DATA FOR LITHIUM FROM LITHIUM CORPORATION OF AMERICA

	ppm in Lithium Metal					
Element	As-Received No. 292	After Filtering No. 293	After Hot Trapping No. 309	After Distilling No. 1355	After Flushing Transfer Sys. No. 1488	After Flushing Loop No. 1492
O	130,130	150,160	106,123	24,19	10	39,39,18
N	801,834, 871	755,778, 841	11,10,5,3	< 5,<5	3,6	< 5
C	134,158	97,101	38,48	26	63	39,50
Ag	< 5	< 5	< 5	< 5	<5	< 5
Al	< 5	< 5	5	75	50	< 25
B	< 50	< 50	< 50	< 50	< 50	< 50
Ba	75	50	< 50	< 50	< 25	< 50
Be	< 5	< 5	< 5	< 5	< 5	< 5
Ca	133	53	5	< 5	25	< 25
Cb	< 25	< 25	< 25	< 50	< 25	< 25
Co	< 5	< 5	< 5	< 5	< 5	< 5
Cr	< 5	< 5	< 5	< 5	< 5	5
Cu	< 5	< 5	28	<125	< 5	5
Fe	< 5	< 5	5	5	5	< 5
K						< 25
Mg	5	5	< 5	< 5	5	5
Mn	< 5	< 5	< 5	< 5	< 5	< 5
Mo	< 5	< 5	< 5	< 5	< 5	< 5
Na	53	133	80		75	125
Ni	< 5	< 5	28	< 5	< 25	< 5
Pb	< 25	< 25	< 25	50	< 50	< 50
Si	5	5	28	5	115	< 25
Sn	< 25	< 25	< 25	< 5	< 25	< 50
Sr	5	5	< 5	< 5	5	5
Ta					< 250	<250
Ti	< 5	< 5	< 5	< 5	< 25	< 5
V	< 25	< 25	< 25	< 50	< 25	< 25
Zr	< 5	< 5	< 5	< 5	< 25	< 25

ORIGINAL PAGE IS
OF POOR QUALITY

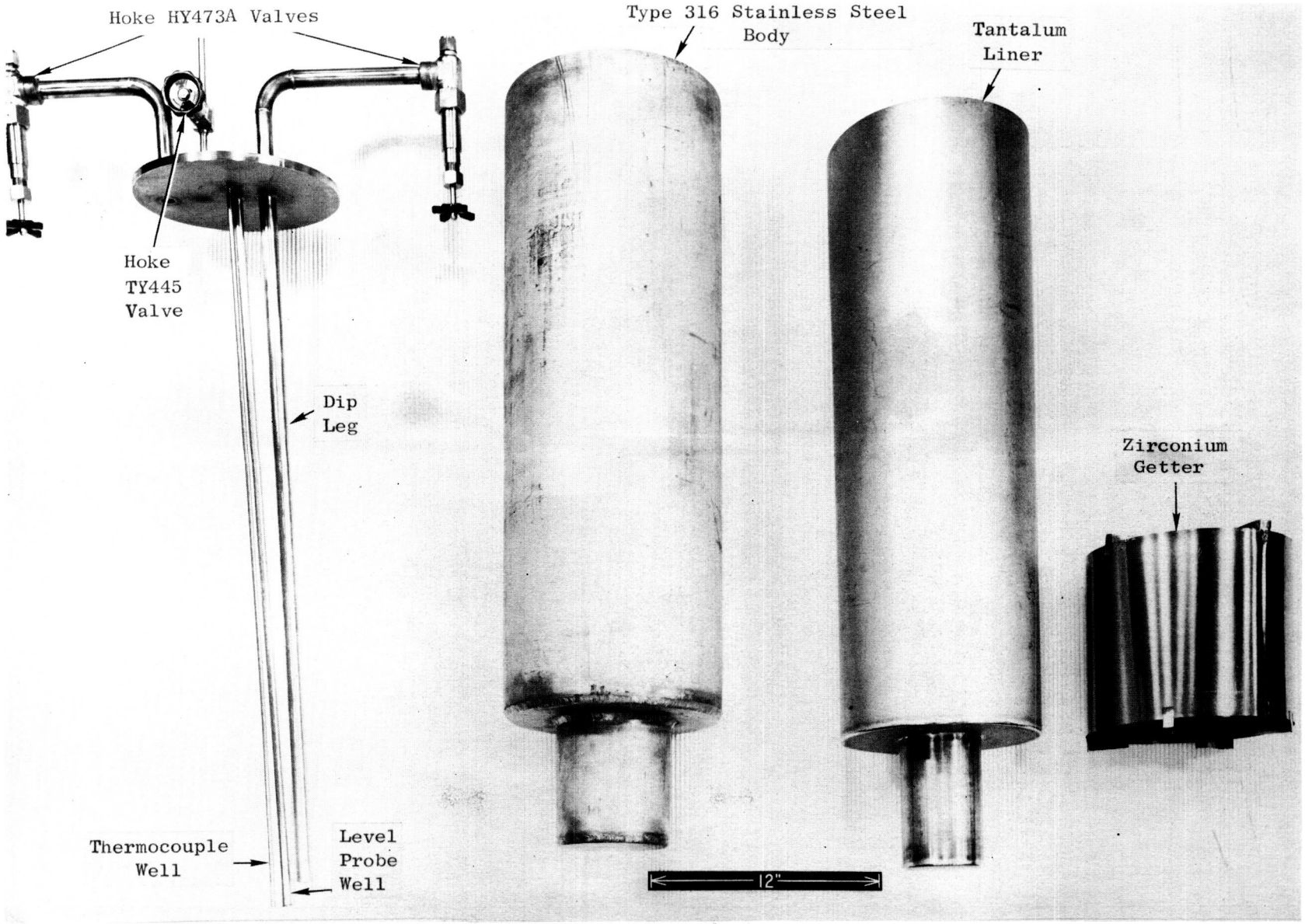


Figure 37. Hot Trap for Purifying Alkali Metals - Before Assembly.
(Orig. 65111625)

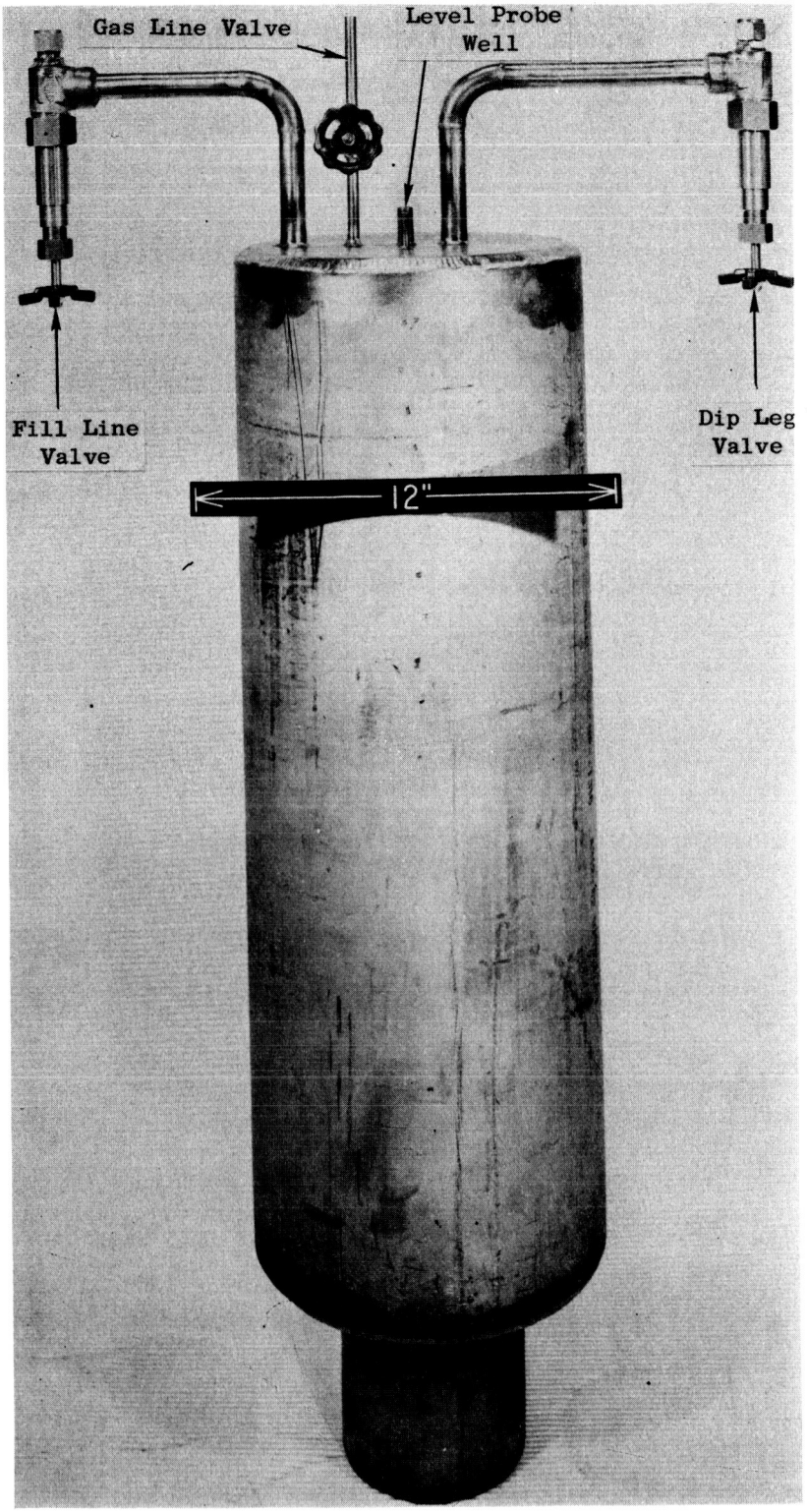


Figure 38. Hot Trap for Purifying Alkali Metals - After Assembly. (Orig. C65111823)

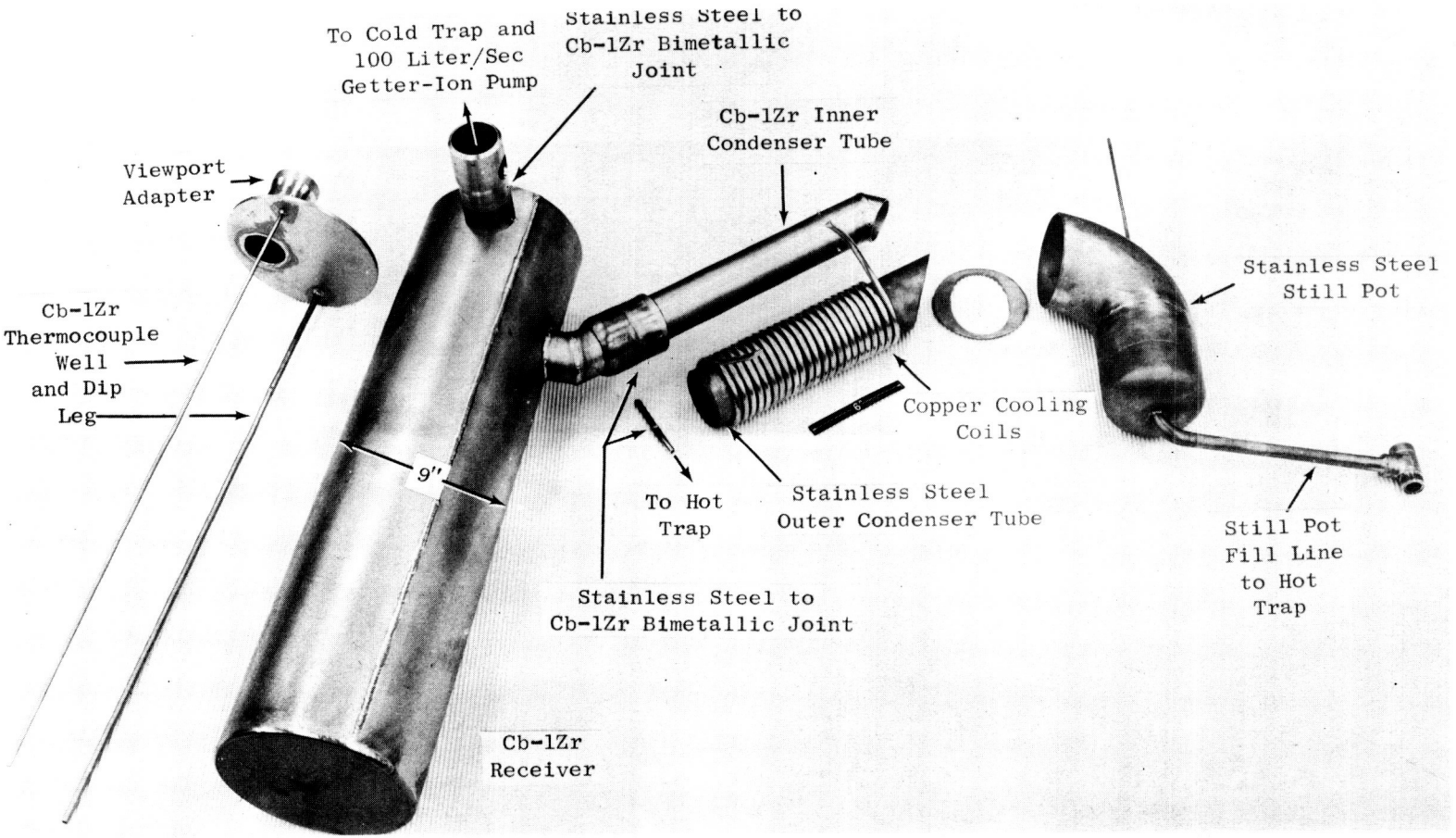


Figure 39. Distillation for Purifying Alkali Metal for the T-111 Corrosion Loop Test. Components of System Shown Prior to Assembly. (Orig. C65062186)

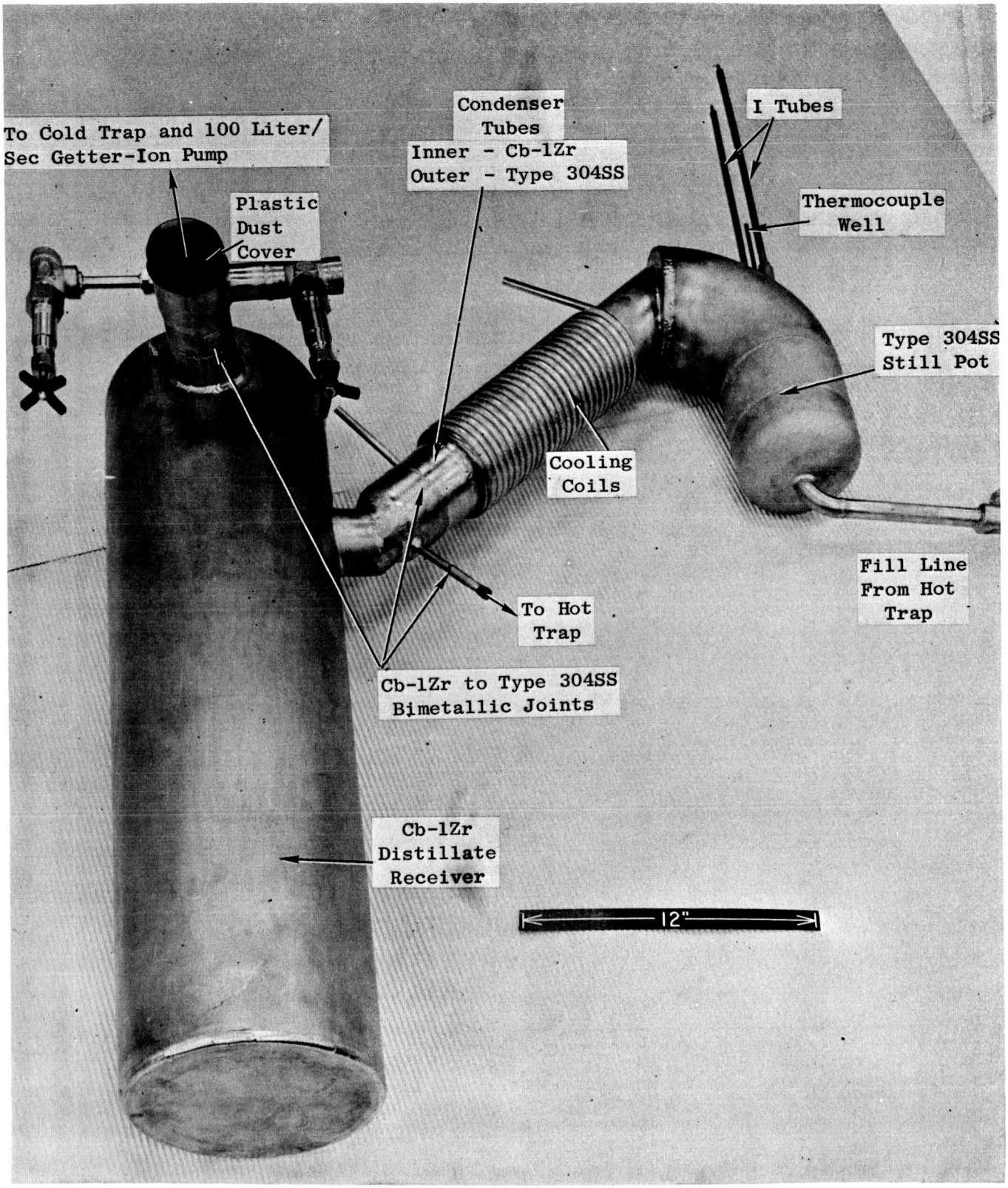


Figure 40. Alkali Metal Still - After Assembly. (Orig. C66121230)

ORIGINAL PAGE IS
OF POOR QUALITY

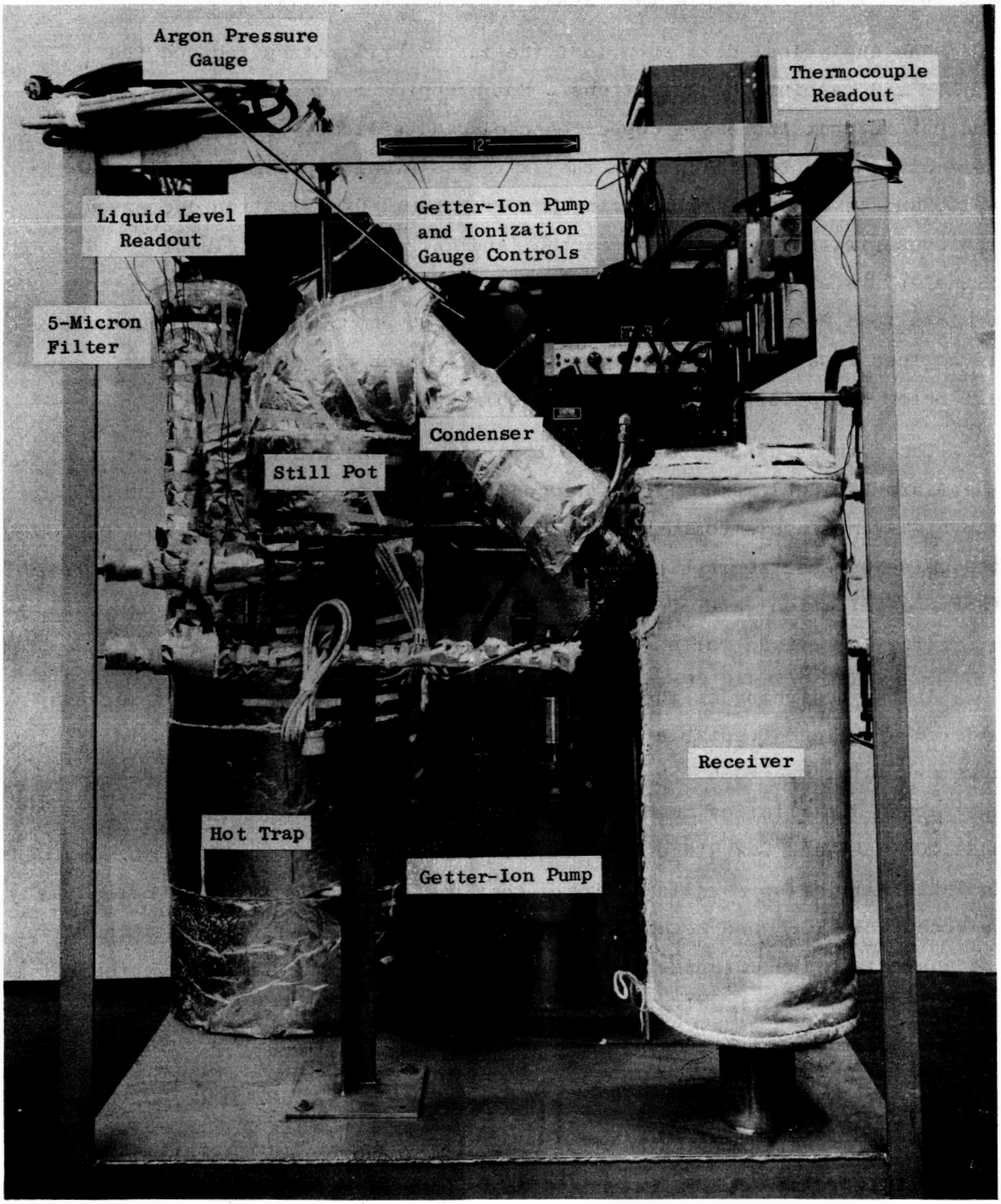


Figure 41. Alkali Metal Purification Facility.
(Orig. C68022909)

ORIGINAL PAGE IS
OF POOR QUALITY

tank and the loop flushed at 1000°F (538°C) and the lithium returned to the surge tank. A sample (No. 1492) was taken and analyzed.

The analytical data show that the initial filtration reduced the carbon and calcium concentrations. Hot trapping reduced nitrogen, carbon, and calcium but increased copper, nickel, and silicon. These increases were attributed to pickup from the stainless steel dip leg, thermocouple well, and level probe well during hot trapping. Distillation decreased the concentrations of oxygen, carbon, and nitrogen. After flushing the transfer system and loop, the lithium was still within the specifications of less than 20 ppm nitrogen and less than 150 ppm oxygen. Although there is no specification for the maximum concentration for other elements, they were all below acceptable limits after flushing the loop.

The methods used to determine impurity concentrations in the lithium were the micro-Kjeldahl method for nitrogen (NSP Specification 03-0056-00-A), the high-temperature combustion method for carbon (NSP Specification 03-0057-00-A), the emission spectrographic method on the carbonate for metallic impurities (NSP Specification 03-0058-00-A), and the fast neutron activation and vacuum distillation methods for oxygen (NSP Specification 03-0079-00-A).

At the beginning of the program, only fast neutron activation was considered to be an acceptable method for the determination of oxygen in lithium. However, later on, both the NASA-Lewis Research Center and GE-NSP developed the vacuum distillation method for this analysis. The results obtained by NASA, GE-NSP, and Oak Ridge National Laboratory are compared for two specimens in Table XIII. The results indicate that the vacuum distillation method is an acceptable in-house method and has been used subsequently. We acknowledge and appreciate the efforts of R. Gahn of the NASA-Lewis Research Center for the vacuum distillation results and E. Strain of the Oak Ridge National Laboratory for the neutron activation results.

B. POTASSIUM PURIFICATION

The high-purity potassium from Mine Safety Research Corporation, Callery, Pennsylvania, was received in one of their special stainless steel drums. On receipt, it was sampled (No. 1901) and analyzed. All analytical results for this potassium are shown in Table XIV.

TABLE XIII

COMPARISON OF RESULTS ON OXYGEN CONCENTRATION IN LITHIUM AS DETERMINED BY THE FAST NEUTRON ACTIVATION AND VACUUM DISTILLATION METHODS - CONCENTRATION IN PPM

Analytical Lab.	Sample Number 1355	1492
NASA-Lewis (Vacuum Distillation)	21,30,37,36	
ORNL (Fast Neutron)	24,19	31,40
ORNL (Thermal Neutron)	42,65	
GE-NSP (Vacuum Distillation)		39,39,18

The same purification, analytical, and transfer methods were used for potassium as for lithium except as indicated below.

Potassium was not filtered from the drum into the hot trap because it is quite pure when received. The hot trap was a duplicate of the lithium hot trap shown in Figures 37 and 38; however, it had a capacity of 50 pounds (23 kg) of potassium. The hot trapping was performed at 1300°F (704°C) for 24 hours. Potassium is not sampled after hot trapping because taking a sample at this stage would require replacing the line and filter between the hot trap and still pot. The potassium was distilled at 550°F (288°C). The distillation rate was about 1 lb/hr (0.13 gm/sec). The potassium still is essentially a duplicate of the system used for lithium previously shown in Figures 39, 40, and 41.

The amalgamation method (NSP Specification 03-0025-00-A) was used to determine oxygen in potassium instead of the distillation method. Potassium does not form a stable nitride, so it is not analyzed for nitrogen following distillation.

The potassium transfer system was baked out and flushed as was the lithium system. The potassium was transferred to the loop surge tank and the loop flushed at 1000°F (538°C). The analytical results for samples taken after these operations are shown in Table XIV.

C. REFILLING OF LOOP CIRCUITS FOLLOWING BOILER REPAIR

The lithium and potassium described above were used during the initial operation of the loop. However, during this initial operation, it was found that a leak had developed between the two loops within the boiler as described in Section VIII. The analytical data for the lithium and potassium which was eventually used in the loops following the repair and flushing of the boiler is given in Table XV. Although the nitrogen concentration was slightly higher than the 20-ppm limit in the specification, the lithium was approved for use since further purification and handling could possibly increase the low concentrations of other impurities. This lithium was obtained from Foote Mineral Company, Exton, Pennsylvania, and was purified using the techniques previously described.

TABLE XIV

ANALYTICAL DATA FOR POTASSIUM

Element	Impurity Concentrations - ppm in Potassium					
	As-Received No. 190	After Distilling No. 1352	After Flushing Transfer System No. 1487A	After Flushing Transfer System No. 1487B	After Flushing Loop No. 1493A	After Flushing Loop No. 1493B
O	4,6	2,1	17,20		14,14	
C		63	37		21	
Ag	< 2	< 2	< 2	< 2	< 2	< 2
Al	2	10	2	< 2	< 2	< 2
B		< 50	< 50	< 10	< 50	< 20
Ba		< 50	< 30	< 10	< 30	< 10
Be		< 2	< 2	< 2	< 2	< 2
Ca	10	2	2	< 2	2	2
Cb	2	< 10	< 20	< 10	< 20	< 10
Co	< 2	< 2	< 2	< 2	< 2	< 2
Cr	< 2	< 2	> 50	< 2	30	2
Cu	< 2	2	< 2	< 2	2	< 2
Fe	2	< 2	20	< 2	> 50	2
Li			< 10			
Mg	< 2	< 2	< 2	< 2	10	2
Mn	< 2	< 2	2	< 2	< 2	< 2
Mo	< 2	< 2	< 2	< 2	< 2	< 2
Na	< 50	< 20	< 50	< 20	< 50	
Ni	< 2	< 2	< 10	< 2	20	< 10
Pb	< 2	< 10	< 30	< 10	< 15	< 10
Si	10	2	2	< 2	2	2
Sn		< 10	< 20	< 10	< 20	< 10
Sr		5	< 2	< 2	< 2	2
Ta						
Ti	< 2	< 2	< 10	< 2	< 10	< 10
V	< 2	< 20	< 30	< 20	< 30	< 10
W						< 100
Zn						< 100
Zr	< 10	< 20	< 30	< 10	< 30	< 10

TABLE XV

ANALYTICAL DATA FOR THE LITHIUM AND POTASSIUM USED IN THE T-111 CORROSION LOOP

	Impurity Concentrations - ppm in Lithium				
	Potassium		Lithium from Foote Mineral Co.		
Element	As-Received No. 1927	Hot-Trapped & Distilled No. 1981	As-Received No. 2039	Hot-Trapped No. 2067	Distilled No. 2081
O	23	6	95		31
N	-	-	278	21,23,33	27,33
C	83	29	75	69	46
Ag	< 2	< 2	< 5	< 5	< 5
Al	2	< 2	< 5	< 5	5
B	< 30	< 20	< 50	< 50	< 50
Ba	< 30	< 20	< 50	< 50	< 75
Be	< 2	< 2	< 5	< 5	< 5
Ca	< 2	< 2	< 5	5	25
Cb	< 10	< 10	< 25	< 25	< 25
Co	< 2	< 2	< 5	< 5	< 5
Cr	< 2	< 2	< 5	< 5	< 5
Cu	< 2	< 2	5	50	< 5
Fe	< 2	< 2	< 5	< 5	< 5
Mg	< 2	< 2	5	< 5	5
Mn	< 2	< 2	< 5	< 5	< 5
Mo	< 2	< 2	< 5	< 5	< 5
Na	< 30	< 20	< 75	< 50	< 10
Ni	< 2	< 2	< 5	< 5	< 5
Pb	< 30	< 10	< 50	< 50	< 50
Si	2	< 2	5	5	< 5
Sn	< 10	< 10	< 25	< 25	< 25
Sr	< 2	< 2	25	25	25
Ti	< 10	< 10	< 25	< 25	< 25
V	< 10	< 10	< 25	< 25	< 25
Zr	< 10	< 10	< 25	< 25	< 25

VI. TEST FACILITY

The test facility utilized for operation of the T-111 Rankine System Corrosion Test Loop is the same as that previously used for the Cb-1Zr Rankine System Corrosion Test Loop. A detailed description of this facility may be found in Reference 1. Figure 42 shows an overall view of the equipment, including the vacuum chamber and control console.

A. VACUUM SYSTEM

The vacuum chamber is feet (1.2 m) in diameter and consists of three sections; the bell jar, the spool piece in which the loop is supported, and the sump. The overall height of the chamber is 11 feet (3.3 m). The three sections are joined together with Wheeler flanges which utilize a 0.125-inch (3.2-mm)-diameter copper wire gasket for sealing. Electrical resistance strip heaters are attached to the chamber wall to permit continuous bakeout of the chamber to 500°F (260°C). The chamber is covered with an aluminum shroud which thermally insulates the chamber, results in more uniform heating, and provides maximum safety to operating personnel. The chamber has water cooling channels welded to the wall which are capable of removing approximately 100 kw of heat during test operation.

The vacuum chamber is rough pumped with a turbomolecular pump (Sargent-Welch Scientific Company, Model 3102A) backed by a 15-cfm (7-ℓ/sec) mechanical forepump. Pumping in the high- and ultrahigh-vacuum ranges is provided by a 2400-ℓ/sec getter-ion pump (Varian Model 912-5002). At the completion of the 5000 hours of testing of the Cb-1Zr Corrosion Loop,[15] the ion pump was removed from the system and returned to the manufacturer for routine cleaning and maintenance. At this time, newly developed insulator assemblies were installed. In addition, the pump elements were replaced with the new "super elements"(slotted cathode) which, according to the manufacturer, have higher pumping speed for the inert gases.

In addition to the getter-ion pump, four titanium sublimation pumps

---

(15) Hoffman, E. E. and Holowach, J., Cb-1Zr Rankine System Corrosion Test Loop, NASA CR-1509, June 1970.

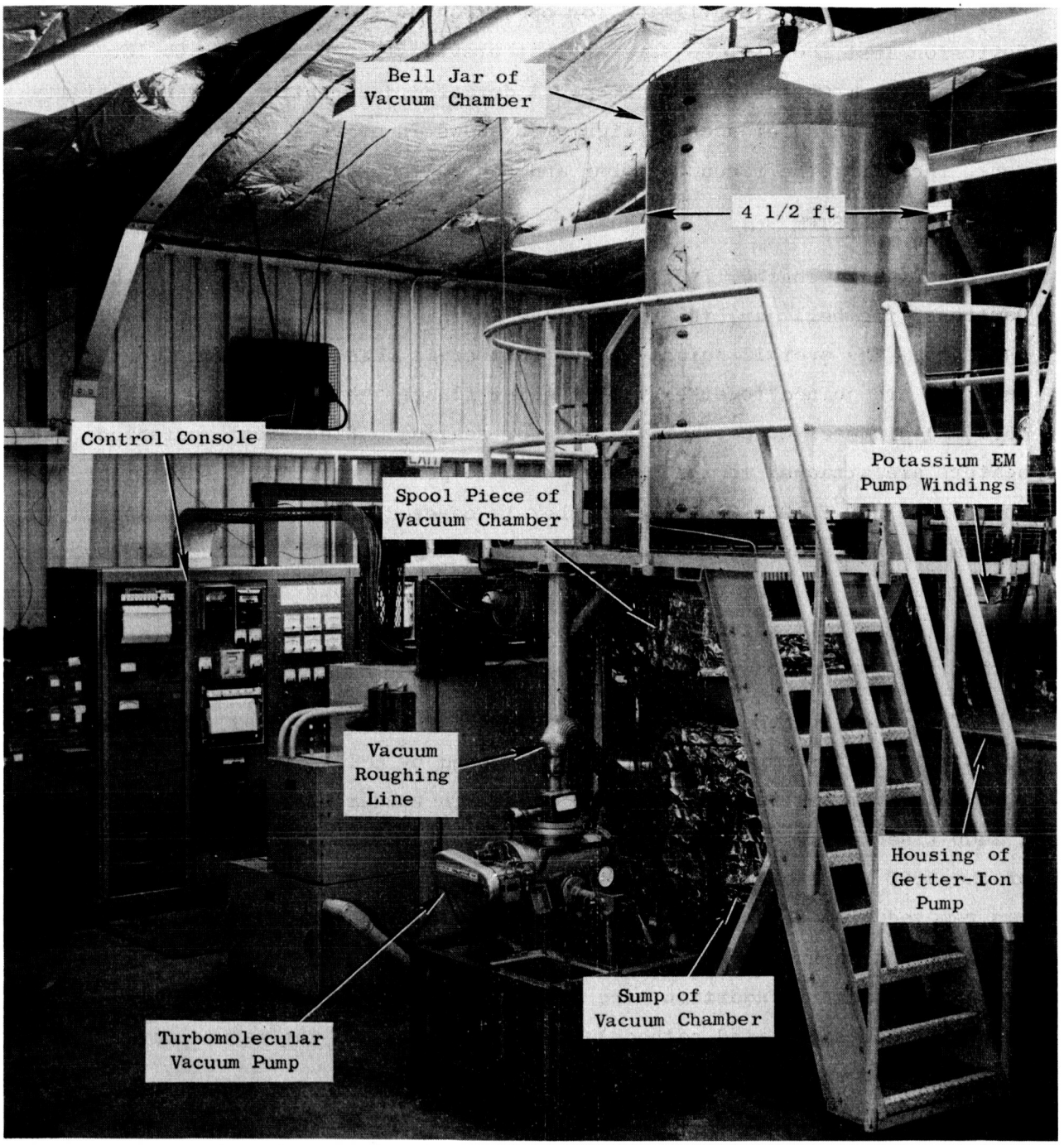


Figure 42. Test Facility for Operation of T-111 Corrosion Test Loop. (Orig. 69-1-63D)

ORIGINAL PAGE IS OF POOR QUALITY

are available for use during period of high outgassing. These pumps are located in the bottom of the sump.

As a result of the stress-corrosion cracking of the wall of the spool piece encountered during operation of the Cb-1Zr Corrosion Loop,[15] a new spool piece was fabricated for the T-111 Corrosion Loop Test. In order to minimize the possibility of further problems with stress-corrosion cracking, the following important changes were made in the design of the new spool piece.

1. The inlet and outlet fittings of the water cooling system on the spool piece were located so as to assure that the channels are completely filled with water during test operation.
2. Water cooling channels were located closer together (minimum spacing of 4 inches (10 cm) in order to reduce the wall temperature gradients.
3. All stainless steel fittings were used in the cooling water circuit.

In addition to these changes in the cooling water circuit, the location of one EM pump port in the spool piece was changed so that there was a 45^{o} angle between the two EM pumps, rather than 90^{o} as was the case with the Cb-1Zr loop. The reason for this change was to facilitate insertion of the loop into the spool piece.

The bell jar section of the chamber is raised and lowered by a 2-ton (1810-kg) chain hoist. Four 4-inch (10-cm)-diameter bakeable Pyrex glass viewing ports are mounted in the wall of the bell jar. These view ports permit observation and photography of loop components during test operation.

B. CHAMBER PRESSURE AND PARTIAL PRESSURE MEASUREMENT

The vacuum chamber contains a hot filament ionization gauge and a mass spectrometer. Reduction of data from these two instruments involves a procedure in which the total pressure is obtained from the ionization gauge reading, connected for relative concentrations of the various gas

species. The relative concentrations are obtained from the mass spectrometer. Details of the mass spectrometer calibration and the data reduction procedure are given in Appendix H, Calibration of the Partial Pressure Gas Analyzer.

The hot filament ionization gauges[a] may be used alone to obtain the approximate total pressure in the chamber, or what is sometimes referred to as the "nitrogen equivalent pressures." The ionization gauge had been calibrated by the manufacturer for nitrogen, as previously reported.[15] The output of the ionization gauge was fed to a strip chart recorder continuously during the test for a permanent record of the chamber pressure.

The mass spectrometer used[b] was a 90° magnetic sector type with a 5-cm radius of curvature. The ion detector is a 10-stage electron multiplier. A 3-kilogauss permanent magnet focuses the ion beam, and electrostatic scanning results in good peak separation in the mass-to-charge range between 2 and 50.

The ionization gauge, partial pressure analyzer tube, and a variable leak valve are mounted in the chamber sump as shown in Figure 43. The variable leak valve is used to introduce gases into the chamber for calibration of the partial pressure analyzer. Figure 44 shows the electronic control unit and the X-Y recorder used for the residual gas analysis.

C. HEATER POWER SUPPLIES

The lithium heater power supply consists of a combined temperature controller and stepless power regulator system with a stepdown current transformer. The system has a continuous power rating of 20 kva with 440-volt, single-phase input. The combined temperature controller and power regulator includes:

1. A manual power adjustment,
2. Automatic set point control,
3. Current limiter control.

(a) Varian, Model UHV-12.

(b) General Electric Partial Pressure Analyzer Model 22PT110 with Model 22PC110 control.

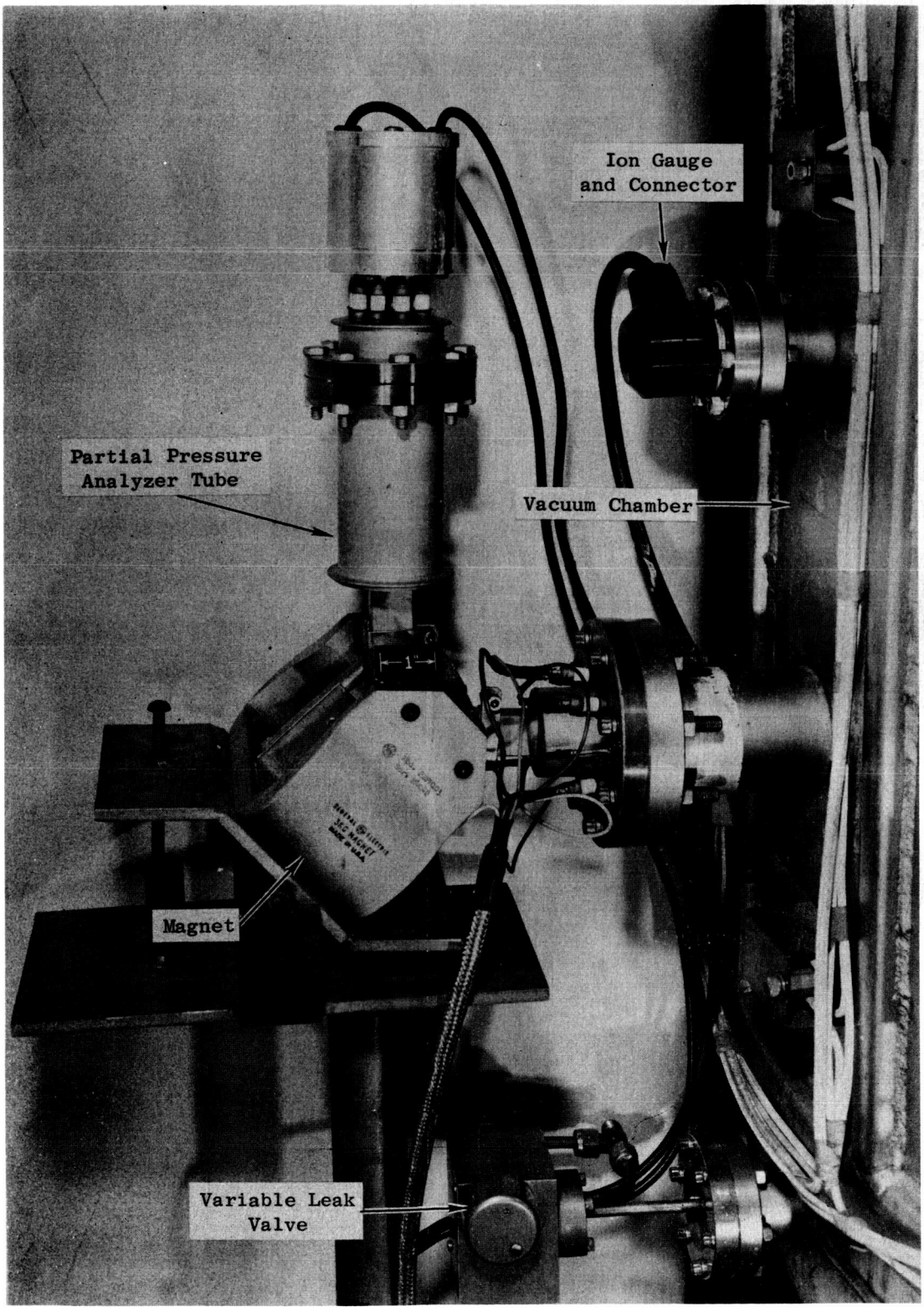


Figure 43. Ion Gauge, Partial Pressure Analyzer Tube, and Variable Leak Valve Mounted on Chamber Sump. (Orig. C66050427)

ORIGINAL PAGE IS
OF POOR QUALITY

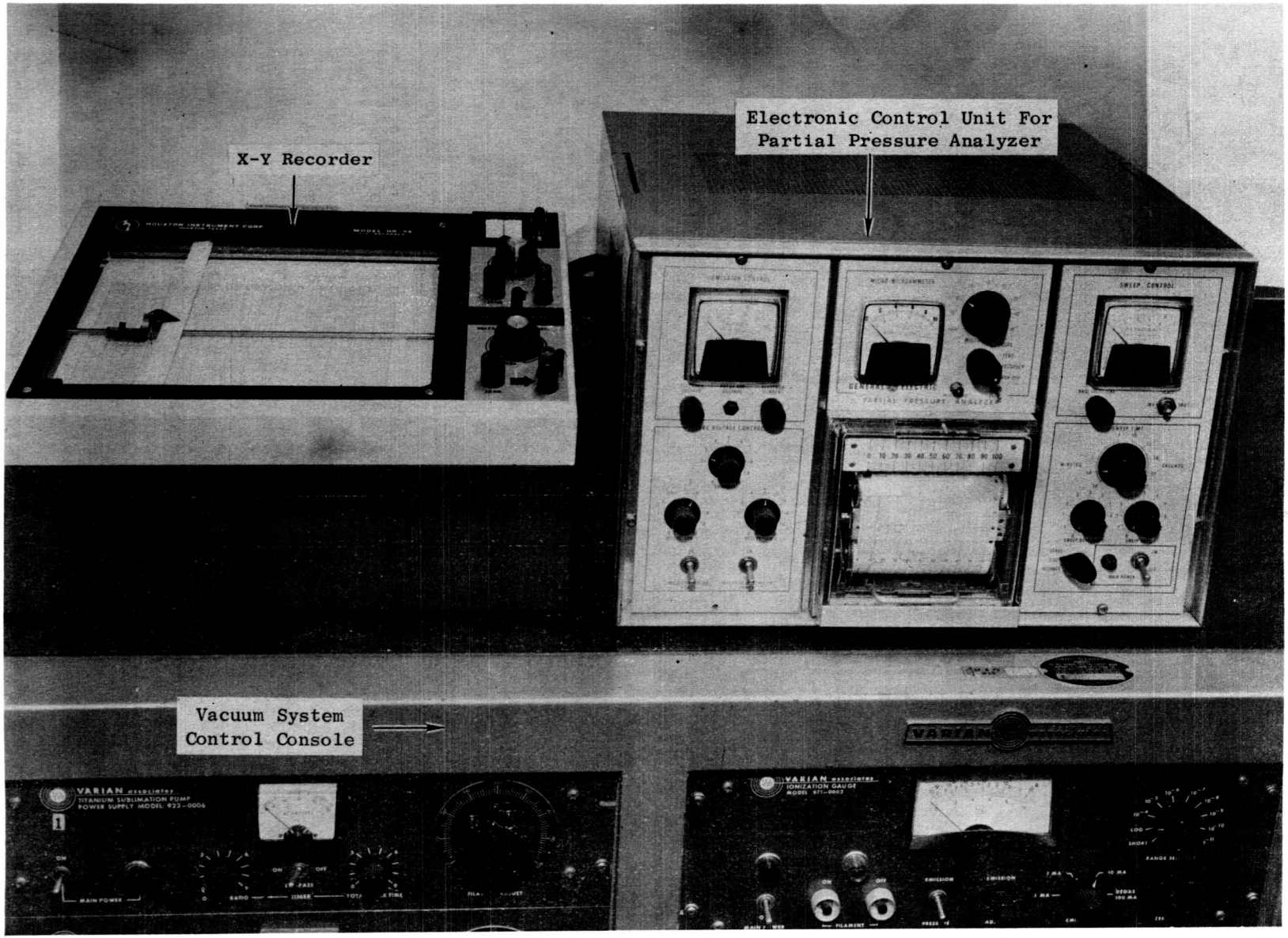


Figure 44. Electronic Control Unit and X-Y Recorder for the Partial Pressure Analyzer. (Orig. C66050426)

The system included a single-pen, 1/4-percent, null-balance, servo-operated recording potentiometer with a General Electric Model 524 controller (3-mode proportional control with rate action and automatic reset), and an amplistat plus a saturable core reactor and current transformer. The system functioned as follows:

An input signal to the recorder is obtained from the control thermocouple and is measured by the recorder. This input signal is compared to a known voltage developed across the measurement slidewire. The slidewire is part of a bridge circuit, the other part of which is located in the 3-mode controller. The output of the controller is directly proportional to the unbalance of the bridge circuit and a provides a dc control signal to an amplistat. The control signal is amplified by the amplistat to a sufficient level to operate a saturable reactor. The output of the saturable reactor is connected to a stepdown transformer rated at 5000 amperes continuous duty. The high current is fed through the vacuum chamber to the loop heaters by water-cooled, 1000-ampere feedthroughs.

Power is supplied to the potassium preheater from a silicon-controlled rectifier unit with a stepdown current transformer. Output of the secondary is rated at 5 kva and 1000 amperes. The preheater temperature is controlled by a proportional temperature controller.

VII. INSTRUMENTATION AND INSTALLATION OF THE LOOP

The test loop was positioned near the vacuum system, and an air shelter was assembled over the loop. The air shelter, which was previously used for instrumentation of the Cb-1Zr Rankine System Corrosion Test Loop,[16] is a reinforced polyethylene hemisphere approximately 15 feet (4.6 m) in diameter by 15 feet (4.6 m) high and is supported by 0.2 psig (3×10^3 N/m^2) air pressure supplied by a centrifugal blower. The loop is at ground level and is readily accessible for instrumentation. All personnel are required to wear clean, white dacron gloves, shoe covers, and coveralls while working in the air shelter.

The temporary support brackets used in the fabrication and transfer of the loop were removed, and permanent support brackets and instrumentation channels for routing thermocouple and pressure sensor lead wires were installed. The copper bus bars for both the potassium preheater and lithium heater were also installed at this time, since they also serve as structural support members to maintain the helical heater coils in position.

A. INSTALLATION OF THERMOCOUPLES AND THERMAL INSULATION

The temperature of the various loop components was measured with thermocouples made of 0.005-inch (0.13-mm)-diameter W-3Re and W-25Re wires. The thermocouple wires inside the chamber were electrically insulated with high-purity, two-hole, 99.5 percent alumina insulators to the point of contact with the material. Beryllium oxide insulators (99.5 percent) were used in contact with the regions of the loop designed to operate at temperatures in excess of 2000°F (1093°C).

All thermocouples were taken from single lots of matched W-3Re and W-25Re wire. This is the same wire that had been previously calibrated and used to instrument the Cb-1Zr Corrosion Test Loop.[16] The calibration data are given in Appendix I of this report, Calibration of W-3Re/W-25Re Thermocouple Wire.

---

(16) Hoffman, E. E. and Holowach, J., Cb-1Zr Rankine System Corrosion Test Loop, NASA CR-1509, June 1970.

The locations and identifications of the 80 thermocouples, which were installed on the loop, are shown in Figure 45. Sixty-seven of the thermocouples are of the wall junction or surface type with each thermocouple wire spot welded directly to the loop components. The remaining thirteen thermocouples were of the well type in which the thermocouple is beaded before insertion in a cavity. The well-type thermocouples were used for components where an accurate average temperature was required, and the geometry of the component permitted the location of a well tube or a drilled hole. These included certain parts of the EM pumps, the turbine simulator, the potassium preheater, and the condenser. A typical thermocouple installation of the wall type may be seen in Figure 46, which shows the instrumented boiler assembly.

Thermal insulation consisting of multiple layers of Cb-1Zr foil was applied to the loop as the thermocouples were installed. The insulation used on all circular pipe sections was 0.002-inch (0.05-mm)-thick x 0.5-inch (1.27-mm)-wide foil which had been dimpled by passing the foil between a hardened steel, coarse-knurled roller working against a hard plastic sheet. The effective thickness of the foil after dimpling was 0.009 to 0.012 inch (0.23 to 0.30 mm). The insulation was attached to the tube by spot welding the foil to the tube and to itself as succeeding layers were applied as shown in Figure 47. A minimum number of spot welds were used to minimize conduction heat losses through the foil. A refractory metal electrode (molybdenum) was used on the spot welder to avoid contamination of the foil surface, and argon cover gas flooded the spot-welded area to prevent oxidation.

The boiler was insulated as a unit by first inserting an inner cylindrical section down the center and placing end shields on the top and bottom. The inner cylinder and bottom shield are in place in Figure 46. Following installation of the thermocouples, the outside of the boiler was wrapped with continuous spiral layers of Cb-1Zr foil, 8 inches (20.3 cm) wide. Spacing between the adjacent layers of insulation was maintained by tantalum wires.

A typical thermocouple circuit originates at the hot junction of the thermocouple, and the thermocouple leads are routed along the support structure

ORIGINAL PAGE IS
OF POOR QUALITY

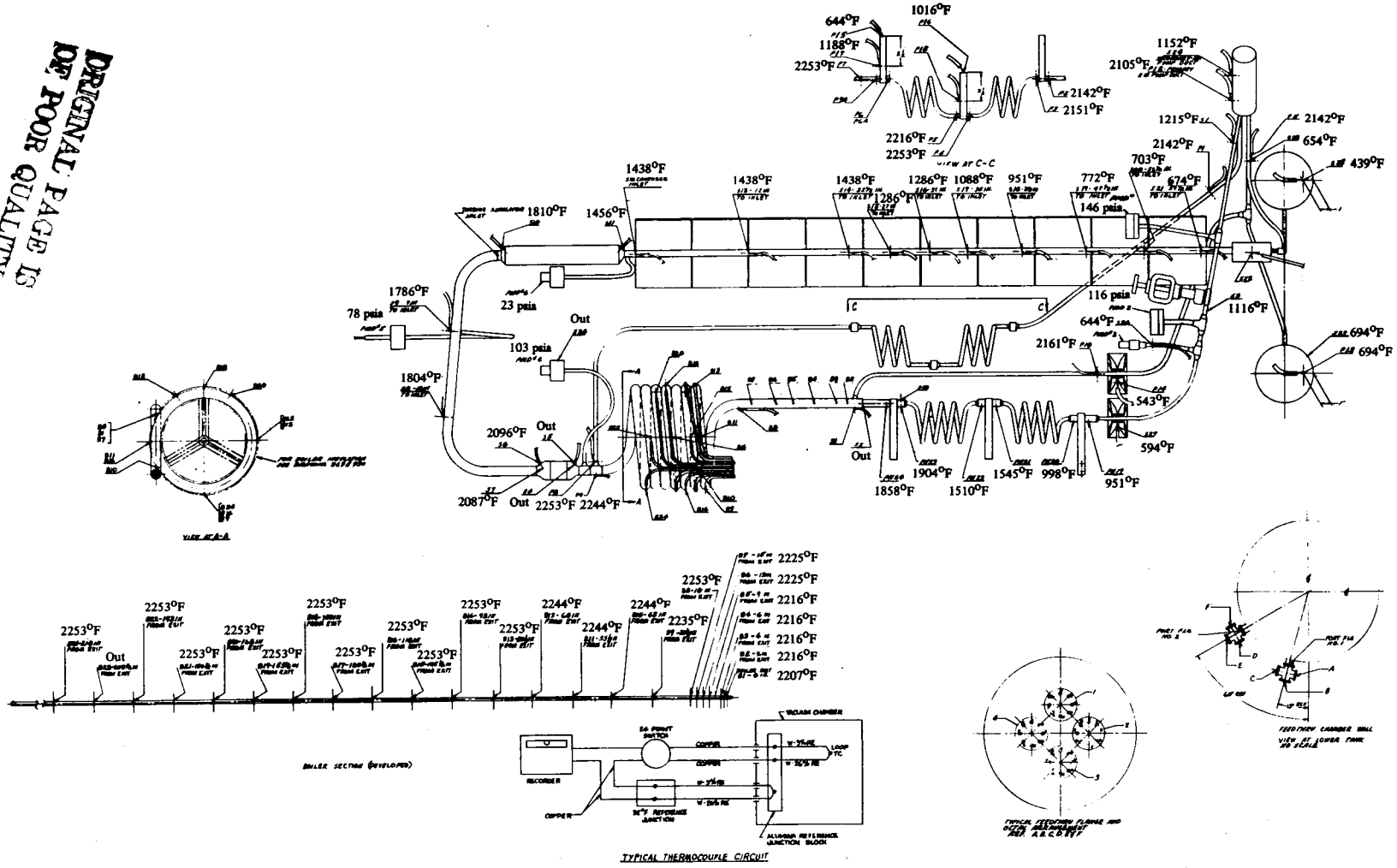


Figure 45. Instrumentation of T-111 Rankine System Corrosion Test Loop Showing Typical Test Conditions.

ORIGINAL PAGE IS
OF POOR QUALITY

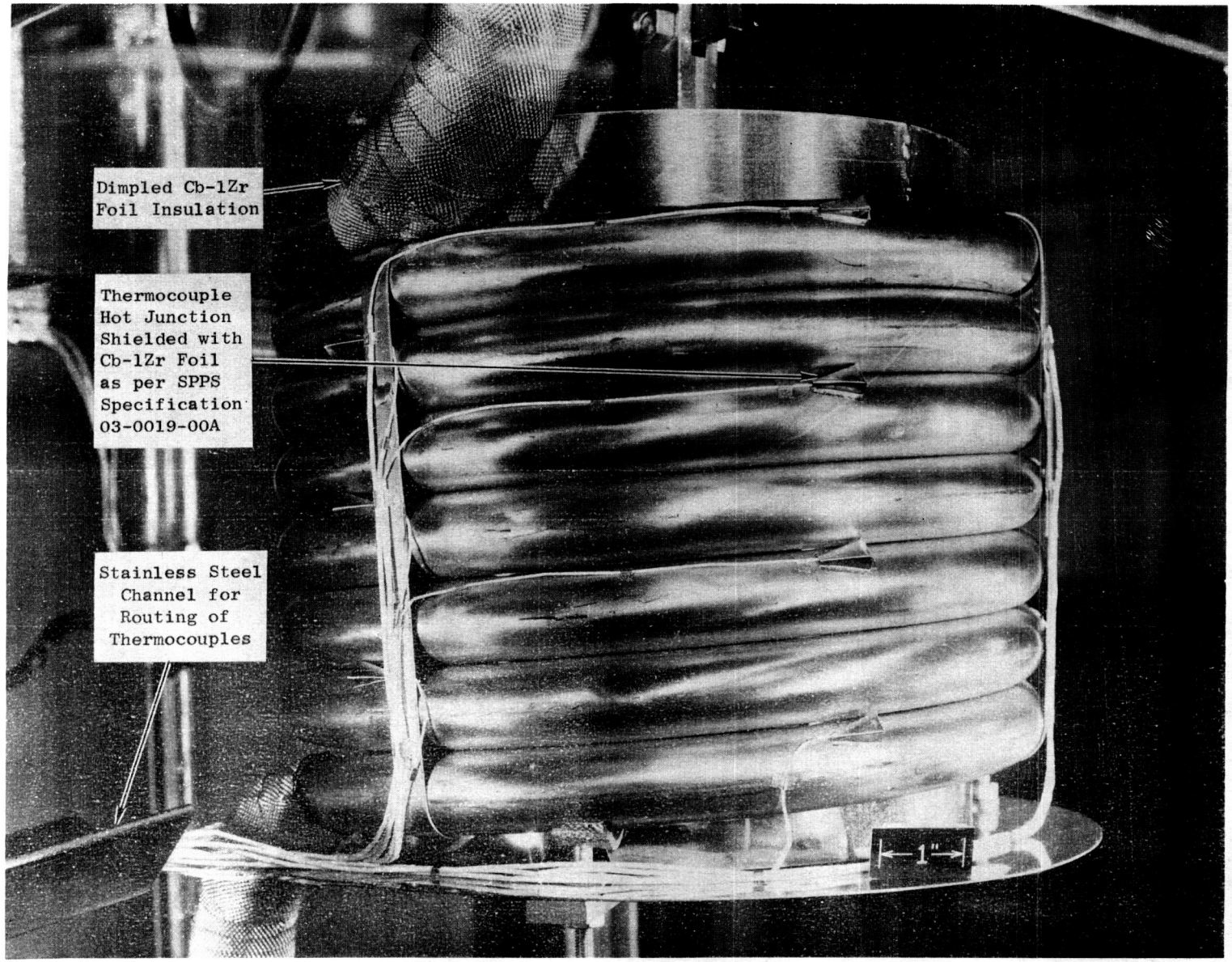


Figure 46. Thermocouple Installation on the Tube-in-Tube Helical Boiler of the T-111 Corrosion Test Loop.

(Orig. C68013186)

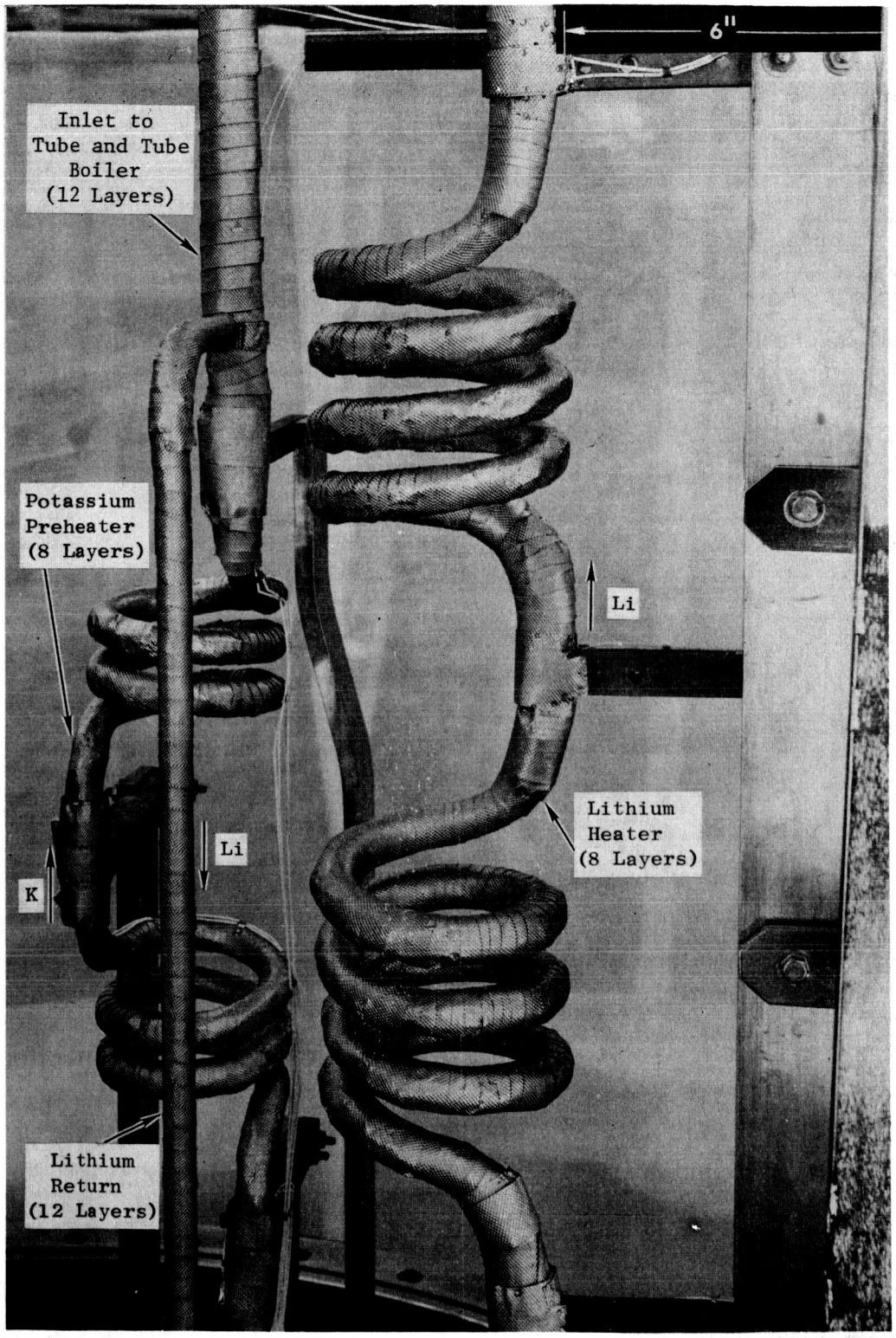


Figure 47. Typical Cb-1Zr Dimpled Foil Thermal Insulation of Various Loop Components. (68013191)

to a thermocouple reference junction block attached to the inside wall of the spool section. The thermocouple reference junction block, shown in Figure 48, consists of a 99.7% Al_2O_3 terminal strip mounted on a copper block and mechanically fastened to the walls of the chamber. The entire assembly is shielded from the loop to minimize temperature gradients in the junction block as well as maintain a lower absolute temperature approaching that of the water-cooled vacuum tank wall. At the reference junction block, a transition from the thermocouple wire to copper wire is made, and the copper wires are routed through the thermocouple vacuum feedthroughs (shown in Figure 49) to three 24-point recording potentiometers.

Automatic compensation of all thermocouples to a thermoelectrically cooled, ice point calibration standard is obtained by use of the circuit shown schematically in the insert of Figure 45. A W-3Re/W-25Re thermocouple is connected with its hot junction at the isothermal reference terminal inside the vacuum chamber and its cold junction at the ice point reference located outside the vacuum chamber. This thermocouple is connected in series with the measuring thermocouples so that a millivolt signal proportional to the difference between the internal reference junction block and the ice point is added to each thermocouple signal. The EMF of each loop thermocouple is thus recorded directly with an ice point reference.

B. TRANSFER OF LOOP AND CHAMBER SPOOL PIECE TO THE TEST FACILITY

In Figure 50, the loop is shown mounted in the spool piece after completion of instrumentation. The entire assembly was then moved from the clean room to the vacuum chamber. The plywood pallet on which the spool section and loop rested was lifted by a fork truck and held above the vacuum sump while the bell jar was lowered and then bolted to the spool flange. The bell jar and the attached spool section were raised together off the pallet and then lowered to the sump. The flanges were bolted together, and the vacuum chamber was evacuated and helium leak-checked. This sequence was required to ensure a leak-tight joint between the sump and lower spool flange because the spool becomes fixed in position when the EM pump windings for the two pumps are attached to their spool flanges and the gas pressurization and liquid metal fill lines are welded to their spool piece ports.

ORIGINAL PAGE IS
OF POOR QUALITY

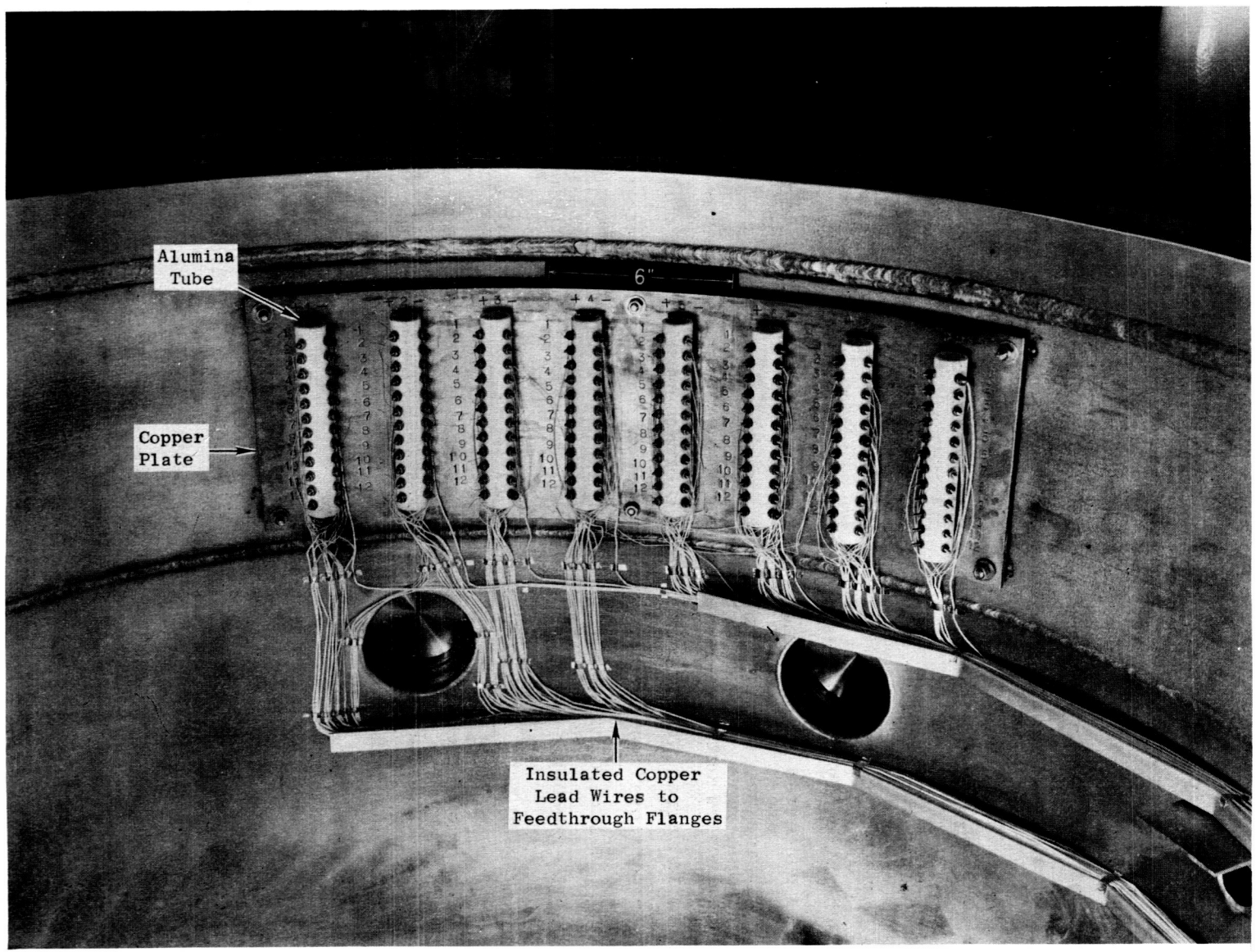


Figure 48. Thermocouple Wire Terminals (192 Total) Located in the Sump of the Test Chamber for the T-111 Corrosion Test Loop.
(Orig. C65062196)

ORIGINAL PAGE IS
OF POOR QUALITY

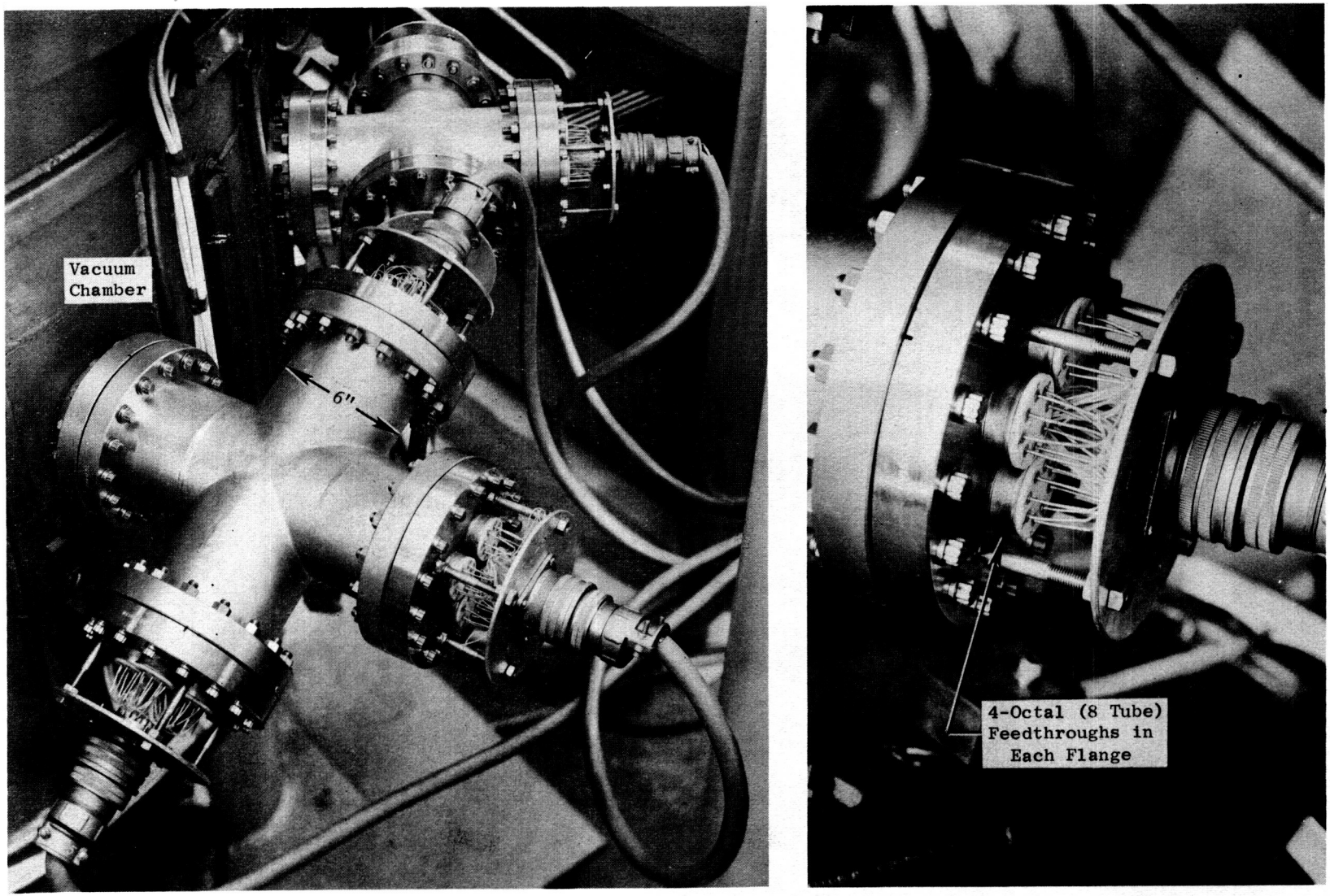


Figure 49. Six Thermocouple Lead Wire Feedthrough Flanges with 32 Wires in Each Flange. An Enlarged View of One of the Flanges is Shown on the Right. (C65062189)

ORIGINAL PAGE IS
OF POOR QUALITY

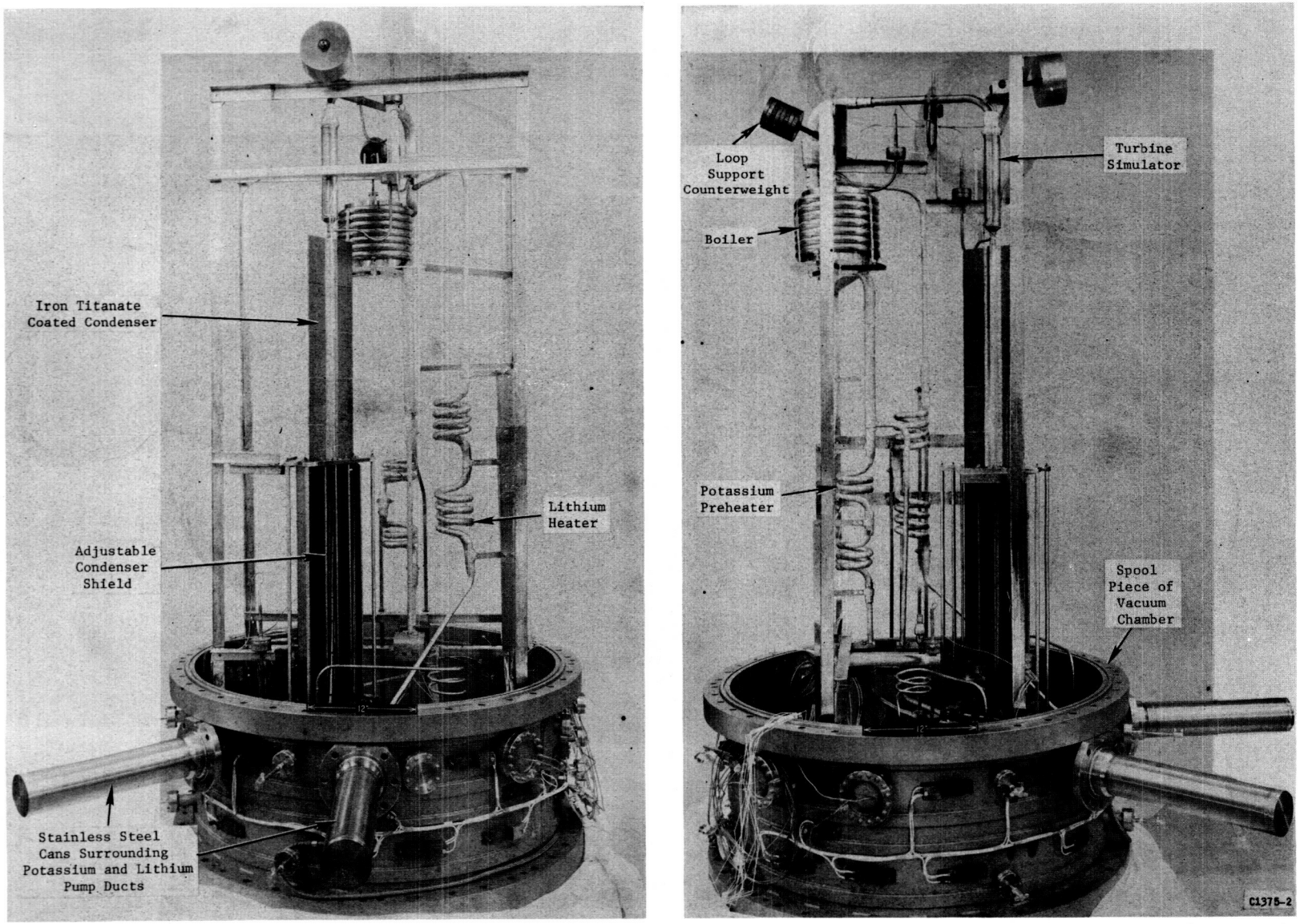


Figure 50. T-111 Rankine System Corrosion Test Loop. Following Instrumentation Before Installation on the Vacuum Chamber Sump. (Orig. C68013187, C68013190)

Upon completion of the helium leak check, the vacuum system air release valve was opened and the chamber was returned to atmospheric pressure. The bell jar was hoisted into the penthouse above the chamber, and the final instrumentation and the installation of loop components, which could only be completed with the loop in its final test position, were resumed.

The metering and on-off isolation valves, as shown in Figure 51, were assembled with their actuating systems which consist of ultrahigh-vacuum rotary feedthroughs[a] with a torque rating of 6 ft-lb (0.8 kg-m) connected by a 0.31-inch (0.8-cm)-diameter, flexible, stainless steel cable to a 3:1-right-angle gear drive mounted on the valve yoke.

A 500-watt, quartz lamp heater,[b] shown in Figure 52, was installed on the shell of the lithium surge tank to supplement the vacuum chamber bakeout heaters in melting the lithium in the surge tank after a loop shutdown. The heater is also used during low-power operation to maintain the surge tank above the melting point (357°F, 180.6°C) of lithium when the bakeout heaters are off.

The adjustable condenser shield assembly, as shown in Figure 53, was the last component to be installed. The shield is actuated by a rack-and-spur gear drive system and consists of eight movable shield fins constructed of Cb-1Zr. A view of the lower section of the test loop is shown in Figure 54.

(a) Varian Associates, Model No. 954-5039.

(b) General Electric Model 500T3CL, 117 v.

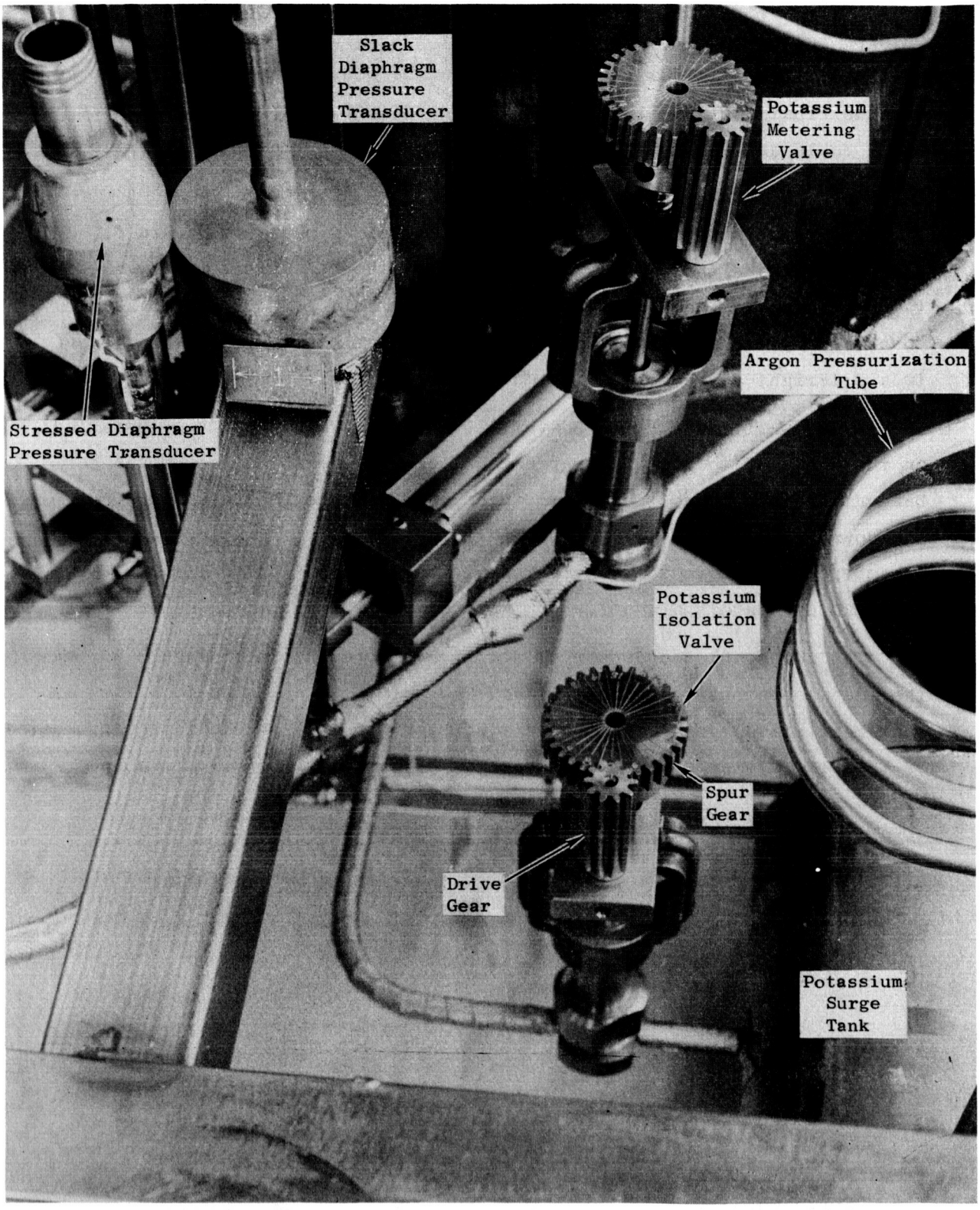


Figure 51. Metering Valve and Isolation Valves of the T-111 Corrosion Test Loop. (68013184)

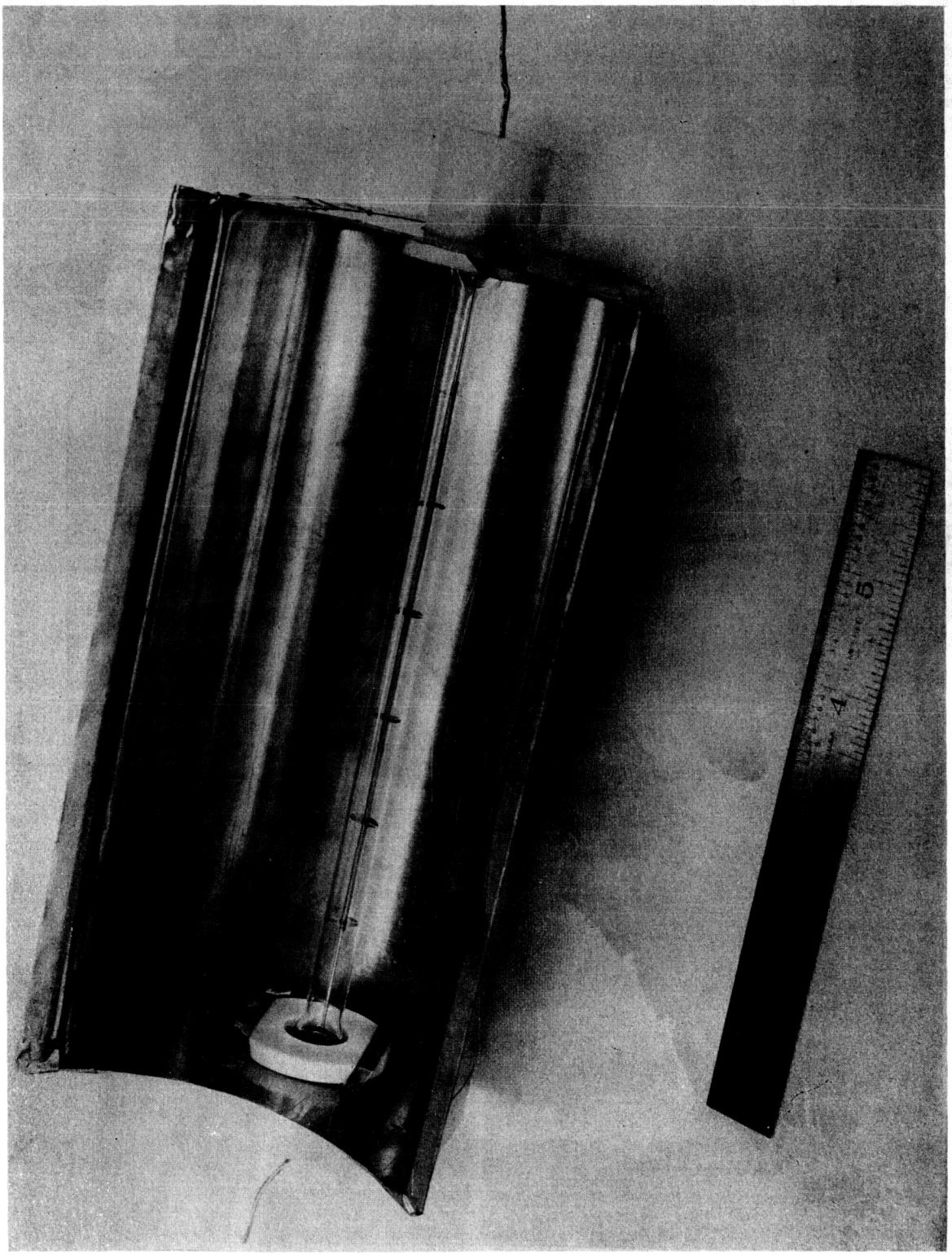


Figure 52. Auxiliary Quartz Lamp Heater Used on the Lithium Surge Tank. (Orig. C68013196)

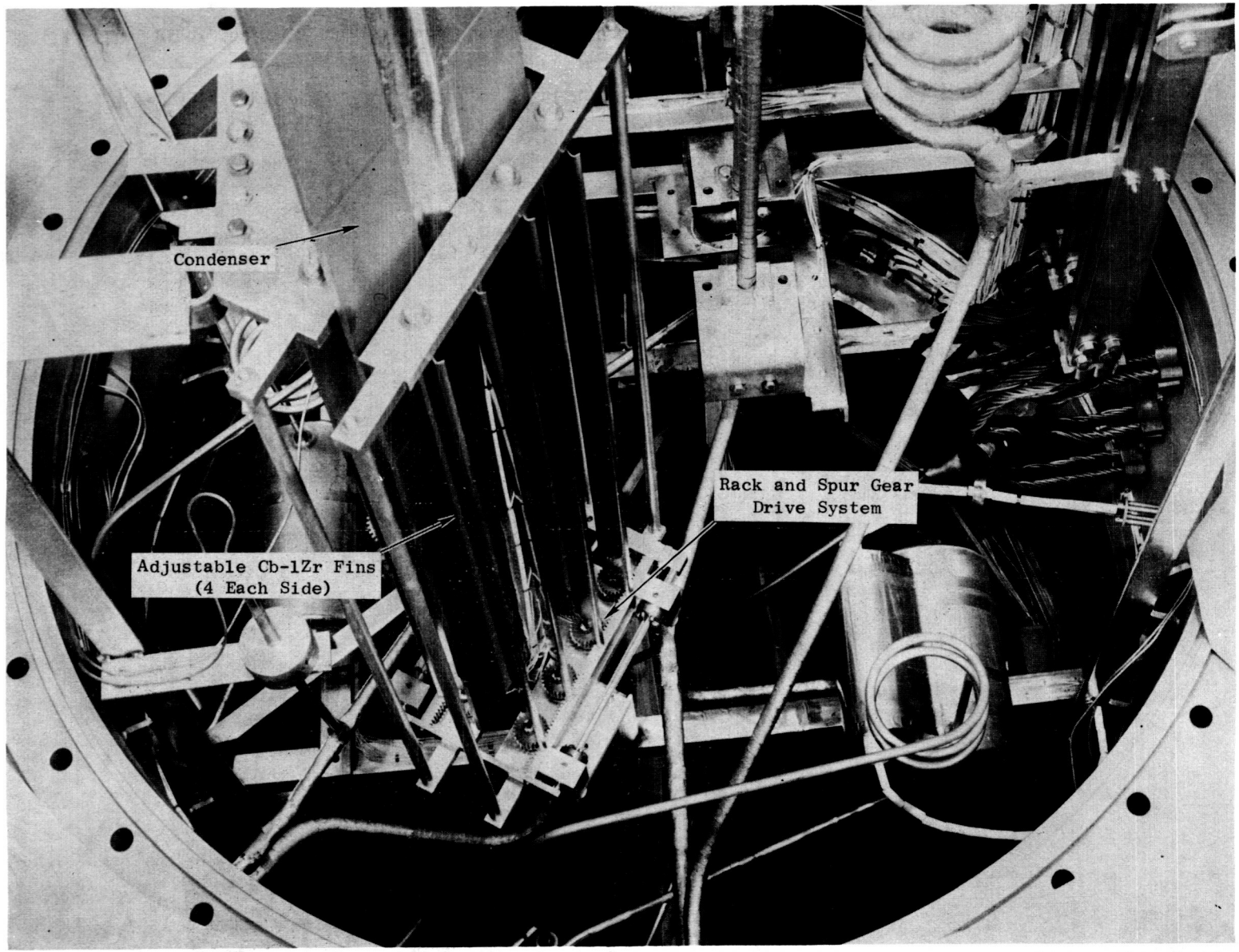


Figure 53. Adjustable Condenser Shield and Drive Mechanism.

(Orig. C68021350)

ORIGINAL PAGE IS
OF POOR QUALITY

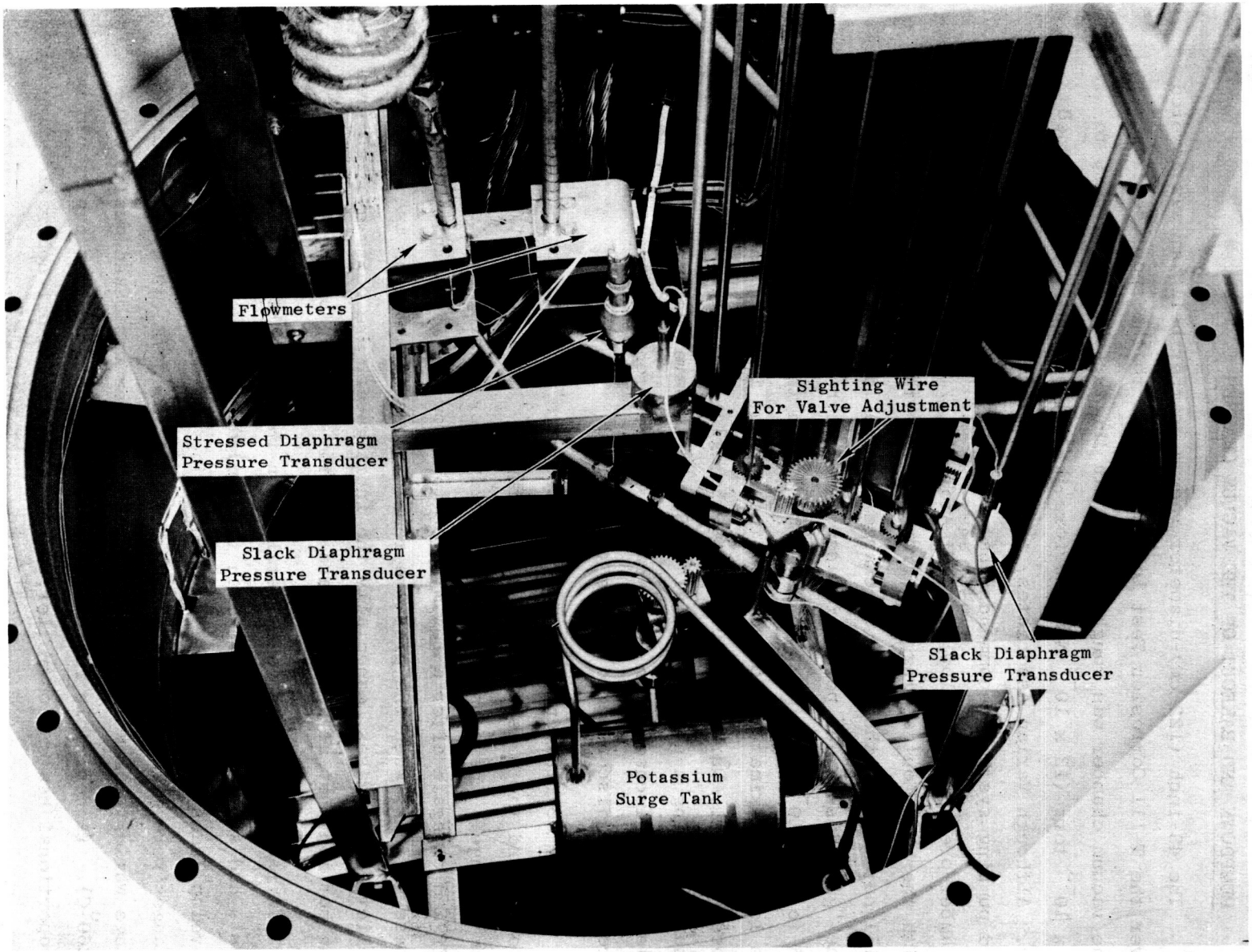


Figure 54. Lower Portion of the T-111 Corrosion Test Loop.
(Orig. C68021351)

VIII. PRETEST OPERATION

A. PUMPDOWN AND BAKEOUT OF THE VACUUM CHAMBER

The 48-inch (122-cm)-diameter vacuum chamber bell jar was lowered over the T-111 Corrosion Test Loop and bolted to the spool section. The vacuum chamber was rough-pumped with the turbomolecular pump to 1×10^{-3} torr (13×10^{-2} N/m^2) before the getter-ion pump was turned on. Although Varian Associates, the manufacturer of the test chamber and pumping system, recommends that the ion pump be turned on when the vacuum chamber pressure is below 15×10^{-3} torr (2 N/m^2), it has been found that with the heavy outgassing load from the loop the ion pump overheats and will not confine the "glow discharge" at the 15×10^{-3} torr (2 N/m^2) level. The "glow discharge" period is associated with the high-pressure operation (5 to 20×10^{-3} torr [0.7 to 2.7 N/m^2]) when the getter-ion pump voltage is low (approximately 200 volts), the current is high, and the pumping speed is low. During the period of the "glow discharge," electrical discharges having a peak potential of 300 volts have been measured, and the electrical discharge can cause damage to electronic controls that are not grounded or disconnected during this period.

After confinement of the "glow discharge," the pumpdown proceeded slowly, and the pressure remained in the 10^{-4} to 10^{-6} torr (10^{-2} to 10^{-4} N/m^2) range. The pumpdown was accelerated by turning the ion pump power off and on again after a few minutes to allow the ion pump to cool. During these periods, when the pressure remains constant or even increases, it is believed that gases, especially the inert gases, are being evolved from the hot ion pump at a higher rate than the ion pump pumping speed.

Air cooling ducts were installed on the main flanges since previous tests had shown that the 48-inch (122-cm)-diameter Wheeler flange would develop leaks when thermally cycled during the bakeout period. The air-cooled flanges were maintained in the 90°F (32°C) to 120°F (49°C) temperature range while the remainder of the vacuum chamber was baked out at 500°F (260°C). (A desirable feature of vacuum chambers of this type would be a proportional heater controller, rather than the on-off controller supplied with the system, which would permit a controlled heating and cooling rate

for the main flange and also provide better control over the outgassing rate of the loop at the start of the bakeout period.)

The vacuum chamber pressure at the start of the bakeout period was 4.8×10^{-8} torr (6.4×10^{-6} N/m^2). The bell jar bakeout heaters were the first to be turned on, followed by the spool section heaters and then the sump heaters as the initial outgassing rate decreased and the getter-ion pump could handle the gas load without overheating. The vacuum chamber pressure increased to the 10^{-6} torr (10^{-4} N/m^2) range during this period. After the vacuum chamber pressure returned into the 10^{-7} torr (10^{-5} N/m^2) range, the EM pump power was turned on at 10 percent of the rated power to inductively heat the pump ducts and the insulation cans to accelerate their outgassing rate. A log of the pressure during bakeout is presented in Table XVI.

B. FINAL HELIUM LEAK CHECK OF THE TEST LOOP

The T-111 Corrosion Test Loop was helium leak checked after the final assembly weld was made, and no indication of a leak was observed at that time. A final leak check of the test loop was made after the loop was installed in the vacuum chamber and during bakeout prior to filling the loop with alkali metal. This leak check was made using the partial pressure gas analyzer of the 48-inch (122-cm)-diameter vacuum chamber system which is used to measure the residual gas in the vacuum chamber during test operations. The leak check was made by comparing the argon background level in the vacuum chamber with the loop evacuated and with an internal argon pressure of 18 psia (124×10^3 N/m^2 abs.). No change in the argon background level was found during the pressurization of the loop with argon.* The total pressure in the vacuum chamber during the leak check remained at 3×10^{-7} torr (4×10^{-5} N/m^2).

Following completion of leak checking, the two circuits of the loop were filled with purified lithium and potassium as described in Section V.

*NOTE: Although a leak check across the wall separating the potassium and lithium regions of the tube-in-tube boiler was performed following fabrication of this component, no leak check of this type was performed following installation in the test facility. It is recommended that a check of the later type be considered mandatory for systems of this type in the future.

TABLE XVI

CHAMBER BAKEOUT
PRESSURE LOG

Date	Hours On Bakeout	Chamber Pressure*	Average Loop Temperature		Remarks
2-16	0	4.8×10^{-8}	Room Temperature		Prior to starting bakeout
2-17	24	3.5×10^{-6}	380°F	193°C	Bell jar bakeout only
2-18	48	1.2×10^{-6}	400°F	204°C	Spool and sump bakeout on
2-19	72	3.0×10^{-7}	400°F	204°C	
2-20	96	3.0×10^{-7}	400°F	204°C	
2-21	120	2.5×10^{-6}	400°F	204°C	Power to EM pumps
2-22	144	3.6×10^{-7}	400°F	204°C	
2-23	168	2.3×10^{-7}	400°F	204°C	
2-24	192	2.7×10^{-7}	400°F	204°C	
2-26	240	1.3×10^{-7}	400°F	204°C	
2-27	264	2.5×10^{-7}	400°F	204°C	Bake out on partial pressure analyzer
2-28	288	1.0×10^{-7}	400°F	204°C	
2-29	312	8.5×10^{-8}	400°F	204°C	
3-1	336	8.6×10^{-8}	400°F	204°C	
3-2	360	1.2×10^{-7}	400°F	204°C	Loop filled with K and Li
3-4	408	1.0×10^{-7}	400°F	204°C	
3-5	432	4.0×10^{-7}	525°F	274°C	Ciculated alkali metals in loop
3-6	456	1.9×10^{-7}	525°F	274°C	Start pretest checkout

* Torr x 133 = N/m^2

C. CHECKOUT AND CALIBRATION OF THE LOOP INSTRUMENTATION

The calibration of all pressure sensors was repeated with the loop filled with potassium at 500°F (260°C) and the vacuum chamber on bakeout. The pressure sensors were originally calibrated at room temperature with argon before the loop was filled with alkali metal. All pressure sensors showed good linearity and excellent repeatability over the operating range. The calibration results for the slack diaphragm pressure transducer No. 1 (potassium pump outlet) are shown in Figure 55 and are typical of the results obtained for the other four slack diaphragm transducers.

The calibration of the fast-response stressed diaphragm pressure transducer with potassium prior to the test startup is shown in Figure 56. The temperature of the transducer during the liquid metal calibration was 400°F (204°C).

The primary loop thermocouples were checked by operating the lithium circuit at near-isothermal conditions and comparing the indicated temperature of each thermocouple with those thermocouples adjacent to it. A near-isothermal condition in the primary circuit was achieved by operating at a high-lithium flow rate (2 gpm [0.45 m^3/hr]) with the potassium loop empty. The calibration is also useful in computing the heat balance in subsequent loop operation because the temperature drop of the lithium can be equated to the heat loss of the boiler. The temperature distribution as a function of boiler length for the calibration run is shown in Table XVII. Although higher temperature calibrations are desirable, they were not made at this time because of the high outgassing rate of the loop.

The primary and secondary flowmeters were calibrated by an energy balance across the preheater and heater during all liquid operation. The results of these tests are shown in Figures 57 and 58. The millivolt output as a function of flow rate was considerably lower than that predicted by the theoretical[17] equation for magnetic flowmeters. This discrepancy in flow rates was also observed in the Cb-1Zr Corrosion Test Loop flowmeter

---

(17) Affel, R. G., Burger, G. H., and Pearce, C. L., Calibration and Testing of 2- and 3 1/2-Inch Magnetic Flowmeters for High-Temperature NaK Service, Oak Ridge National Laboratory, ORNL-2793, p. 16.

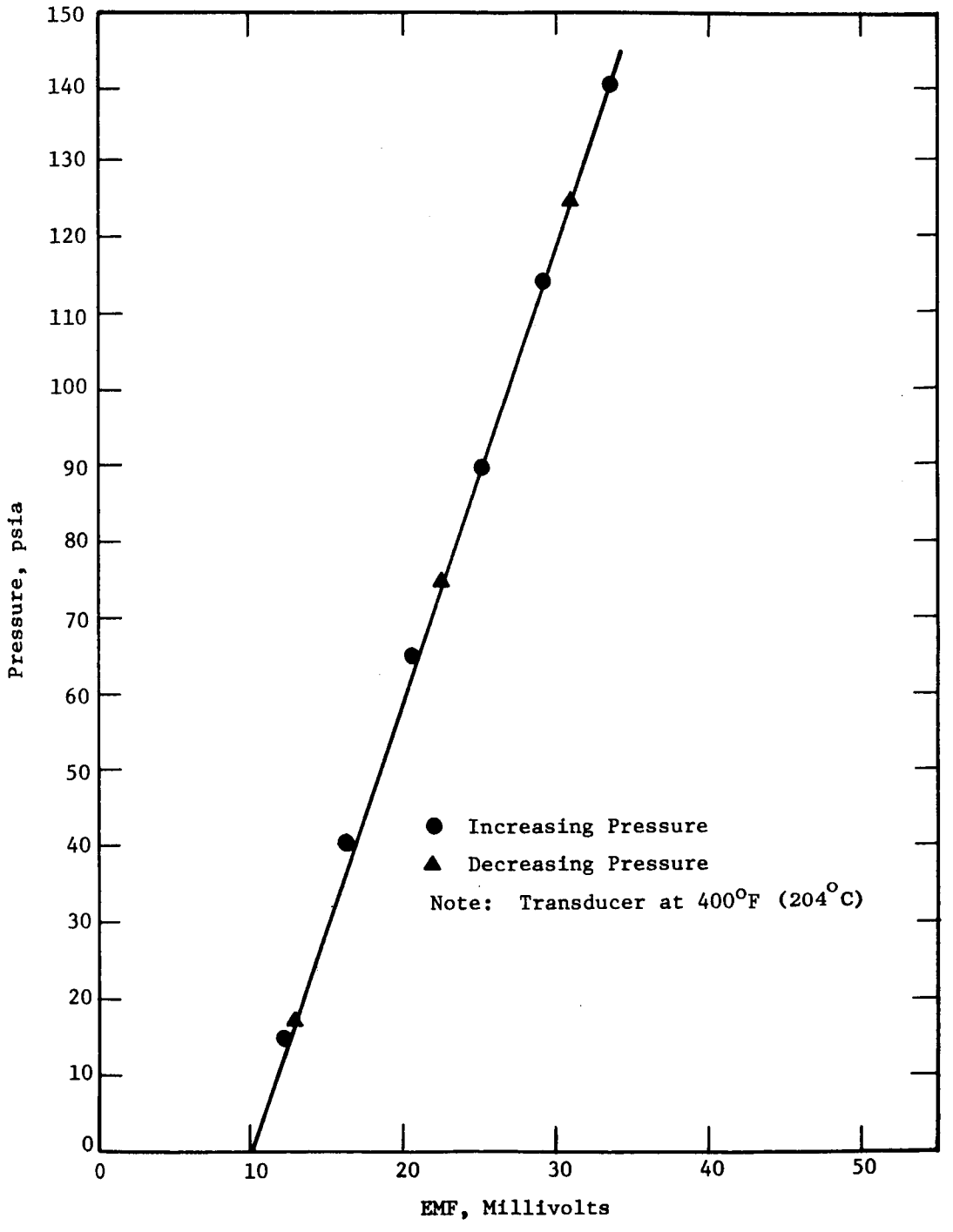


Figure 55. Calibration of Slack Diaphragm Pressure Transducer No. 1 for the T-111 Corrosion Test Loop.

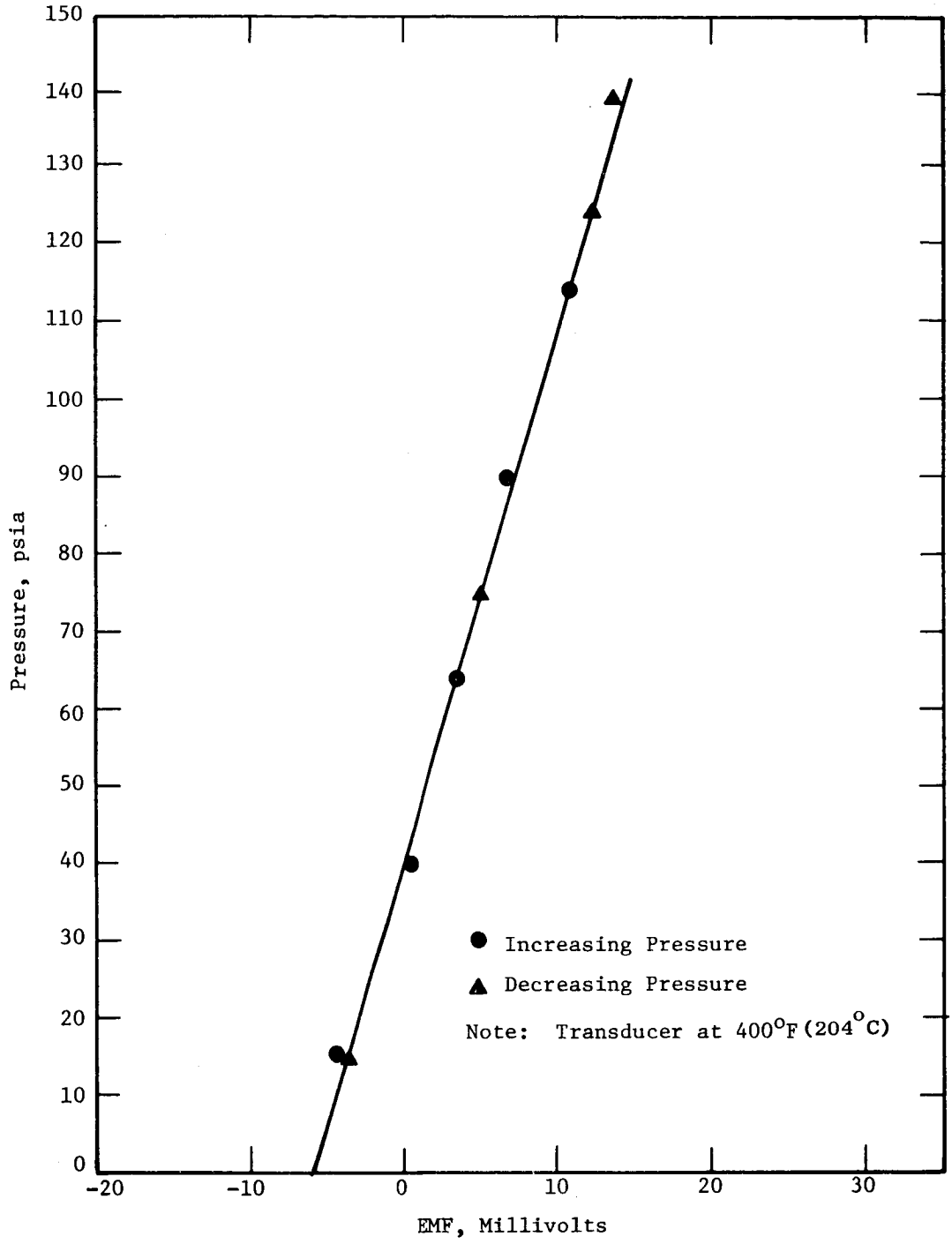


Figure 56. Calibration of Fast-Response Stressed Diaphragm Pressure Transducer for the T-111 Corrosion Test Loop.

TABLE XVII

RESULTS OF CALIBRATION[a] OF W-3Re/W-25Re THERMOCOUPLES IN THE BOILER SECTION OF THE T-111 CORROSION LOOP

Thermocouple No.	Temperature °F	Temperature °C	Location Inches From Boiler Exit[b]
B1	905	485	0
B2	903	484	2
B3	902	483	4
B4	903	484	6
B5	916	491	9
B6	914	490	12
B7	914	490	15
B8	914	490	18
B9	910	488	30
B10	908	486	43
B11	908	486	55
B12	908	486	68
B13	908	486	80
B14	908	486	93
B15	908	486	105
B16	908	486	118
B17	914	490	130
B18	914	490	143
B19	914	490	155
B20	911	488	168
B21	909	487	180
B22	909	487	193
B23	908	486	205
B24	908	486	218

(a) Calibration test conducted with a lithium flow of 2.0 gpm (0.45 m^3/min) in the primary circuit and no potassium in the secondary circuit.

(b) Lithium exit, potassium inlet.

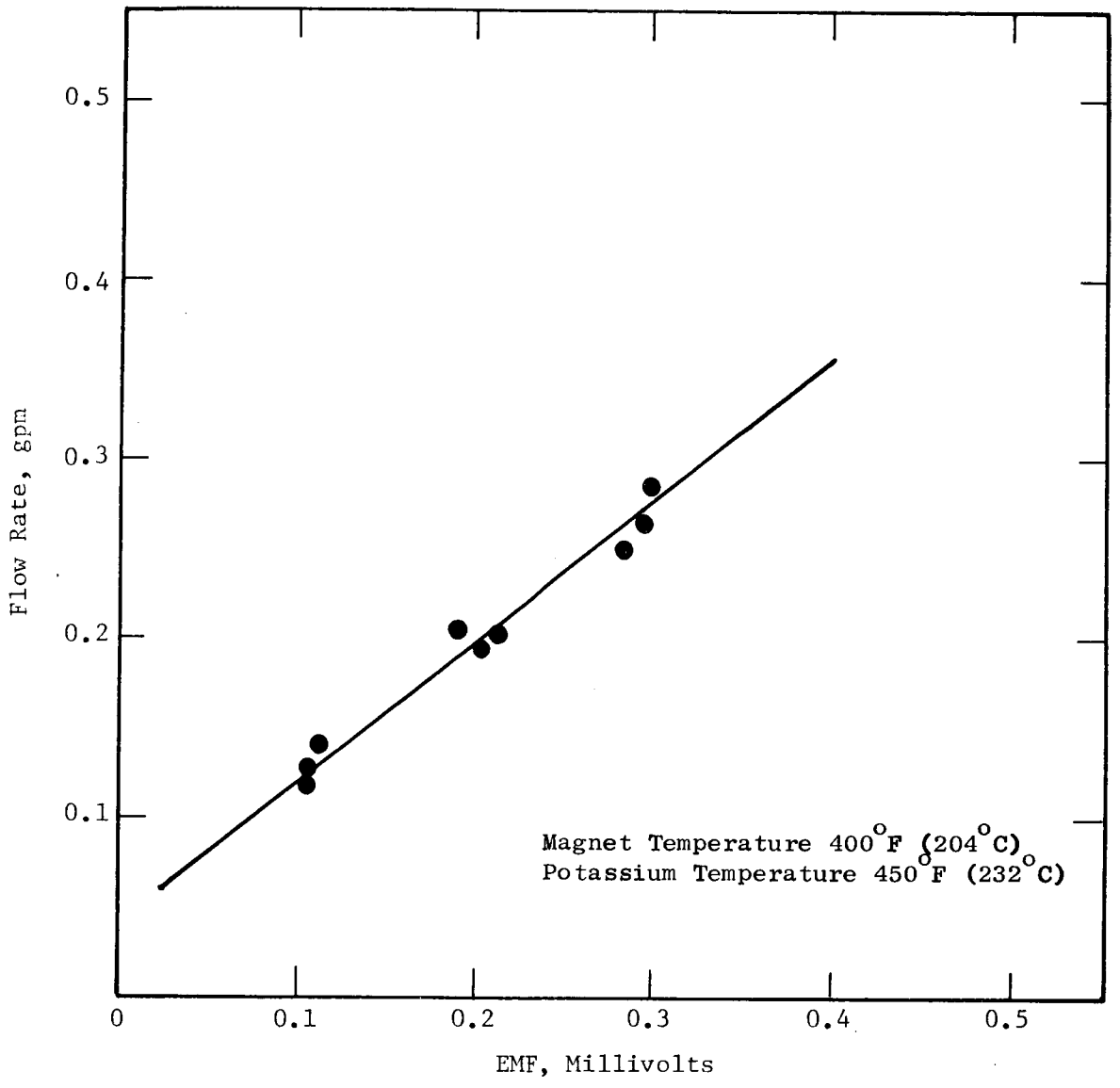


Figure 57. Potassium Flowmeter Calibration for T-111 Corrosion Test Loop.

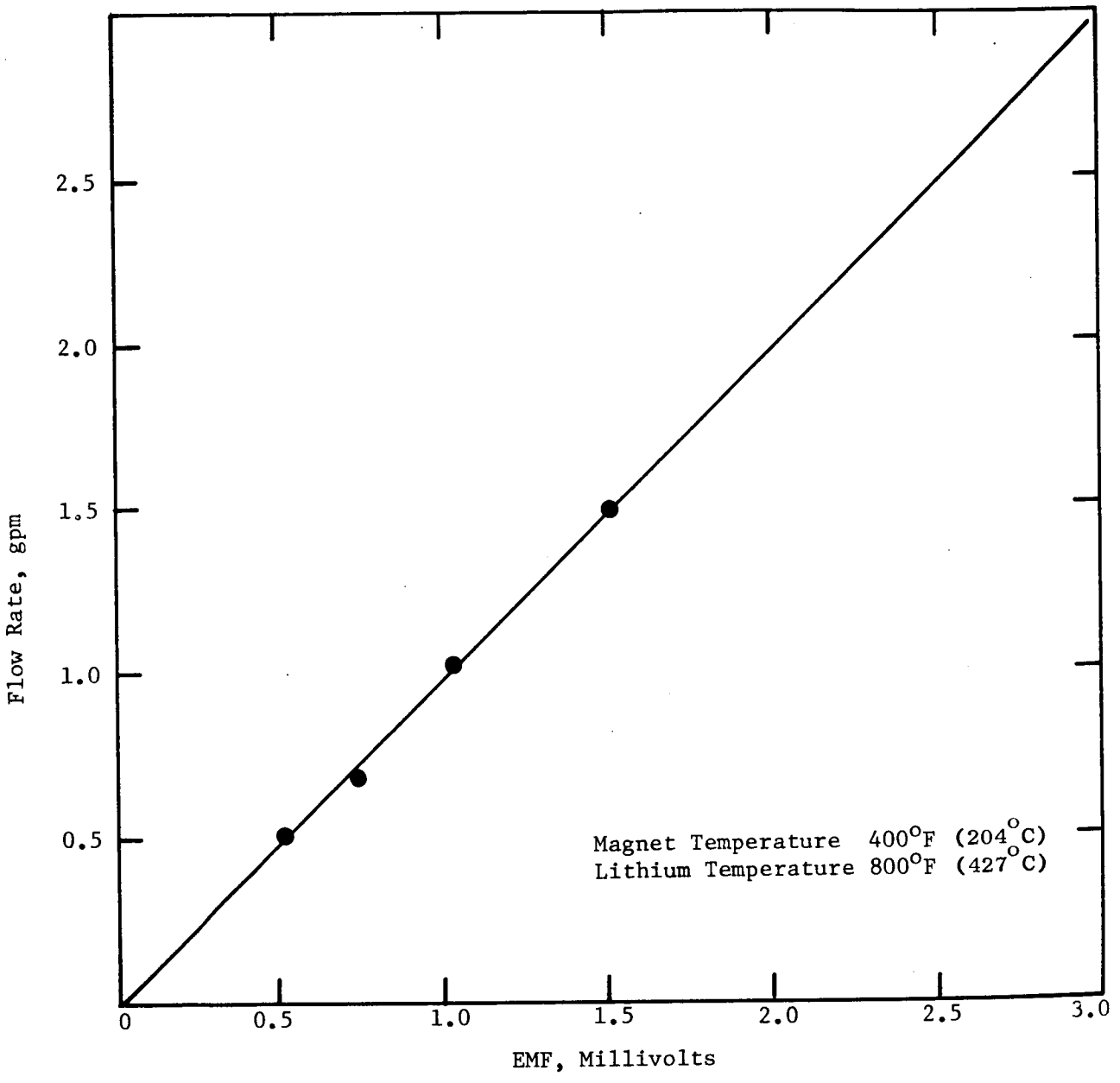


Figure 58. Lithium Flowmeter Calibration for the T-111 Corrosion Test Loop.

calibration.[18] The T-111 Corrosion Loop flow tubes are 0.25-inch (0.63-cm) ID x 0.065-inch (0.16-cm) wall thickness with a ratio of outer diameter to inner diameter of 1.5:1, which is considerably larger than the diameter ratio (1.12:1) used by Affel, et al. in the referenced report.[17]

After completion of the calibration tests, the loop safety circuits were checked and set according to the procedures outlined in the test plan.[19]

D. BOILING AND CONDENSING OPERATION

The boiling and condensing operation of the T-111 Corrosion Test Loop was started after completion of the checkout of the loop control and safety circuits. The test loop had completed one week of outgassing with all-liquid operation and was at the test conditions listed below at the start of the boiler and condensing operation:

Vacuum Chamber Pressure	4×10^{-7} torr (5×10^{-5} N/m^2)
Lithium Flow Rate	2 gpm (0.45 m^3/hr)
Potassium Flow Rate	0.2 gpm (0.045 m^3/hr)
Lithium Temperature	1180°F (638°C)
Potassium Temperature	1140°F (616°C)

The potassium loop was dumped by evacuating the surge tank and gravity draining the potassium from the loop into the surge tank. The metering valve was adjusted to 3/16 open which is the position determined from the valve calibration test as the setting required for a 10- to 25-psia (6.9×10^4 to 17.2×10^4 N/m^2 abs.) pressure drop across the valve at the design operating conditions.

The potassium surge tank was pressurized with argon to 2.0 psia (13.8×10^3 N/m^2 abs.), forcing the liquid potassium out of the surge tank into the loop. This pressure is sufficient to partially fill the loop to

---

(18) Potassium Corrosion Test Loop Development Program, Quarterly Progress Report No. 8 for Period Ending July 15, 1965, NASA Contract NAS 3-2547, NASA-CR-54843, November 23, 1965, p. 25.

(19) Advanced Refractory Alloy Corrosion Loop Program, Test Plan for T-111 Rankine System Corrosion Test Loop, NASA Contract NAS 3-6474.

the inlet to the boiler and approximately two-thirds of the condenser. The boiling operation was started by turning on the potassium EM pump at low power and forcing liquid potassium into the boiler. The potassium flow rate and the lithium temperature were slowly increased and allowed to stabilize at a potassium vapor temperature of 1250°F (677°C) and a lithium temperature of 1366°F (741°C). The vacuum chamber pressure increased to the 10^{-6} torr (10^{-4} N/m^2) range as the loop temperature reached a new high and further power increases were delayed until the vacuum chamber pressure decreased into the 10^{-7} torr (10^{-5} N/m^2) range.

During the next several hours, the loop temperature and potassium flow rate were slowly increased until the potassium flow rate slowly decreased to zero flow. At this time, all pressure gauges in the potassium loop were at the same pressure indicating the flow blockage between the condenser and the pump inlet. The potassium flow direction was reversed and the pressure gauges No. 2, 4, 5, and 6 then read the same pressure, but pressure No. 1 read zero indicating the flow blockage was then at the metering valve. The metering valve was then opened from 3/16 open to full open and all pressure gauges responded and a high-potassium flow rate was established.

The potassium surge tank was immediately evacuated in an attempt to dump the loop and remove the plugging material from the loop to the surge tank. The loop would not dump indicating that a flow blockage was present between the surge tank and the loop. The potassium surge tank was pressurized in an attempt to dislodge the plugging material; however, no immediate response on the loop pressure gauges was observed. After a few minutes, the loop pressure slowly increased to 80 psia (5.5×10^5 N/m^2 abs.), the pressure in the surge tank. The surge tank was again evacuated but the loop would not dump, and the pressure in the loop remained at 80 psia (5.5×10^5 N/m^2 abs.). The vacuum chamber bakeout system was turned on since the loop was now operating at a lower power level, and the alkali metal could freeze if additional heat was not supplied to the loop. Communication between the surge tank and the loop was established suddenly and the loop and surge tank pressures equalized to 18 psia (1.2×10^5 N/m^2 abs.). The potassium EM pump was turned on, and potassium could be circulated at

a high flow rate. The plug between the loop and the potassium surge tank could have been frozen potassium in a cooler location; however, the temperatures in this general region were significantly above the 147°F (64°C) melting point of potassium.

On the following day, a second attempt to reach the design operating conditions was made. The loop power was slowly increased, but extremely large flow fluctuations made the loop difficult to control. The possibility that additional plugging material remained in the loop after the previous dump was considered as a potential source of the instabilities and, consequently, the potassium circuit was dumped and the loop refilled after holding the loop charge of potassium in the surge tank for 10 minutes. Loop operation continued and the lithium temperature was increased to 1770°F (966°C), but again large pressure and flow fluctuations prevented reaching design operating conditions. Additional attempts to reach design conditions in the next few days were also plagued by pressure and flow fluctuations.

An attempt to maintain the loop at the maximum power level and obtain steady-state test data was not successful because of the changing potassium flow rate. The potassium flow rate steadily decreased, and the pressure drop across the valve increased indicating that the valve was plugging with particulate matter. The metering valve was opened from 3/16 open (the original setting) to 1/4 open with an instantaneous increase in the potassium flow rate and decrease in the pressure drop across the metering valve as shown in Figure 59. The flow rate again decreased as the valve was opened in steps up to full open and the plugging noted above occurred after holding for a few minutes at each new valve opening. When this occurred with the valve fully open, the heater and preheater power were quickly reduced to a safe level to avoid overtemperaturing of these components. The vacuum chamber bakeout heaters were turned on to maintain the loop above the melting point of the alkali metals.

E. DRAINING OF LOOPS AND DISCOVERY OF THE BOILER LEAK

The potassium surge tank was then evacuated to dump the potassium into the surge tank in an attempt to remove the plugging material from the loop. The potassium was allowed to settle in the surge tank for approximately

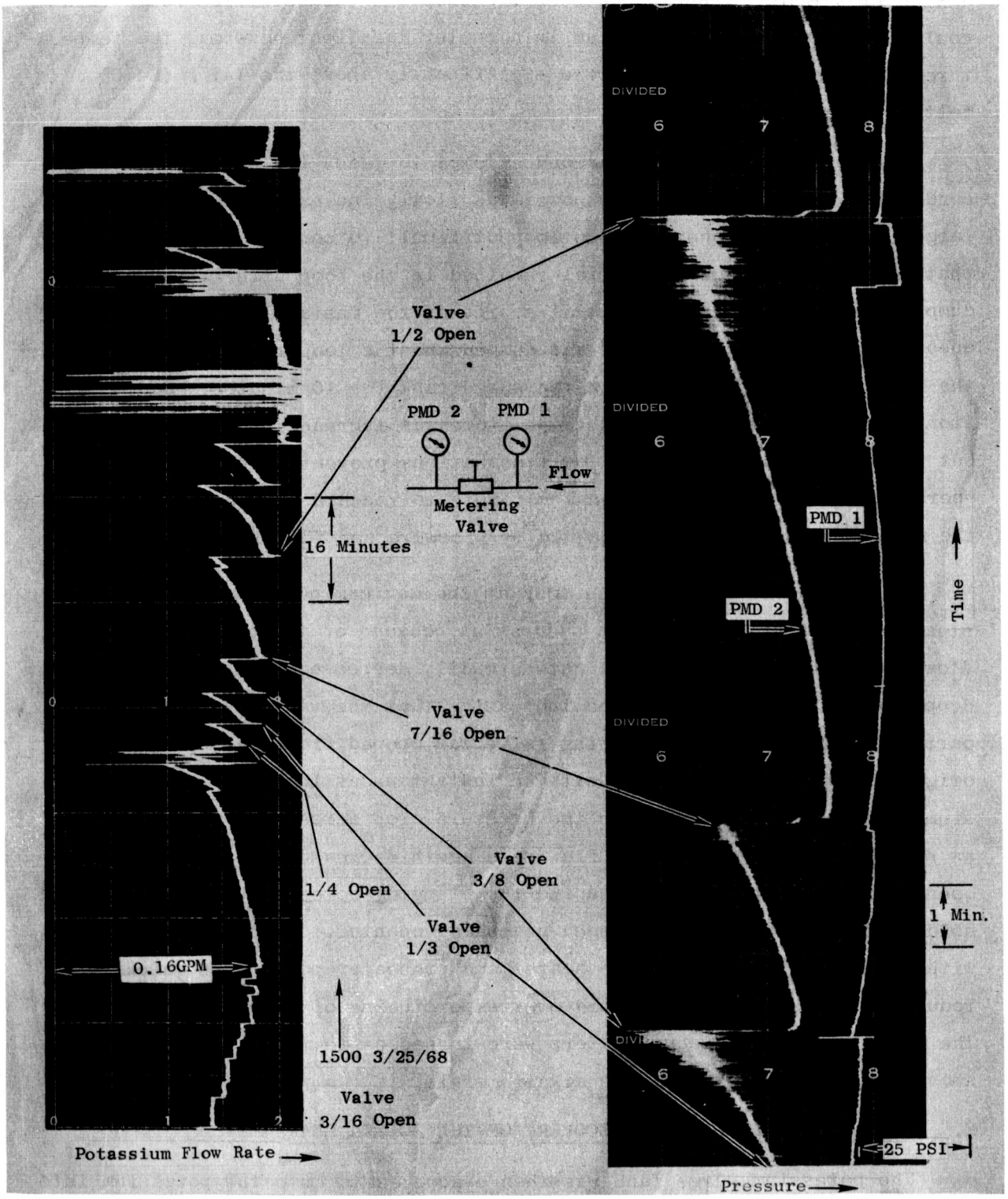


Figure 59. The Effect of Plugging the Metering Valve on Potassium Flow Rate and Pressure Drop Across the Metering Valve During Operation of the T-111 Rankine System Corrosion Test Loop.

ORIGINAL PAGE IS
OF POOR QUALITY

10 minutes before the loop was refilled by pressurizing the surge tank. The potassium pump power leads were changed for reverse flow and a high potassium flow could be maintained, indicating the loop had unplugged. The loop was again dumped, refilled with potassium and circulated in the reverse direction as before. The dumping procedure was repeated for the third time, and again the normal flow rate was initially established but then it slowly decreased to zero. The EM pump was rewired for forward flow but potassium circulation could not be established.

The potassium and lithium were dumped into the surge tanks, and plans were made to sample the potassium inventory in an attempt to identify the plugging material before the test operation could continue. The draining and sampling of the loop circuits are described in Section XV, Appendix K, of this report. Sampling indicated communication between the lithium and potassium circuits of the loop. Subsequently, a leak was discovered in the boiler between these circuits. The repair of the boiler and reinstallation in the loop are described in detail in Appendix K of this report.

IX. TEST STARTUP AFTER REPAIR OF BOILER

As indicated in the preceding section, a leak was discovered in the potassium containment tube during the initial attempt to reach the test conditions. An extensive effort was required to remove the boiler, locate the leak, repair the boiler, and replace it in the test system. The details of these operations as well as the flushing operations utilized to clean the two circuits of the test system are given in considerable detail in Section XV, Appendix K, of this report.

Boiling operation of the corrosion loop was initiated by first increasing the lithium temperature to 1350°F (732°C) at a flow rate of approximately 2 gpm. The secondary EM pump was adjusted to supply a low flow of potassium to the boiler, and the flow rate and primary temperature were gradually increased at a rate to maintain the chamber pressure below 5×10^{-7} torr (7×10^{-5} N/m^2). The outgassing rate increased considerably as the loop temperatures were increased, and the titanium sublimation pumps were used to assist the getter-ion vacuum pumps in maintaining a 10^{-7} torr (10^{-5} N/m^2) pressure level in the vacuum chamber.

The rate of increase to the test conditions was limited by the outgassing of the loop components. The chamber pressure and the partial pressures of the principal residual gases during this period when the test conditions were being approached are shown in Figure 60. Hydrogen accounted for over 95 percent of the total residual gas pressure. Although the chamber pressure reached the 10^{-6} torr (10^{-4} N/m^2) scale during startup, the partial pressures of oxygen-bearing residual gases were 10^{-8} torr (10^{-6} N/m^2) or lower. Additional discussion of the partial pressure gas analysis of the test chamber environment is covered in Section X, Loop Operation.

Short periods of unstable boiling were noted during the startup of the loop as adjustments to the lithium temperature and potassium flow caused boiling to move out of the plug section. This effect was observed in the operation of the Cb-1Zr Rankine System Corrosion Test Loop and is described in detail in the topical report.[20] The typical effect of these

---

(20) Hoffman, E. E. and Holowach, J., Cb-1Zr Rankine System Corrosion Test Loop, NASA CR-1509, June 1970.

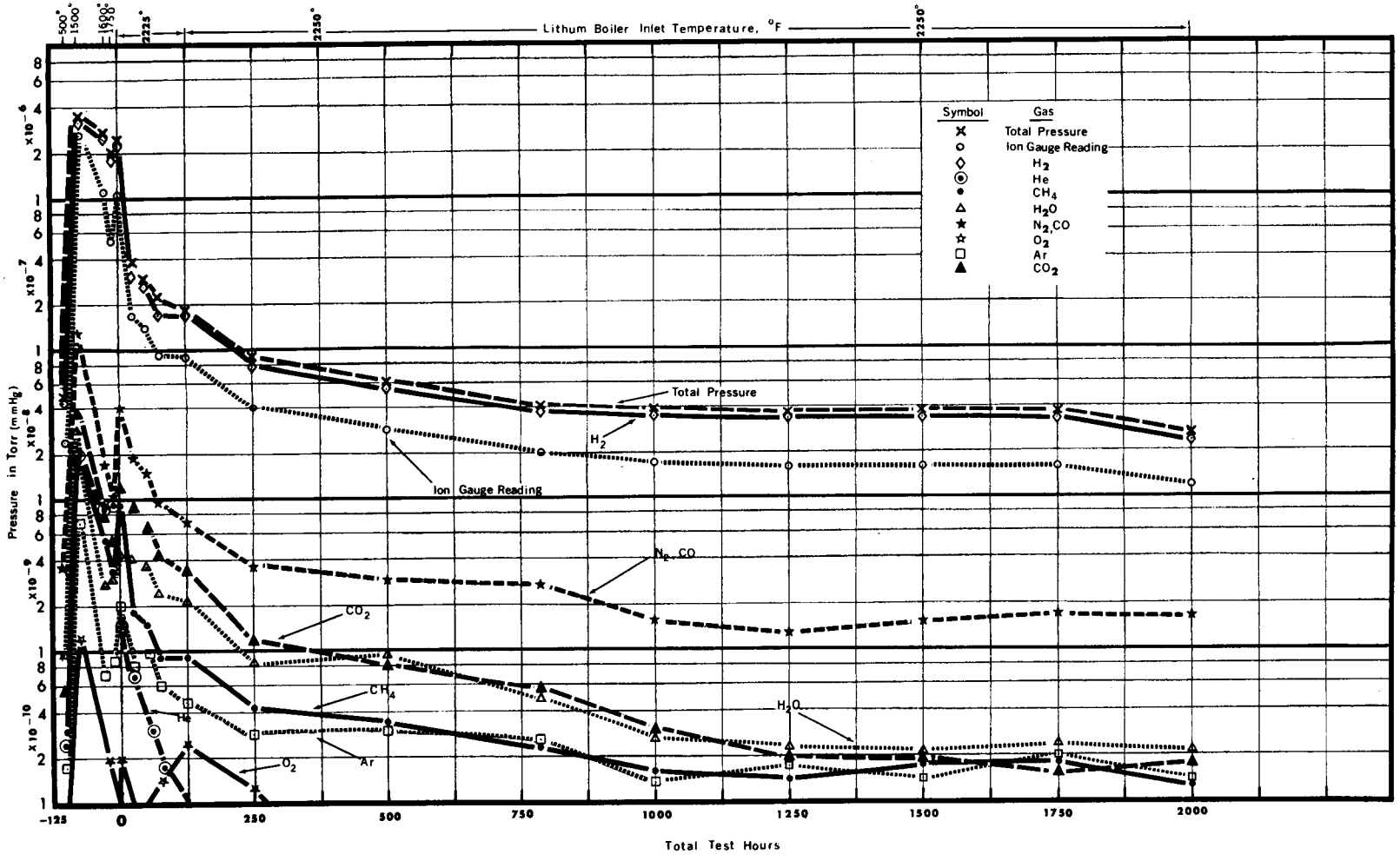


Figure 60. Test Chamber Environment During Startup and Early Operation Testing of the T-111 Corrosion Loop.

boiling instabilities on the potassium pressure and flow is shown in Figure 61. After a short period of time (approximately 22 minutes) of unstable boiling, the potassium EM pump power was decreased with a corresponding decrease in potassium flow and pressure. Boiling returned to the plug section and became stable.

The primary loop temperature, secondary flow rate, and preheater temperature were increased until the design conditions were met. These conditions are listed below:

Boiling temperature	$2050^{o} \pm 25^{o}F$ ($1121^{o} \pm -3.9^{o}C$);
Superheat temperature	$2150^{o} \pm 10^{o}F$ ($1177^{o} \pm -12.2^{o}C$);
Condensing temperature	$1400^{o} \pm 25^{o}F$ ($760^{o} \pm -3.9^{o}C$);
Potassium flow rate	35 lb/hr $\pm$ 5 lb/hr (15.9 kg/hr $\pm$ 1.7 kg/hr).

The T-111 Rankine System Corrosion Test Loop began logging hours at 1630 hours on January 25, 1969.

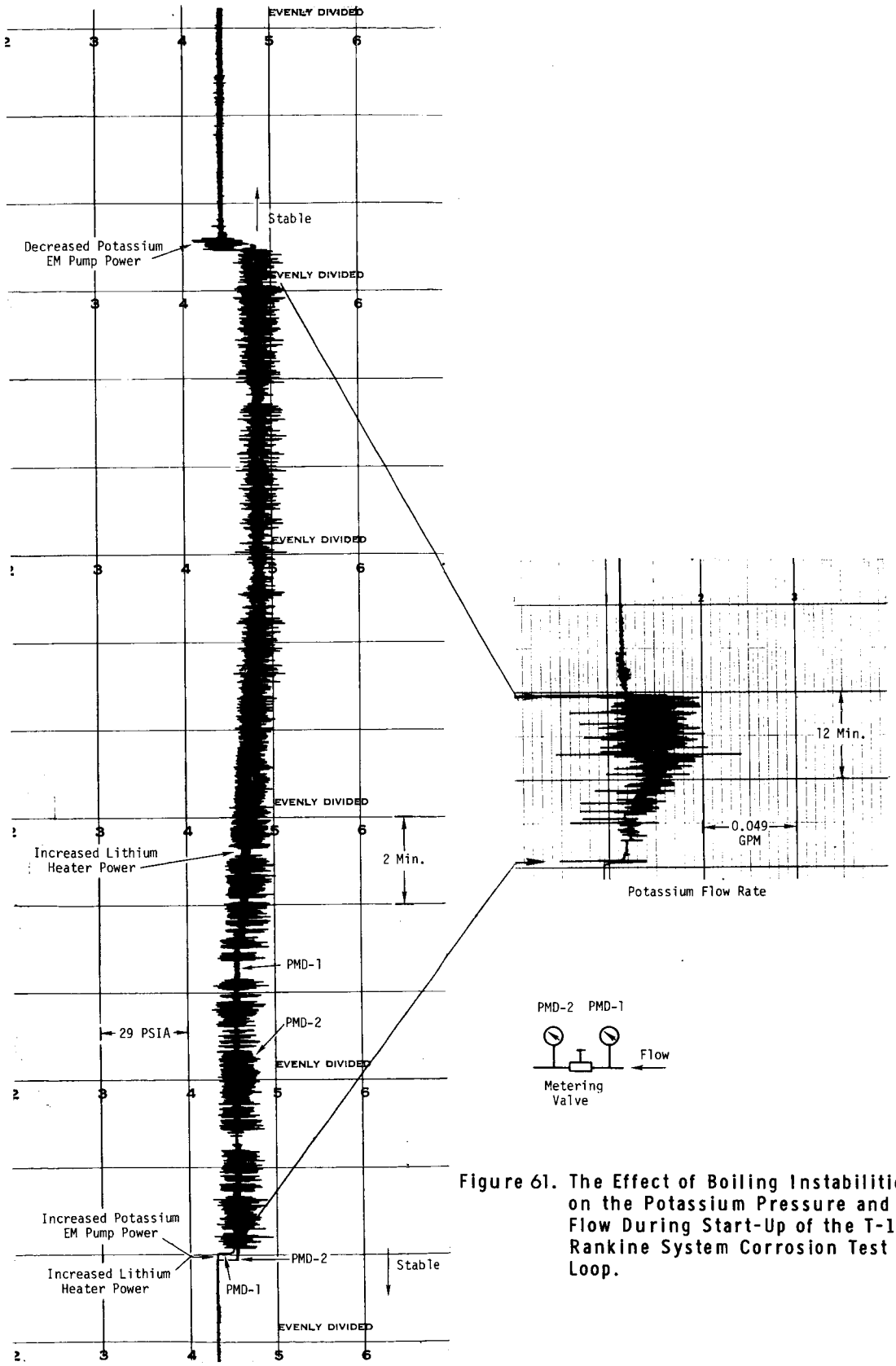


Figure 61. The Effect of Boiling Instabilities on the Potassium Pressure and Flow During Start-Up of the T-111 Rankine System Corrosion Test Loop.

X. LOOP OPERATION

The required test conditions for initiation of the 10,000-hour test were reached at 1630 on January 25, 1969. The conditions at this time were described in Section IX. This section of the report will describe the endurance test, the shutdown of the system following completion of the test, and a review of the total pressure and partial pressures of the vacuum environment during the test.

A. LOOP OPERATION DURING THE 10,000-HOUR TEST

On March 8, 1969, the T-111 Corrosion Test Loop completed 1000 hours of operation. As a result of the stable and trouble-free operation of the loop during this period, constant surveillance appeared to be less of a necessity than originally anticipated. Furthermore, adjustments made during this testing period were limited predominantly to slight adjustments to the lithium heater to compensate for minor line voltage fluctuations.

The effect of these fluctuations on the lithium boiler inlet temperature was examined during the period March 11, 1969, to March 17, 1969, with no adjustments being made from 1600 hours to 0800 hours. It was found that anticipatory adjustments to the lithium heater power made by daytime shift operators could result in maintaining the lithium boiler inlet temperature within $\pm$ 25°F ($\pm$ 14°C).

On March 22, 1969, loop operation was reduced to the daytime shift with unattended operation from 1600 hours to 0800 hours. No difficulties were encountered in maintaining stable loop operation, and the lithium boiler inlet temperature was easily maintained within a $\pm$ 25°F ($\pm$ 14°C) band as indicated in the data shown in Figure 62. The potassium vapor temperature at the exit of the boiler was maintained within a $\pm$ 20°F ($\pm$ 11°C) band. The boiling temperature, which is determined by the boiler inlet pressure, was maintained within $\pm$ 2°F ($\pm$ 1°C). This further confirmed the stability of the inlet pressure and concomitant boiler outlet pressure, of prime interest in turbine operation.

On April 10, 1969, continuous surveillance of the loop was restored at the request of the NASA Program Manager. With continuous surveillance the lithium boiler inlet temperature could be maintained within a $\pm$ 15°F ($\pm$ 8°C) band by adjustments to the lithium heater power when required as indicated in Figure 63.

ORIGINAL PAGE IS
OF POOR QUALITY

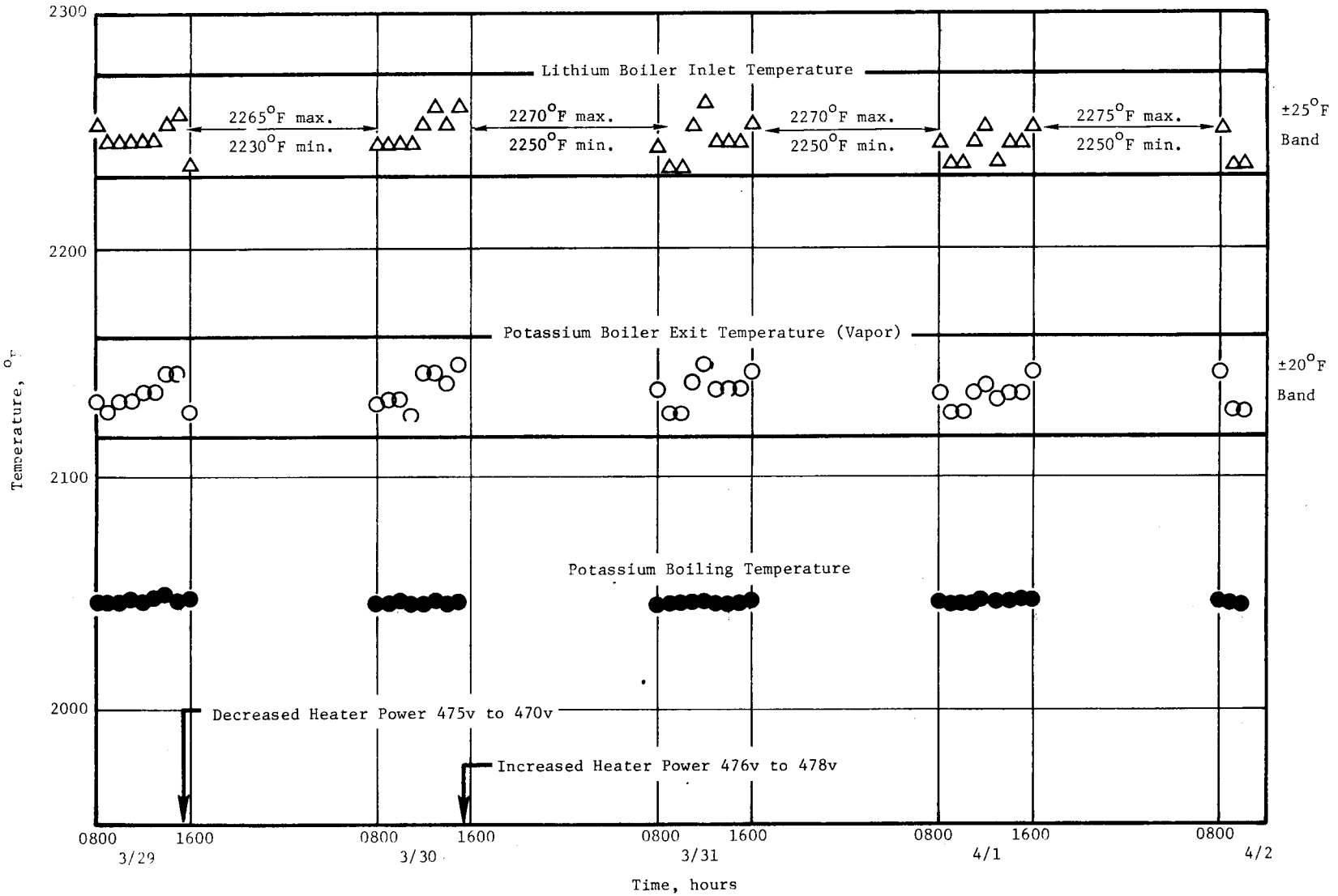


Figure 62. Temperatures of Interest Recorded During Operation of the T-111 Corrosion Test Loop on the Daytime Shift Only With Unattended Operation Between 1600 Hours and 0800 Hours.

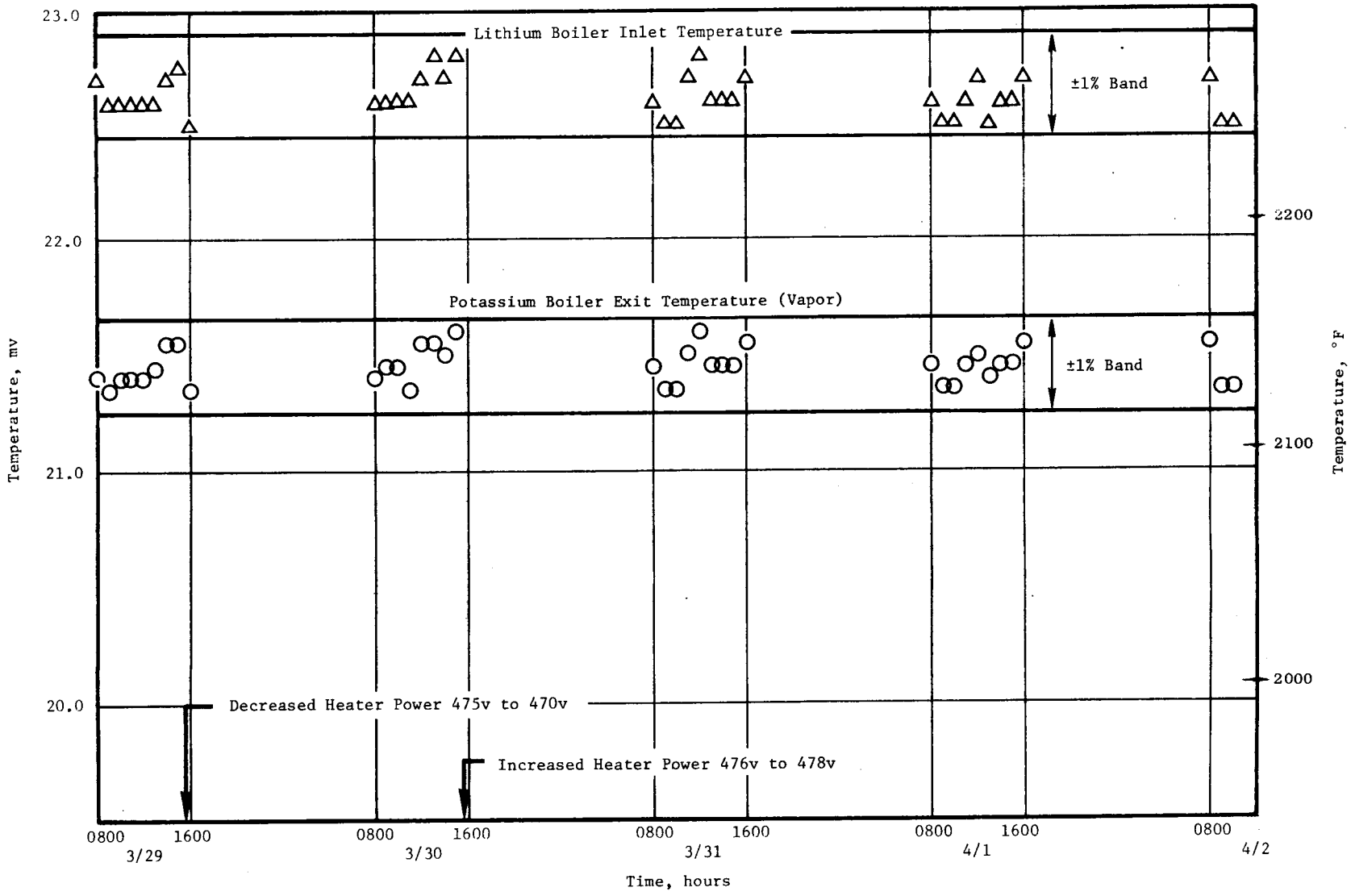


Figure 63. Temperatures of Interest Recorded During Operation of the T-111 Corrosion Test Loop on the Daytime Shift Only With Unattended Operation Between 1600 Hours and 0800 Hours.

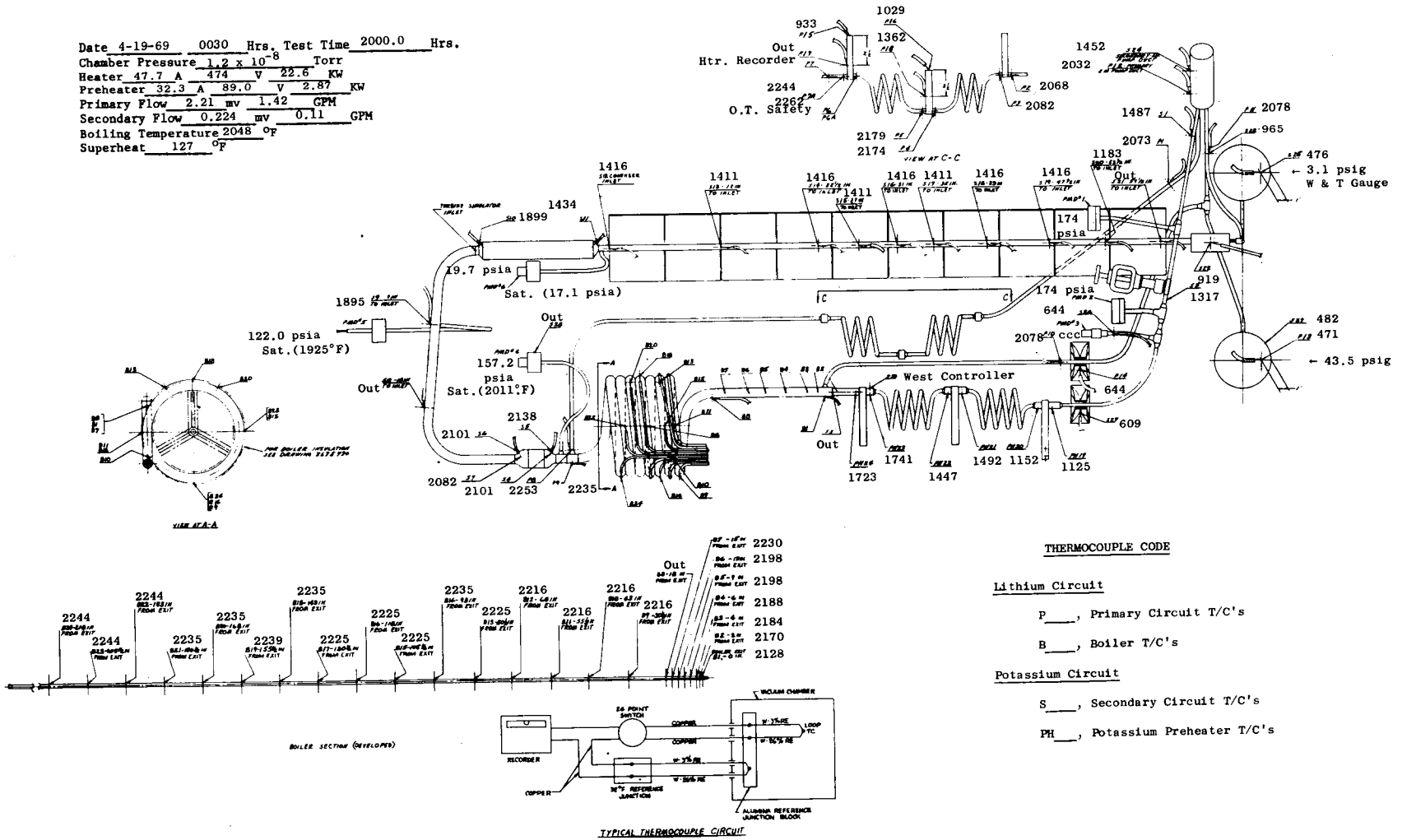
On April 19, 1969, the T-111 Corrosion Loop completed 2000 hours of operation. The loop temperatures recorded at that time are shown in Figure 64, and temperatures of major interest are shown on the loop schematic in Figure 65. The performance of the loop has been excellent in that control adjustments have been limited to minor changes in the power input to the lithium heater to compensate for small line voltage changes not compensated for by the voltage stabilizer. A comparison of the data obtained at 1000 hours with the 2000-hour data shown in Table XVIII further indicates the stability of the loop's performance.

The lithium temperature profile in the boiler and the calculated potassium quality and temperature as a function of boiler length are given in Figure 66. The calculated qualities indicated are based on thermal calculations involving potassium flow, potassium boiler inlet temperature, lithium flow, and the drop in the measured lithium temperatures as a function of boiler length. Calculations indicate approximately 100-percent-quality vapor is attained at the exit of the plug section, 18 inches (46 cm) from the boiler inlet. In the remaining 195 inches (495 cm), the vapor is superheated to 2147°F (1175°C). The 135°F (75°C) of superheat is the difference between the measured temperature of the potassium vapor at the boiler exit, 2147°F (1175°C), and the saturation temperature, 2012°F (1100°C), as determined by the boiler exit pressure, 158 psia (10.9×10^5 N/m^2). The pressure and flow traces shown in Figure 67 indicate the stability of the boiling in the loop. Pressure flucutations noted on the Taylor gauges are less than 1 psia (6.9×10^3 N/m^2).

At 0400 on July 6, 1969, after 3870 hours of loop operation, the lithium heater and potassium preheater power was interrupted during a violent electric storm. In reducing the EM pump power, a carbon brush on the powerstat was broken as a result of having become bonded in place during the long-term operation. The brush was replaced and the loop brought back to conditions by 0600 with no additional problems. The lithium temperature did not fall below 1000°F (538°C) during this period.

The test continued without incident, and on August 22, 1969, the T-111 Corrosion Test Loop successfully completed the first half of the planned 10,000 hours of operation. The principal loop temperatures recorded at the

ORIGINAL PAGE IS
OF POOR QUALITY



THERMOCOUPLE CODE

Lithium Circuit

P___, Primary Circuit T/C's

B___, Boiler T/C's

Potassium Circuit

S___, Secondary Circuit T/C's

PH___, Potassium Preheater T/C's

Figure 64. T-111 Corrosion Test Loop Temperatures at 2000 Hours.

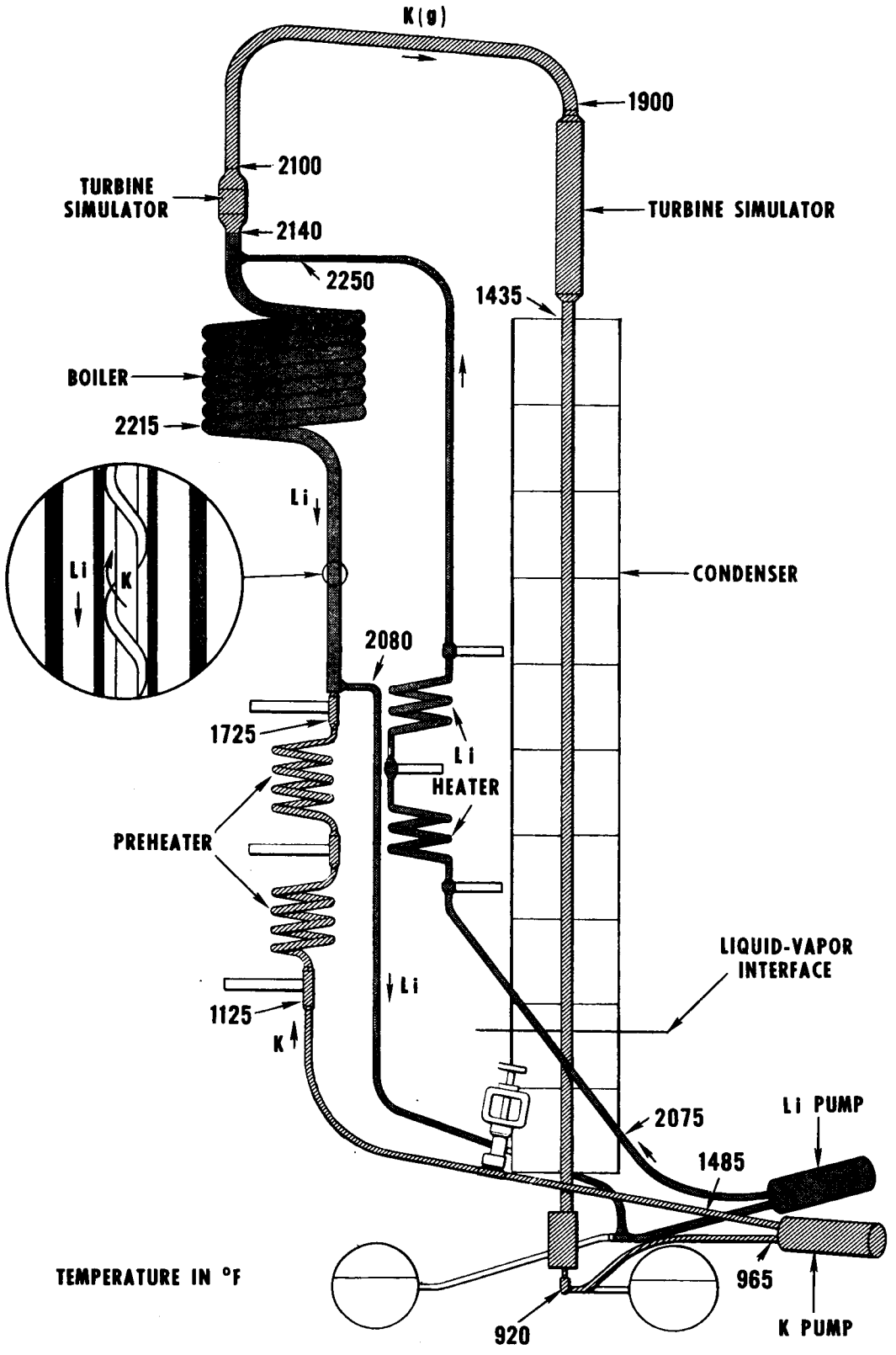


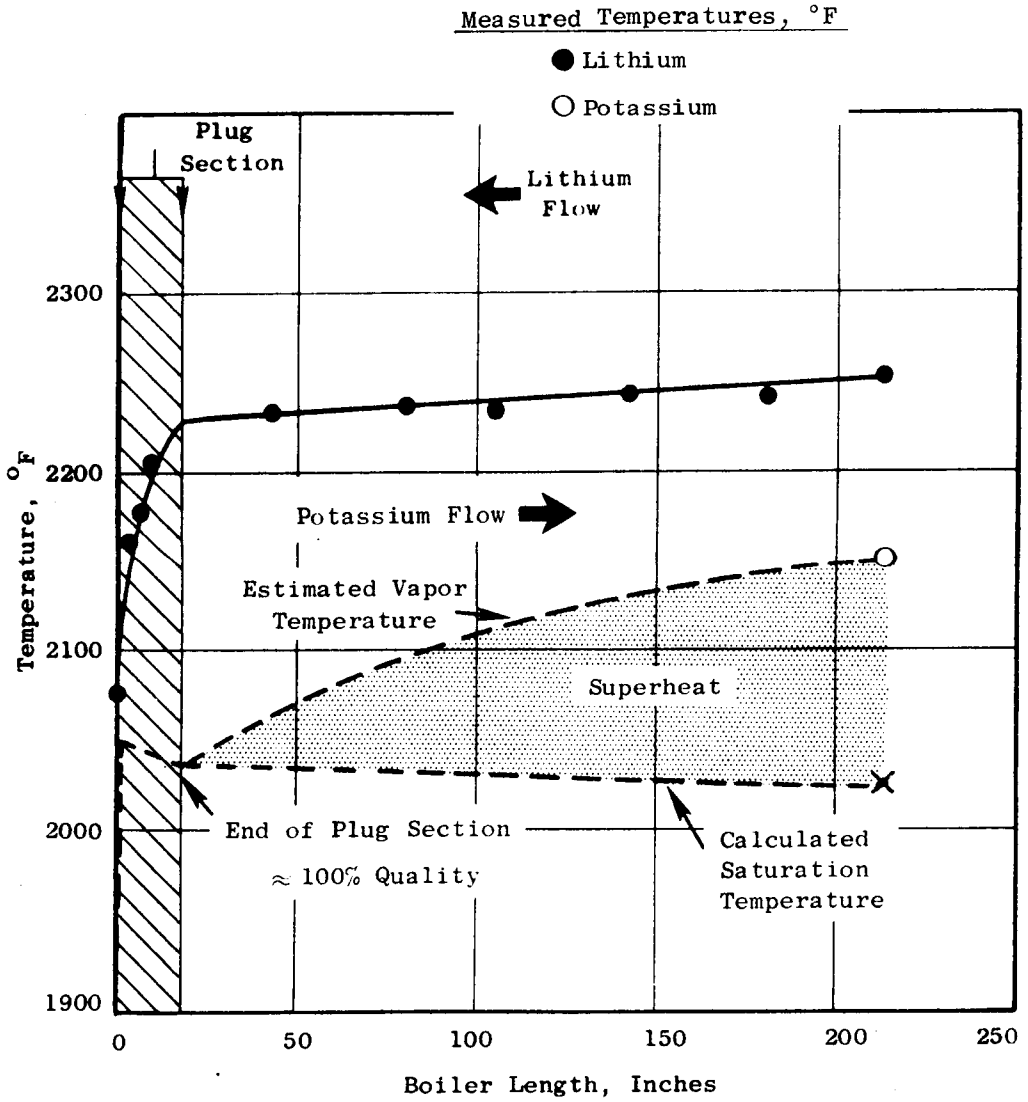
Figure 65. T-111 Corrosion Test Loop Operating Temperatures - 2000 Hours.

TABLE XVIII

T-111 RANKINE SYSTEM CORROSION TEST LOOP PERFORMANCE

Date	3-8-69	4-19-69
Test Hours	1000	2000
Lithium Flow Rate	205 lb/hr (93 kg/hr)	207 lb/hr (94 kg/hr)
Lithium Temperature, In	2253°F* (1234°C)	2253°F* (1234°C)
Lithium Temp., Out	2078°F (1248°C)	2078°F (1248°C)
Lithium ΔT	175°F (97°C)	175°F (97°C)
Potassium Flow Rate	36 lb/hr (16.3 kg/hr)	37 lb/hr (16.8 kg/hr)
Plug Boiling Temperature	2048°F (1120°C)	2048°F (1120°C)
Boiler Exit Vapor Temperature	2147°F (1175°C)	2138°F (1170°C)
Boiler Exit Saturation Temperature	2012°F (1100°C)	2011°F (1100°C)
Potassium Vapor Superheat	135°F (75°C)	127°F (70°C)
Condensing Temperature	1416°F (769°C)	1416°F (769°C)
Potassium Heat Input		
1. Preheat	2280 Btu/hr (0.67 kw)	2340 Btu/hr (0.68 kw)
2. Heat of Vaporization	26,300 Btu/hr(7.7 kw)	26,950 Btu/hr(7.6 kw)
3. Superheat	1040 Btu/hr (0.30 kw)	947 Btu/hr (0.28 kw)
Total	29,620 Btu/hr(8.7 kw)	30,237 Btu/hr(8.9 kw)
Total Power to Lithium Heater	13.2 kw	13.7 kw
Total Power to Potassium	8.7 kw	8.9 kw
Net Heat Loss	4.5 kw	4.8 kw

* The lithium boiler inlet temperature is maintained within ± 15°F (± 8°C) by appropriate adjustments to the lithium heater power.



Boiler Conditions

Net Heat Transfer - 8.65 KW

Lithium
- Flow Rate, 205 lbs/hr
- Inlet Temp., 2253°F
- Outlet Temp., 2078°F

Potassium
- Flow Rate, 36 lbs/hr
- Inlet Temp., 1723°F
- Outlet Temp., 2147°F
- Inlet Pressure, 174 psia
- Outlet Pressure, 157 psia

Boiler Components

Lithium Tube, OD - 1.0-Inch
ID - 0.8-Inch
Potassium Tube, OD - 0.375-Inch
ID - 0.250-Inch

Plug, 18 Inch Long, Formed by Wrapping a 0.06 Inch Diameter Wire on a 1-Inch Pitch Helix on a 0.125-Inch Diameter Center Rod.

Figure 66. T-111 Corrosion Test Loop Boiler Conditions After 1000 Hours Operation.

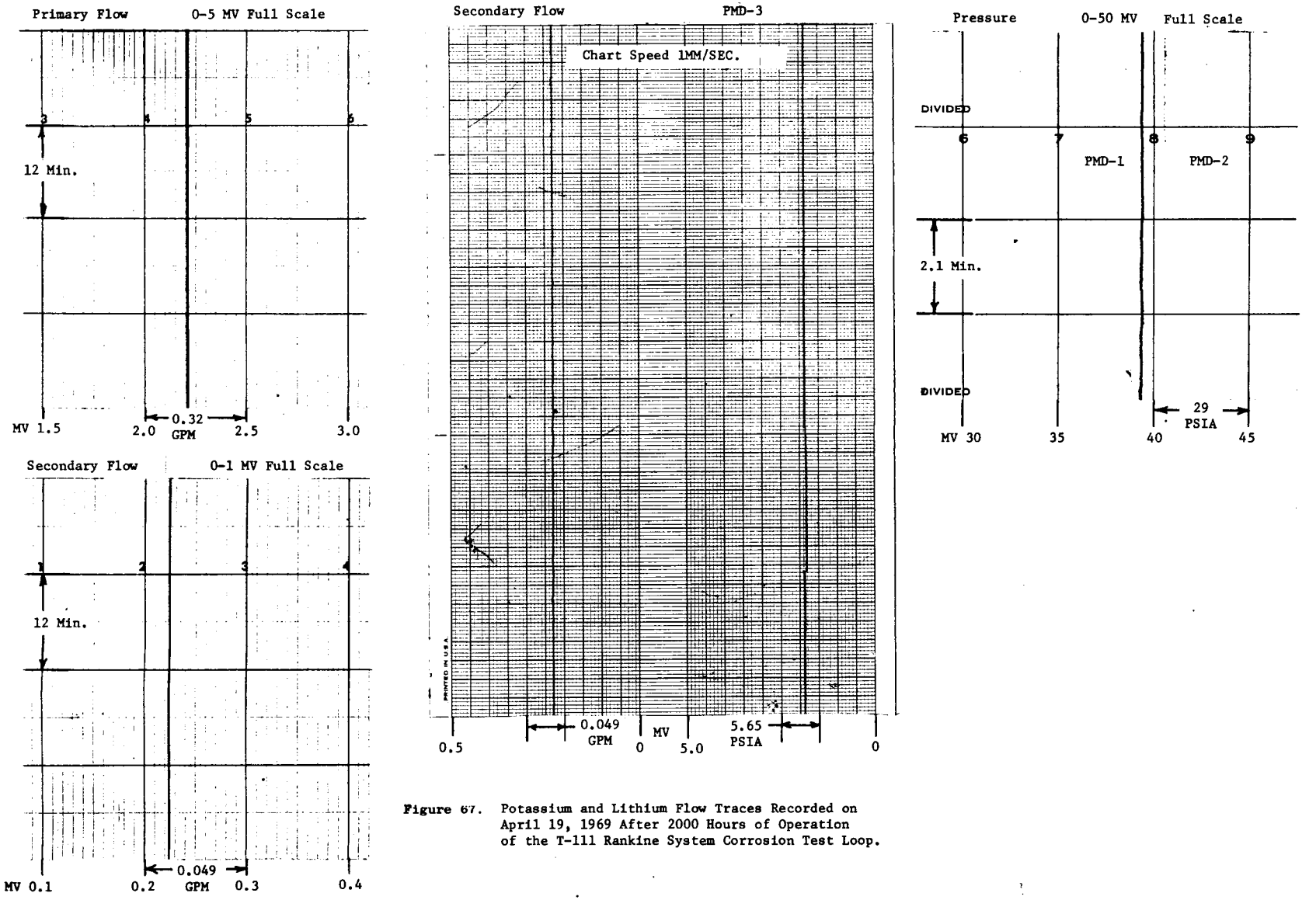


Figure 67. Potassium and Lithium Flow Traces Recorded on April 19, 1969 After 2000 Hours of Operation of the T-111 Rankine System Corrosion Test Loop.

5000-hour test time are shown in Figure 68. The performance of the loop continued to be excellent in that control adjustments were limited to minor changes in the power input to the lithium heater to compensate for small line voltage changes not compensated for by the voltage stabilizer. A comparison of the data obtained at 2000 hours and 5000 hours, shown in Table XIX, further exemplifies the continued stability of the loop's performance.

The calculated vapor velocities of the turbine simulator nozzles at 5000 hours are presented in Table XX for a mass velocity of 36.7 lb/hr (20.6 kg/hr) of potassium. The vapor velocity in the superheated first stage was 1080 ft/sec (329 m/sec). The vapor velocity in the 88-percent-quality region ranged from a high of 1280 ft/sec (390 m/sec) in the second-stage nozzle to a low of 1150 ft/sec (351 m/sec) in the tenth-stage nozzle. All vapor velocities were higher than the 1000 ft/sec (305 m/sec) design velocity.

The higher-than-design velocity is attributed to the lower-than-predicated vapor pressure at the inlet to the turbine simulator due to a higher-than-predicated pressure drop in the boiler. The higher-than-predicated pressure loss in the boiler is due to the high heat transfer rate in the 18-inch (46-cm)-long plug and the resulting high vapor quality in the entrance section of the boiler. For a given mass flow rate, the pressure drop in the tube is inversely proportional to the vapor density.

As a result of the stable and trouble-free operation of the loop during the first 5000 hours of operation, the need for constant surveillance was reevaluated. During constant surveillance, operation adjustments to the loop controls were limited to manual adjustments to the lithium heater power control, a General Electric Type 524 Current-Modulation Controller. This unit was capable of automatically controlling the power to maintain a specific temperature when used in conjunction with a General Electric Type HF temperature recorder. On September 29, 1969, the lithium heater power was placed on automatic control.

Appropriate adjustments to the control band width resulted in control of the lithium heater exit temperature within a $20^{o}F$ ($11^{o}C$) band at

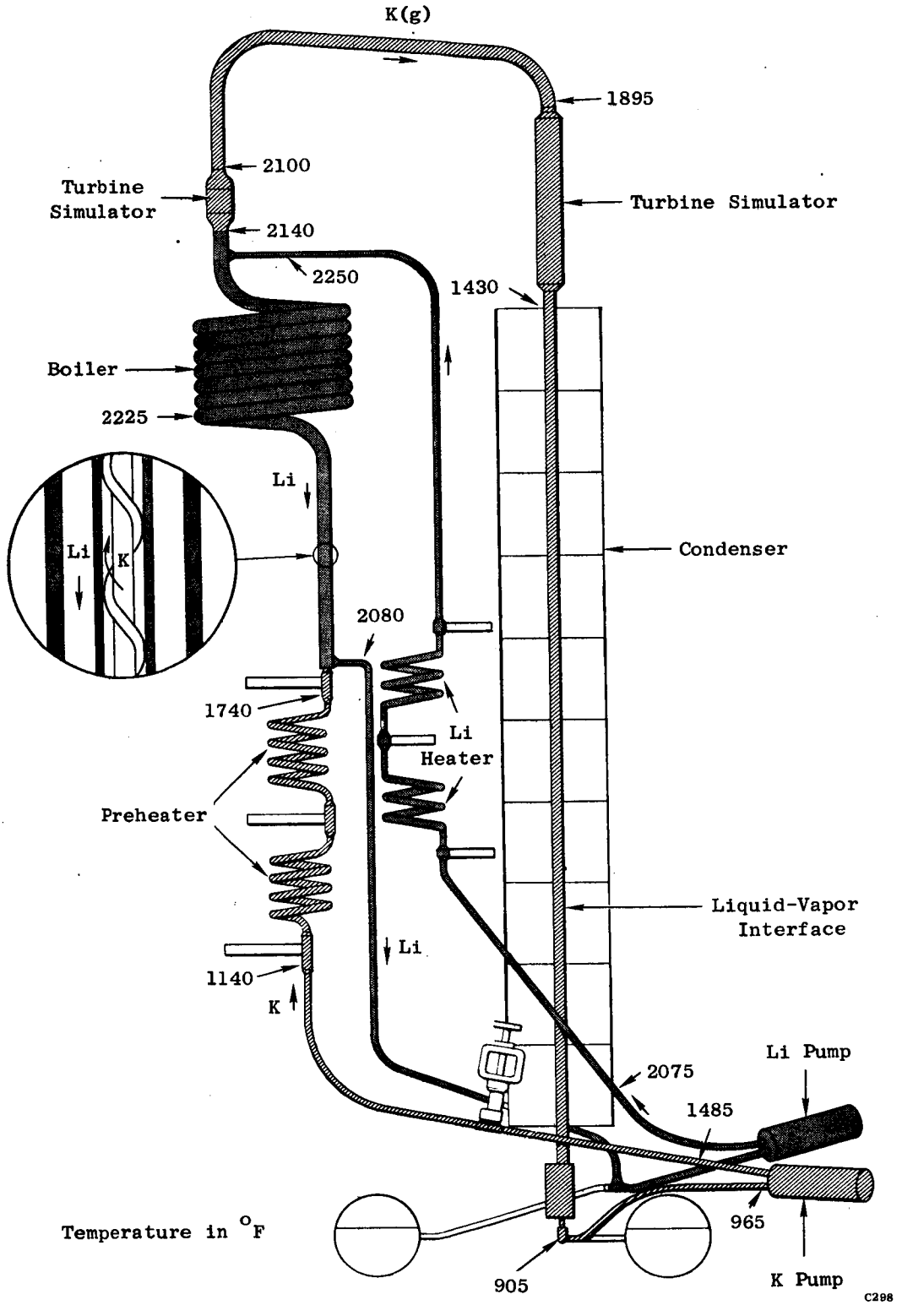


Figure 68. T-111 Corrosion Test Loop Operating Temperatures - 5000 Hours.

TABLE XIX

T-111 RANKINE SYSTEM CORROSION TEST LOOP PERFORMANCE

Date	4-19-69	8-22-69
Test Hours	2000	5000
Lithium Flow Rate	207 lb/hr (94 kg/hr)	229 lb/hr (104 kg/hr)
Lithium Temperature, In	2253°F (1234°C)	2239°F (1226°C)
Lithium Temperature, Out	2078°F (1248°C)	2078°F (1136°C)
Lithium ΔT	175°F (97°C)	161°F (72°C)
Potassium Flow Rate	37 lb/hr (16.8 kg/hr)	38 lb/hr (17.2 kg/hr)
Plug Boiling Temperature	2048°F (1120°C)	2052°F (1123°C)
Boiler Exit Vapor Temperature	2138°F (1170°C)	2137°F (1169°C)
Boiler Exit Saturation Temperature	2011°F (1100°C)	2012°F (1100°C)
Potassium Vapor Superheat	127°F (70°C)	125°F (52°C)
Condensing Temperature	1416°F (769°C)	1411°F (767°C)
Potassium Heat Input		
1. Preheat	2340 Btu/hr (0.68 kw)	2410 Btu/hr (0.71 kw)
2. Heat of Vaporization	26,950 Btu/hr(7.6 kw)	27,600 Btu/hr (8.1 kw)
3. Superheat	947 Btu/hr (0.28 kw)	960 Btu/hr (0.28 kw)
Total	30,237 Btu/hr(8.9 kw)	30,970 Btu/hr (9.1 kw)
Total Power to Lithium Heater	13.7 kw	13.8 kw
Total Power to Potassium	8.9 kw	9.0 kw
Net Heat Loss	4.8 kw	4.8 kw

TABLE XX

T-111 RANKINE SYSTEM CORROSION TEST LOOP TURBINE SIMULATOR PERFORMANCE AT 5000 HOURS

Nozzle Number	Material	Nozzle Diameter * inch	cm	Inlet Temperature °F	°C	Exit Pressure psia	$N/m^2 \times 10^{-3}$	Vapor Velocity ** ft/sec	m/sec
1	Mo-TZC	0.0892	0.226	2137	1169	112.4	775	1080	330
2	Mo-TZC	0.0881	0.234	1899	1037	92.5	647	1280	390
3	Mo-TZC	0.0964	0.245	1839	1003	75.0	524	1280	390
4	Mo-TZC	0.1083	0.275	1777	969	61.0	427	1240	378
5	Mo-TZC	0.1181	0.300	1720	938	49.5	346	1260	384
6	Cb-132M	0.1292	0.328	1664	907	40.0	280	1280	390
7	Mo-TZC	0.1457	0.370	1611	878	32.5	227	1215	371
8	Mo-TZC	0.1598	0.406	1562	850	26.3	184	1230	375
9	Cb-132M	0.1784	0.453	1514	824	21.5	150	1190	363
10	Mo-TZC	0.1986	0.504	1471	800	17.6	125	1150	351

* Measured at room temperature.

** Nozzle exit.

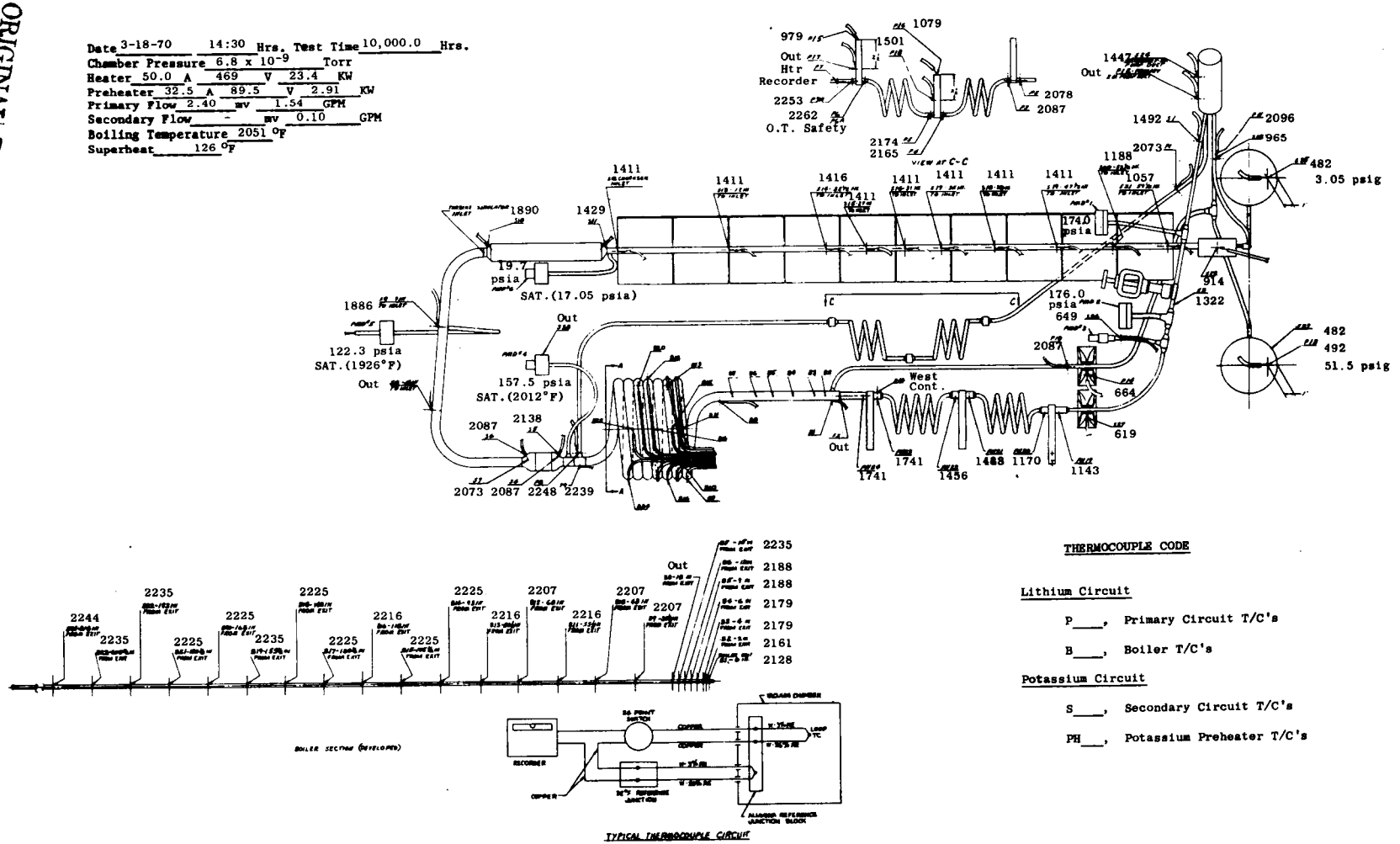
2250°F (1232°C) with no difficulties. On October 3, 1969, the loop had completed 6000 hours of operation, and surveillance was reduced to one shift for data-taking purposes only since no adjustments in power were required. Automatic and unattended operation of a corrosion loop of this complexity can be considered a major accomplishment and was only possible due to the stable and trouble-free operation of the test loop.

The test continued with no significant changes in operating conditions until a malfunction in the Simplytrol on the primary EM pump windings caused the loop to shut down at 0515 on 1-10-70 after 8385 hours of operation. The loop was brought back to test conditions with a loss of approximately one hour of test time. During the shutdown, the secondary flowmeter became inoperative; however, this was not a serious problem since the flow could be calculated from ΔT measurements in the loop.

The T-111 Corrosion Test Loop successfully completed the planned 10,000 hours of continuous operation on March 18, 1970. The loop temperatures recorded just prior to the shutdown are shown in Figure 69, and the temperatures of major interest are summarized in the schematic in Figure 70. The performance of the loop was excellent, and the power input to the lithium heater remained on automatic control for the final 4000 hours of the test with excellent temperature control being maintained. A comparison of the operating conditions at 5000 hours and 10,000 hours shown in Table XXI further exemplifies the stability of the loop's performance.

The calculated vapor velocities of the turbine simulator nozzles at 10,000 hours are presented in Table XXII for a mass flow rate of 36 lb/hr (16.3 kg/hr) of potassium. The vapor velocity in the superheated first stage was 1030 ft/sec (314 m/sec). The vapor velocity in the 88-percent-quality region ranged from a high of 1240 ft/sec (378 m/sec) in the second-stage nozzle to a low of 1095 ft/sec (334 m/sec) in the tenth-stage nozzle. As may be noted by comparing the turbine simulator conditions in Tables XX (5000-hour operation) and XXII (10,000-hour operation), no significant changes in pressure or temperatures occurred during this test period.

ORIGINAL PAGE IS
OF POOR QUALITY



AS-885

Figure 69. T-111 Rankine System Corrosion Test Loop Thermocouple Instrumentation Layout.

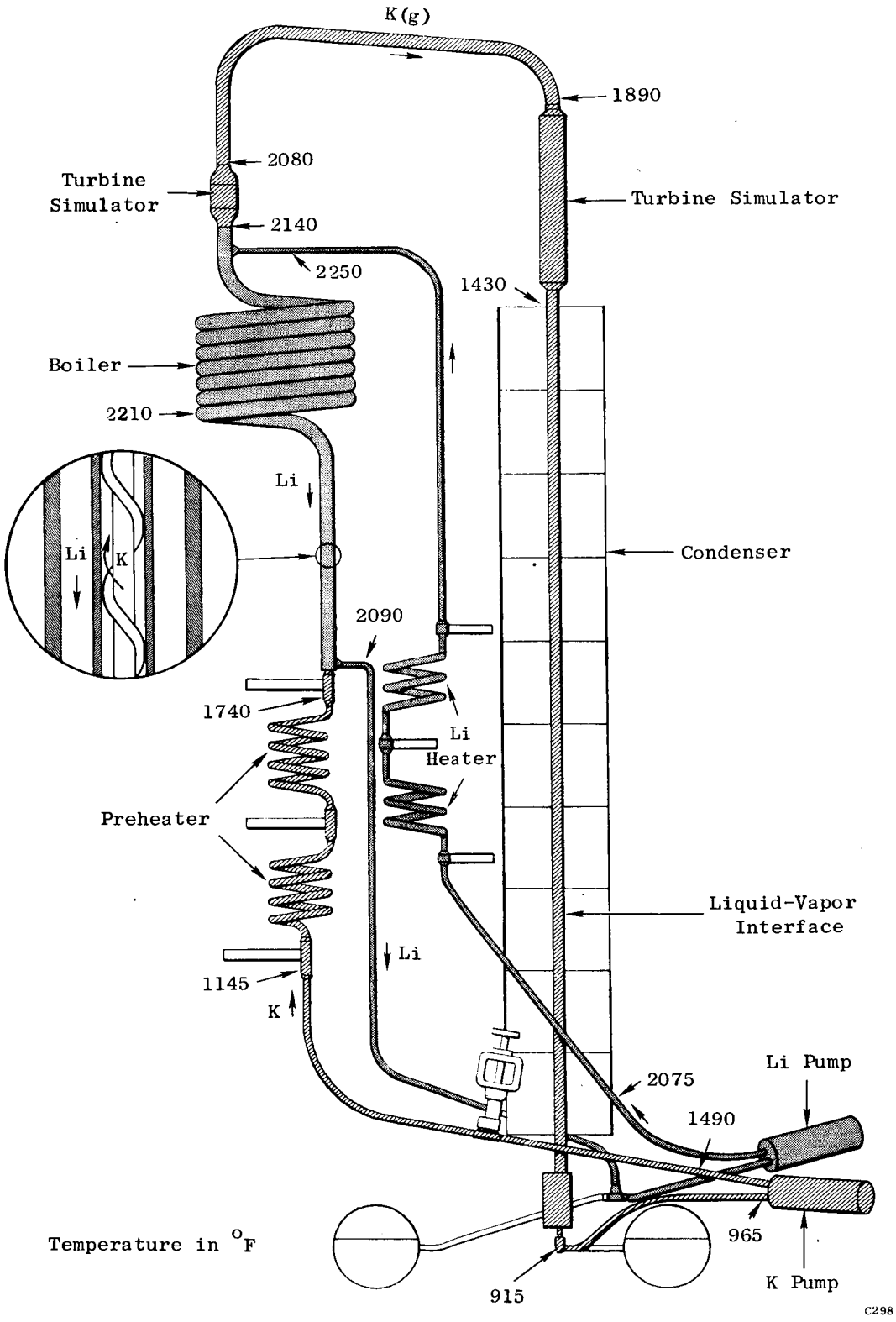


Figure 70. T-111 Corrosion Test Loop Operating Temperatures - 10,000 Hours.

TABLE XXI

T-111 RANKINE SYSTEM CORROSION TEST LOOP PERFORMANCE

Date	8-22-69	3-18-70
Test Hours	5000	10,000
Lithium Flow Rate	229 lb/hr (104 kg/hr)	234 lb/hr (106 kg/hr)
Lithium Temperature, In	2239°F (1226°C)	2239°F (1226°C)
Lithium Temperature, Out	2078°F (1136°C)	2087°F (1141°C)
Lithium ΔT	161°F (72°C)	152°F (68°C)
Potassium Flow Rate	38 lb/hr (17.2 kg/hr)	36 lb/hr (16.3 kg/hr)
Plug Boiling Temperature	2052°F (1123°C)	2050°F (1121°C)
Boiler Exit Vapor Temperature	2137°F (1169°C)	2138°F (1169°C)
Boiler Exit Saturation Temperature	2012°F (1100°C)	2012°F (1100°C)
Potassium Vapor Superheat	125°F (52°C)	126°F (53°C)
Condensing Temperature	1411°F (767°C)	1411°F (727°C)
Potassium Heat Input		
1. Preheat	2410 Btu/hr (0.71 kw)	2260 Btu/hr (0.66 kw)
2. Heat of Vaporization	27,6000 Btu/hr(8.1 kw)	26,500 Btu/hr(7.8 kw)
3. Superheat	960 Btu/hr (0.28 kw)	920 Btu/h4 (0.27 kw)
Total	30,970 Btu/hr(9.1 kw)	29,680 Btu/hr(8.7 kw)
Total Power to Lithium Heater	13.8 kw	14.0 kw
Total Power to Potassium	9.0 kw	8.7 kw
Net Heat Loss	4.8 kw	5.3 kw

TABLE XXII

T-111 RANKINE SYSTEM CORROSION TEST LOOP TURBINE SIMULATOR PERFORMANCE AT 10,000 HOURS

Nozzle Number	Material	Nozzle Diameter* inch	Nozzle Diameter* cm	Inlet Temperature °F	Inlet Temperature °C	Exit Pressure psia	Exit Pressure $N/m^2 \times 10^{-3}$	Vapor Velocity** ft/sec	Vapor Velocity** m/sec
1	Mo-TZC	0.0892	0.226	2142	1172	110.0	760	1030	314
2	Mo-TZC	0.0881	0.234	1890	1032	91.0	627	1240	378
3	Mo-TZC	0.0964	0.245	1834	1001	74.0	510	1245	380
4	Mo-TZC	0.1083	0.275	1774	969	60.0	413	1200	366
5	Mo-TZC	0.1181	0.300	1716	935	49.5	341	1205	367
6	Cb-132M	0.1292	0.328	1664	907	40.0	276	1220	372
7	Mo-TZC	0.1457	0.370	1611	878	32.5	224	1165	355
8	Mo-TZC	0.1598	0.406	1562	850	26.3	174	1180	360
9	Cb-132M	0.1784	0.453	1514	824	21.5	148	1140	348
10	Mo-TZC	0.1986	0.504	1471	800	17.6	121	1095	334

*Measured at room temperature.

**Nozzle exit.

B. TERMINATION OF THE TEST

The loop test was terminated at 1430 hours on March 18, 1970. Only four one-hour interruptions in the testing were experienced during the 10,000-hour test, and they resulted from power interruptions to the test facility and not from loop performance. The continuous operation of the T-111 Rankine System Corrosion Test Loop can be considered a significant milestone in the development of the technology for advanced space power systems.

The loop shutdown was performed in gradual steps to reduce the possibility of large thermal shocks from boiling instabilities. The plot of the pressures on either side of the metering valve, Figure 71, best illustrates the loop shutdown procedure and the small instabilities which were observed when the potassium temperature was reduced below 1600°F (871°C). At each step, the power to the lithium heater, potassium preheater, and both EM pumps and the potassium surge tank pressure was reduced. The surge tank pressure was finally reduced to 0 psia, and the potassium dumped into the surge tank.

C. TOTAL PRESSURES AND PARTIAL PRESSURES DURING THE 10,000-HOUR TEST

During operation of the loop test, the total pressure and the partial pressures of the individual residual gases in the test chamber were determined every 12 hours at a minimum utilizing the equipment previously described in Section VI.B of this report. The methods used to calibrate the mass spectrometer and subsequently calculate the partial pressures of the various residual gases in the test chamber are described in Section XV, Appendix H, of this report.

The chamber pressure and partial pressures of the various gaseous species in the test chamber during the period of loop operation up to 2000 hours were shown earlier in Figure 60. The total pressure (sum of partial pressures) was consistent with the ion gauge reading, even though it is nearly a factor of two greater. The reason for this is that the major species is hydrogen, which has a rather low ionization efficiency, the ion gauge sensitivity relative to nitrogen being only 0.42.

At the start of loop operation at design conditions, the ion gauge

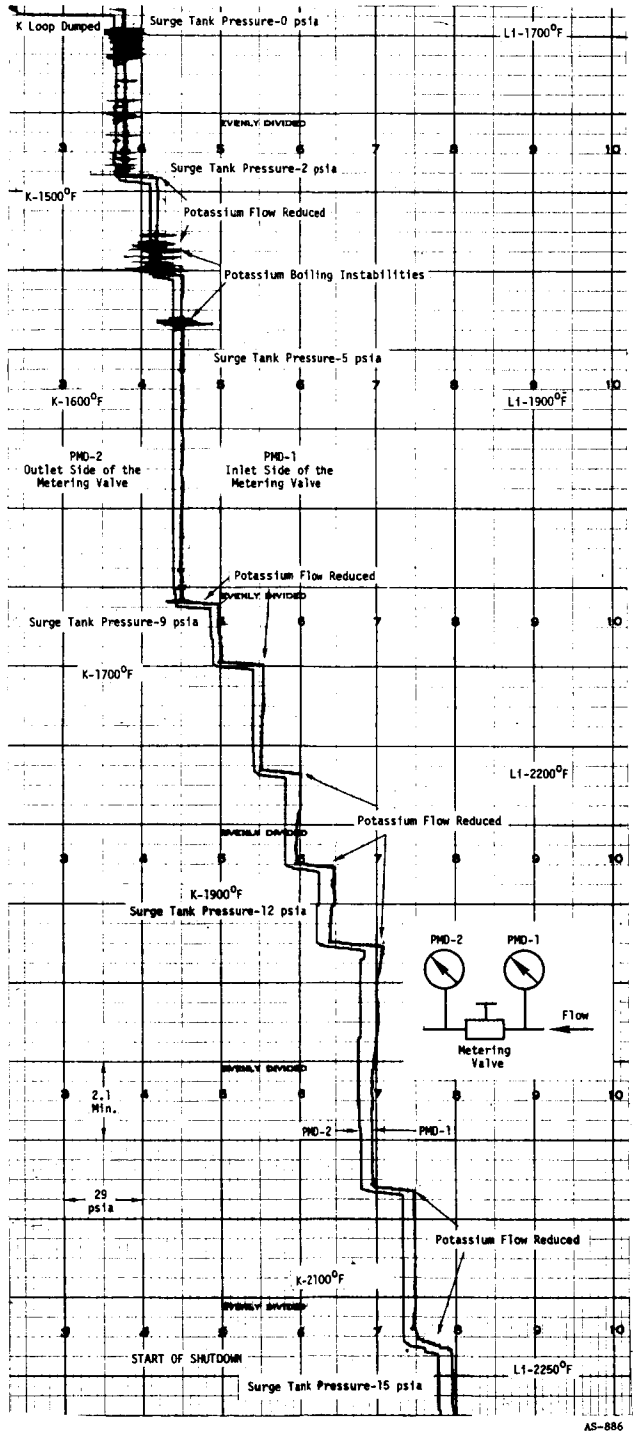


Figure 71. Potassium Pressure on Either Side of the Metering Valve During the Shutdown Completing the 10,000 Hours of Testing of the T-111 Rankine System Corrosion Test Loop.

ORIGINAL PAGE IS
OF POOR QUALITY

reading was 1 x 10^{-6} torr (1.3 x 10^{-4} N/m^2) but dropped rapidly reaching the 10^{-8} torr (10^{-6} N/m^2) range in less than 100 hours. Throughout the 2000-hour test period, 90 to 95 percent of the residual gas in the chamber was hydrogen. The source of this gas is probably outgassing of heated metal parts, either the loop itself or the supporting structure. The fact that the N_2 and CO, Ar, and O_2 concentrations were so low this early in the test indicated the absence of any appreciable leakage in the system.

It is of interest to compare the residual gas composition in the present test with that obtained under similar conditions in the previous Cb-1Zr Corrosion Rankine System Loop Test.[21] For the Cb-1Zr loop after 1000 hours of loop operation, the total pressure was about 4 x 10^{-8} torr (5 x 10^{-6} N/m^2) with major species N_2 + CO, Ar, and H_2 in approximately equal proportions. For the T-111 loop after 1000 hours, the total pressure was about 4 x 10^{-8} torr (5 x 10^{-6} N/m^2) with major species H_2. This comparison thus shows that the same total pressure was obtained in both tests after 1000 hours, and it indicates that much more hydrogen outgassing occurs in the present T-111 loop test while the oxygen-bearing gases were higher in the Cb-1Zr loop test. No significant changes in total pressure or the partial pressures occurred during the 2000-hour to 10,000-hour period of test operation. The chamber pressure and partial pressures of the various gas species in the test chamber during the entire 10,000 hours of loop operation are summarized in Figure 72. The data for the initial 1000 hours of testing are shown on an expanded scale since this is where the largest changes were observed. Following this initial large decrease, there was a continued gradual decrease in most species for the period of 1000 to 6500 hours, at which time all pressures essentially leveled off and remained constant until the shutdown at 10,000 hours. A very slight increase in the N_2 + CO and Ar pressures was noted after 3500 hours of test operation. This increase, which was most likely due to a minute air leak, had no significant effect on the total pressure in the test chamber. Only a limited number of data points are shown for clarity; however, residual gas analyses were obtained at least

(21) Hoffman, E. E. and Holowach, J., Cb-1Zr Rankine System Corrosion Test Loop, NASA CR-1509, June 1970, p. 196.

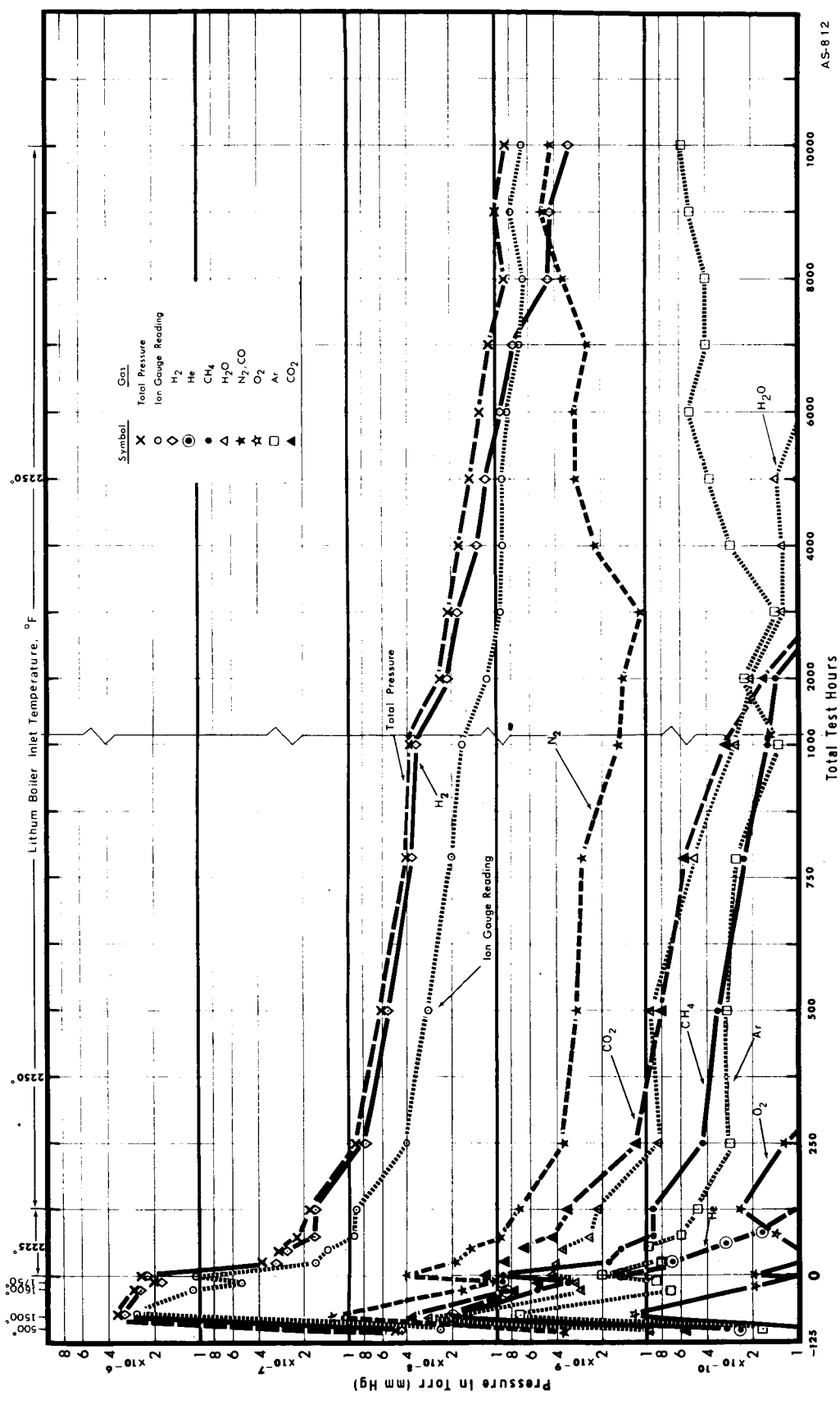


Figure 72. Test Chamber Environment During Testing of the T-111 Rankine System Corrosion Test Loop.

every 24 hours. The ion gauge pressure at the completion of the 10,000-hour test was 8.5×10^{-9} torr (1×10^{-7} N/m^2).

The effectiveness of the close control of the test chamber pressure during the 10,000-hour test in minimizing the environmental contamination of the T-111 test components is illustrated by the chemical analysis results obtained on samples of the Cb-1Zr alloy foil insulation taken from the vapor carryover tube. The very limited oxygen increase noted in these specimens, as well as the limited pickup noted on the loop tubing proper, is discussed in Section XII, Chemical and Metallurgical Evaluation of Loop Components.

XI. DRAWING, DISASSEMBLY, AND CLEANING OF LOOP COMPONENTS

A. ALKALI METAL SAMPLING, DRAINING, AND ANALYSIS

At the completion of the shutdown operation described in the previous section, the potassium was allowed to cool to 1000°F (540°C) and then sampled using the system shown schematically in Figure 73. The potassium remaining in the surge tank was then immediately gravity drained into the potassium still pot. This potassium was subsequently vacuum distilled at 800°F (425°C). The pot was opened and approximately 19 mg of a black, powdery residue was recovered and analyzed. The analyses of the potassium sample and the black residue are shown in Table XXIII. No major changes in the potassium were observed as a result of the 10,000-hour exposure to T-111 at a maximum temperature of 2150°F (1175°C). The black residue contained the elements of stainless steel plus lithium, all of which were also observed after draining the original potassium charge for the pretest boiler repair described in Appendix K.

The initial lithium draining and sampling system was identical to that for potassium as shown previously in Figure 73; however, failure of the bellows in the original fill valve required replacement of this valve and the modified sampling system, shown in Figure 74, was installed. The lithium was dumped from the loop into the surge tank at a temperature of 1100°F (595°C). Approximately 300 cc of lithium was drained into the waste tank, and a sample was obtained in sample tube No. 1 between the dump valve and the fill valve. This sample was removed, and the fill and dump valves were cleaned. In-line sample tube No. 2, shown by the dotted line in Figure 74 was then installed. Following leak checking and bakeout of the system, the remaining lithium in the surge tank was drained into the waste tank at 1000°F (538°C), thereby obtaining a second lithium sample in the transfer line. The lithium samples were analyzed, and the results are presented in Table XXIII. The results indicate that the oxygen concentration in the lithium increased about ten-fold during the test which could be expected as lithium exposure normally reduces the oxygen concentration of the T-111 piping during elevated-temperature testing.

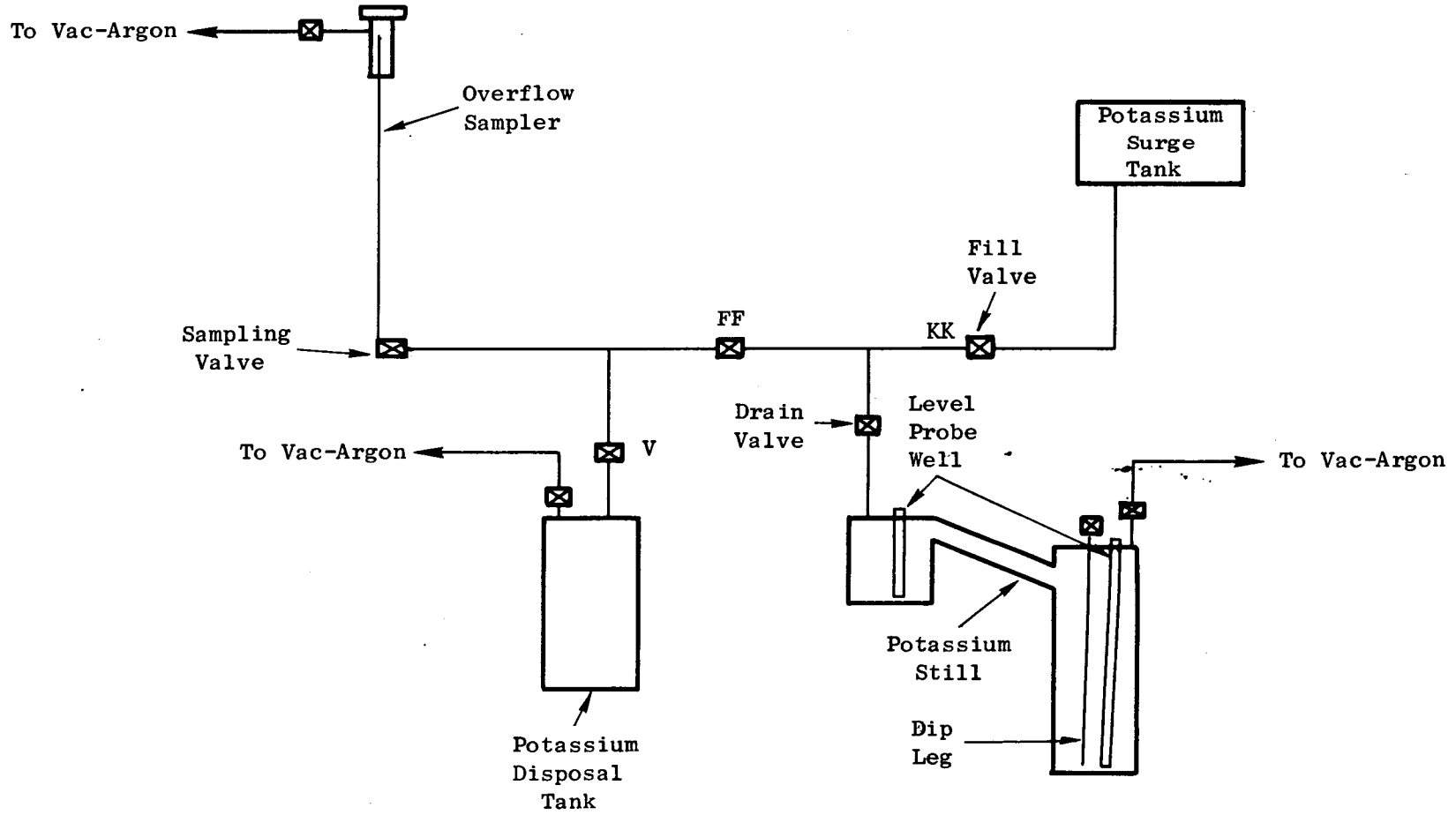


Figure 73. T-111 Corrosion Test Loop Potassium Draining and Sampling Schematic.

TABLE XXIII

ANALYSES OF POTASSIUM AND LITHIUM BEFORE AND AFTER THE 10,000-HOUR TEST AND THE ANALYSIS OF A RESIDUE RECOVERED FROM THE POTASSIUM BY DISTILLATION FOLLOWING THE TEST

	Potassium		Lithium		
	Pretest ppm	After 10,000 Hours ppm	Pretest ppm	After 10,000 Hours ppm	ppm
O	3,4	6,11	49	460,554	386,413
C	32	41	31	81	65
N	-	-	38,47	48,53	44,48
Ag	< 2	< 2	< 5	< 5	< 5
Al	10	2	5	5	< 5
B	< 30	< 30	< 50	< 75	< 75
Ba	< 20	< 10	< 50	< 75	< 75
Be	< 2	< 2	< 5	< 5	< 5
Ca	10	2	5	5	5
Cb	< 10	< 10	< 25	< 25	< 25
Co	< 2	< 2	< 5	< 5	< 5
Cr	< 2	< 2	< 5	< 5	< 5
Cu	2	< 2	5	5	5
Fe	2	< 2	< 5	< 5	< 5
Mg	2	< 2	5	5	5
Mn	< 2	< 2	< 5	< 5	< 5
Mo	< 2	< 2	< 5	< 5	< 5
Na	< 20	< 30	< 50	< 125	< 125
Ni	< 2	< 2	5	< 5	< 5
Pb	< 20	< 20	< 50	< 50	< 50
Si	2	2	5	5	5
Sr	< 2	< 2	5	5	5
Sn	< 10	< 10	< 25	< 25	< 25
Ti	< 10	< 10	< 25	< 25	< 25
V	< 10	< 10	< 25	< 25	< 25
Zr	< 10	< 10	< 25	< 25	< 25
Li	31	-	K = 106		

Black residue from potassium distillation after 10,000-hour test.

Major (10 - 100%): Cr, Fe
Minor (1 - 10%): Ni, Ti, Li
Trace (0 - 1%): Ag, Al, Cu, Mg, Mn, Mo, Si, V

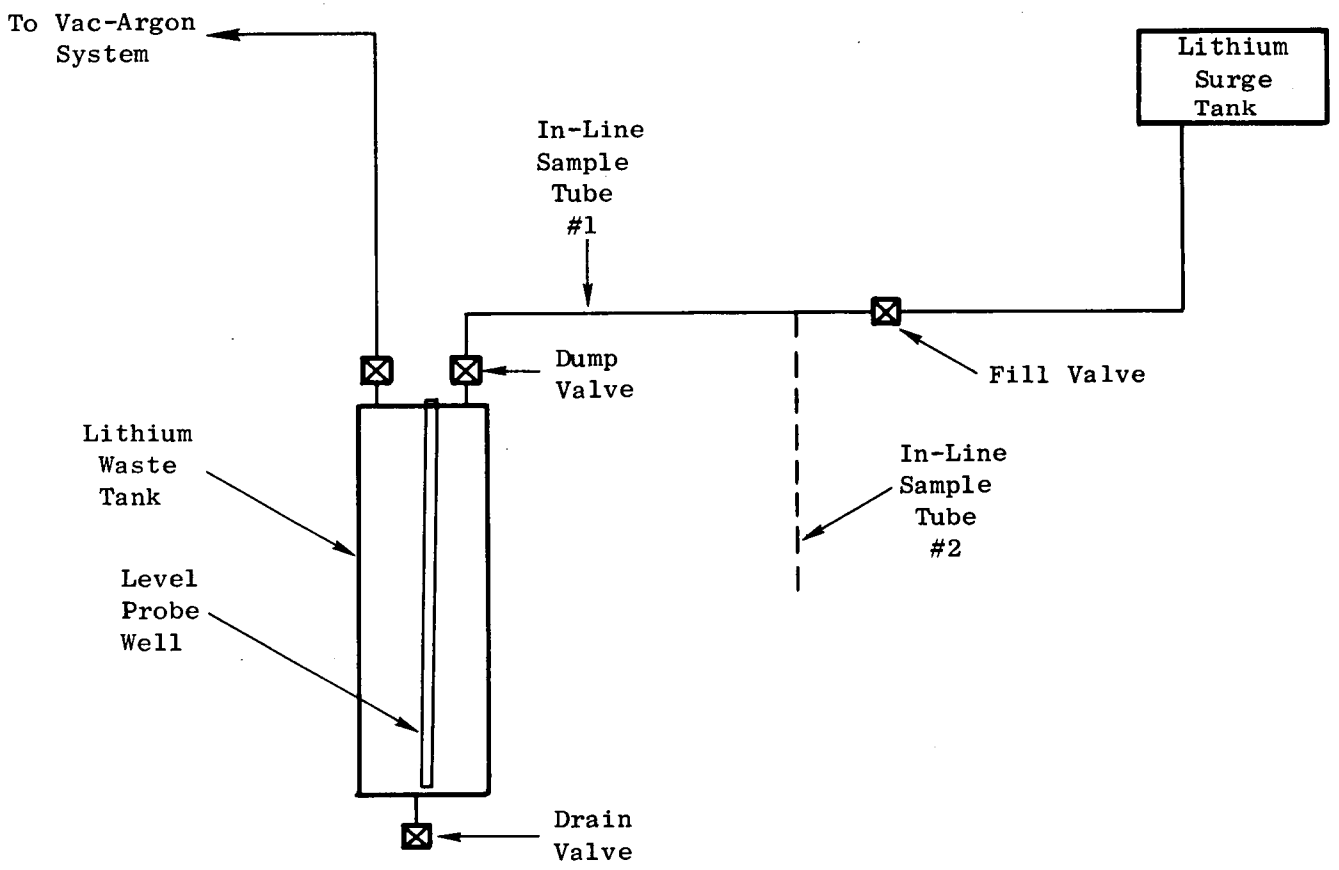


Figure 74. T-111 Corrosion Test Loop Lithium Draining and Sampling Schematic.

B. INITIAL PREPARATION FOR POSTTEST EVALUATION

Following removal of the alkali metal from the loop and surge tanks, all electrical power and water cooling was turned off. After the loop and vacuum chamber had cooled to room temperature, the bell jar was removed. Visual inspection of the loop and all related components showed them to be in excellent condition. Except for isolated areas in close proximity to the stainless steel support structure, there was no discoloration of the Cb-1Zr dimpled-foil, thermal insulation. Photographs of the loop prior to any disassembly or removal of foil are shown in Figures 75, 76, 77. Figure 75 shows the boiler (insulation package still in place, lithium inlet line to boiler, both turbine simulators, crossover line, the top of the condenser section, and two of the pressure transducers. Figure 76 shows the bottom of the boiler insulation package, boiler plug section, condenser, potassium preheater, lithium heater, and lithium inlet and return lines. Figure 77 is a photograph looking down into the spool piece illustrating, in addition to the items described above, the shutter assembly, potassium surge tank, and both valve assemblies. Close examination of the metering valve revealed that the reason it became inoperative during the test is because the coupling connecting the spur gear shaft with the flexible cable had become disengaged.* Following this initial visual examination, thermocouples and the thermal insulation were removed from the boiler, turbine simulators, and crossover line, the loop components which were to undergo posttest evaluation. All the Cb-1Zr thermal insulating foil removed from the loop was ductile, and no visible evidence of contamination was noted. After removal of the thermal insulation, these components were reinspected visually. Again, they were found to be in excellent condition as shown in the photographs of the boiler and plug regions in Figures 78 and 79.

Auxiliary supports were installed as needed to support the loop during

---

* In future valve actuation systems of this type, the coupling between the flexible drive cable and the spur gear shaft should be accomplished by means of a pin rather than a set screw as used in this test to achieve a more positive connection.

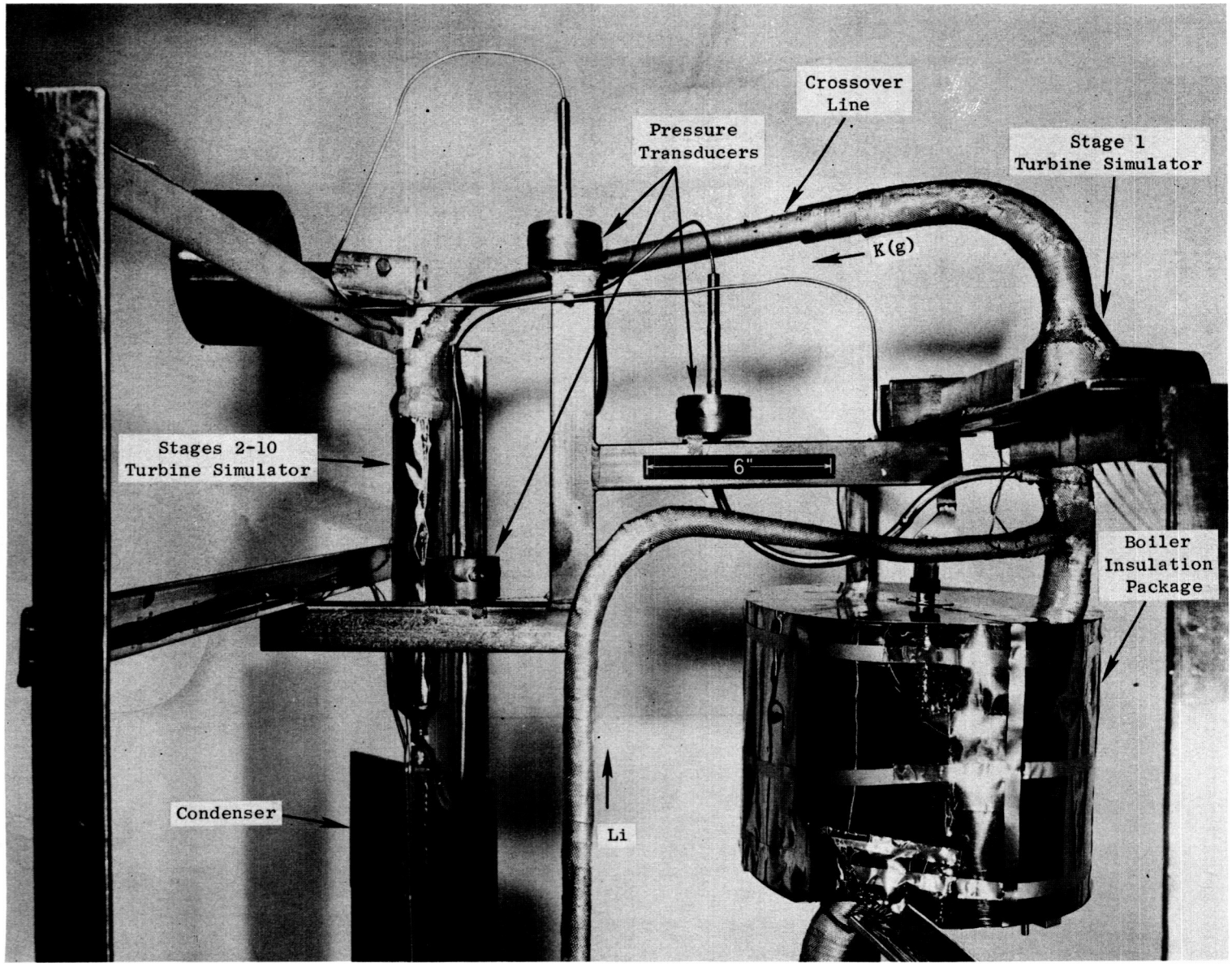


Figure 75. Top Portion of T-111 Corrosion Test Loop After Completion of 10,000 Hours of Testing. (Orig. P70-3-22G)

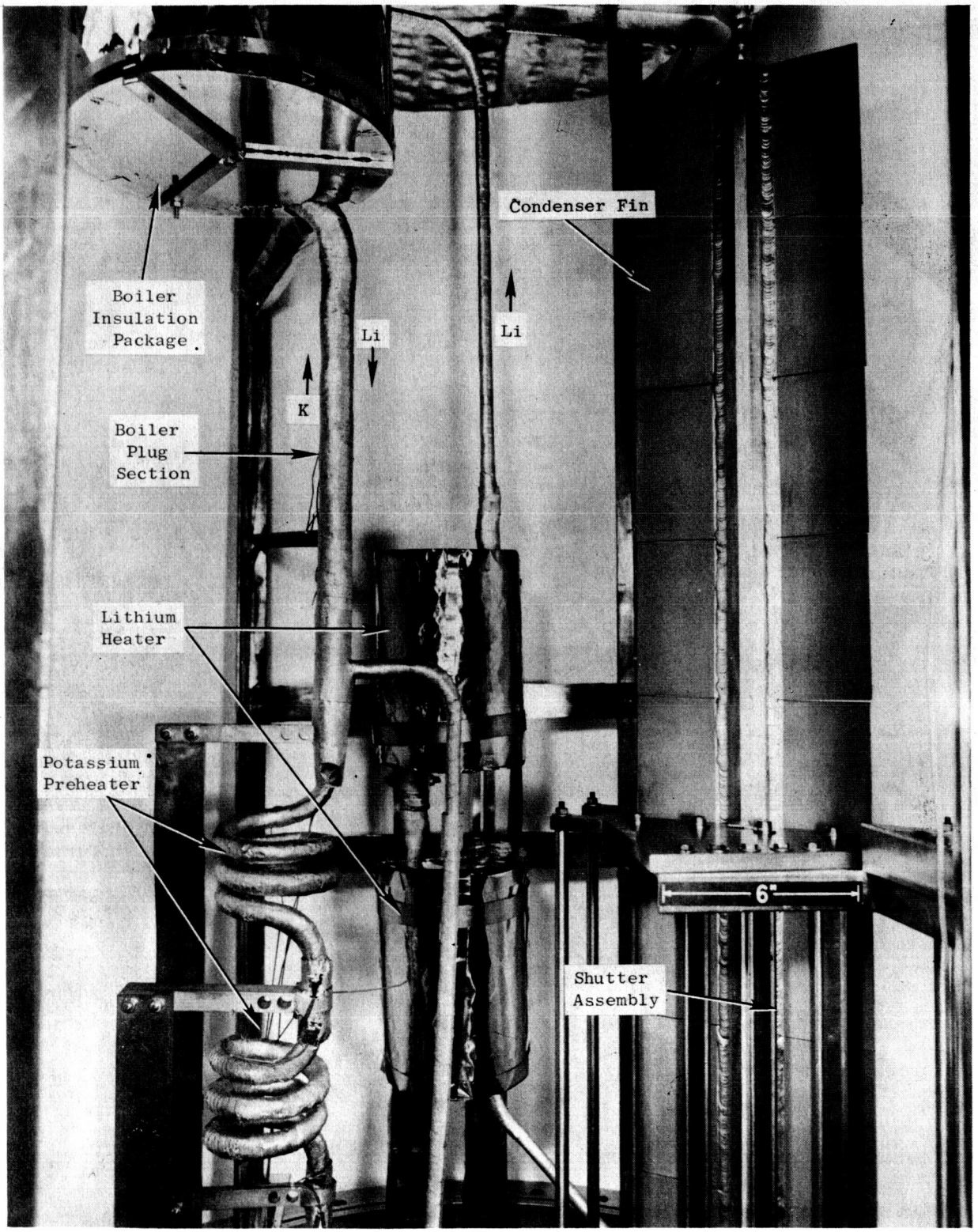


Figure 76. T-111 Corrosion Test Loop After Completion of 10,000 Hours of Testing. (Orig. P70-3-22C)

ORIGINAL PAGE IS OF POOR QUALITY

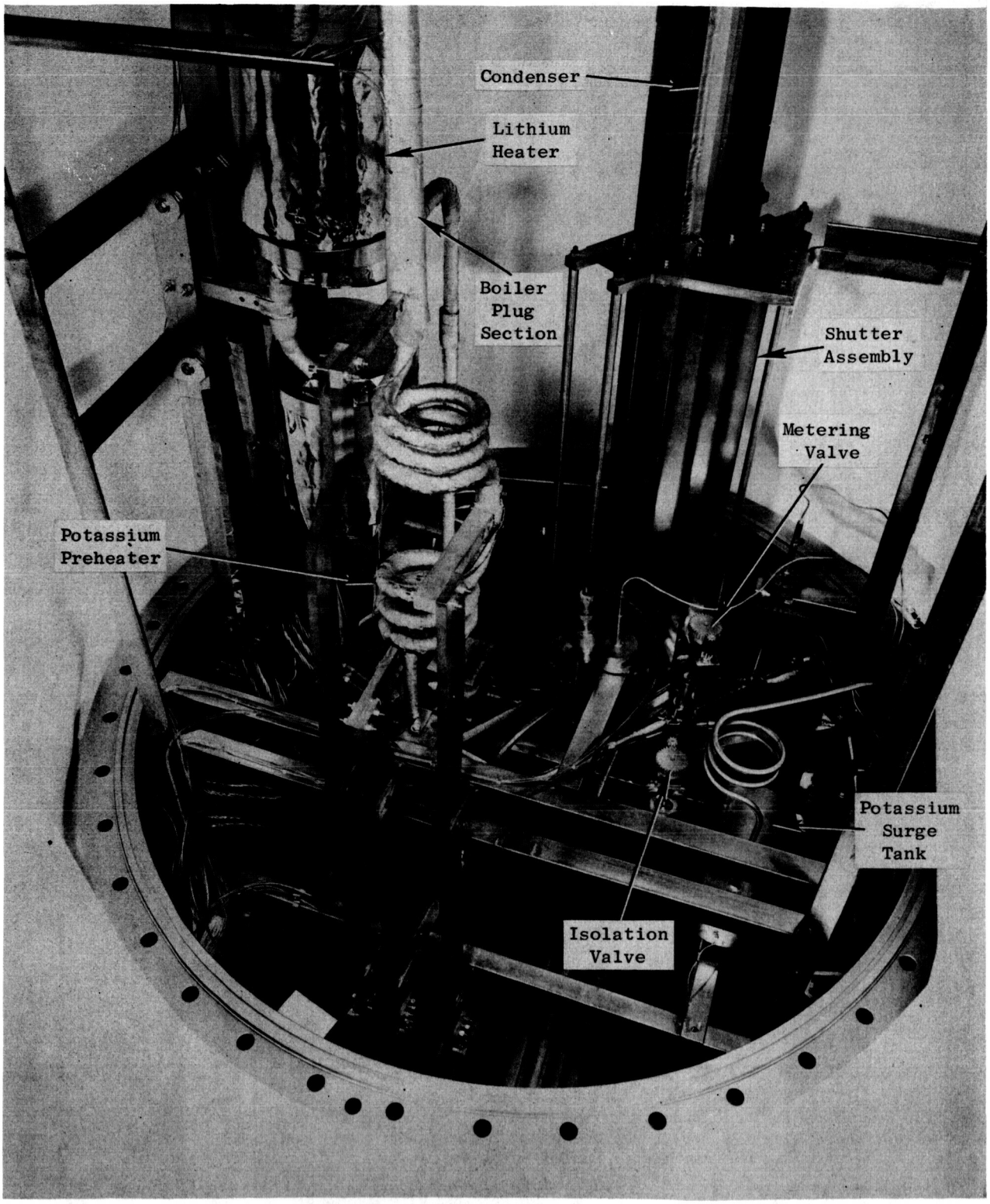


Figure 77. Lower Portion of T-111 Corrosion Test Loop After Completion of 10,000 Hours of Testing. (Orig. P70-3-22F)

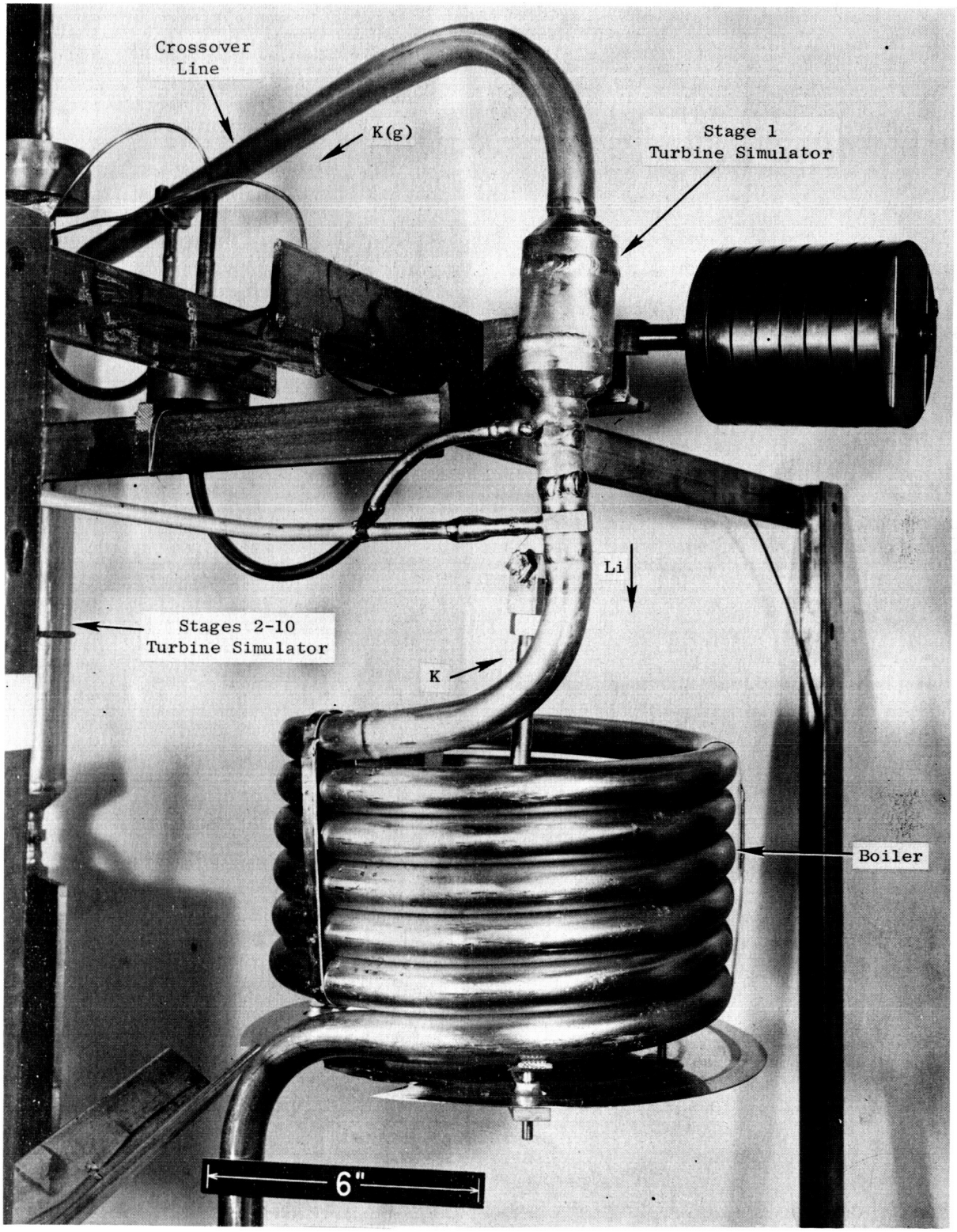


Figure 78. T-111 Corrosion Test Loop Boiler and Turbine Simulator Following Removal of the Thermal Insulation. (Orig. P70-4-1A)

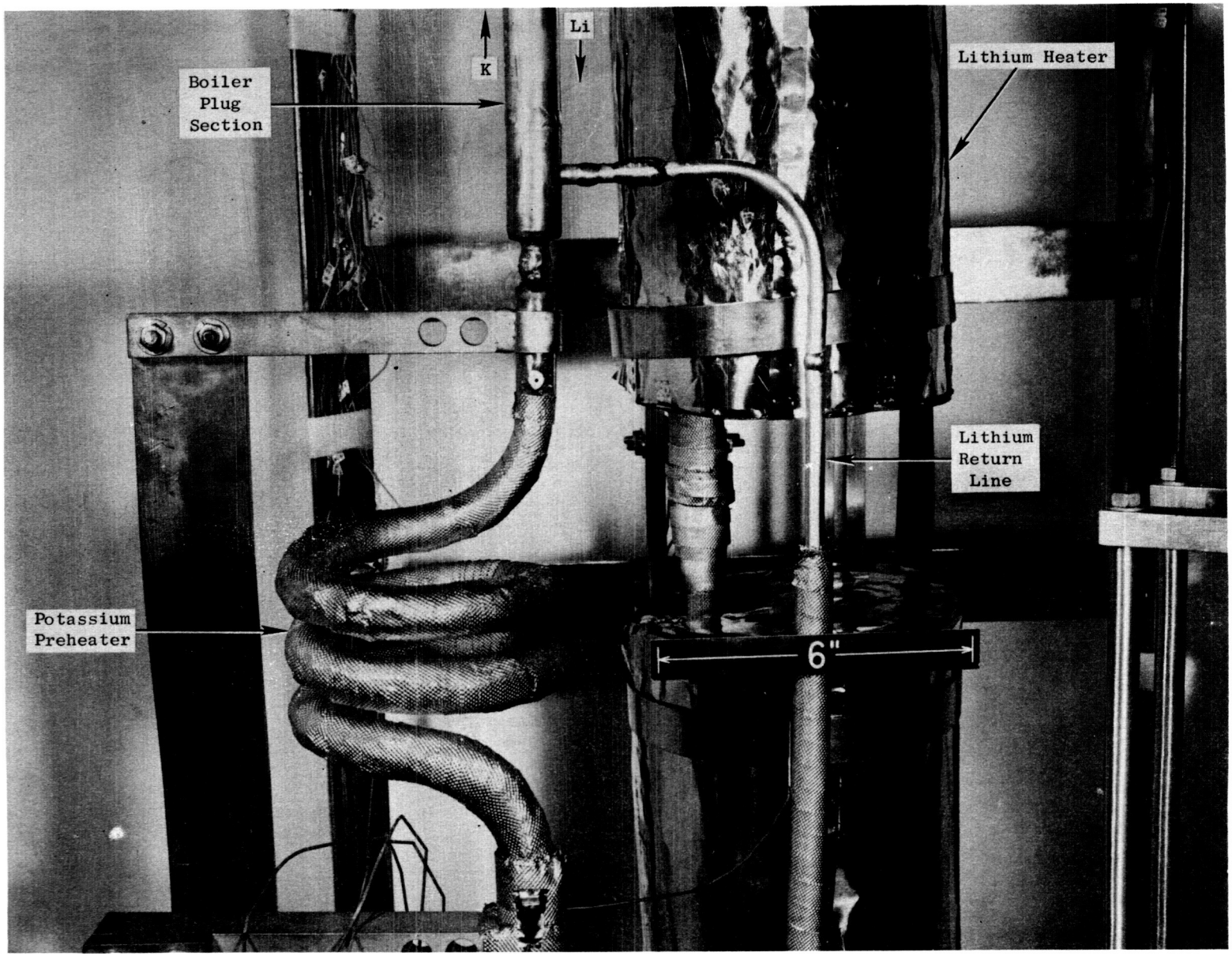


Figure 79. Components of T-111 Corrosion Loop After Removal of Thermal Insulation From Areas to Undergo Posttest Evaluation. (Orig. P70-4-1C)

removal of the components for complete evaluation. The techniques employed were similar to those developed during removal of the boiler, as described in Appendix K. The protective vinyl chamber was placed over the loop, sealed to the spool piece, evacuated, and backfilled with helium in preparation for cutting and removal of the desired components. The loop enclosed in the vinyl chamber and ready for cutting is shown in Figure 80. After filling the bag with helium, areas to be cut were first hand-filed as necessary to remove weld metal buildup or to reduce sufficiently the wall thickness to simplify the final cutting using a tubing cutter. All final cutting was performed with a tubing cutter at the locations shown in Figure 81 to eliminate the possibility of introducing chips inside the loop tubing. After making the cuts, both the potassium and lithium circuits were pressurized with argon to verify that no blockage occurred. Upon verification of a gas path, the open tube ends were plugged or capped with stainless steel "Swagelok" fittings.

The protective vinyl chamber was removed and finally, the boiler and turbine simulators were removed from the chamber and placed on a lab bench for closer visual examination. The bell jar was replaced and the chamber evacuated to maintain the remainder of the loop under vacuum for possible future use.

The boiler and turbine simulators after removal from the loop are shown in Figure 82. This assembly was then transferred to the weld chamber for attachment of valves to the potassium and lithium inlet tubing to facilitate removal of residual alkali metals with liquid ammonia.

C. REMOVAL OF RESIDUAL ALKALI METAL

After the assembly was transferred to the weld chamber, the chamber was evacuated and backfilled with argon. Valves were attached to the lithium and the potassium circuits, and the assembly was removed from the weld chamber to be connected to the liquid ammonia system described in Appendix K. The assembly was maintained at -60°F (-50°C) in a liquid nitrogen-cooled, 50-percent (by volume) mixture of methanol and water held in insulated containers as shown in Figure 83. When the assembly reached -60°F (-50°C), the temperature

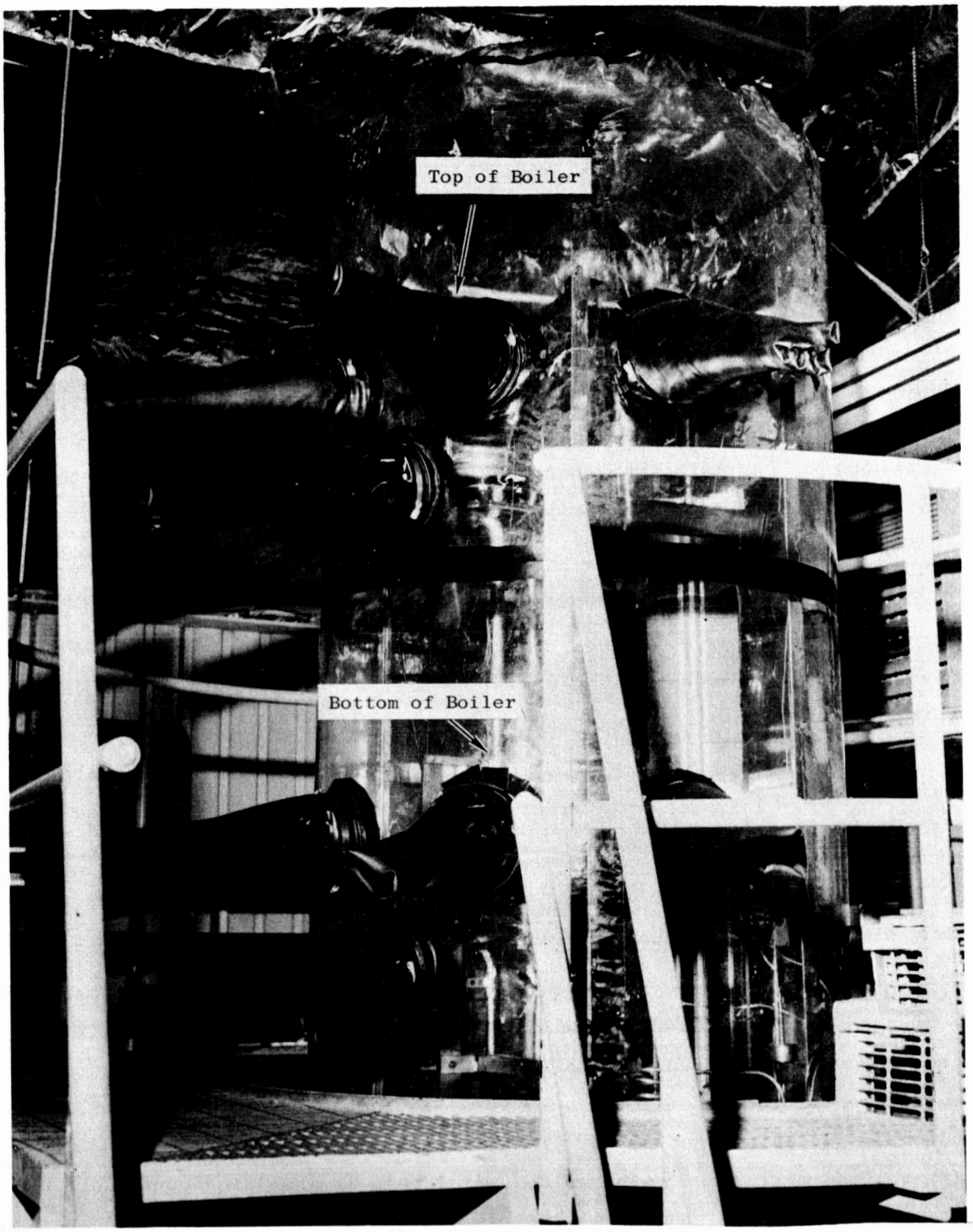


Figure 80. Vinyl Chamber Used for Cutting Operations on T-111 Corrosion Test Loop. (Orig. C68062842)

ORIGINAL PAGE IS
OF POOR QUALITY

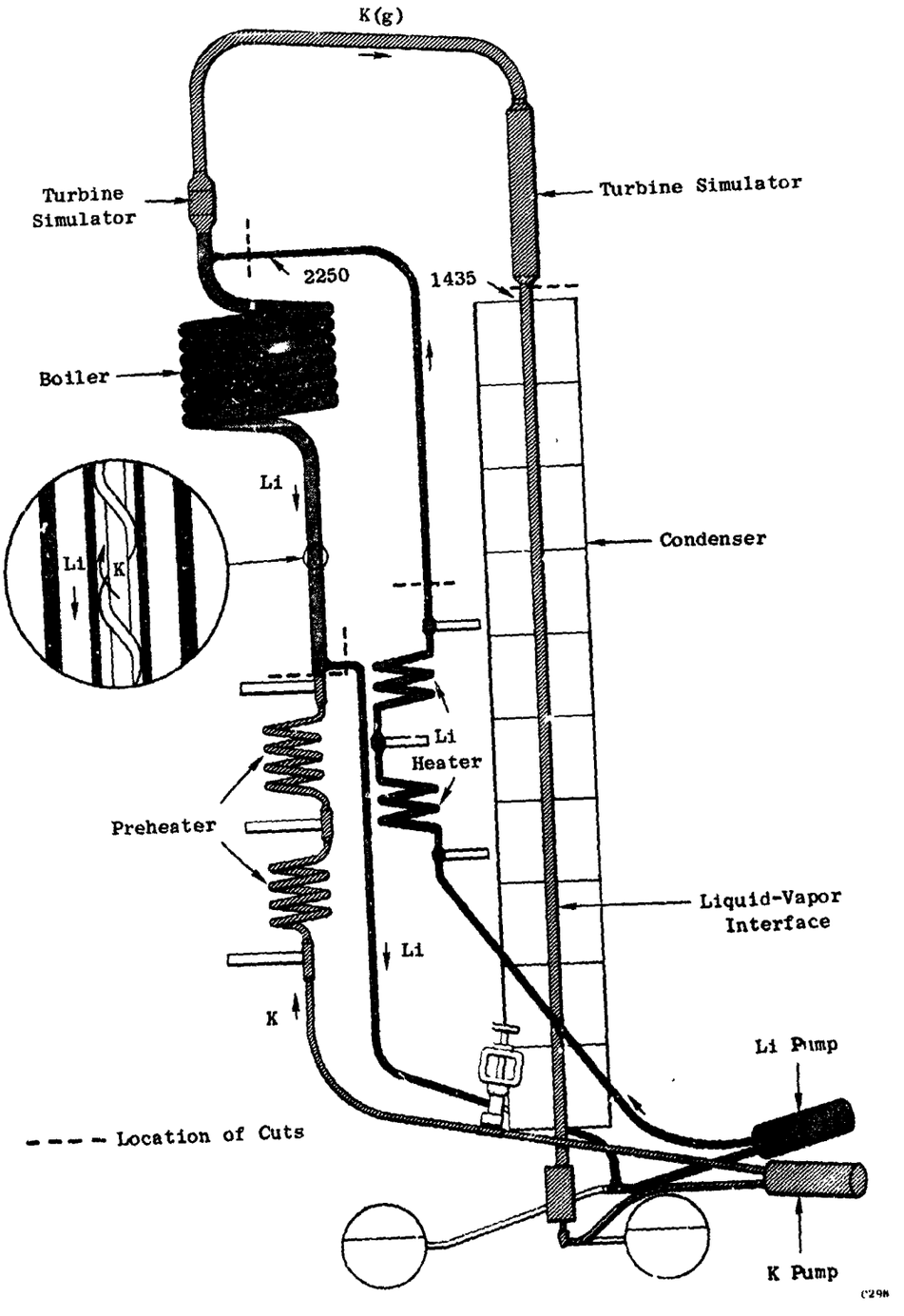


Figure 81. T-111 Corrosion Test Loop Showing Location of Cuts Necessary to Remove Boiler and Turbine Simulators for Evaluation at the Completion of 10,000 Hours of Testing.

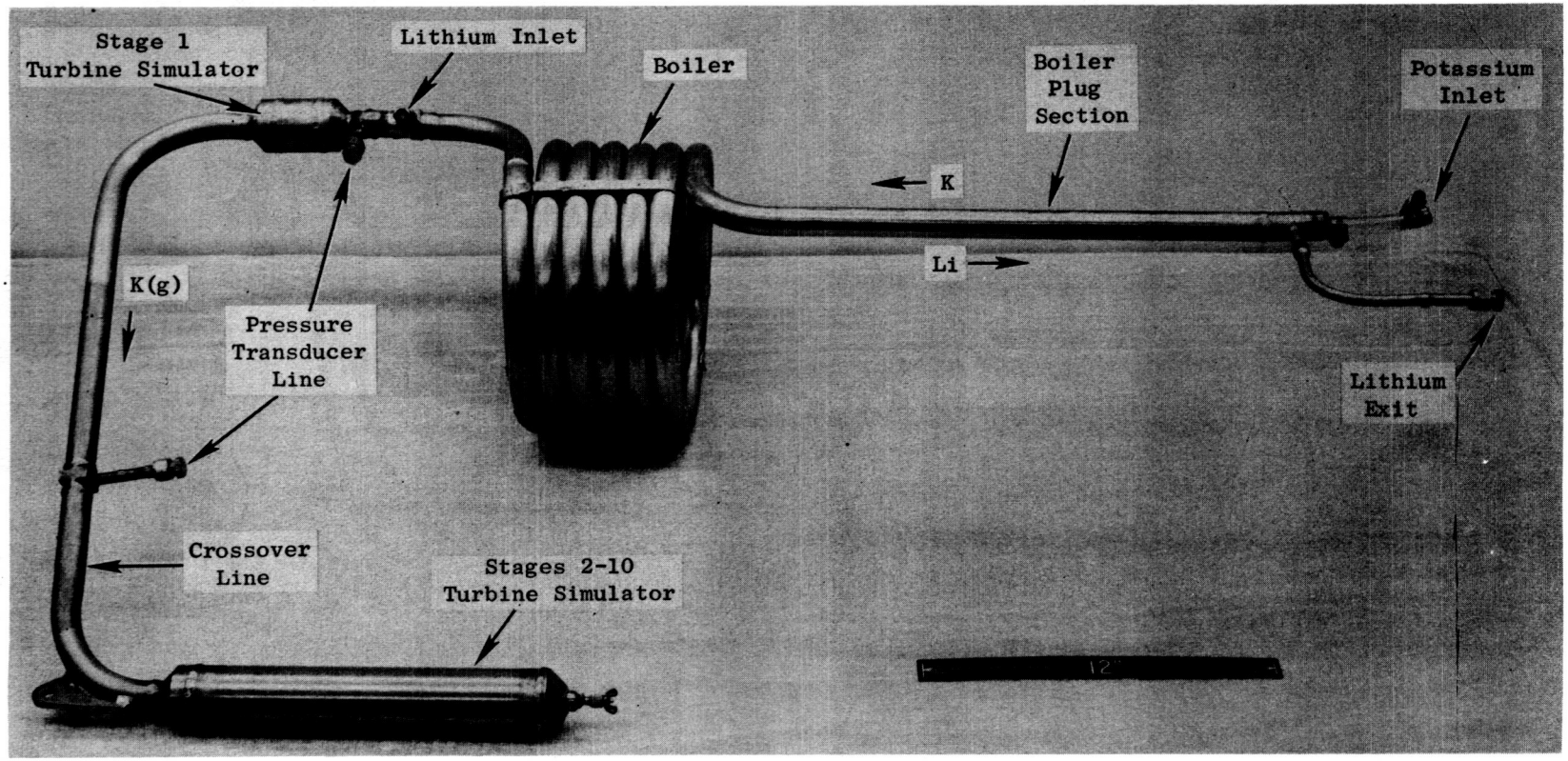


Figure 82. Boiler, Crossover Line, and Turbine Simulators After Removal From T-111 Corrosion Test Loop. (Orig. P70-4-14A)

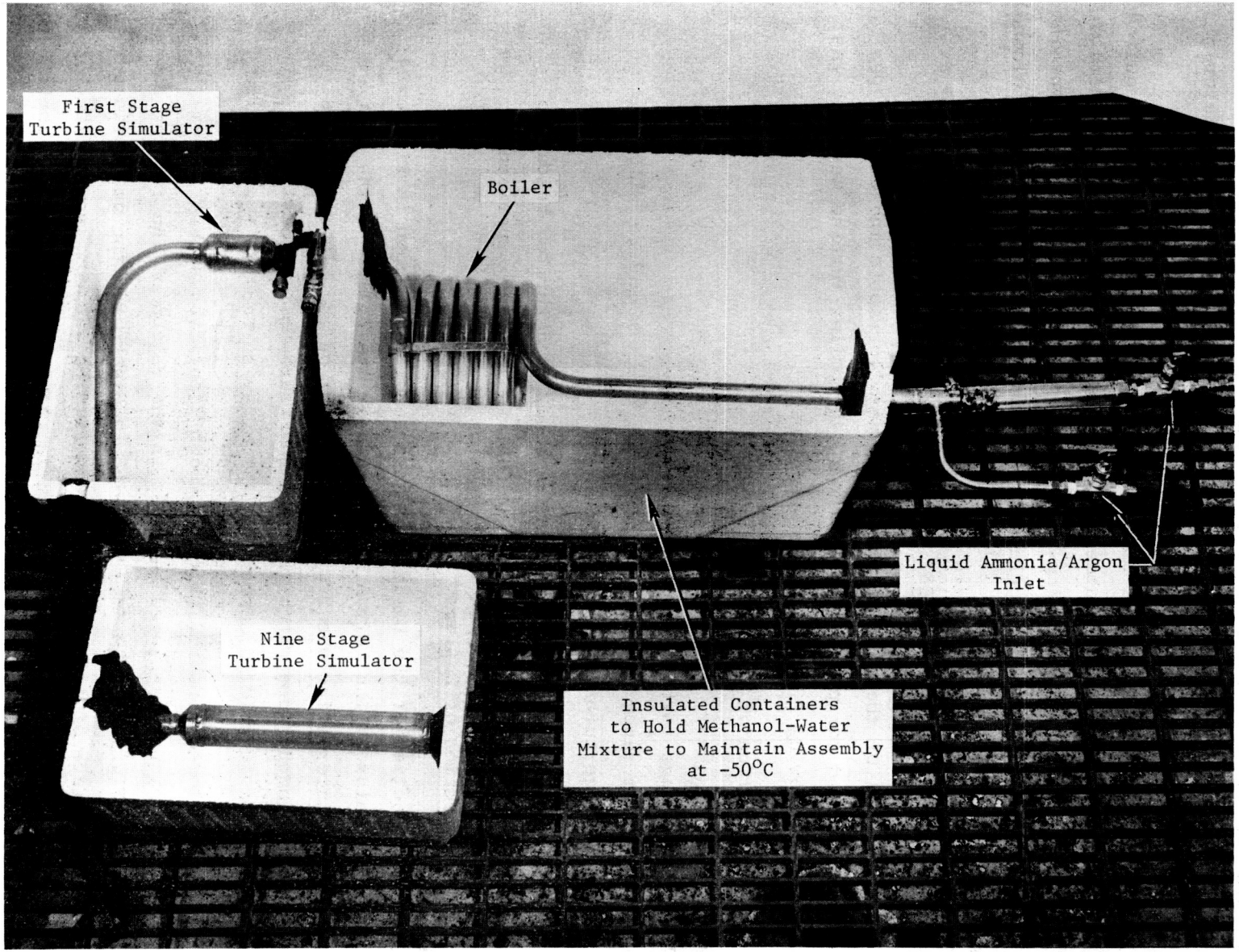


Figure 83. Setup for the Removal of Residual Alkali Metals from T-111 Rankine System Corrosion Test Loop Components by Reaction with Liquid Ammonia. (Orig. P70-4-18B)

necessary to maintain the ammonia in a liquid state, the argon flow was closed, and the valve to the ammonia bottle opened. The ammonia flow through the assembly was maintained until the effluent was clear and colorless. The lithium circuit contained a greater quantity of alkali metal than the potassium circuit, based on the quantities of liquid ammonia required to clean each circuit. Similar observations were made when the alkali metals were removed from the boiler during the repair operation described in Appendix K. Each circuit of the assembly was flushed with distilled water and ethyl alcohol and allowed to dry.

D. FINAL PREPARATION FOR POSTTEST EVALUATION

To obtain all of the desired chemistry, metallographic and other types of specimens needed for posttest evaluation, the boiler-turbine assembly was cut into the following five major subassemblies:

1. Plug section of the boiler;
2. Boiler;
3. First-stage turbine simulator;
4. Potassium vapor crossover line;
5. Nine-stage turbine simulator.

These subassemblies were further dissected, as described below, to facilitate further visual examination and obtain necessary specimens.

1. Plug Section of Boiler

The plug section of the boiler was disassembled as shown in Figure 84 by filing the welds at the bottom fitting and at the bottom of the swirler wire. The most interesting observations were made on the 3/8-inch (0.95-cm) potassium containment tube which is shown in Figure 85. Of particular interest is the gold-colored deposit on the outer surface of the tube.

The gold-colored deposit, which has been identified as HfN by X-ray diffraction techniques, appeared heaviest in the region of the fitting shown in the inset of Figure 85. As may be noted in Figure 85, the deposition on the outer surface of the boiler tube and fitting was confined to the last five inches of the lithium flow path in the boiler (first five inches

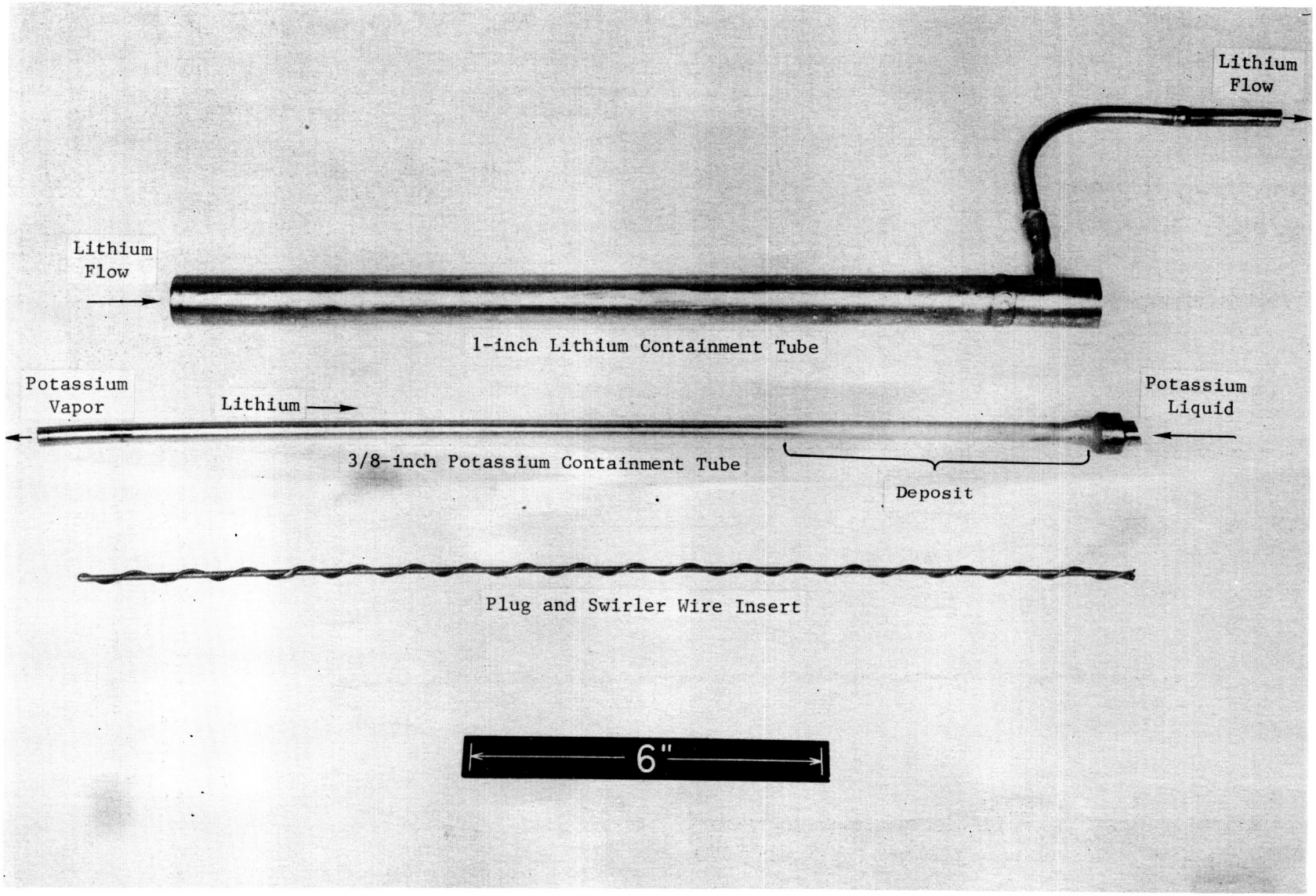


Figure 84. Components of Boiler Plug Section of T-111 Rankine System Corrosion Test Loop Following 10,000 Hours of Continuous Operation. (Orig. P70-5-1M)

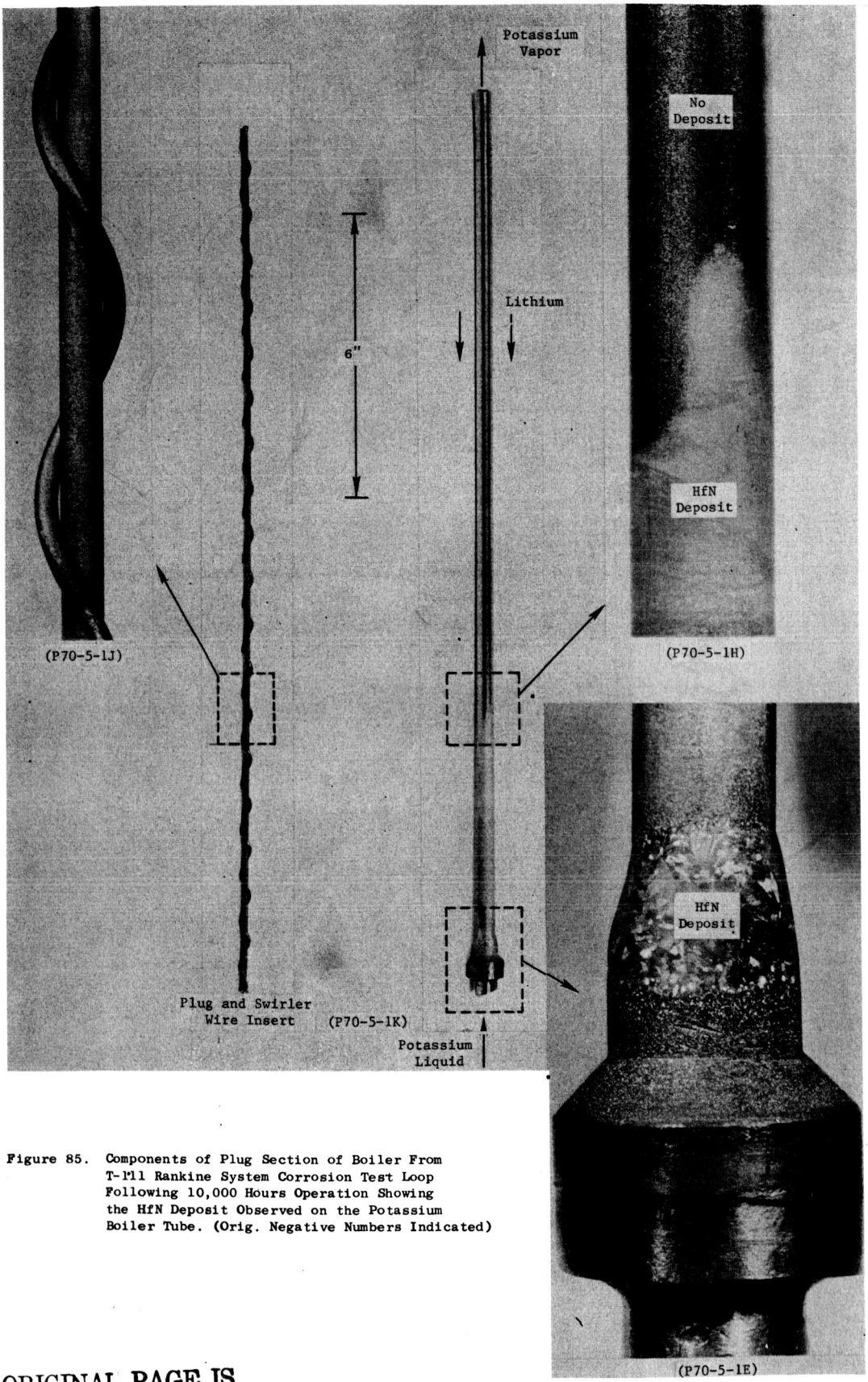


Figure 85. Components of Plug Section of Boiler From T-111 Rankine System Corrosion Test Loop Following 10,000 Hours Operation Showing the HfN Deposit Observed on the Potassium Boiler Tube. (Orig. Negative Numbers Indicated)

ORIGINAL PAGE IS
OF POOR QUALITY

of the potassium flow path). In this relatively short length, the lithium temperature dropped approximately 50°F. This temperature drop was approximately 40 percent of the entire lithium temperature drop in the boiler and corresponds to the high heat flux potassium nucleate boiling region of the plug section of the boiler. This sharp temperature drop in the lithium made the outer surface of the boiler tube, which was the lowest temperature surface in contact with the lithium in the entire lithium circuit, an ideal location for deposition of elements which are in solution in the flowing lithium. A very similar deposition of zirconium and oxygen was noted in the plug section of the boiler in the 5000-hour Cb-1Zr Rankine System Corrosion Test Loop.[22] The wavy appearance of the deposit - no deposit transition evident in Figure 85 - probably results from the potassium flow pattern induced by the swirler wire in the plug section. No deposit or discoloration was observed on the swirler wire-plug insert, as can be seen in Figure 85.

2. Boiler

The boiler was further cut, as shown in Figure 86, to allow closer examination of each coil. Initial plans were to remove the 3/8-inch (0.95-cm) tube from each coil; however, the eliptical cross section of the 1-inch (2.54-cm) lithium containment tube resulting from the forming operation prevented removal of the spacers holding the 3/8-inch (0.95-cm) tube in place. Because of this problem, only two coils were cut up for complete examination. The coil of primary interest contained the boiler repair welds and is shown in Figure 87. As can be seen in the inset, no evidence of corrosion or discoloration was observed.

3. Turbine Simulators

The nozzles and blades were removed from the turbine simulators by making a longitudinal cut in each of the housings, as described previously.[23] The appearance of all blades and nozzles was very good, and no signs of gross corrosion or erosion were observed. Potassium vapor flow patterns were observed on the blades, as seen in Figures 88 and 89. The flow patterns

(22) Hoffman, E. E. and Holowach, J., Cb-1Zr Rankine System Corrosion Test Loop, NASA CR-1509, June 1970, p. 270.

(23) Ibid, p. 231.

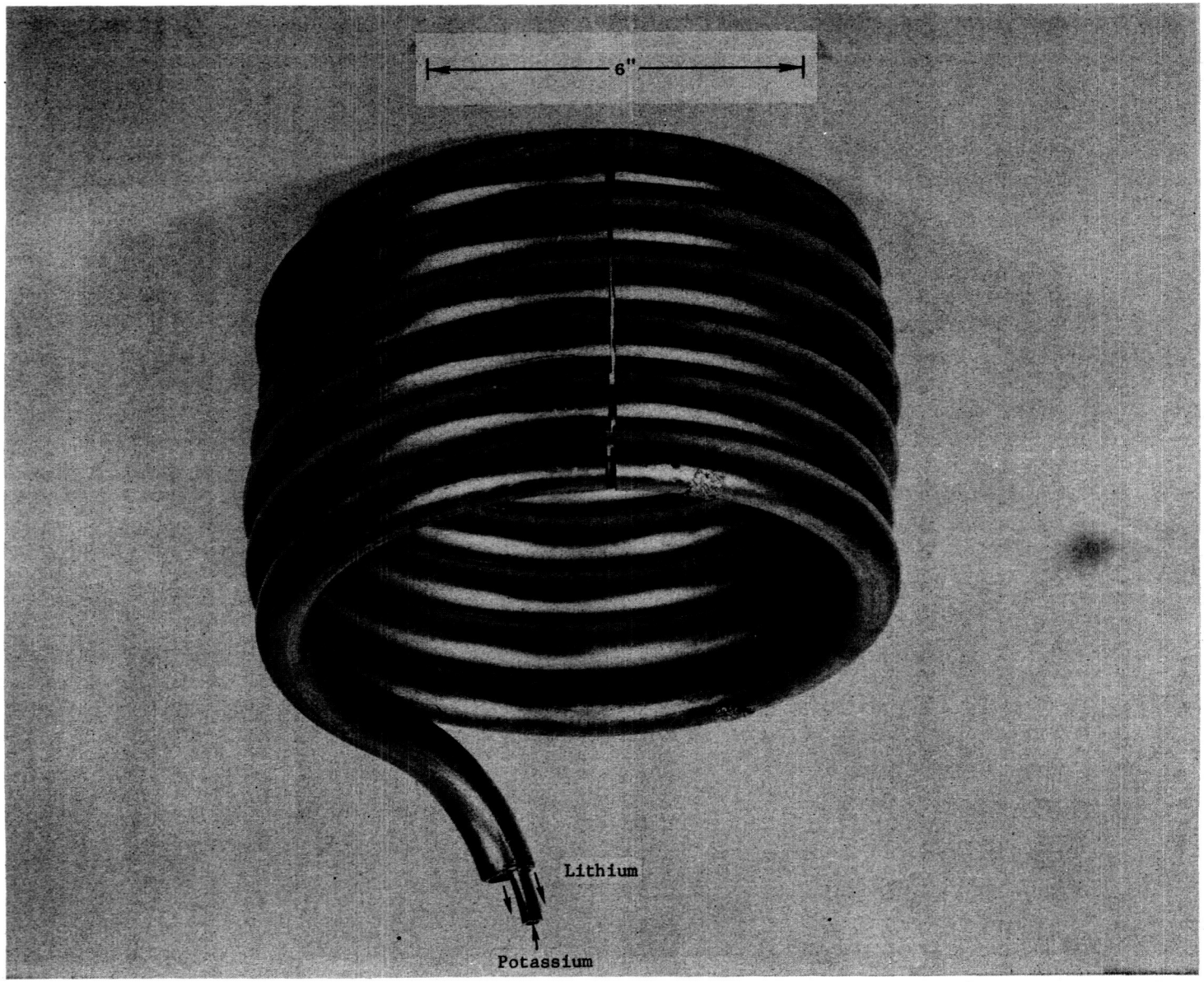


Figure 86. Boiler from T-111 Rankine System Corrosion Test Loop Following 10,000 Hours of Operation Illustrating Location of Cut Providing Removal and Inspection of Individual Coils. (Orig. P70-5-12A)

ORIGINAL PAGE IS
OF POOR QUALITY

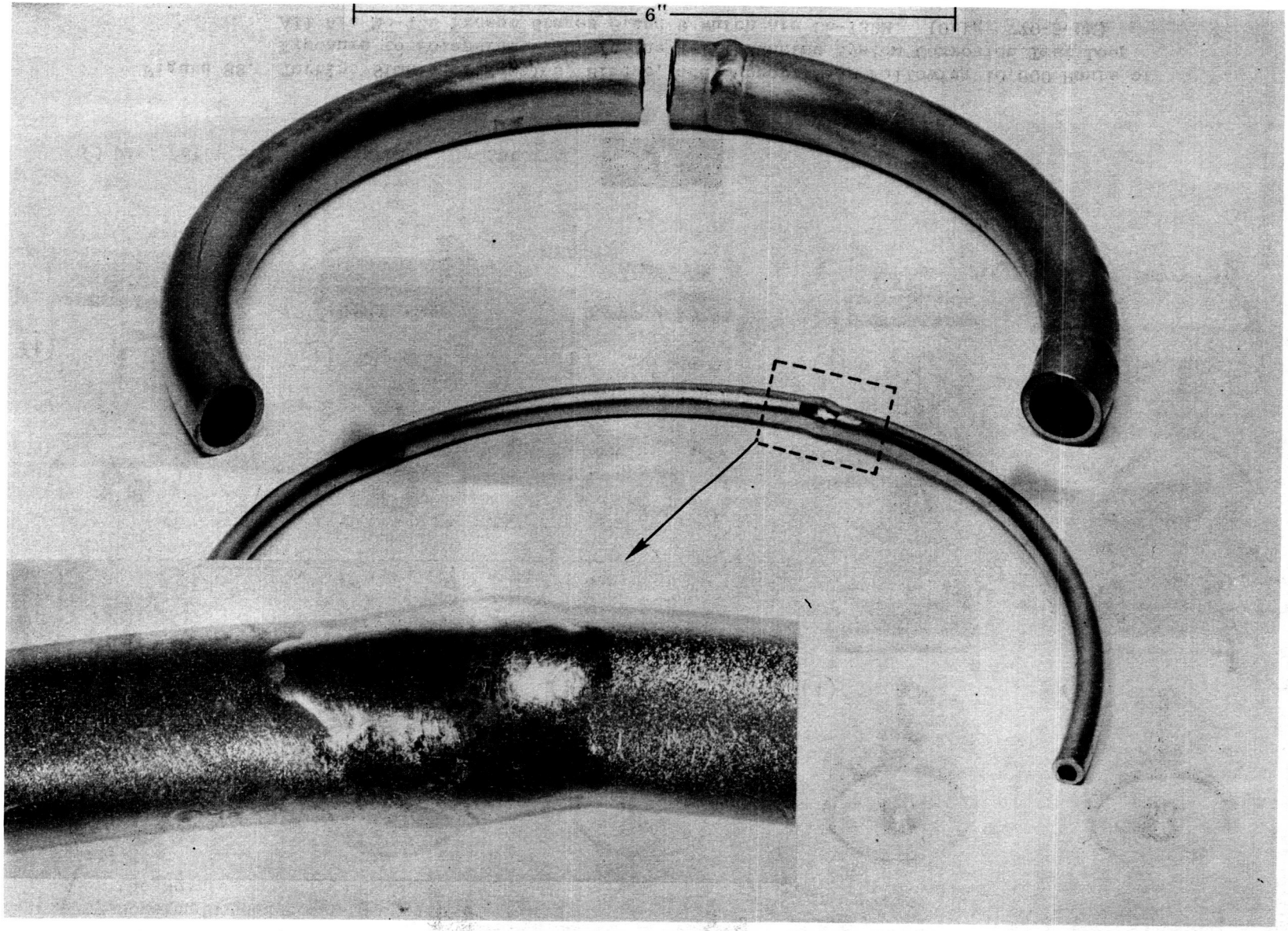


Figure 87. Repair Welds in Boiler Tubes of T-111 Rankine System Corrosion Test Loop Following 10,000 Hours of Operation. (Orig. P70-5-12E, P70-5-12B)

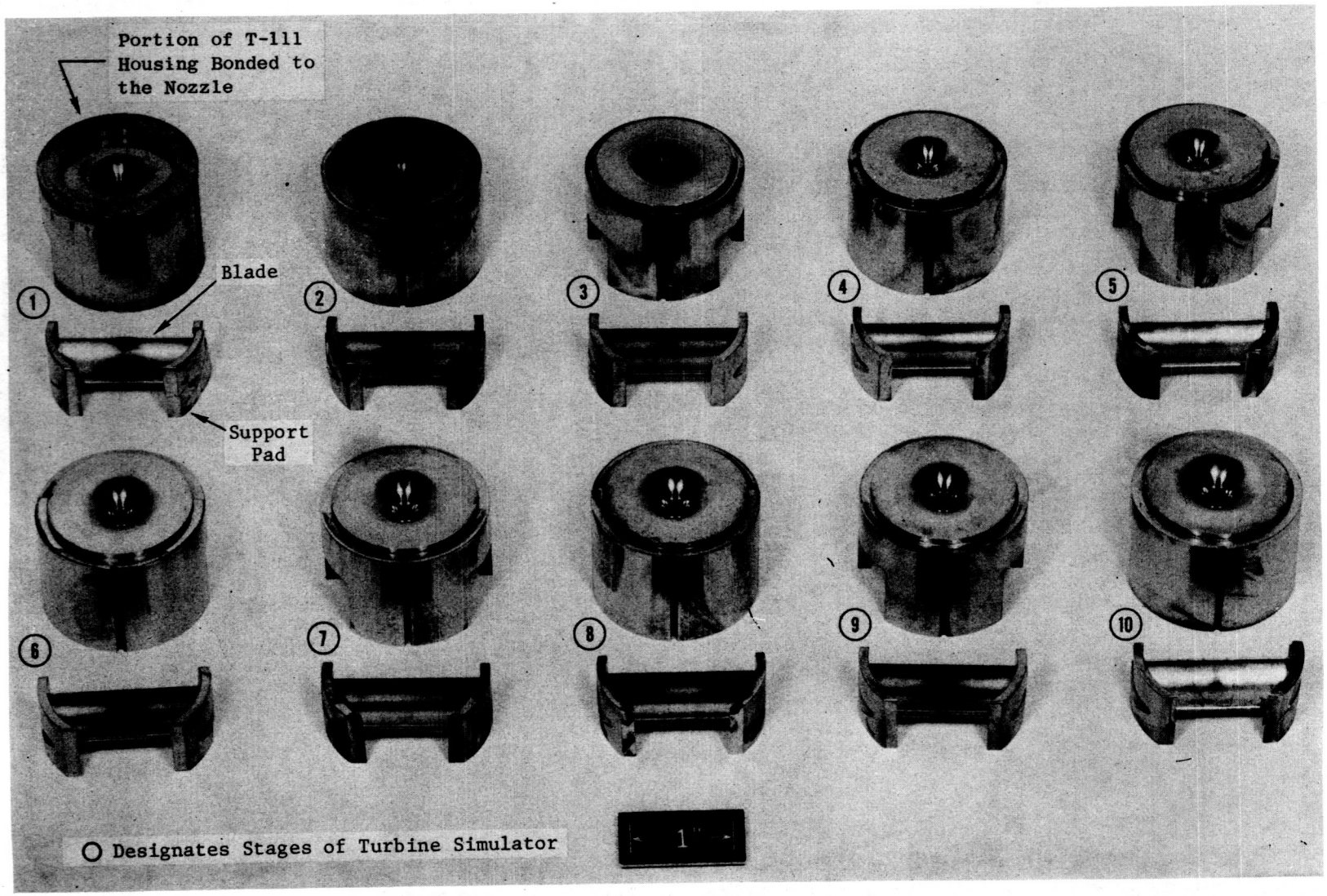


Figure 88. Turbine Simulator Nozzles, Blades, and Support Pads Following 10,000 Hours of Exposure to Potassium Vapor in the T-111 Rankine System Corrosion Test Loop. All Are Mo-TZC Except Stages 6 and 9 Which Are Cb-132M. (Orig. P70-5-6M)

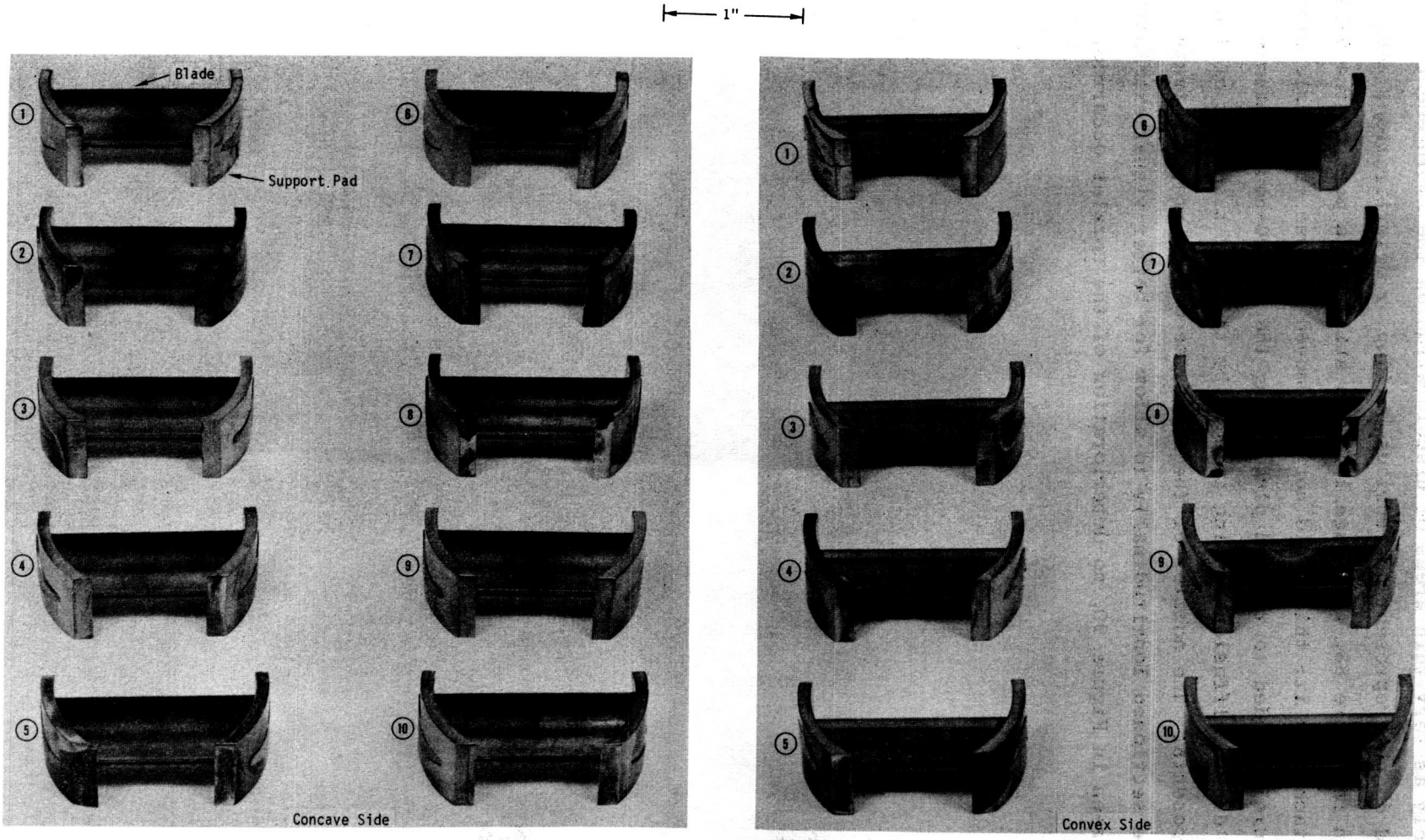


Figure 89. Concave and Convex Side of Turbine Simulator Blades Following 10,000 Hours Exposure to Potassium Vapor in the T-111 Rankine System Corrosion Test Loop. All Are Mo-TZC Except Stages 6 and 9 Which Are Cb-132M.
(Orig. P70-5-6P and P70-5-6N)

appear merely as very thin areas of discoloration on the impingement surface and do not represent any serious buildup or deterioration. As can be seen in Figure 88, the stage 1 nozzle still has a part of the T-111 housing attached to it; this could not be removed because the nozzle had become securely bonded to the end plug during the 10,000-hour exposure, apparently due to diffusion bonding induced by the very tight fit of the mating components. The nozzles of the first, second, sixth, and tenth stages were sectioned longitudinally to allow for better visual examination. As can be seen in Figure 90, no deterioration of the nozzles occurred.

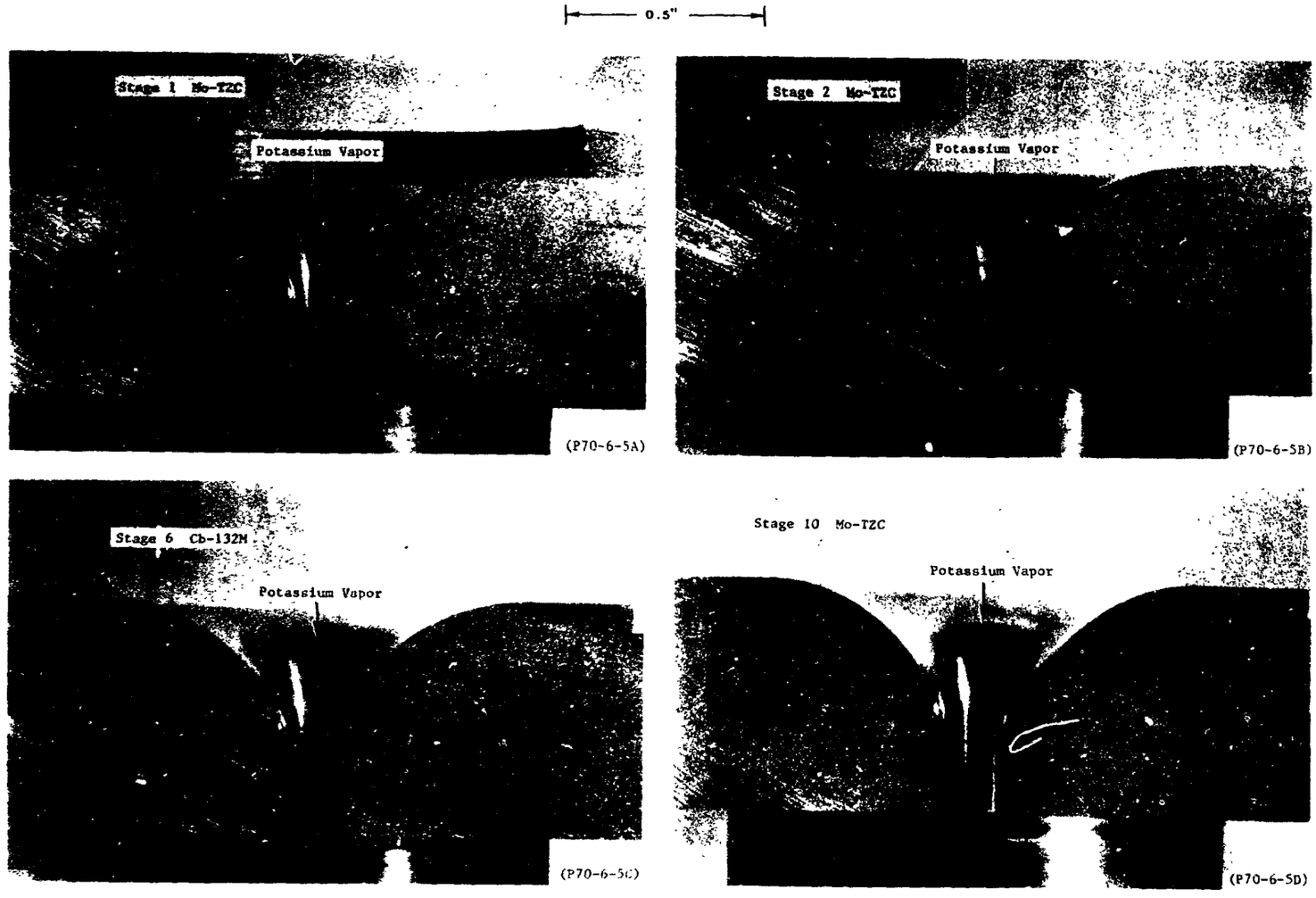


Figure 90. Longitudinal Cross Section of Turbine Simulator Nozzles Following 10,000 Hours of Exposure to Potassium Vapor in the T-111 Rankine System Corrosion Test Loop.

XII. CHEMICAL AND METALLURGICAL EVALUATION OF LOOP COMPONENTS

Extensive posttest evaluation was performed on the T-111 alloy loop components and the Mo-TZC and Cb-132M alloy nozzle and blade specimens from the turbine simulator. The evaluation included chemical analysis of loop components, weight change, and dimensional analysis of nozzles and blades, metallographic and microprobe examination of a large number of specimens, and tensile testing of T-111 alloy tube specimens. The greatest emphasis was placed on chemical analysis and metallographic examination in evaluating the compatibility of the various loop components with the lithium and potassium environments.

A. CHEMICAL ANALYSIS OF LOOP COMPONENTS

Chemical analyses for carbon, oxygen, hydrogen, and nitrogen were obtained on specimens from the locations shown in Figure 91. The results of all analyses are presented in Tables XXIV, XXV, and XXVI. The results of oxygen analyses are summarized in Figure 92.

The oxygen concentrations in the 1-inch (2.54-cm)-diameter T-111 tubing, the ID of which was exposed to lithium, are all $\leq$ 10 ppm. This clearly indicates dissolution of oxygen from the T-111 by the lithium. The oxygen concentrations in the 3/8-inch (0.95-cm)-diameter T-111 tubing exposed to lithium on the OD and potassium on the ID are less consistent, with some large highly localized oxygen concentrations indicated. The analytical results of the inner and outer wall segment specimens of the potassium containment tube coupled with the oxygen dissolution observed in the 1-inch (2.54-cm)-diameter tube indicates that the most likely oxygen source is the high-temperature regions of the potassium circuit. The oxygen concentration of the potassium boiler tube as a function of distance from the potassium inlet to the boiler is summarized in Table XXVII. Two high-oxygen peaks were observed; the first was found 5 to 6 inches (12.7 - 15.2 cm) from the potassium inlet (lithium exit), and the second was found 16 to 18 inches (40.6 - 45.7 cm) from the potassium inlet. It is currently believed that the first oxygen peak is associated with the region where the inner wall of the potassium containment tube (3/8 inch, 0.95 cm) becomes essentially dry. From this region to the end of the plug section most of

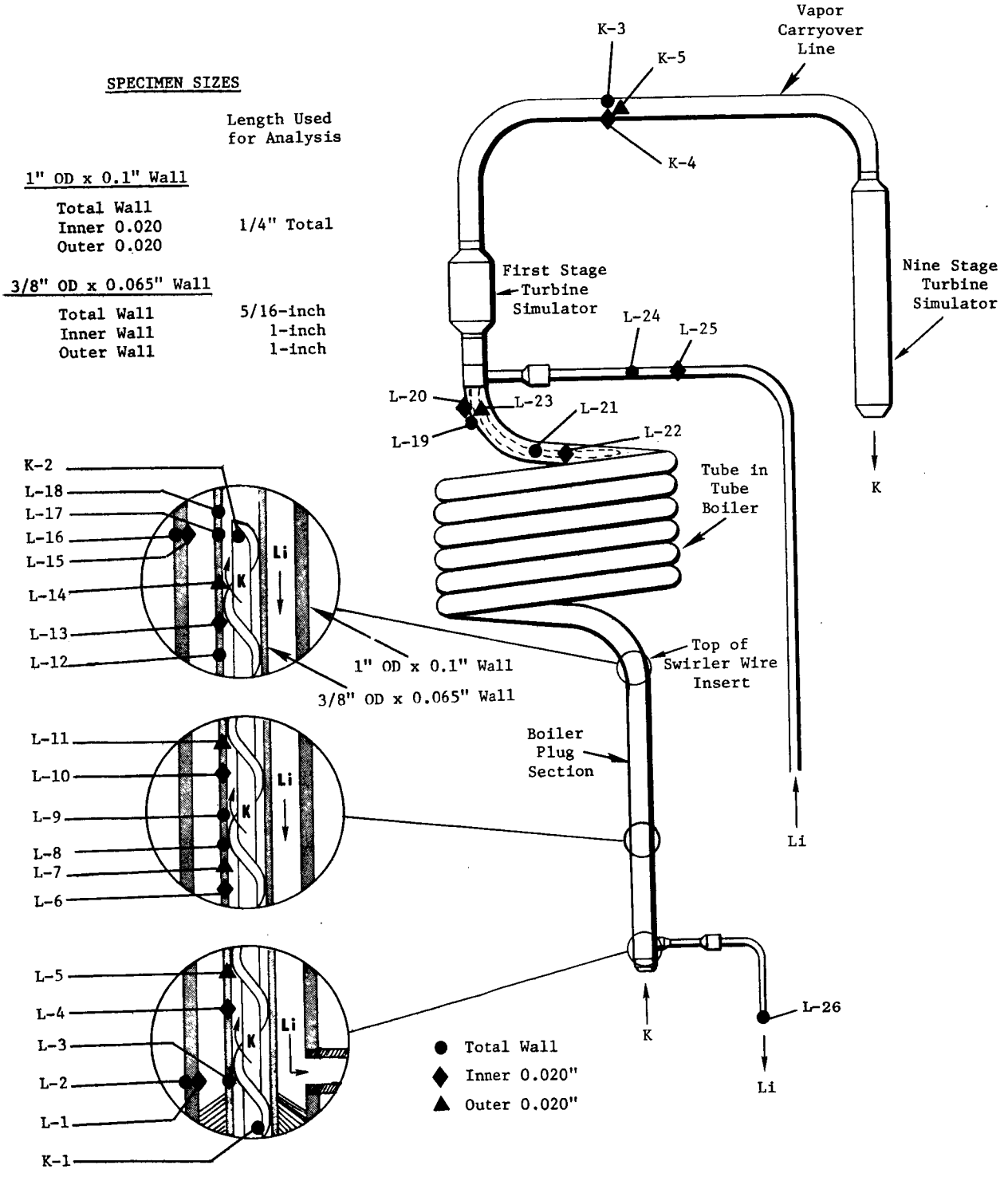


Figure 91. Location of Specimens Used for Chemical Analyses of Loop Components From the T-111 Corrosion Test Loop Following 10,000 Hours of Continuous Operation.

TABLE XXIV

RESULTS OF CHEMICAL ANALYSIS OF SPECIMENS OF T-111 ALLOY LITHIUM CONTAINMENT TUBE[a] FROM THE BOILER

Specimen Identification and Description		Temperature °F	Temperature °C	Chemical Analysis, ppm O	N	H	C
(L-1)[b]	Bottom of plug section at lithium exit, inner 0.020 inch of wall	2128	1165	1	18	< 1	19
				2	19	1	17
			Avg.	1	18	< 1	18
(L-2)	Bottom of plug section at lithium exit, total wall	2128	1165	11	14	< 1	16
				10	13		16
			Avg.	10	13	< 1	16
(L-15)	Top of plug section 18 inches from lithium exit, inner 0.020 inch of wall	2200	1204	8	16	< 1	25
				12	21		24
			Avg.	10	18	< 1	24
(L-16)	Top of plug section 18 inches from lithium exit, total wall	2200	1204	2	13	< 1	34
				2	14		34
			Avg.	2	13	< 1	34
(L-19)	Top of boiler 1 1/2 inches from lithium inlet, total wall	2244	1229	5	13	< 1	37
				6	12		49
			Avg.	5	12	< 1	43
(L-20)	Top of boiler 1 1/2 inches from lithium inlet, inner 0.020 inch of wall	2244	1229	1	14	< 1	37
				4	15		46
			Avg.	2	14	< 1	41
	Before test			17	2	1	44

a) 1-inch OD x 0.10-inch wall thickness.

b) Specimen location indicated in Figure 10.

TABLE XXV

RESULTS OF CHEMICAL ANALYSIS OF SPECIMENS OF T-111 ALLOY POTASSIUM CONTAINMENT TUBE[a] FROM THE BOILER

Specimen Identification and Description		Estimated Temperature °F		Chemical Analysis, ppm O	N	H	C
(L-3)	Bottom of plug section at lithium exit, total wall[b]	1900		2	73	1	32
				7	75	1	34
			Avg.	4	74	1	34
(L-4)	Bottom of plug section, 1/2 inch from lithium exit, inner 0.020 inch of wall	1925		14	15	< 1	54
				16	20		61
			Avg.	15	17	< 1	57
(L-5)	Bottom of plug section, 1 1/2 inch from lithium exit, outer 0.020 inch of wall[b]	1950		30	217	2	91
				37	90	1	94
			Avg.	33	153	1	92
(L-6)	2 1/2 inches from lithium exit, inner 0.020 inch of wall	2050		14	26	1	66
				18	27	1	45
			Avg.	16	26	1	55
(L-7)	3 1/2 inches from lithium exit, outer 0.020 inch of wall[b]	2050		25	67	1	62
				27	38	1	81
			Avg.	26	52	1	71
(L-8)	4 inches from lithium exit, total wall[b]	2050		6	41	2	31
				10	65	1	43
			Avg.	8	53	1	37
(L-9)	5 inches from lithium exit, total wall[b]	2040		378	26	5	36
				236	23	3	41
			Avg.	307	24	4	38
(L-10)	5 1/2 inches from lithium exit, inner 0.020 inch of wall	2040		1051	9	10	40
				845	12	5	49
			Avg.	948	10	7	44
(L-11)	6 1/2 inches from lithium exit, outer 0.020 inch of wall[b]	2040		4	16	< 1	46
				8	21	1	42
			Avg.	6	18	< 1	44
(L-12)	Top of plug section 14 inches from lithium exit, total wall	2040		56	17	1	
				32	17	1	
			Avg.	44	17	1	
(L-13)	Top of plug section 14 3/4 inches from lithium exit, inner 0.020 inch of wall	2040		7	14	1	55
				3	20	< 1	52
			Avg.	5	17	< 1	53
(L-14)	Top of plug section 15 3/4 inches from lithium exit, outer 0.020 inch of wall	2040		4	11	< 1	47
				2	11	2	36
			Avg.	3	11	1	41
(L-17)	Top of plug section 16 3/4 inches from lithium exit, total wall	2040		545	30	4	47
				648	28	10	39
			Avg.	596	29	7	43
(L-18)	Top of plug section 17 1/4 inches from lithium exit, total wall	2040		789	17	5	
				1414	16	5	
			Avg.	1101	16	5	
(L-21)*	Top of boiler 6 1/2 inches from lithium inlet, total wall	2140		3	9	< 1	24
				2	8		25
			Avg.	2	8	< 1	24
(L-22)*	Top of boiler 6 1/2 inches from lithium inlet, inner 0.020 inch of wall	2140		4	3	2	63
				1	3	1	63
			Avg.	2	3	1	63
(L-23)*	Top of boiler 1 1/2 inches from lithium inlet, outer 0.020 inch of wall	2140		2	10	2	43
				4	9	1	33
			Avg.	3	9	1	38
	Before test, original boiler tube			16	5	1	42
	*Before test, replacement tube used for boiler repair			8	2	< 1	29

a) 3/8-inch OD x 0.065-inch wall thickness.

b) Includes HfN surface layer on OD.

ORIGINAL PAGE IS OF POOR QUALITY

TABLE XXVI

RESULTS OF CHEMICAL ANALYSIS OF MISCELLANEOUS SPECIMENS OF T-111 ALLOY EXPOSED TO POTASSIUM OR LITHIUM DURING THE 10,000-HOUR TEST

	Specimen Identification and Description	Temperature °F	Temperature °C		Chemical Analysis, ppm O	N	H	C
	Potassium Circuit							
(K-1)	Centerbody and swirl wire,[a] bottom of plug section	1850	1010		53	8	2	51
					36	7	1	48
				Avg.	44	7	1	49
(K-2)	Centerbody and swirl wire,[a] top of plug section	2040	1116		196	7	3	31
					271	5	2	45
				Avg.	233	6	2	38
	Before test				8	3	8	24
(K-3)	Vapor carryover tube,[b] uninsulated, 1/2 inch from end of insulation, total wall	1900	1038		38	7	1	71
					24	5	< 1	61
				Avg.	31	6	< 1	66
(K-4)	Vapor carryover tube, uninsulated, 1/2 inch from end of insulation, inner 0.020 inch of wall	1900	1038		17	4	< 1	67
					16	4		67
				Avg.	16	4	< 1	67
(K-5)	Vapor carryover tube, uninsulated, 1/2 inch from end of insulation, outer 0.020 inch of wall	1900	1038		50	4	1	58
					53	6	1	67
				Avg.	51	5	1	62
	Before test				17	2	1	44
	Lithium Circuit							
(L-24)	Lithium heater exit tube,[c] 9 inches from boiler inlet, total wall	2250	1232		4	4	< 1	23
					6	1		30
				Avg.	5	2	< 1	26
(L-25)	Lithium heater exit tube,[c] 9 inches from boiler inlet, inner 0.020 inch of wall	2250	1232		11	3	< 1	39
					17	10		50
				Avg.	14	6	< 1	44
(L-26)	Lithium return line to EM Pump[c] (10 inches from boiler exit) total wall	2090	1143		15	26	< 1	34
					9	28	< 1	33
				Avg.	12	27	< 1	33
	Before test				16	5	1	42

a) 0.060-inch swirl wire wrapped on and tack-welded to 0.125-inch-OD centerbody.

b) 1-inch OD x 0.10-inch wall thickness.

c) 3/8-inch OD x 0.065-inch wall thickness.

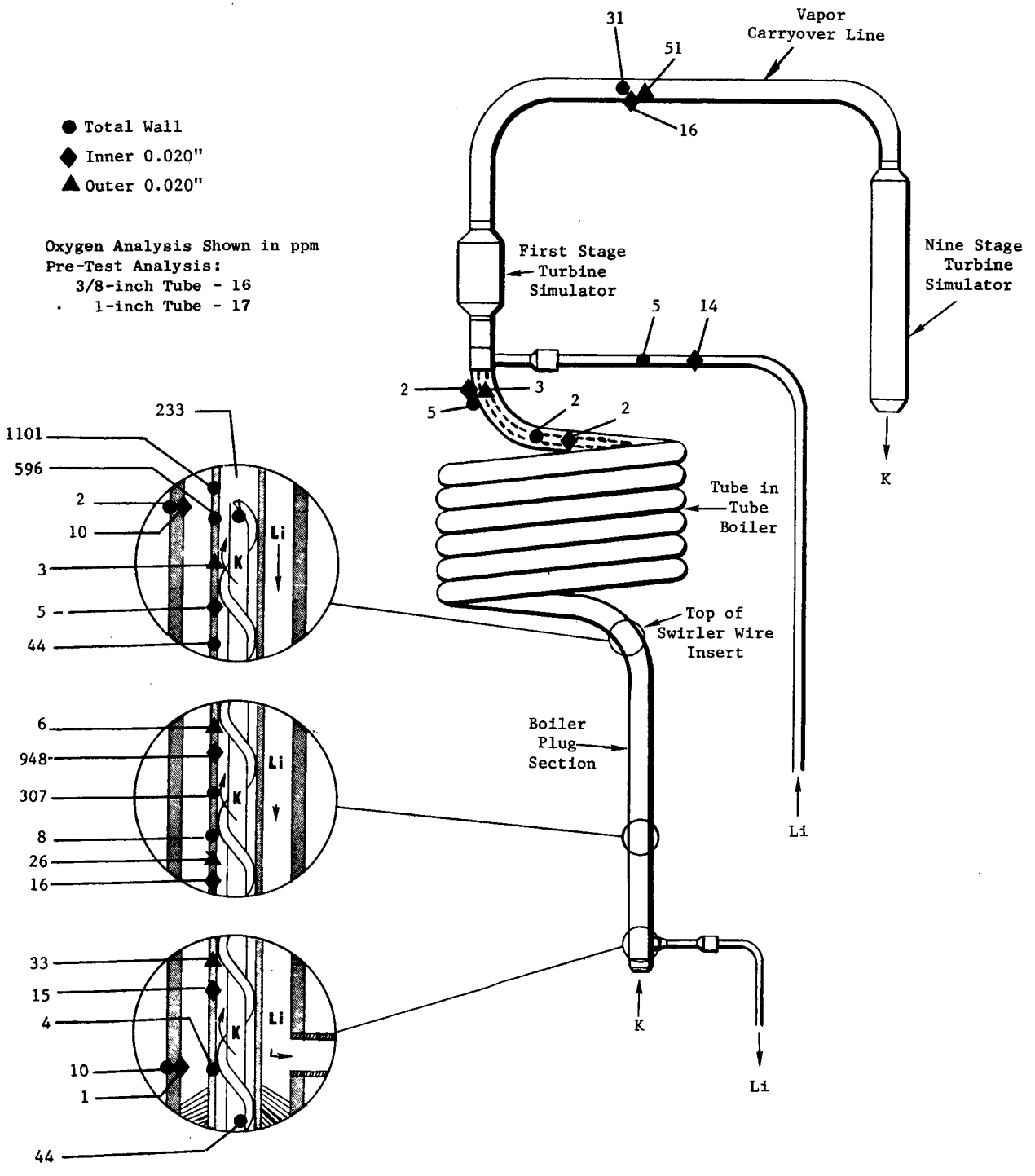


Figure 92. Results of Oxygen Analysis of Loop Components.

TABLE XXVII

OXYGEN CONCENTRATION OF POTASSIUM BOILER TUBE[a] AS A FUNCTION OF DISTANCE FROM POTASSIUM INLET

Distance from Potassium Inlet		Oxygen Concentration, ppm[b]		
			Inner	Outer
Inches	cm	Whole Wall	0.020 Inch (0.05 cm) of Wall (K Side)	0.020 Inch (0.05 cm) of Wall (Li Side)
0	0	4		
1	2.5		15	
2	5.1			33
3	7.6		16	
4	10.3	8		26
5	12.7	307		
6	15.2		948	
7	17.8			6
8	20.3			
9	22.9			
10	25.4			
11	27.9			
12	30.4			
13	33.0			
14	35.5	44		
15	38.1		5	
16	40.7			3
17	43.1	596		
18	45.7	1101		

a) 0.375-inch (0.95-cm) OD x 0.065-inch (0.16-cm) wall; oxygen concentration before test, 16 ppm.

b) Average of duplicate analyses.

the remaining potassium liquid is assumed to be carried along on the swirler wire and centerbody. It is hypothesized that as liquid potassium is converted to vapor in this area, the oxygen concentration of the remaining liquid becomes increasingly higher until it finally is concentrated at the wall and contaminates the T-111 either by absorption and interstitial diffusion and/or reaction (corrosion). Metallographic examination of specimens from this area, which will be discussed later in this section, shows some localized corrosion in this area.

As indicated, the second oxygen peak occurs near the end of the swirler wire-plug insert. A recently completed experimental study at GE-NSP on air-water flow has shown the behavior of liquid in tubes containing swirl generators similar to that employed in the T-111 Corrosion Loop. The results of the air-water flow study as applied to the T-111 Corrosion Loop would indicated that the ID of the potassium containment tube will become void of liquid potassium downstream from the end of the insert; however, liquid potassium will still flow on the plug insert since the pressure is relatively low in the center. At the end of the insert, this liquid potassium is thrown to the ID of the potassium containment tube where it immediately is converted to vapor. The transfer of liquid from the plug insert to the containment tube wall is illustrated for the air-water flow tests in Figure 93.[24] Since the air-water tests are performed at ambient temperatures, the conversion to vapor on contact with the tube wall does not occur as it does for the case when the tube walls are hot, as in a boiler. Oxygen contamination of the T-111 wall in this area can therefore occur by the same process as described in the preceding paragraph. The oxygen concentrations of the centerbody and swirl wire at the top end of the plug were also high, supporting this postulate.

A comparison of the oxygen concentration in the inner and outer wall segments (Table XXVI) of the uninsulated vapor carryover line indicates very minor oxygen pickup (34 ppm) in the outer 0.020 inch (0.051 cm) of the tube wall from the chamber environment during the 10,000-hour test.

---

(24) Bond, J. A., "The Design of Components for an Advanced Rankine Cycle Test Facility," Fifth Intersociety Energy Conversion Engineering Conference in Las Vegas, Nevada, September 21-25, 1970.

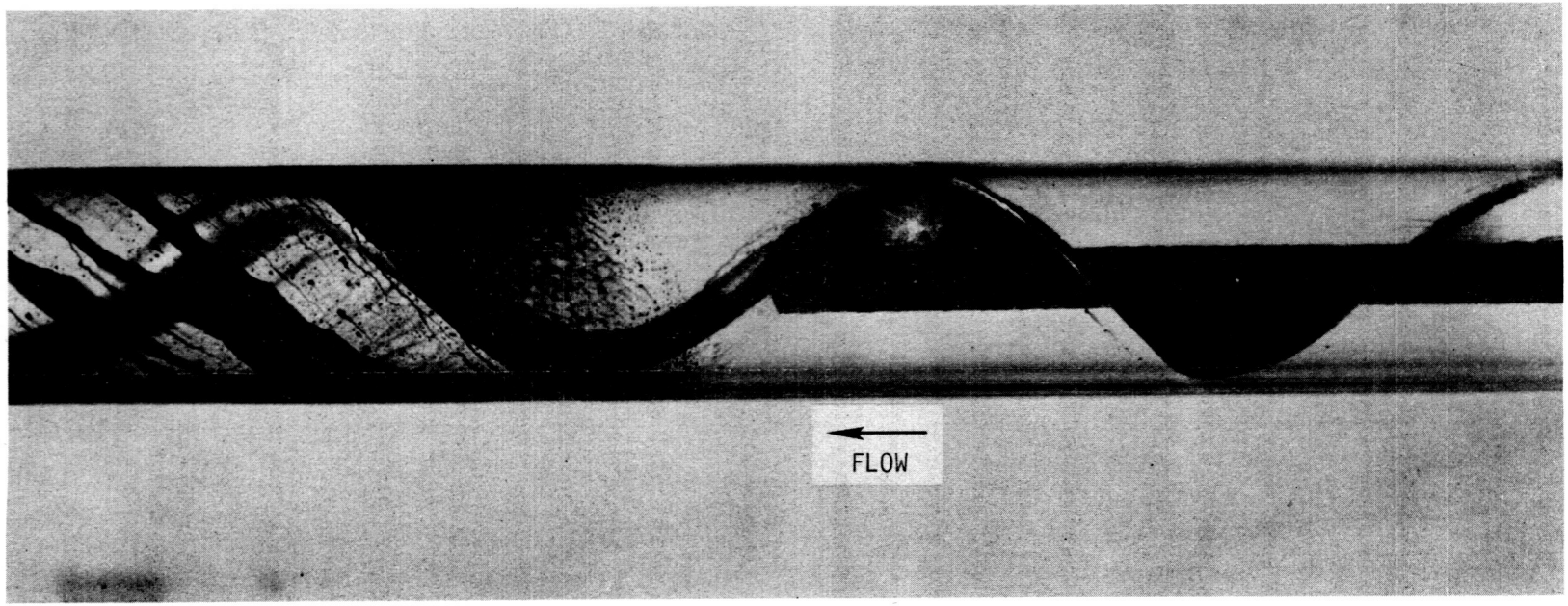


Figure 93. Flow Pattern at End of Swirler Wire Plug Insert in Water Test.

As shown by item L-5 in Table XXV, the nitrogen and carbon concentrations in the outer 0.020-inch (0.051-cm) wall specimens taken from the 3/8-inch (0.95-cm) potassium containment tube in the area of the HfN deposit are higher than for any other evaluated portion of the loop. Since essentially all of the carbon and nitrogen concentrations shown in Table XXIV, XXV, and XXVI are at least equal to the pretest value, it must be assumed that the source of these elements is the unevaluated portions of the lithium circuit. It is postulated that the principal source of the carbon and nitrogen was the lithium heater section since the tendency for these elements to transfer from the hot region of the loop to the cooler regions has been noted in a number of liquid metal systems.

In addition, the performing chemical analyses on the loop components, the vapor impingement areas of Stages 1, 2, 4, and 6 blades were also analyzed for carbon, oxygen, hydrogen, and nitrogen. As can be seen in Table XXVIII, no significant changes in the concentrations of these elements results from the 10,000 hours of exposure to high-velocity potassium.

Also, analyses were performed on three layers of the 0.002-inch (50-micron)-thick Cb-1Zr dimpled foil. Table XXIX summarizes these results and shows that the oxygen increased by a maximum of 293 ppm. It should be noted that this is equivalent to an increase of 6 ppm in the 0.1-inch (0.25-cm) pipe wall assuming uniform distribution across the pipe wall if the foil contamination is assumed to occur from one side. This calculated increase is in reasonably good agreement with the 14-ppm measured increase shown in Table XXVI based on the comparison of the "before test" oxygen concentration and the value obtained for specimen K-3.

As is also shown in Table XXIX, the carbon concentration of the foil increased significantly. This increase is currently not understood; however, a significant increase in the carbon concentration was also observed for the thermal insulation foil from the 5000-hour Cb-1Zr test previously reported.[25]

---

(25) Hoffman, E. E. and Holowach, J., Cb-1Zr Rankine System Corrosion Test Loop, NASA CR-1509, June 1970, p. 250.

TABLE XXVIII

RESULTS OF CHEMICAL ANALYSIS OF TURBINE SIMULATOR BLADE SPECIMENS* FOLLOWING THE 10,000-HOUR TEST

Specimen Description	Nozzle Inlet Temperature °F	Nozzle Inlet Temperature °C		Chemical Analysis, ppm O	N	H	C
Stage No. 1 Blade	2142	1173		12	3	< 1	1700
Mo-TZC Alloy				6	6		1800
			Avg.	9	4	< 1	1750
Stage No. 2 Blade	1890	1032		3	3	< 1	1700
Mo-TZC Alloy				8	6		1800
			Avg.	5	4	< 1	1750
Stage No. 10 Blade	1471	800		14	4	< 1	1600
Mo-TZC Alloy				9	5		1500
			Avg.	11	4	< 1	1550
Before Test				1	1	< 1	1600
				5	1		1600
			Avg.	3	1	< 1	1600
Stage No. 6 Blade	1664	906		19	9	1	1600
Cb-132M Alloy				17	12	1	1600
			Avg.	18	11	1	1600
Before Test				7	7	< 1	1900
				15	8		1500
			Avg.	11	7	< 1	1700

* Chemical analysis sample taken from the vapor impingement region of each blade.

TABLE XXIX

RESULTS OF CHEMICAL ANALYSIS OF Cb-1Zr FOIL* TAKEN FROM THE VAPOR CARRYOVER TUBE FOLLOWING THE 10,000-HOUR TEST

Specimen	Estimated Temperature °F	Estimated Temperature °C		Chemical Analysis, ppm O	N	H	C
Outer Layer	1000	538		498	37	7	284
				501	32	3	248
			Avg.	499	34	5	266
Middle Layer	1350	732		332	32	4	150
				348	31	3	168
			Avg.	340	31	3	159
Inner Layer	1800	982		381	35	2	137
				305	14	7	133
			Avg.	343	24	4	135
Before Test				199	30	2	76
				213	32	2	79
			Avg.	206	31	2	77

*Chemical analysis sample taken from the start of the heat rejection zone. Foil thickness 0.002 inch.

B. WEIGHT CHANGE AND DIMENSIONAL ANALYSIS OF NOZZLES AND BLADES

Pre- and posttest dimensional and weight measurements performed on the turbine simulator nozzles and blades, summarized in Table XXX and Table XXXI, indicate no significant change due to the 10,000 hours' exposure to the flowing potassium vapor.

C. RESULTS OF METALLOGRAPHIC AND MICROPROBE EVALUATIONS

Metallographic examination was performed on specimens cut from the locations shown in Figure 94. Specimens from both the lithium and potassium circuits were examined and the microstructures compared with untested (pretest) specimens from the same lot of material. All pretest specimens were heat treated for 1 hour at 2400°F (1315°C) to simulate the loop post-weld anneal. Differences in microstructure observed, therefore, are a result of the test exposure. Typical microstructure of the pretest material is shown in Figure 95. All specimens were nickel plated prior to mounting to facilitate edge retention during polishing. T-111 specimens were etched with 30 grams NH_4F-50 ml HNO_3-20 ml H_2O. In addition to the T-111 specimens from the loop, samples were also examined from the nozzles and blades of the first-, second-, sixth-, and tenth-stage turbine simulators all of which were made from Mo-TZC except the sixth stage which was made of Cb-132M alloy.

1. Plug Section of Boiler

As can be seen in Figure 94, over one-third of the specimens examined were from the plug section of the boiler since, based on previous experience,[26] this is one of the more critical areas of a loop of this type with respect to changes in microstructure. Particular attention was given to the 3/8-inch (0.95-cm)-diameter potassium containment tube because of the high heat flux across the wall of this tube and the fact that visual examination of the lithium-exposed side showed the lower six inches to be coated with HfN. The appearance and identification of this deposit were covered in Section XI of this report. A longitudinal section was cut from the bottom of the 3/8-inch (0.95-cm) tube where it was welded to the fitting; also transverse sections

---

(26) Hoffman, E. E. and Holowach, J., Cb-1Zr Rankine System Corrosion Test Loop, NASA CR-1509, June 1970.

TABLE XXX

WEIGHTS OF TURBINE SIMULATOR NOZZLES AND BLADES BEFORE AND AFTER 10,000 HOURS EXPOSURE IN THE T-111 RANKINE SYSTEM CORROSION TEST LOOP

Stage No.	Material	Temperature F	Temperature C	Weight,(a) grams Blade Before Test	Blade After Test	Blade Change	Nozzle Before Test	Nozzle After Test	Nozzle Change
1	Mo-TZC	2142	1173	25.1496	25.1490	-0.0006	265.4495	(b)	-
2	Mo-TZC	1890	1032	25.3640	25.3640	0.0000	263.9073	263.9007	-0.0066
3	Mo-TZC	1834	1001	25.1849	25.1832	-0.0017	257.1087	257.0958	-0.0129
4	Mo-TZC	1774	968	25.3275	25.3262	-0.0013	257.6389	257.6286	-0.0103
5	Mo-TZC	1716	936	25.1817	25.1803	-0.0014	257.6719	257.6620	-0.0099
6	Cb-132M	1664	906	26.5918	26.5918	0.0000	272.0057	272.0074	+0.0017
7	Mo-TZC	1611	878	25.3579	25.3565	-0.0014	256.7299	256.7234	-0.0065
8	Mo-TZC	1562	850	25.2678	25.2656	-0.0022	253.1244	253.1165	-0.0079
9	Cb-132M	1514	829	26.5369	26.5364	-0.0005	268.8649	268.8658	+0.0009
10	Mo-TZC	1471	800	25.2144	25.2127	-0.0017	251.5495	251.5372	-0.0123

(a) Average of duplicate measurements

(b) Not measured; bonded to T-111 alloy fitting

TABLE XXXI

TURBINE SIMULATOR NOZZLE THROAT DIAMETERS BEFORE AND AFTER 10,000 HOURS EXPOSURE IN THE T-111 RANKINE SYSTEM CORROSION TEST LOOP

Stage No.	Material	Temp. °F	Temp. °C	Diameter,[a] inches Before Test	After Test	Change
1	Mo-TZC	2142	1173	0.089175	0.089327	+ 0.000152
2	Mo-TZC	1890	1032	0.087925	0.087810	- 0.000115
3	Mo-TZC	1834	1001	0.096380	0.096215	- 0.000165
4	Mo-TZC	1774	968	0.108275	0.108307	+ 0.000032
5	Mo-TZC	1716	936	0.118060	0.118050	- 0.000010
6	Cb-132M	1664	906	0.129225	0.129185	- 0.000040
7	Mo-TZC	1611	878	0.145737	0.145800	+ 0.000063
8	Mo-TZC	1562	850	0.159837	0.159790	- 0.000047
9	Cb-132M	1514	829	0.178425	0.178562	+ 0.000137
10	Mo-TZC	1471	800	0.198644	0.198595	- 0.000049

[a] Measurements performed by Sheffield Corporation, Dayton, Ohio. Reported accuracy is 0.00005 inch and is the average in duplicate measurements 90° apart.

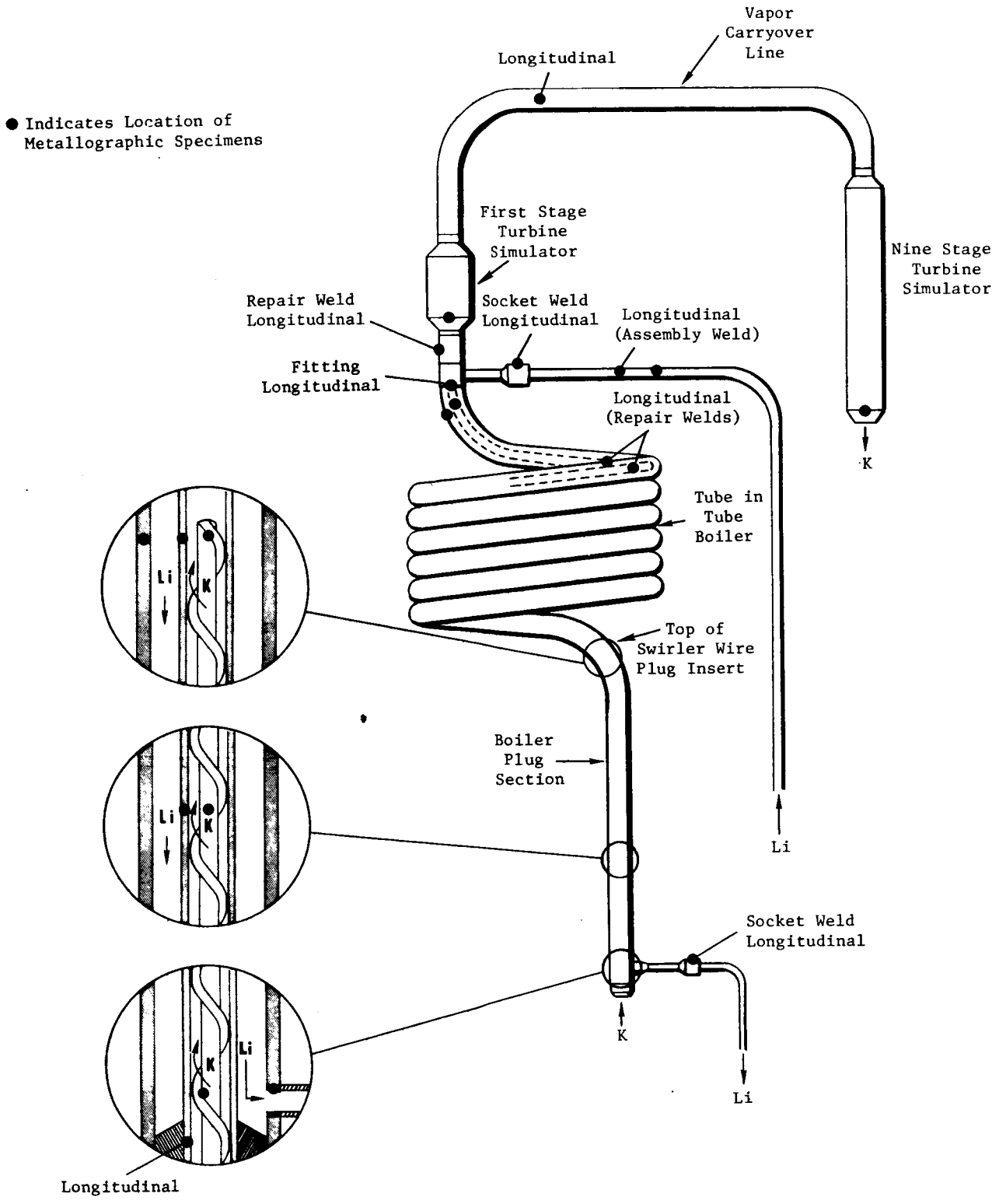
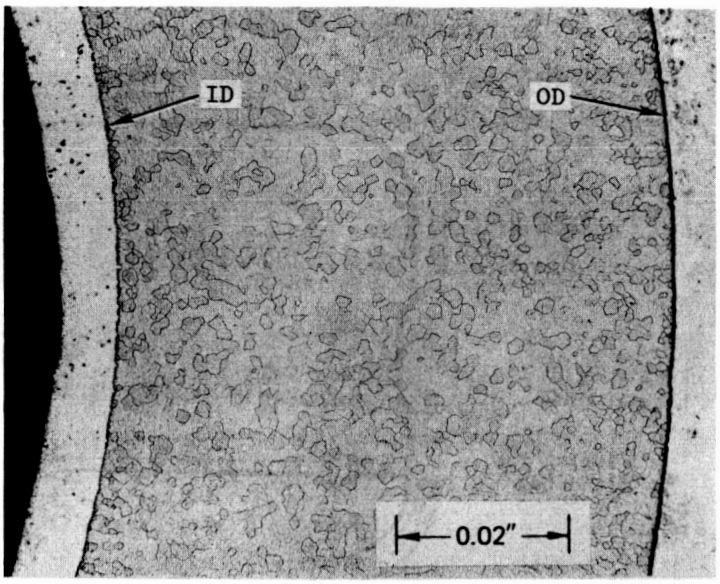
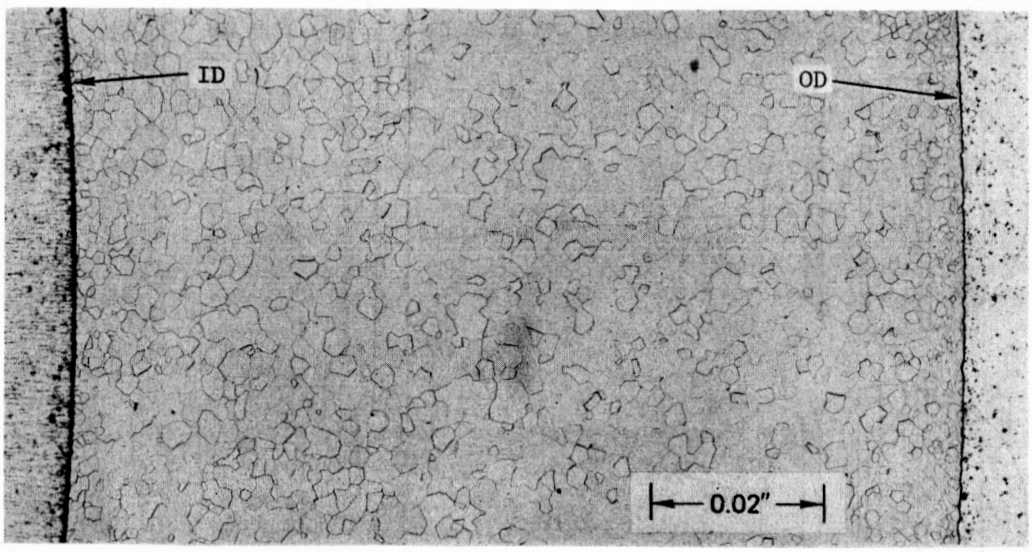


Figure 94. Location of Specimens for Metallographic Examination From the T-111 Corrosion Test Loop. (All Are Transverse Section Unless Noted Otherwise.)



H67031B Etched

a. 3/8-inch OD tubing

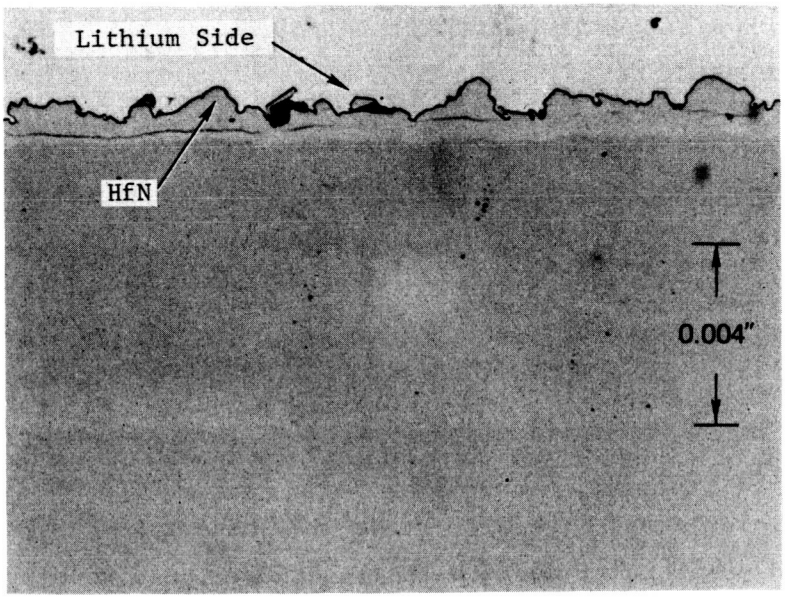


H67011A,B Etched

b. 1-inch OD tubing

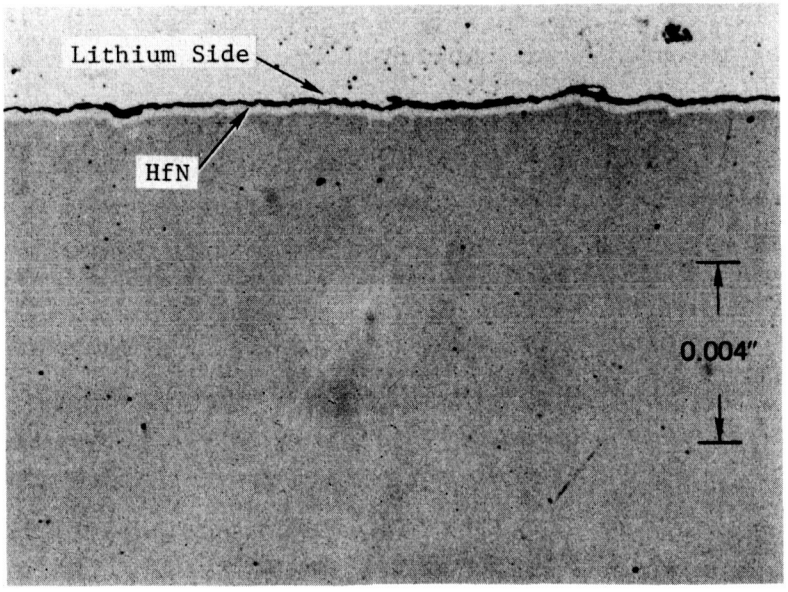
Figure 95. Pretest Microstructure of the T-111 Tubing.

were taken about six inches above the fitting and from two areas near the top of the swirler wire insert. The HfN coating was best examined in the as-polished condition, as shown in Figure 96, since the etchant used for T-111 attacked the HfN rather rapidly. The major difference between the microstructure shown in Figure 96a, which is taken from the weld area, and that shown in Figure 96b, which represents the tube OD surface about 1/2 inch above the weld, is the thickness of the HfN coating. The weld region operated at the lowest temperature in the plug region, and in this area the coating on the weld is much thicker than the coating on the tube. Examination of the ID (potassium) surface of this specimen indicated anomalous microstructural features at the fitting weld metal and tube weld metal interfaces. The microstructure shown in Figure 97 is from the fitting weld metal interface and is typical of these anomalous microstructural features. In the as-polished condition they appear as a light and dark island within the normally gray-colored T-111 matrix; however, after etching, the affected area is seen to be much larger than indicated in the as-polished condition and generally contains a relatively heavily etched (black) core. Note also the evidence of grain-boundary attack on the periphery which does not show up in the as-polished condition. Whether this grain-boundary structure results from potassium attack or reaction of material in the grain boundaries with the etchant is difficult to ascertain. Microprobe analysis of this area for Ta, Hf, W, K, Fe, and Cr showed the area to be rich in Fe and Cr as illustrated by the X-ray scans in Figure 98; no other elements were detected. Although the source of the Fe and Cr cannot be readily explained, their presence in the potassium circuit is undoubtedly related to the previous findings of Fe, Cr, and Ni in the residue from the distillation of the potassium drained from the loop as discussed in Section XI. Presumably the original source is inadvertent contamination by stainless steel; however, the exact source and the reason for the particularly high concentration in this one weld area are currently unknown. It should be pointed out that all other areas where microprobe evaluation was performed were also checked for Fe and Cr; however, no indications were found. Microhardness traverses in the vicinity of these areas showed them to have a hardness of 200-225 units higher than the average matrix hardness of about 225 DPH (100-gram load).



H64011E As-Polished

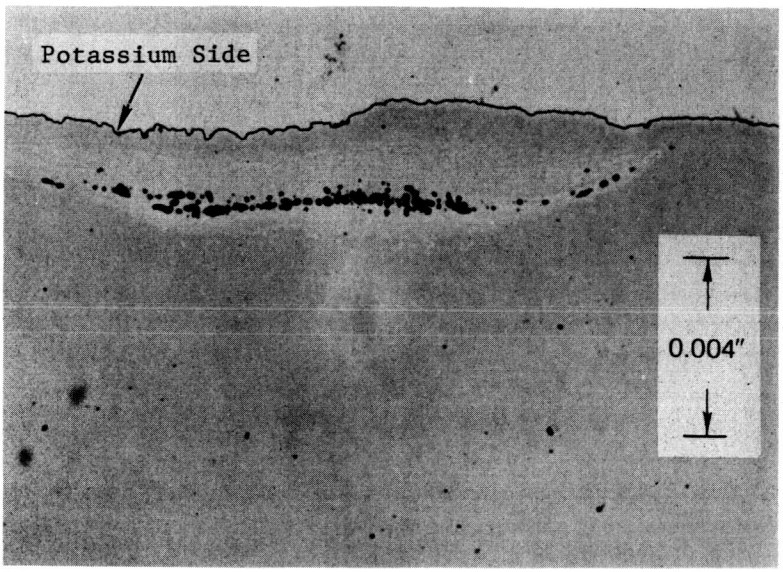
a. On weld metal at tube-fitting interface



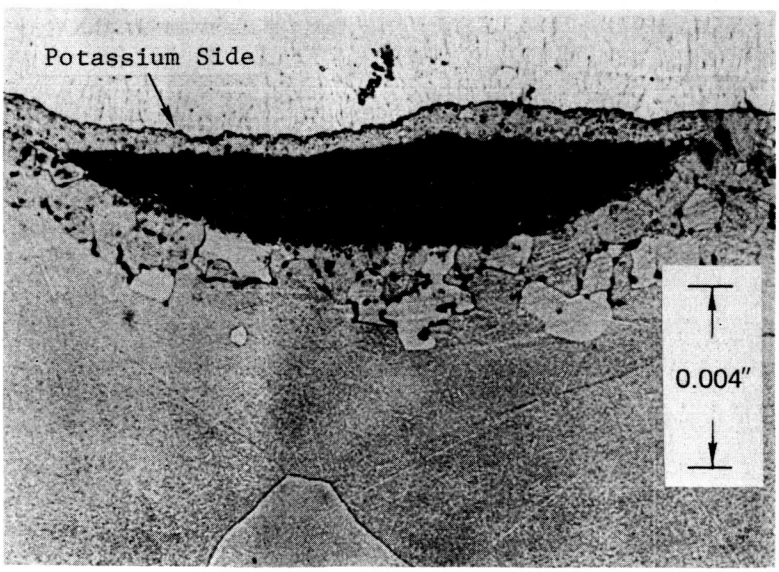
H64011H As-Polished

b. On tube approximately 1/2-inch above fitting

Figure 96. Hafnium Nitride Deposit Near Bottom of 3/8-Inch (0.95-cm)-OD T-111 Tube in Plug Section of Boiler.



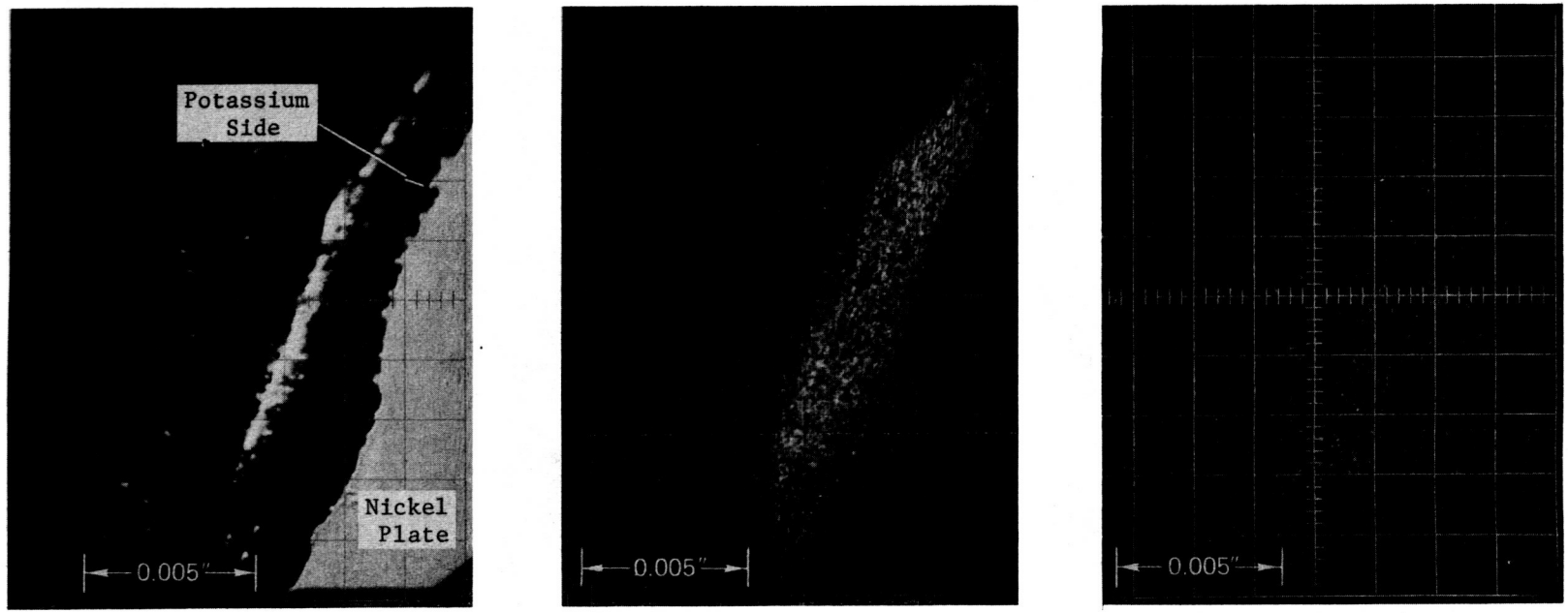
H64011A As-Polished



H64011K Etched

Figure 97. Base Metal - Weld Interface at Bottom of the 3/8-Inch (0.95-cm)-OD T-111 Potassium Containment Tube in the Plug Section of the Boiler Before and After Etching.

ORIGINAL PAGE IS
OF POOR QUALITY



a. Sample current image

b. Iron X-ray image

c. Chromium X-ray image

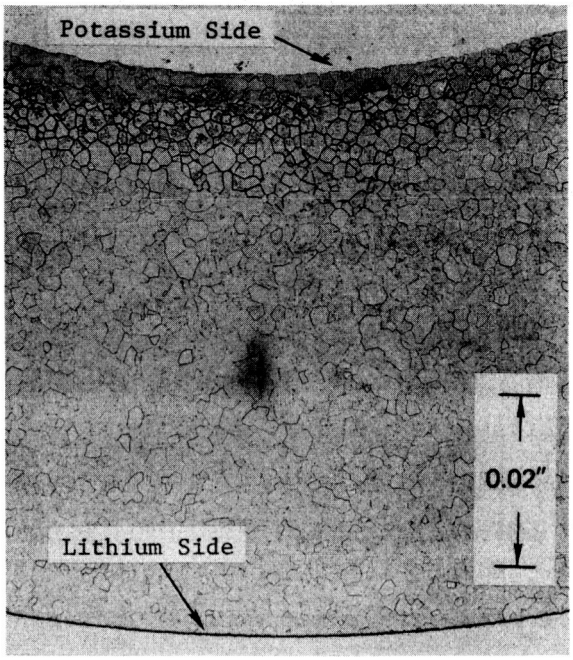
Figure 98. Microprobe Scans of the Base Metal - Weld Interface at the Bottom of the 3/8-Inch (0.95-cm)-OD T-111 Potassium Containment Tube in the Plug Section of the Boiler. Same Area as Figure 97.

A transverse specimen from the 3/8-inch (0.95-cm) tube was cut from an area near the edge of the HfN-coated region which occurred six inches (15 cm) above the lithium exit. This region of the tube is believed to correspond to the area where the ID of the tube begins to be exposed to vapor approaching 100-percent quality, as supported by the fact that the oxygen concentration at the ID below the interface was 16 ppm while just above the interface it was 948 ppm (Table XXV). Some evidence of localized corrosion was evident in this area as shown in Figure 99. The corrosion area was localized, i.e., it did not extend around the total ID surface but was essentially confined to the area shown in Figure 99. This localized effect is believed to be associated with the swirling of the flow path and probably corresponds to transformation of high-oxygen liquid to pure potassium vapor in this local area. Microhardness measurements showed no difference or gradients among various locations in the specimen.

The transverse specimen was reground, repolished, and rough polished dry to attempt to determine if any free potassium was present in the corroded area. Water was applied to the surface of the freshly polished surface while observing the specimen under the microscope. No evidence of gas evolution was detected which indicates that there was no free potassium metal present in the corroded area. Additional polishing and examination in the unetched condition revealed a nonmetallic, semicontinuous phase in the grain boundaries of the corroded region. The phase may be potassium tantalate (K_3TaO_4) since this phase has been detected in solubility experiments of oxygen-doped tantalum in potassium.[27] Also, microprobe examination of the swirler insert, discussed later in this section, revealed the presence of potassium in similar-appearing grain-boundary precipitates.

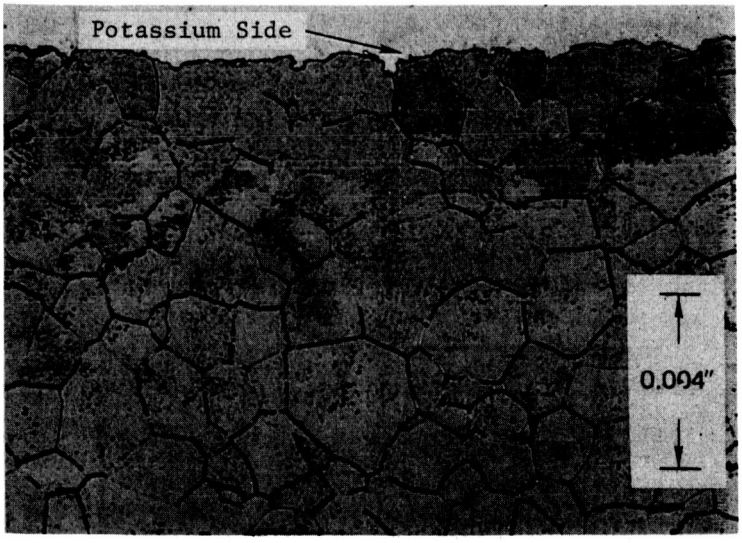
Two specimens were obtained from the 3/8-inch (0.95-cm) tube near the top of the plug section. The first section to be examined was cut essentially even with the top of the swirler wire insert and consisted of a clean, equiaxed microstructure as shown in Figure 100. Since the chemical analysis in this region of the tube had indicated both high oxygen concentration (1100 ppm) and a very steep oxygen gradient, it was decided that an additional

[27] Stecura, Stephan, Apparent Solubilities of Commercially Pure and Oxygen-Doped Tantalum and Niobium in Liquid Potassium, NASA TN D-5875, July 1970.



H64021A Etched

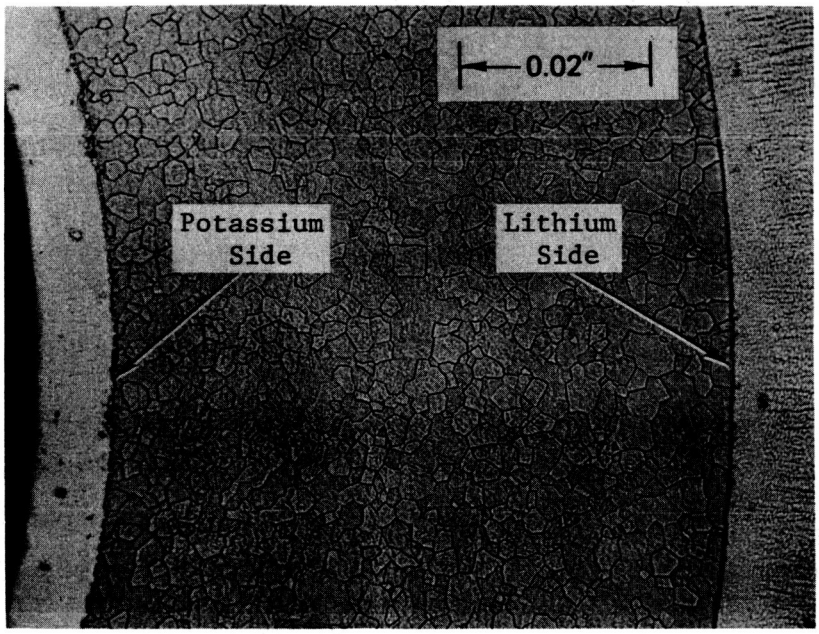
a. Total wall



H64021D Etched

b. Inner wall

Figure 99. T-111 Potassium Containment Tube to the Plug Section Approximately 6 Inches (15 cm) Above Lithium Exit From Boiler.



H64031A Etched

Figure 100. T-111 Potassium Containment Tube in the Plug Section of the Boiler Adjacent to the Top of the Swirler Wire Insert.

specimen should be taken from an area closer to the higher oxygen specimen (1/2 inch, 1.3 cm) above the end of the swirler insert. The microstructure of the second specimen, shown in Figure 101 revealed an uneven zone near the ID. This region is assumed to be the high-oxygen region. The postulated reason for the high oxygen concentration in these regions was discussed earlier in this section. It can be seen in Figure 101 that the reaction zone at the tube ID is not uniform in thickness. This nonuniformity could be a result of the swirling action of the potassium being ejected from the end of the swirler wire insert. The reaction zone consists of three different regions as shown in Figure 102. The microstructure of the region closest to the ID, Figure 102a, consists primarily of a very fine, evenly divided precipitate in the matrix and a slightly coarser grain-boundary precipitate. Near the midwall, the microstructure, illustrated in Figure 102c, is dominated by a relatively large grain-boundary precipitate and somewhat fewer in number but equally large matrix precipitate. The transition region, shown in Figure 126, consists primarily of a fine matrix precipitate and an area immediately adjacent to it of large grain-boundary precipitates but clean matrix. Microprobe analyses were performed on this specimen to determine the identity of the precipitate particles. Although the identity of the fine particles could not be determined, because the size is below the resolution limit of the microprobe, the larger particles are believed to be hafnium oxide because (1) the hafnium content in the region of the larger particles was approximately four times that of the matrix and (2) all of the larger particles fluoresced in the electron beam, a characteristic unique to oxides.

Specimens of the swirler wire insert from the lower portion of the plug section, six inches (15 cm) from the lithium exit, and from the top region of the plug were also examined. The microstructures of these specimens are shown in Figure 103. Microprobe analyses were performed on these specimens in an attempt to characterize the dark regions in these specimens. Results from the top sample showed the hafnium content of some of the dark particles to be three times that of the matrix; however, analyses of the bottom specimen did not reveal anything of significance. The metallographic specimen from six inches above the lithium exit represents a specimen adjacent to the 3/8-inch (0.95-cm) tube section shown in Figure 99. As seen in Figure 104, a similar effect was observed in the swirl wire as was seen in the tube section, i.e., a very localized area of intergranular corrosion. To determine

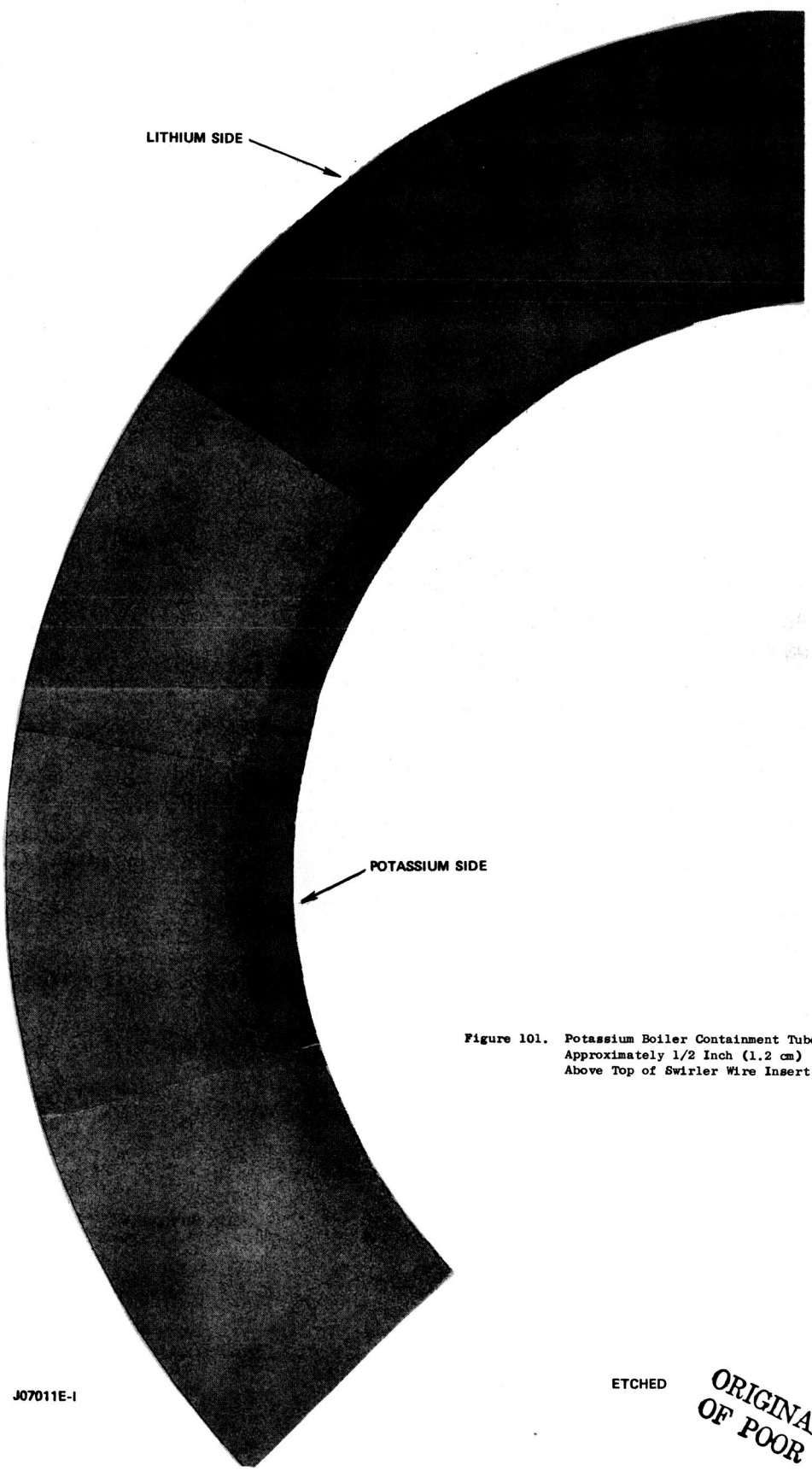
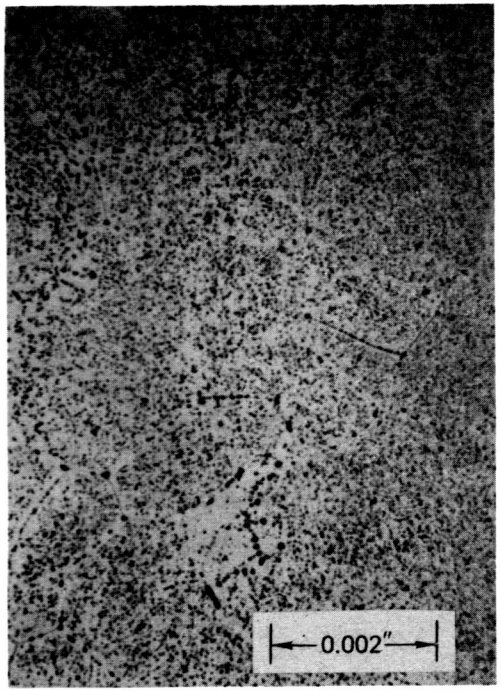


Figure 101. Potassium Boiler Containment Tube Approximately 1/2 Inch (1.2 cm) Above Top of Swirler Wire Insert.

J07011E-I

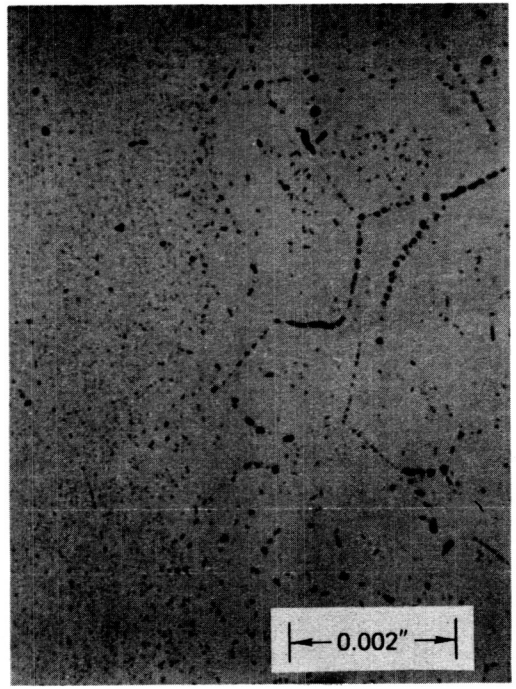
ETCHED

ORIGINAL PAGE IS OF POOR QUALITY



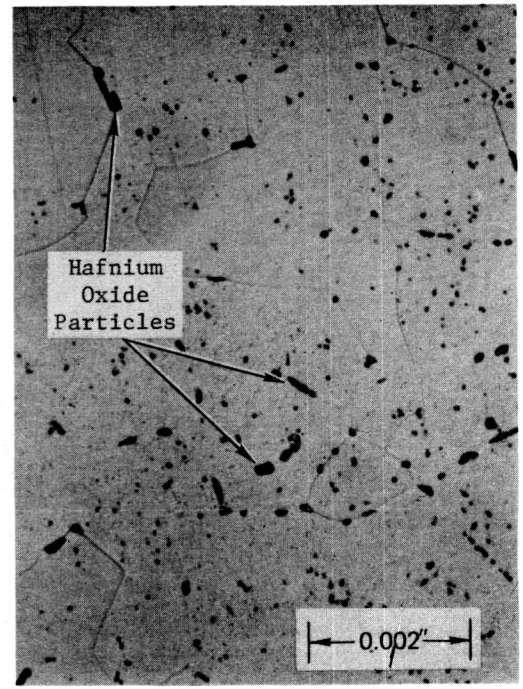
J07011N Etched

a. Near potassium side



J07011C Etched

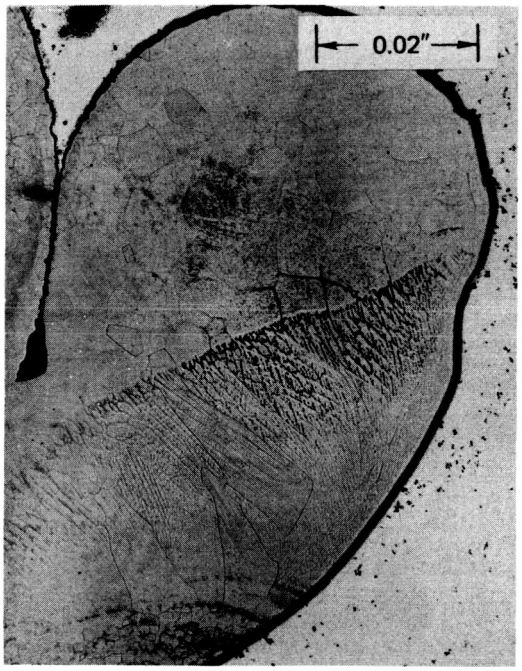
b. Approximately 0.015 inch from potassium side

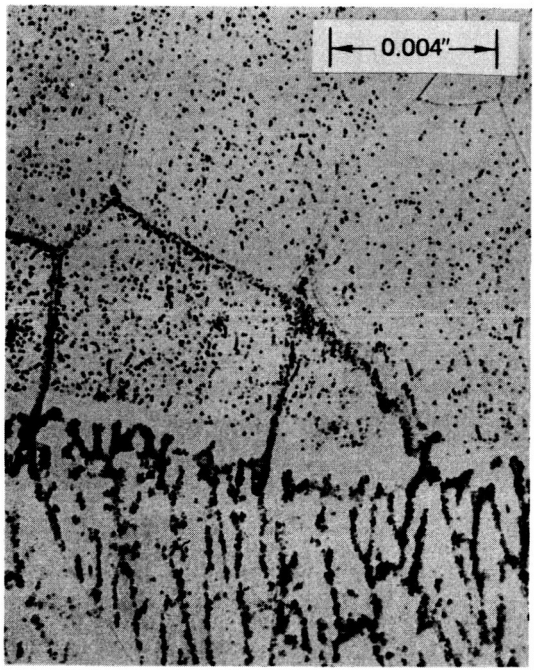


J07011M Etched

c. Approximately 0.030 inch from potassium side - near mid-wall

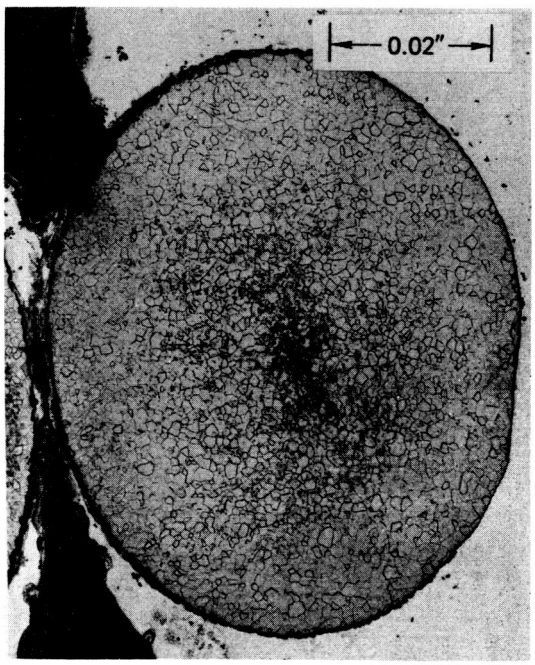
Figure 102. T-111 Potassium Containment Tube 1/2 Inch (1.2 cm) Above the Top of the Swirler Wire Insert. Same Area as Figure 101.

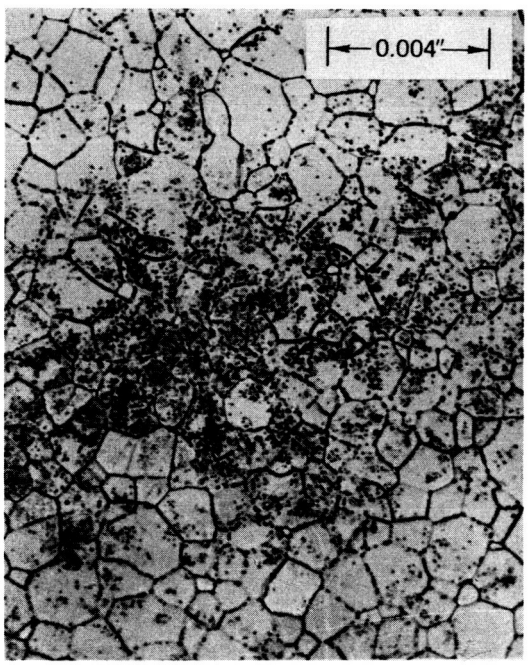




H64081A Etched H64081D Etched

a. Near bottom - potassium inlet showing tack weld joining wire and centerbody

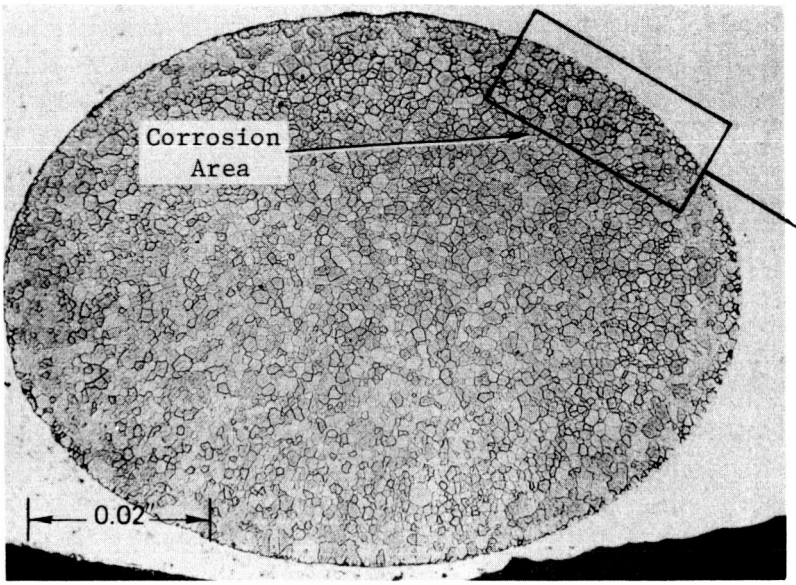




H64061A Etched H64061B Etched

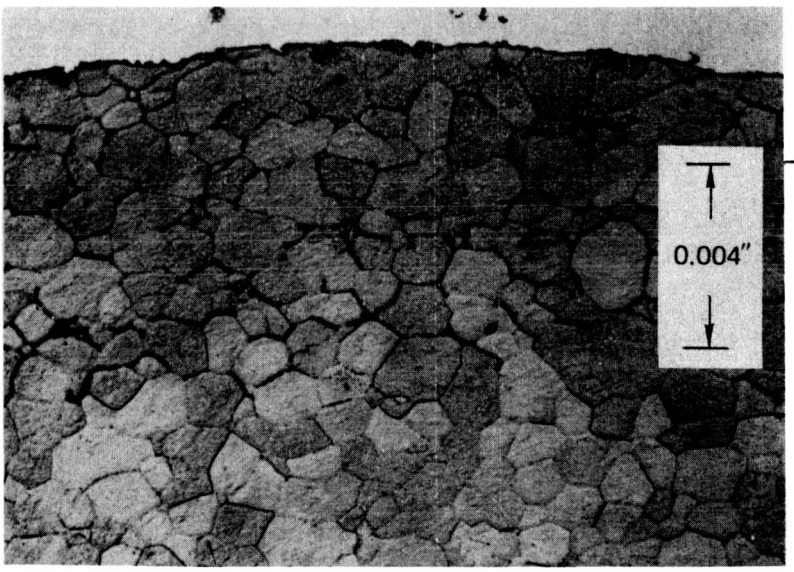
b. Near top of insert

Figure 103. T-111 Swirler Wire From Plug Section of Boiler.



H64071A Etched

a. Overall



H64071B Etched

b. Corrosion area

Figure 104. T-111 Swirler Wire From Plug Section of the Boiler Approximately 6 Inches (15 cm) From the Lithium Exit.

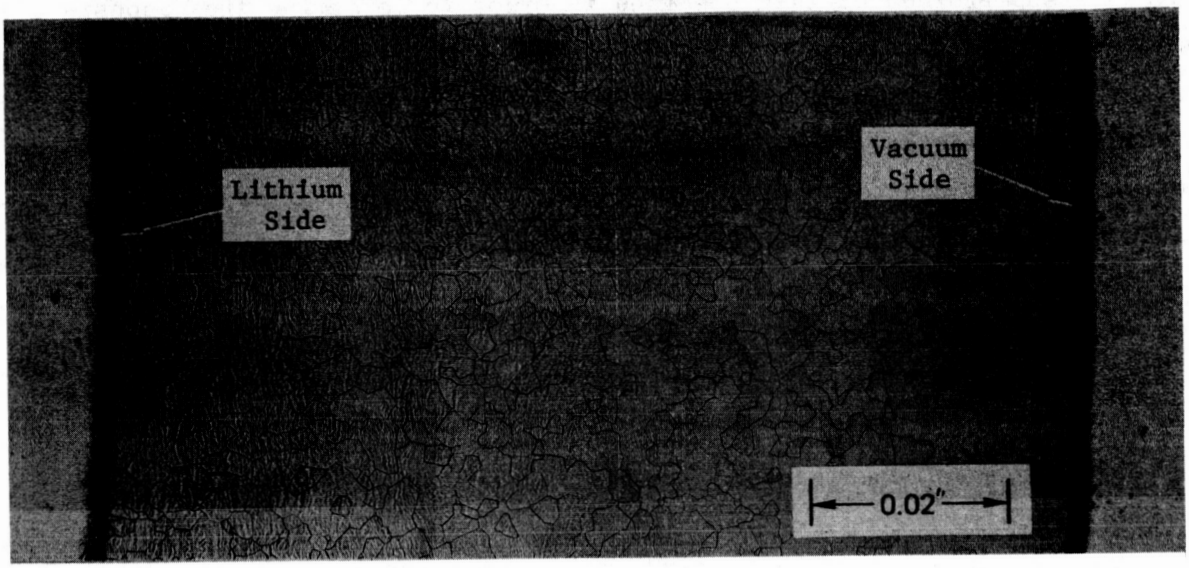
if this effect was assocated with the swirling action as proposed earlier, the specimen was reground to determine if the corrosion area appeared in a different location. On re-etching it was found that, indeed, the area had rotated significantly from the original location supporting the swirling effect. Microhardness traverses in several areas of these specimens showed no significant deviation from the nominal matrix hardness. Microprobe analysis was performed on this specimen in order to determine the composition of the grain-boundary phase. The results show that the grain-boundary phase contains small concentrations of potassium and carbon; no other elements were detected. Since the particles did not fluoresce in the electron beam, it can be concluded that they are not pure oxides; however, it does not preclude the possibility of oxygen being present in quantities below the detection limit of the microprobe or possibly K_3TaO_4 as mentioned in connection with Figure 99. The precipitate particles were too small and the signals too weak in order to further identify their exact composition. Based on these results and the work performed on the adjacent 3/8-inch (0.95-cm) tube specimen discussed earlier in this section, it appears that the precipitate is a complex potassium compound.

Specimens were also examined from the 1-inch (2.54-cm) tube at the top and bottom of the plug section. No differences could be seen from the pretest material except perhaps a very slight amount of grain growth as shown in Figure 105 (compare with Figure 95).

2. Other Regions of the Boiler

Two areas were examined from the coiled portion of the tube-in-tube boiler: (a) the repair weld region and (b) sections from the top of the boiler which were representative of the hottest (2240°F, 1225°C) part of the boiler. The repair welds on both the 3/8- (0.95-) and 1-inch (2.54-cm) tubing appeared to be in excellent condition as shown in Figure 106. The areas shown represent the weld metal - base metal interface, which past experience has shown to be the most critical from the standpoint of alkali metal compatibility. No evidence of any corrosion could be detected.

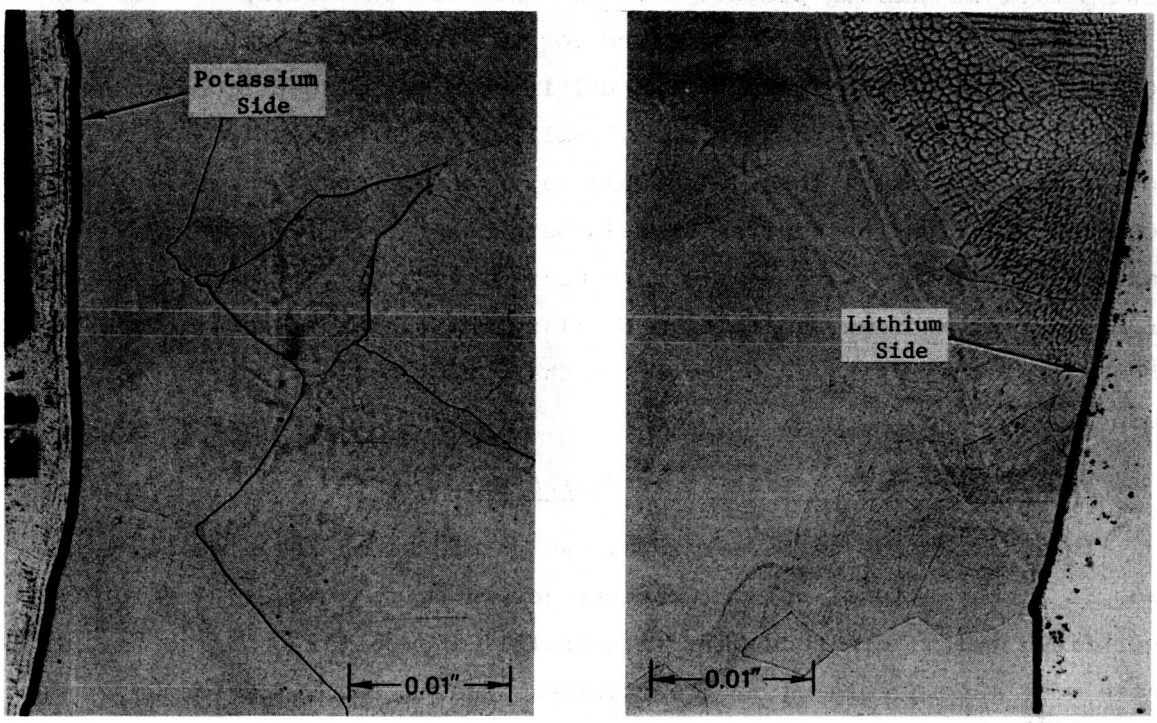
The specimens from the hottest portion of the boiler showed evidence of strain-induced grain growth in both the 3/8- (0.95-) and 1-inch (2.54-cm) tubes. These specimens were taken from a section of tubing that had been



H64101A,B

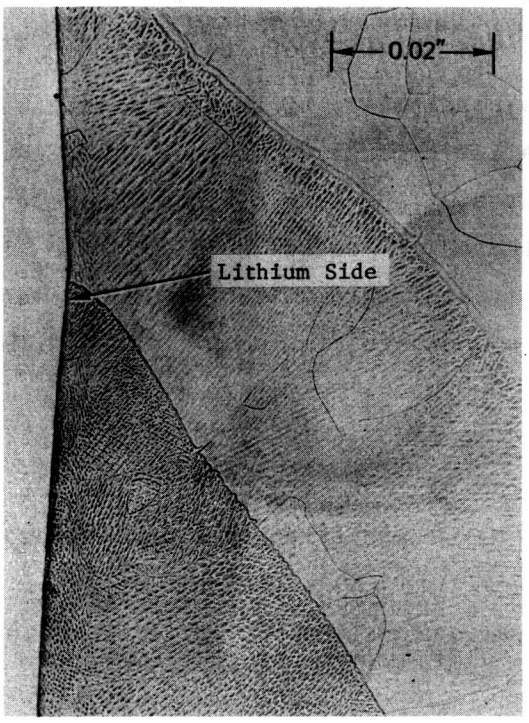
Etched

Figure 105. Lithium Containment Tube (1-Inch, 2.5-cm OD) From Top of Plug Section.



H64041E Etched H64041C Etched

a. 3/8-inch OD potassium containment tube



H64121A Etched

b. 1-inch OD lithium containment tube

Figure 106. Repair Welds in Top Coil of the 3/8-Inch (0.95-cm) and 1-Inch (2.5-cm) T-111 Tubing From the Boiler.

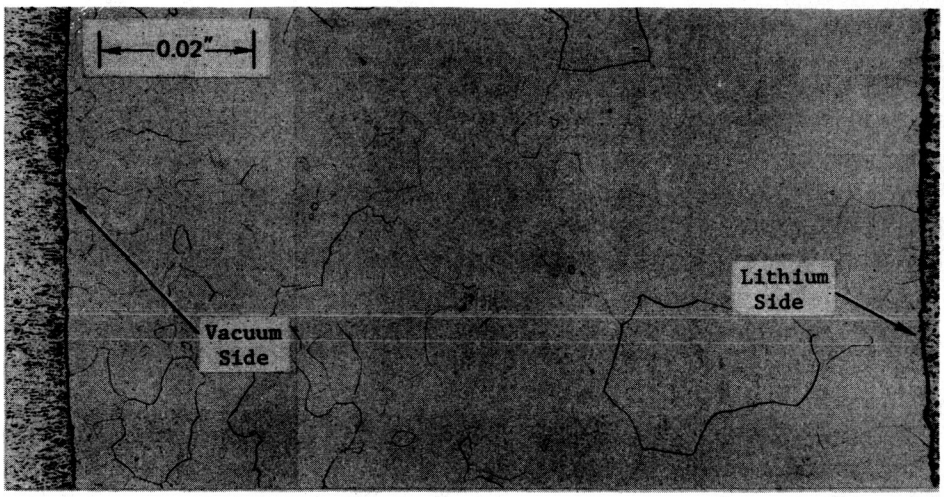
bent almost 90° during pretest forming. As seen in Figures 107 and 108, strain-induced grain growth occurred completely across the 0.1-inch (0.25-cm) wall of the 1-inch (2.54-cm) lithium containment tube and over one-half of the 0.060-inch (0.15-cm) wall of the 3/8-inch (0.95-cm) potassium containment tube. As would be expected, maximum grain growth occurred 90° from the neutral axis in both cases. In areas between the maximum and minimum stress axes, the microstructure (not shown) consisted of mixed fine and coarse grains. Similar, but much more spectacular abnormal grain growth was observed in the Cb-1Zr boiler from the earlier loop test.[28]

3. Field Repair Boiler Installation Welds

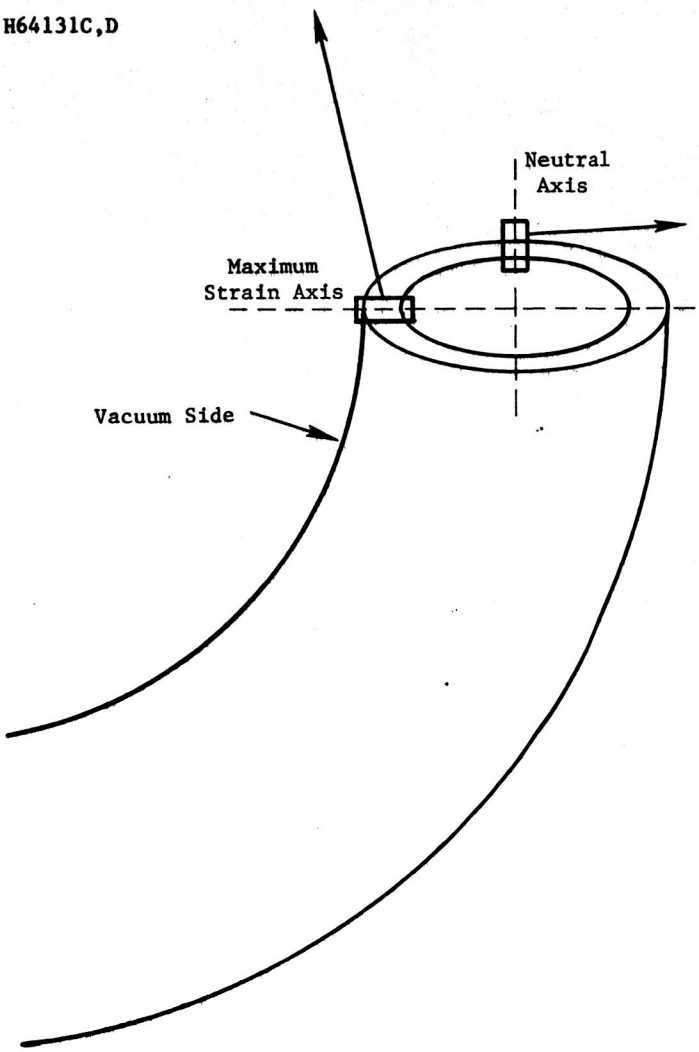
In addition to the boiler repair welds discussed above which were made in a conventional welding chamber according to standard weld practice, four field welds were necessary to reinstall the boiler into the test loop. These were made according to the existing welding specifications for refractory alloys; however, they were performed in a portable weld chamber attached to the 48-inch (122-cm)-diameter spool piece of the test chamber. The details of the procedures used to install the boiler and photographs of the installation welds are included in Appendix K of this report.

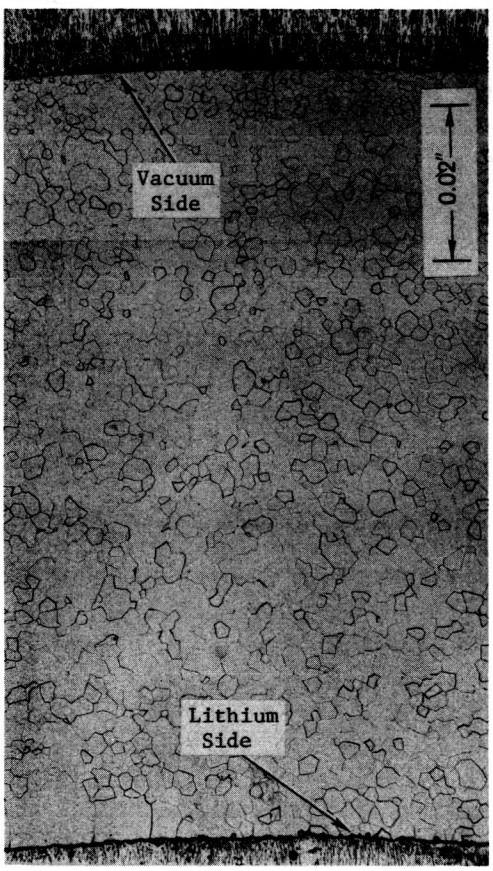
Since there was a possibility of unknown variables which could have influenced the weld quality because of the new techniques utilized in the field installation, three of the four field welds were examined metallographically. Two of these were socket welds, in the lithium circuit. The weld exposed to the hottest lithium (2250°F, 1230°C) at the inlet to the boiler (heater exit) is shown in Figure 109. No detrimental effects were detected due to the 10,000 hours' exposure to flowing lithium. The second socket weld was located on the lithium exit line from the boiler (2090°F, 1145°C). Although no indications of typical alkali metal attack were observed in this weldment, a very fine, somewhat banded, general precipitate was present as shown in Figure 110. This same type of structure was also seen to a somewhat lesser degree at the bottom of the plug section discussed

(28) Hoffman, E. E. and Holowach, J., Cb-1Zr Rankine System Corrosion Test Loop, NASA CR-1509, June 1970, p. 269.



H64131C,D Etched

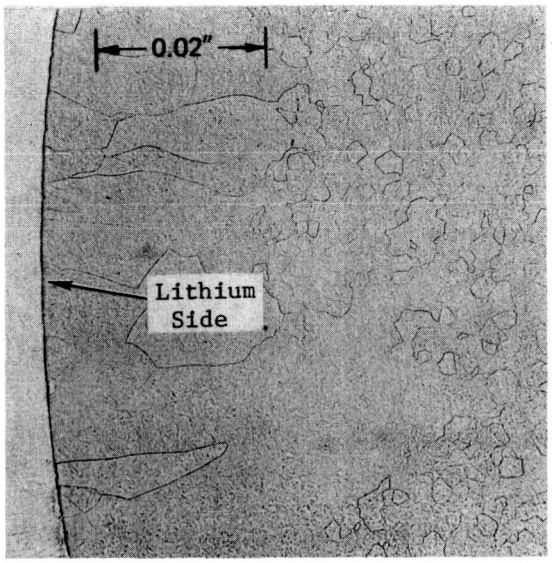




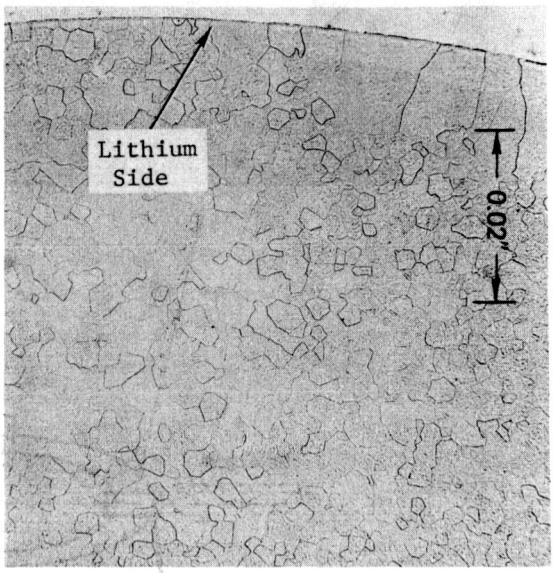
H64131A,B Etched

Figure 107. Lithium Containment Tube From Top of Boiler Following 10,000 Hours of Continuous Operation at Approximately 2240°F (1227°C) Illustrating Effect of Strain From Pretest Forming Operation on Grain Growth.

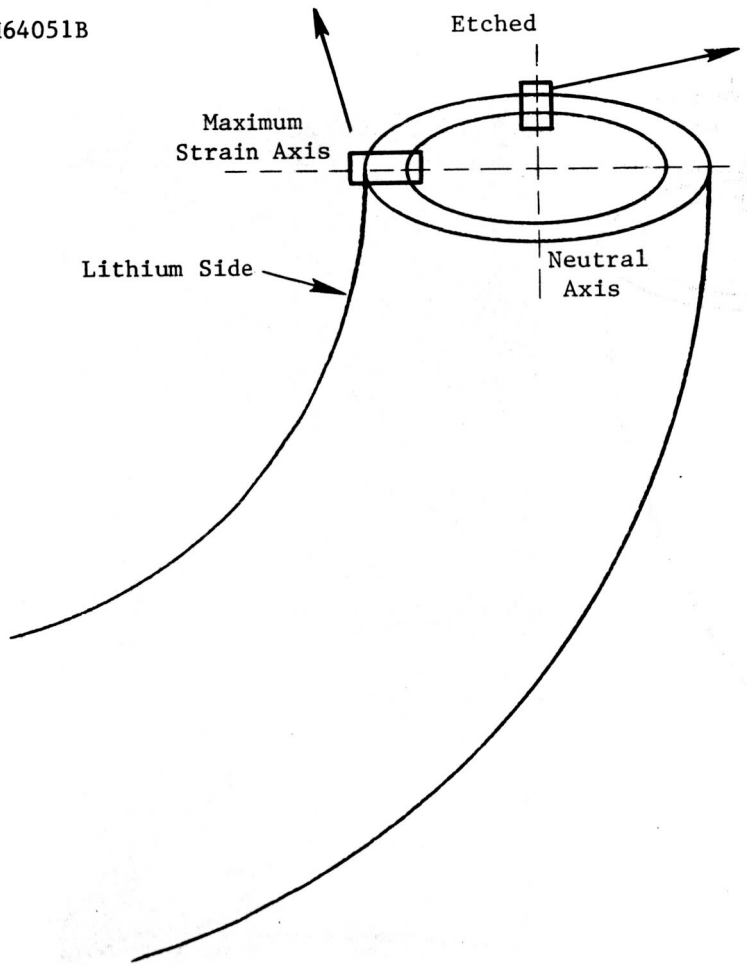
ORIGINAL PAGE IS OF POOR QUALITY



H64051B



H64051A



Etched

Figure 108. 3/8-Inch (0.95-cm) Potassium Containment Tube From Top of Boiler Illustrating Effect of Strain From Pretest Forming on Grain Growth During the 10,000-Hour Test. Adjacent to Sample in Figure 107.

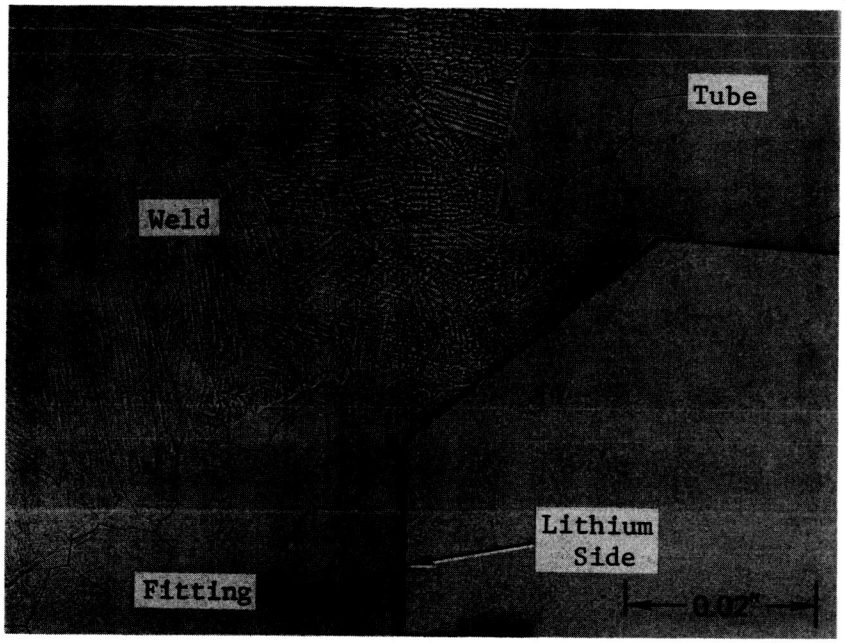
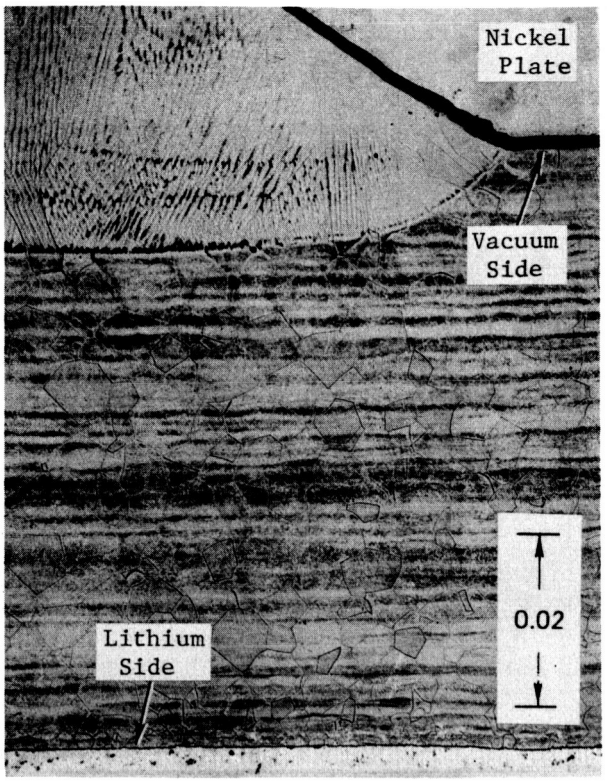


Figure 109. Repair Socket Weld in 3/8-Inch (0.95-cm) Lithium Inlet to the Boiler.



H64151 I,J Etched

a. Fitting



H64151H Etched

b. Tube-weld interface

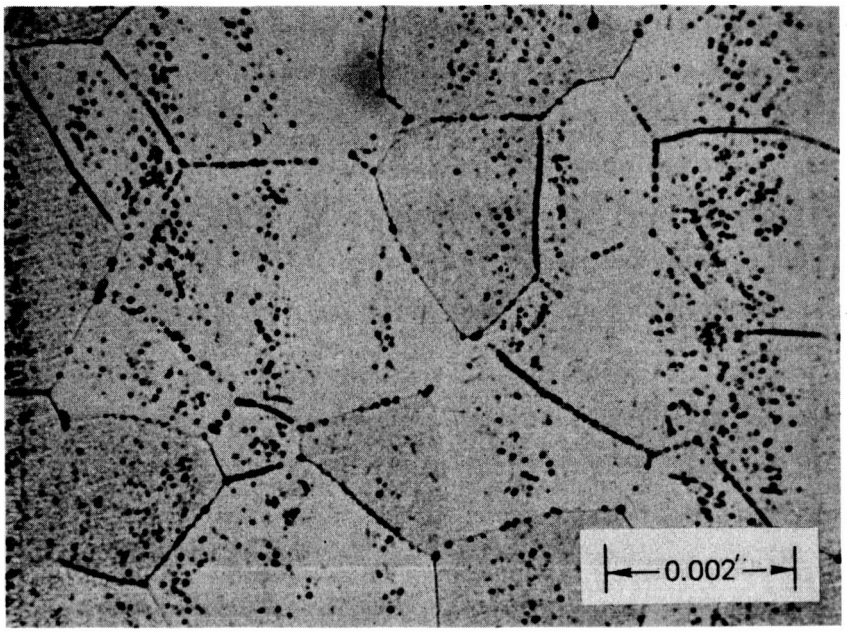
Figure 110. Repair Socket Weld in 3/8-Inch (0.95-cm)-OD Lithium Exit Line From Boiler.

earlier in this report and also in the T-111 portion of the High-Temperature Alkali Metal Valve Loop.[29] Note in Figure 110 that although the second phase extends completely through the 0.062-inch (0.16-cm) wall of the 3/8-inch (0.95-cm)-OD tube, only about 1/3 of the outer portion of the fitting wall shows the precipitate. As shown in the higher magnification photomicrographs of Figure 111, the precipitate appears as small, individual, globular-type precipitates in both the matrix and grain boundaries. Since this precipitate does not appear to adversely affect the reliability of the alloy in an alkali metal system in any obvious manner, no attempts were made to identify it. The random locations of this fine precipitate in tested T-111 components suggests that its presence is related to compositional inhomogeneities and thermal effects rather than liquid metal interactions.

Although no attack was observed in the installation welds discussed above, intra- as well as intergranular alkali metal attack was detected in the heat-affected zone of the field repair weld joining the boiler exit to the first-stage turbine simulator housing inlet. The attacked area was relatively small, and maximum penetration was about 0.005 inch (0.013 cm) as shown in Figure 112. Also indicated in Figure 112 is a very fine reaction layer in addition to the gross grain-boundary attack. This same type of reaction layer can also be seen in the corrosion area of the 3/8-inch (0.95-cm) tube from the plug section previously shown in Figure 99.

The metallographic appearance of the attack suggests that it resulted from localized oxygen contamination and this might be possible despite the fact that (a) extreme care was taken during all phases of the repair and installation sequence to avoid contamination and (b) similar procedures were utilized for the other installation welds, and they showed no evidence of attack. At any rate there is no known mechanism which would suggest that the attack continued with test duration, and only an insignificant portion of the wall thickness was affected. The attack observed in this specimen again points out the usefulness of extensive metallographic examination in detecting areas of localized attack.

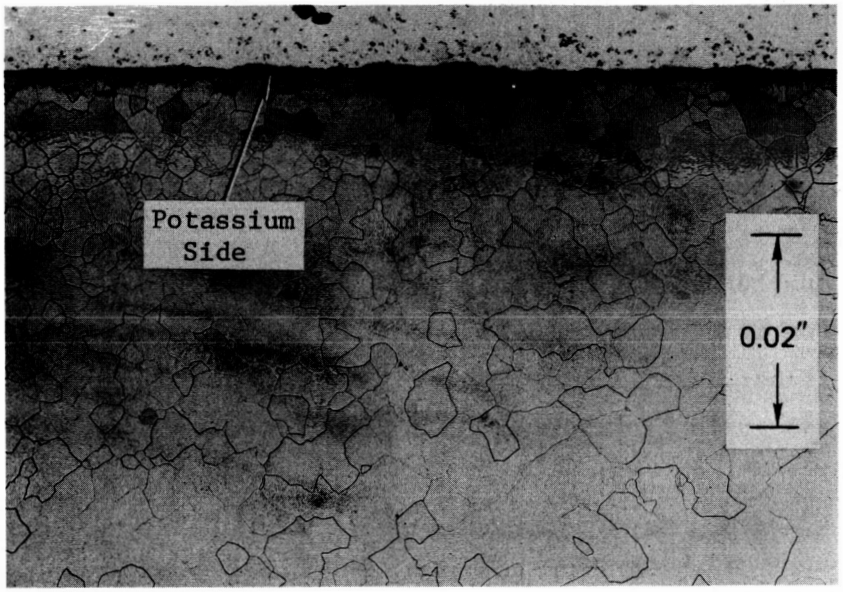
(29) Harrison, R. W. and Holowach, J., Refractory Metal Valves for 1900°F Service in Alkali Metals Systems, NASA Contract NAS 3-8514, General Electric Report No. GESP-508, April 15, 1970.



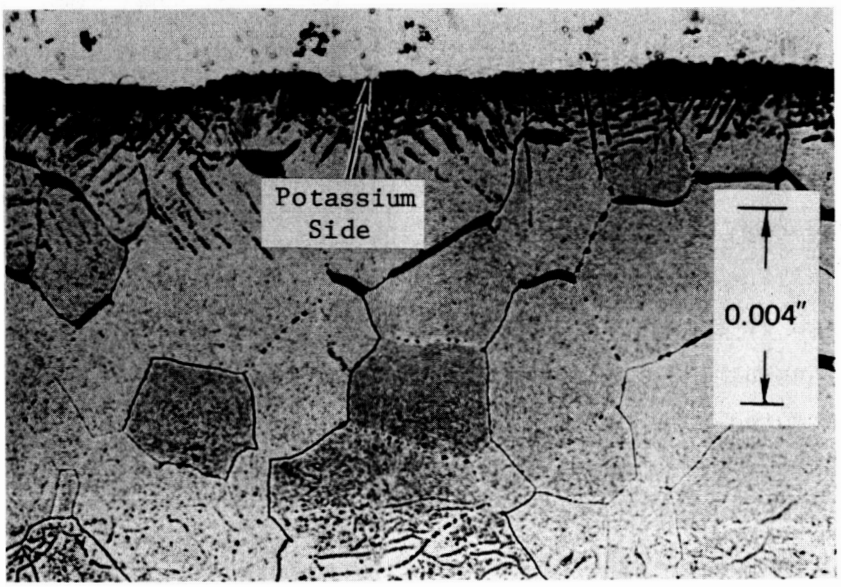
H64151K

Etched

Figure 111. Repair Socket Weld in Lithium Exit Line From Boiler. Same Area as Figure 110.



H64161D Etched



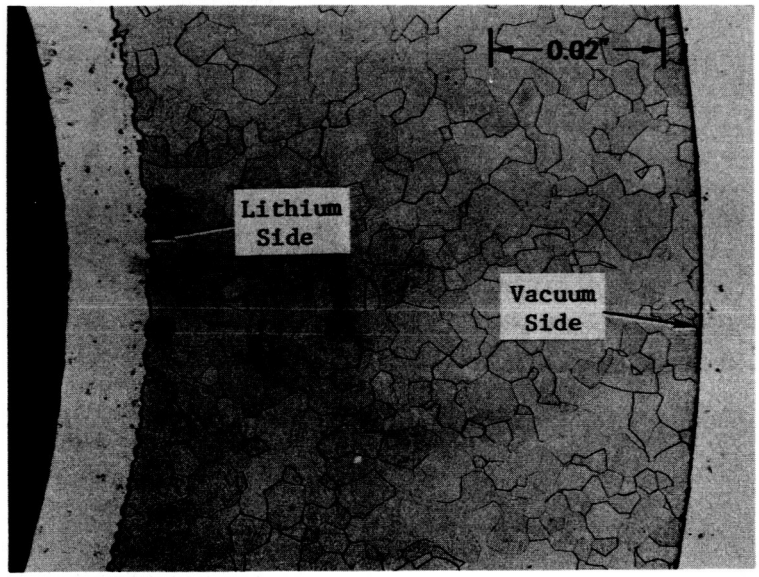
H64161E Etched

Figure 112. Heat-Affected Zone of Field Weld Joining Top of Bo
Bottom of First-Stage Turbine Simulator.

4. Miscellaneous Loop Components

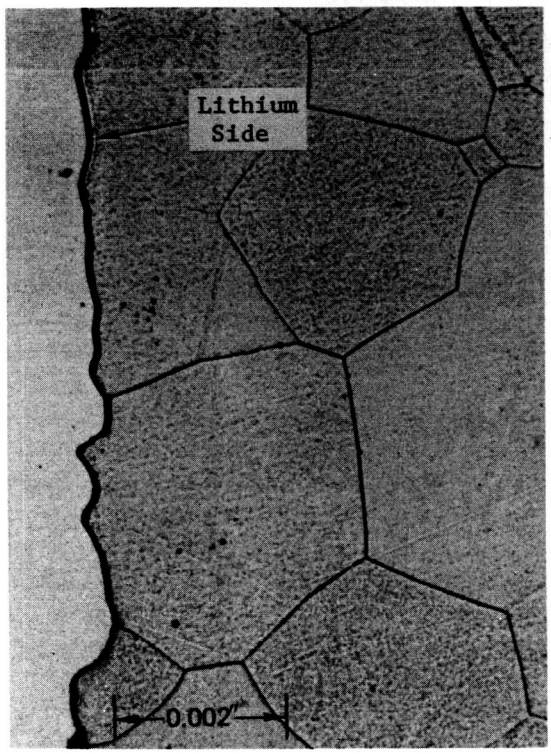
A section from the 3/8-inch (0.95-cm) line between the lithium heater and boiler inlet was examined since it represents tubing exposed to the highest loop temperature (2250°F, 1230°C). This material exhibited the cleanest microstructure of any of the tubing examined as shown in Figure 113. This is consistent with the very low posttest oxygen concentration (5 ppm) of this tubing. It may also be noted in Figure 113 that the grain size is approximately three times that of the pretest material previously illustrated in Figure 95a. Also, note that this is still considerably less grain growth than was noted at the top of the boiler (Figures 107 and 108) where strain during boiler fabrication resulted in nonuniform grain growth during the test.

The vapor crossover line was examined because flattening tests showed this material to be the most brittle in the loop. As shown in Figure 114, compressing of ring segments from the crossover line caused fracture with little or no deformation while similar tests on specimens of pretest material and boiler pipe exhibited excellent ductility. Although some very small cracks were observed in the boiler specimens, they occurred only after considerable deformation and did not propagate rapidly. On the other hand, the crossover line cracked with little or no deformation, and the crack propagated instantaneously across the wall. Except in rare occasions, most cracks initiated on the ID at the location of the maximum tensile strain. Optical microscopy of a specimen from the vapor crossover line showed the presence of a fine, grain-boundary precipitate throughout the cross section as illustrated in Figure 115. Because of the low ductility of this material, Scanning Electron Microscopy (SEM) was performed on specimens from the fractured ring specimens. For comparison, the SEM study also included ductile specimens from the boiler and the pretest material. The results showed, in agreement with the optical microscopy, that the grain boundaries of the vapor crossover tube contain a fine precipitate, and the samples break essentially 100 percent intergranularly as shown in Figure 116c. On the other hand, the boiler material and the pretest material broke in a much more ductile manner as shown in Figures 116a and 116b, and, where visible, the grain boundaries are void of precipitate particles. Qualitative



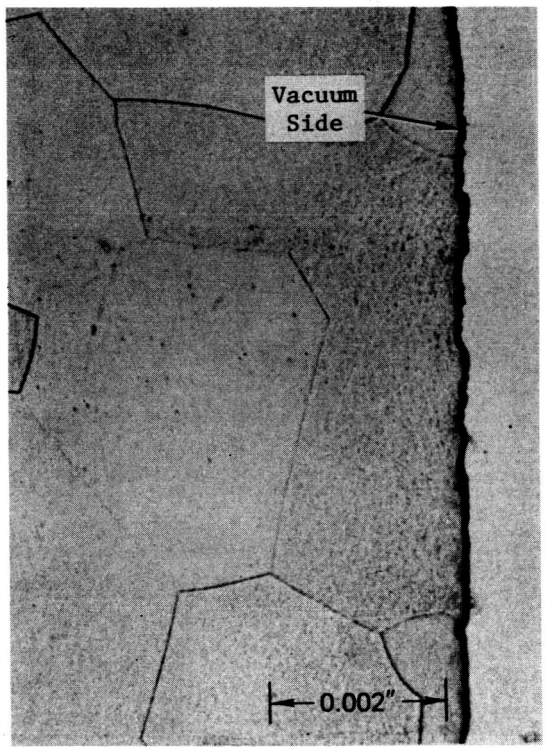
H64181A Etched

a. Total Wall



H64181B Etched

b. Inner Wall



H64181C Etched

c. Outer Wall

Figure 113. Lithium Line Connecting Heater Exit to the Boiler Inlet.

ORIGINAL PAGE IS
OF POOR QUALITY

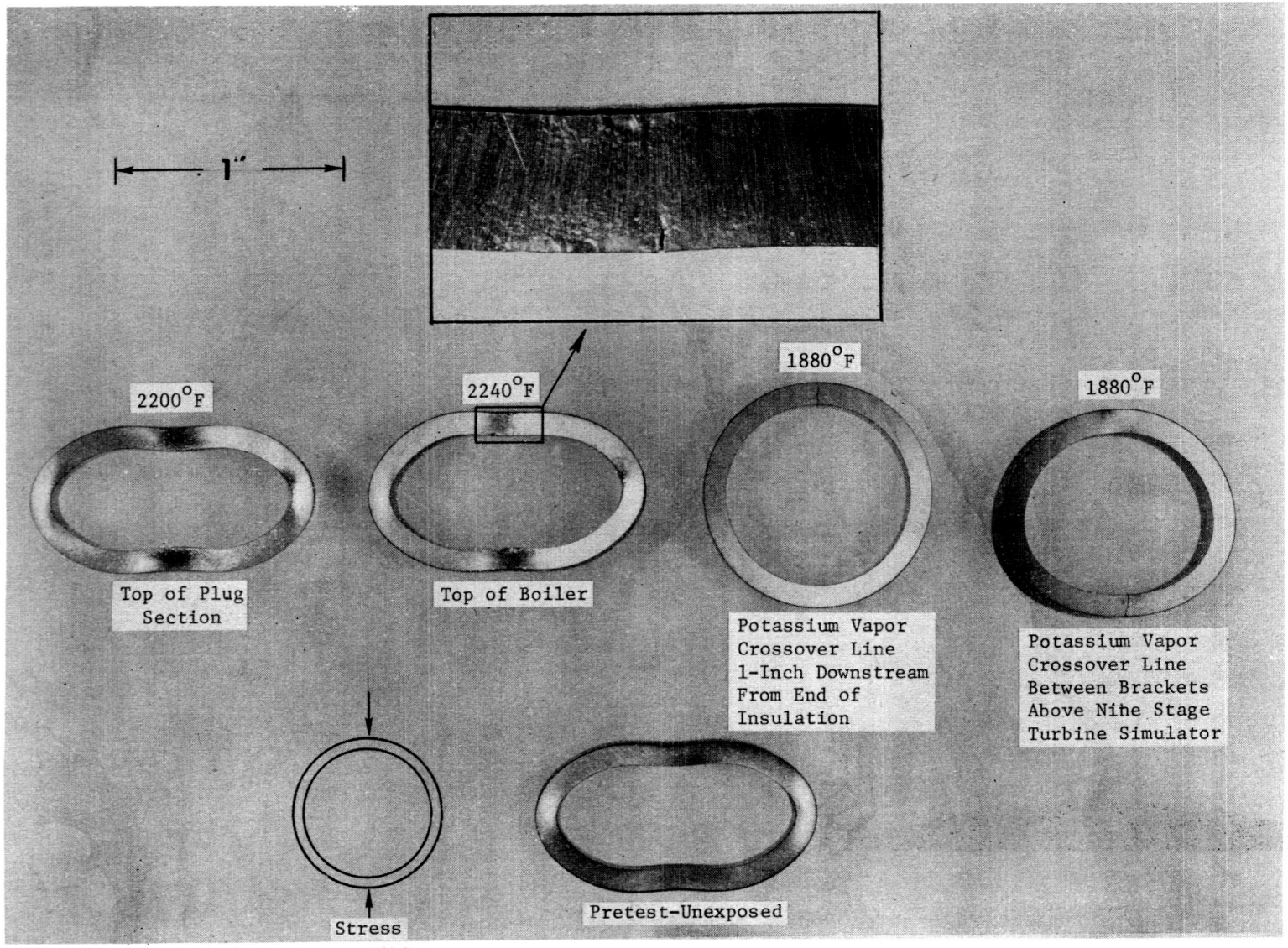
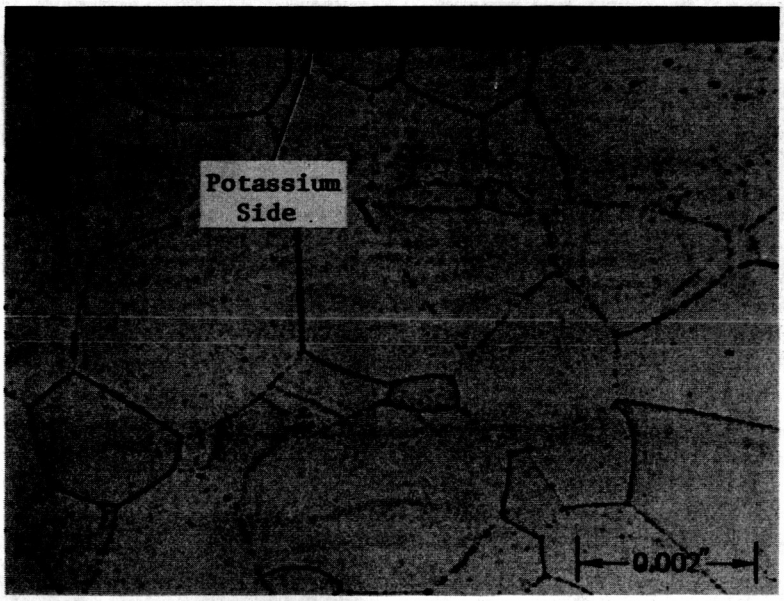
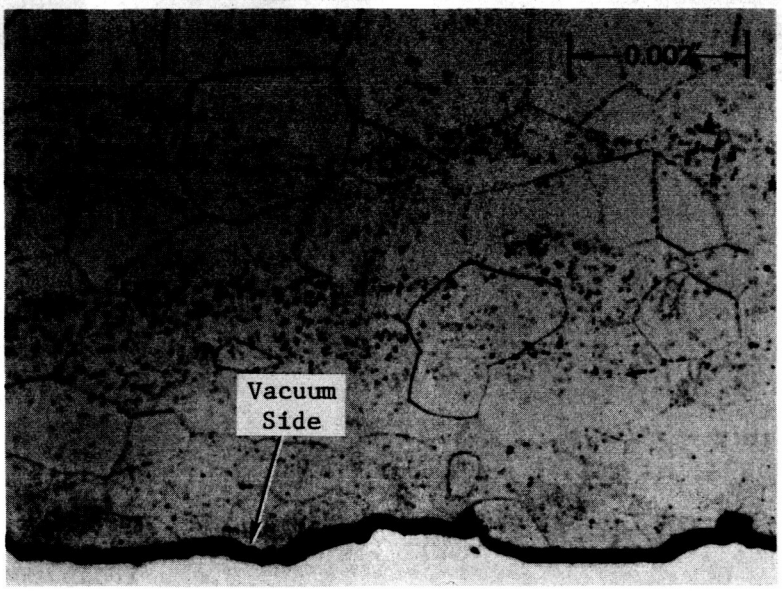


Figure 114. Specimens of 1-Inch (2.5-cm)-OD x 0.1-Inch (0.25-cm)-Wall T-111 Pipe Following 10,000 Hours' Exposure in the T-111 Rankine System Corrosion Test Loop. Ring Specimens Deformed at Room Temperature. (Orig. P70-6-4D)



H64191B Etched

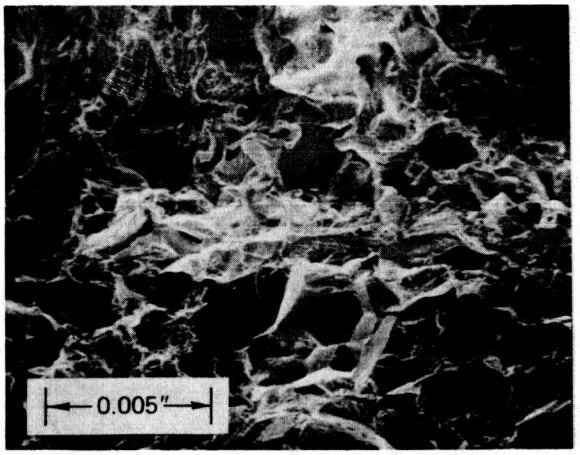
a. Inner Wall



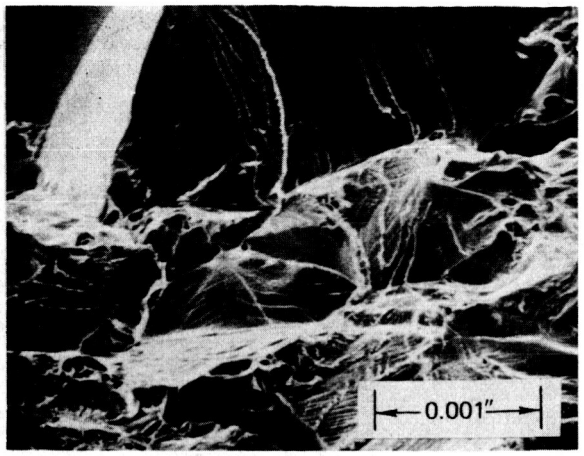
H64191I Etched

b. Outer Wall

Figure 115. 1-Inch (2.5-cm)-OD Potassium Vapor Crossover Line Following 10,000 Hours of Continuous Operation at Approximately 1880°F (1027°C).

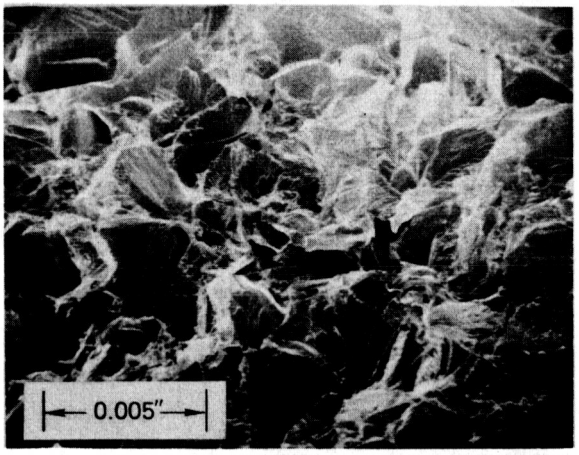


S-2663 As-Fractured

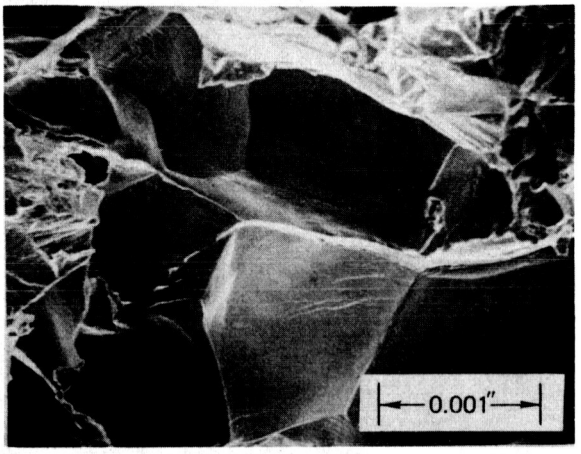


S-2659 As-Fractured

a. Pretest

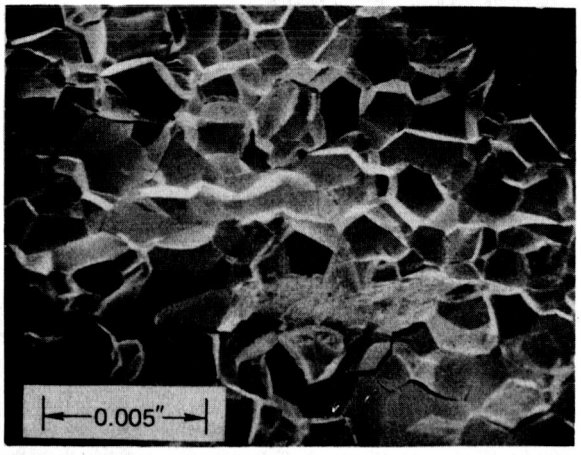


S-2657 As-Fractured

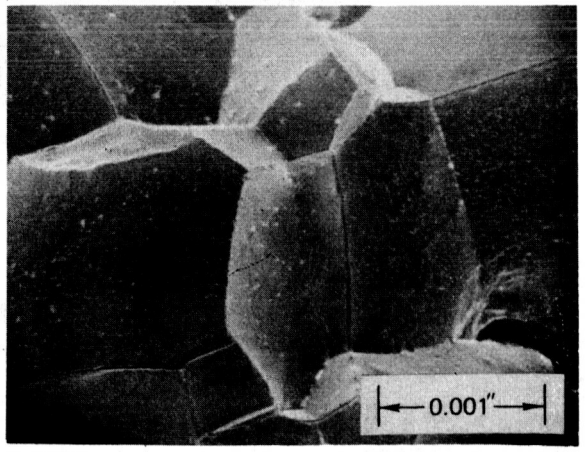


S-2651 As-Fractured

b. Boiler - 2240°F



S-2646 As-Fractured



S-2648 As-Fractured

c. Vapor Crossover Line - 1880°F

Figure 116. Scanning Electron Micrographs of Various Components of T-111 Rankine System Corrosion Test Loop. All Are Fractures From Compression Tests on Rings From 1-Inch (2.5-cm)-OD Tubing.

analyses using the SEM have shown that the particles contain 1.2 - 2.1 times more hafnium than the nominal matrix composition and 0.3 - 0.6 times the tantalum content of the matrix. Tungsten, carbon, oxygen, nitrogen, or hydrogen, which are also possible constituents of the particles, could not be detected because of equipment limitations. Further examination in order to positively identify the precipitate was not undertaken because it was considered to be beyond the scope of the contract.

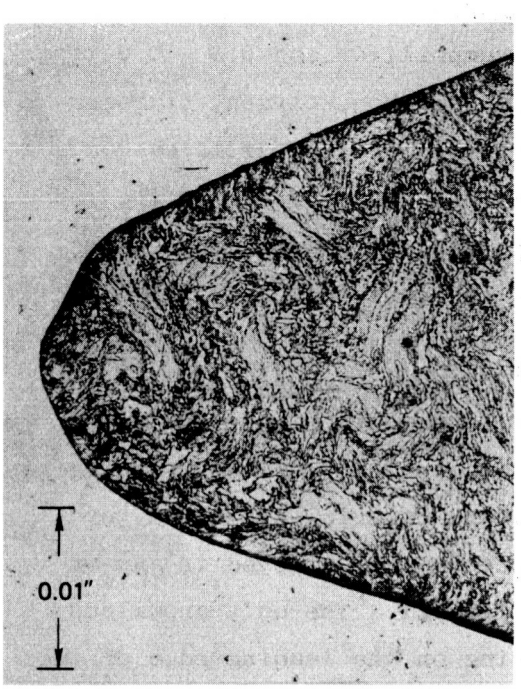
5. Turbine Simulator Nozzles and Blades

Sections from the Mo-TZC first, second, and tenth stages and the Cb-132M sixth-stage nozzle and blades were examined in the vapor impingement area. Typical pretest photomicrographs of each material are shown in Figure 117. No change in general microstructure was observed in any of the specimens examined as shown in Figures 118-121. The only anomalous feature is the 0.0003-inch (0.0007-cm) coating on the leading edge of the second-stage blade and nozzle as seen in Figure 119.

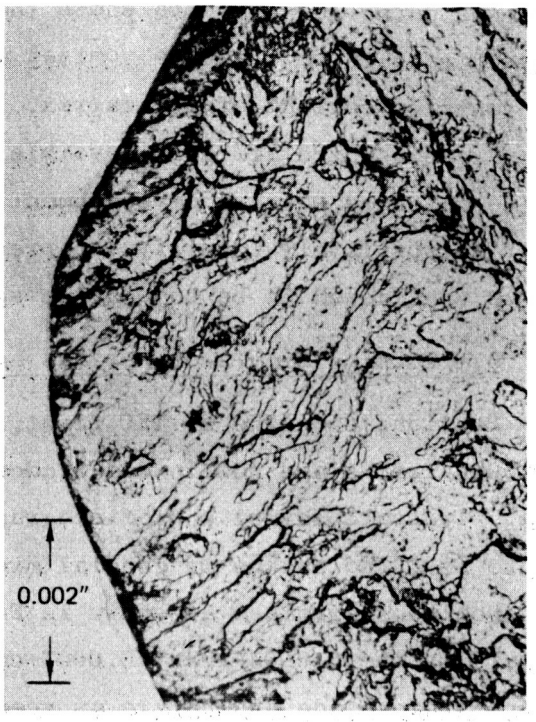
Microprobe examination was performed on the turbine simulator second-stage blade (Mo-TZC) in order to identify the deposit shown in Figure 119. The microprobe results showed that the coating actually consists of two separate layers. The outer layer was found to be essentially pure hafnium. The second layer, located between the outer layer and the Mo-TZC substrate, and much thinner than the outer layer, contained hafnium, but in much lower quantities than the outer layer. Also, the inner layer contained Ti and Zr in about the same quantities as the Mo-TZC substrate. These results indicate that the hafnium was deposited from the potassium vapor onto the surface of the blade and then diffused into the blade. Similar transfer of hafnium from the hot to the cold portions of the lithium circuit was noted earlier in this report in connection with the hafnium nitride coating on the inner tube of the plug section of the boiler.

D. TENSILE TEST RESULTS ON T-111 TUBING

Tensile tests were performed on specimens cut from the 1-inch-OD x 0.1-inch-wall (2.54 x 0.25-cm) T-111 pipe from the top of the plug section and from the potassium vapor crossover line. These two areas were

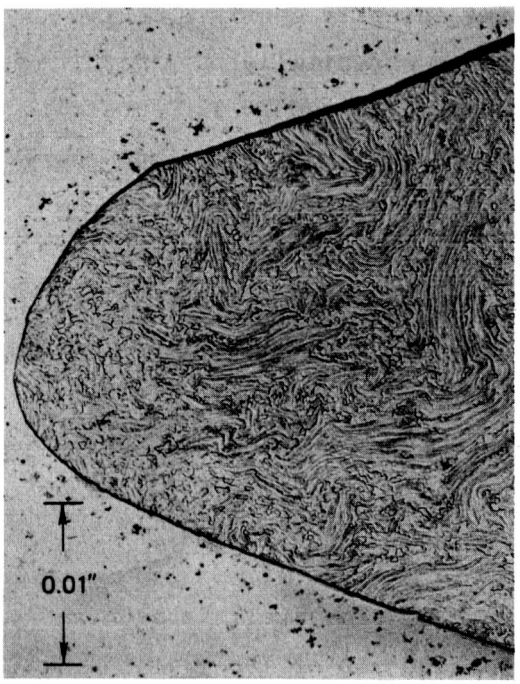


H66081A Etched



H66081B Etched

a. Mo-TZC Alloy



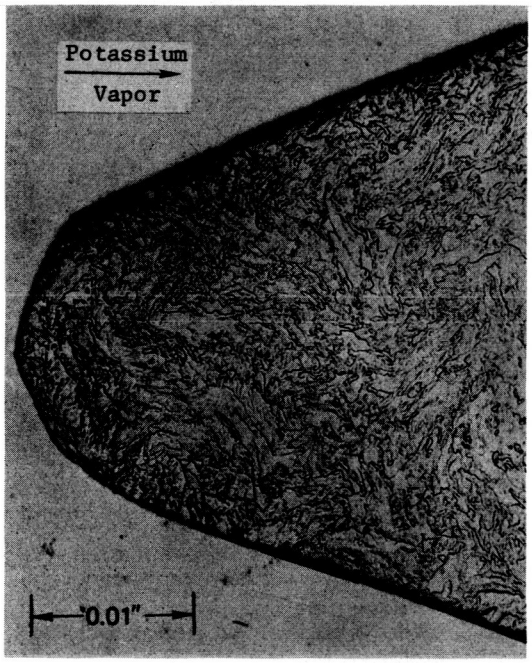
H65031B Etched



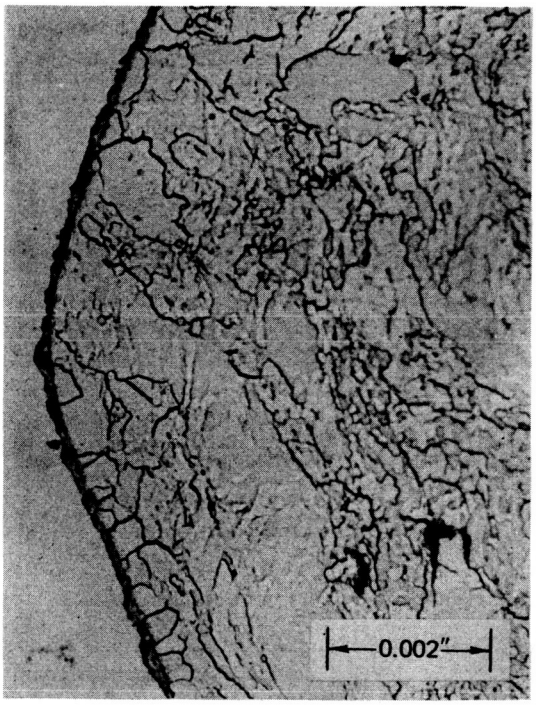
H65031A Etched

b. Cb-132M Alloy

Figure 117. Pretest Microstructure of Materials Used for the Turbine Simulator.

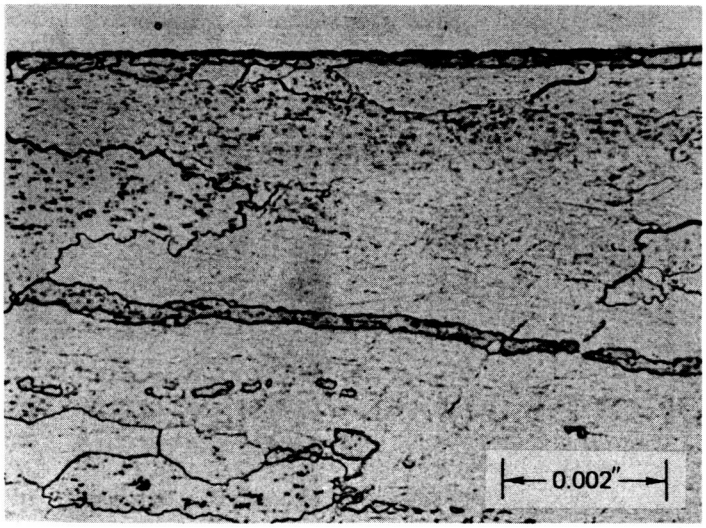


H66011A Etched



H66011B Etched

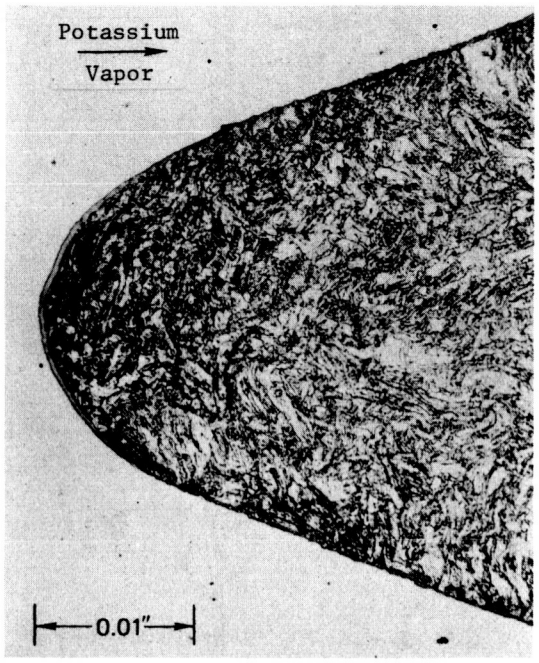
a. Blade



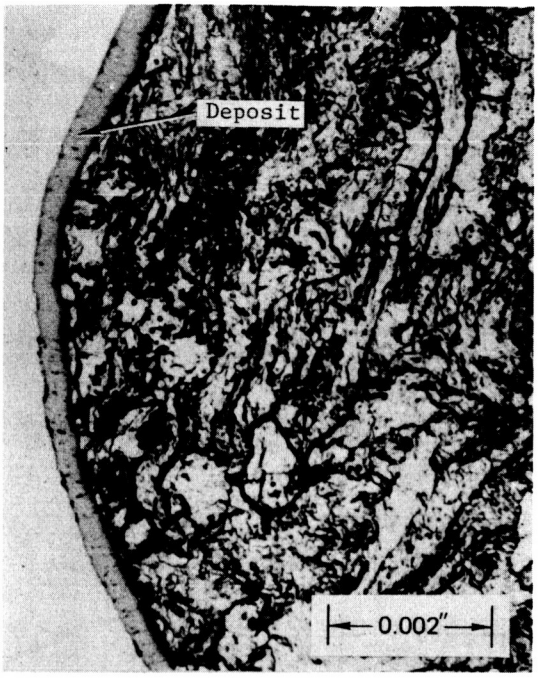
H66021B Etched

b. Nozzle

Figure 118. Mo-TZC Alloy First-Stage Nozzle and Blade Turbine Simulator Following 10,000 Hours of Continuous Exposure to Flowing Potassium Vapor in the Corrosion Test Loop.

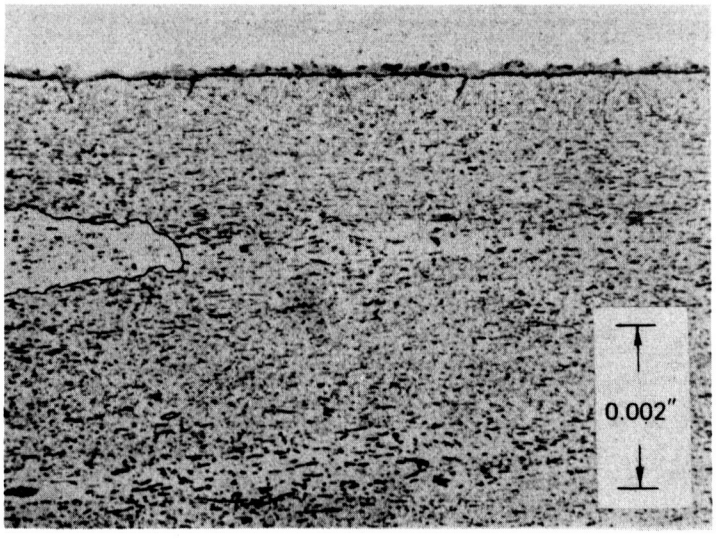


H66041A Etched



H66041C Etched

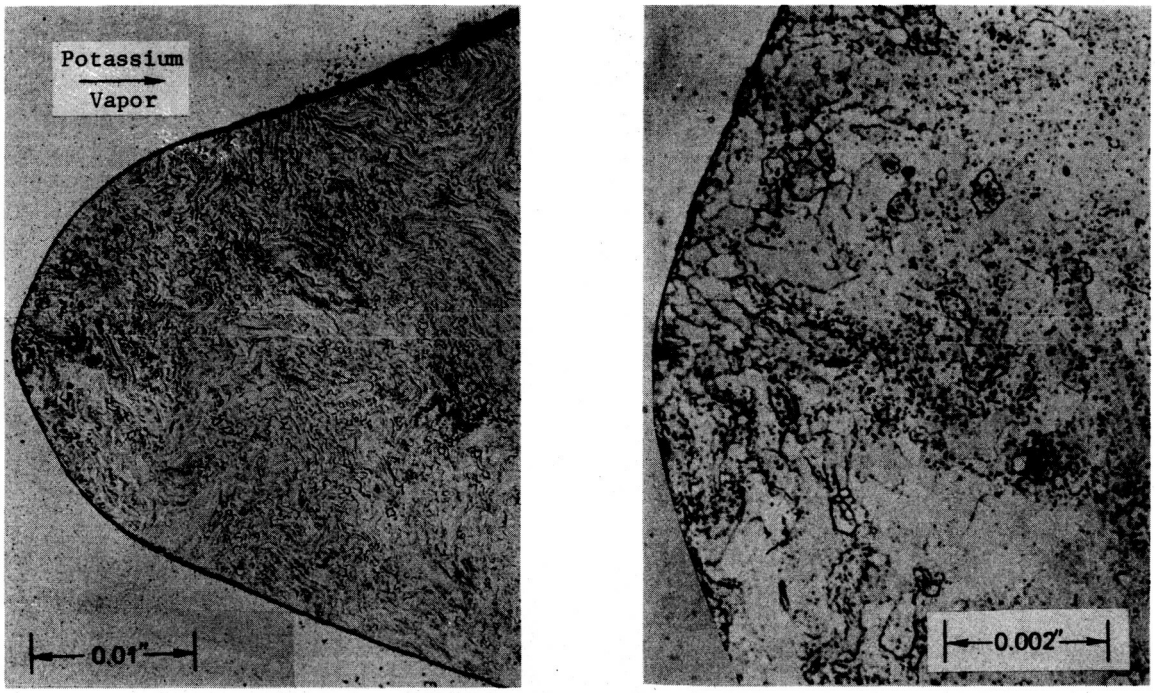
a. Blade



H66051C Etched

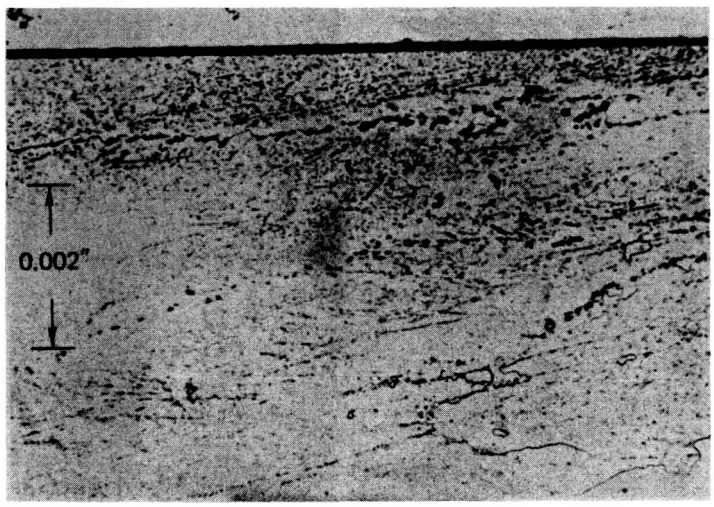
b. Nozzle

Figure 119. Mo-TZC Alloy Second-Stage Nozzle and Blade Turbine Simulator Following 10,000 Hours of Continuous Exposure to Flowing Potassium Vapor in the T-111 Corrosion Test Loop.



H65011B Etched H65011A Etched

a. Blade



H65021A Etched

b. Nozzle

Figure 120. Cb-132M Alloy Sixth-Stage Nozzle and Blade Turbine Simulator Following 10,000 Hours of Continuous Exposure to Potassium Vapor in the T-111 Corrosion Test Loop.

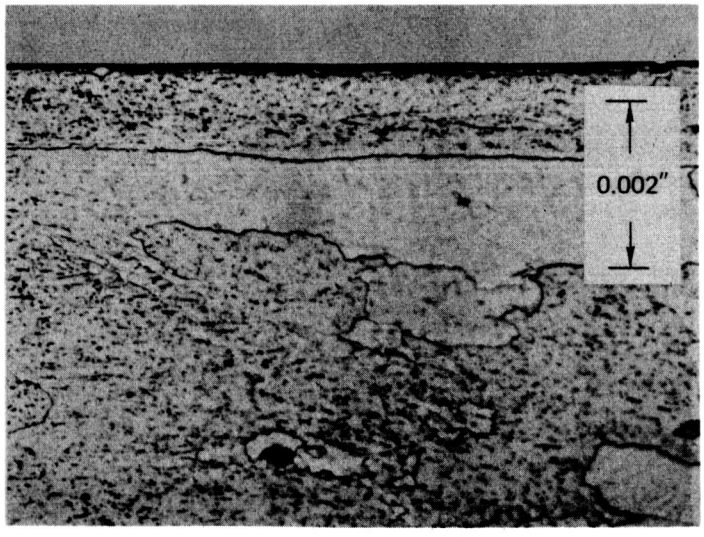


H66061A Etched



H66061B Etched

a. Blade



H66071A Etched

b. Nozzle

Figure 121. Mo-TZC Alloy Tenth-Stage Nozzle and Blade Turbine Simulator Following 10,000 Hours of Continuous Exposure to Potassium Vapor in the T-111 Corrosion Test Loop.

selected because they represent the longest straight sections from the loop which were exposed to the lowest (1900°F, 1040°C) and highest (2200°F, 1205°C) operating temperatures. Also, preliminary screening tests by crushing ring sectors at room temperature from several locations in the loop, discussed earlier in this section (Figure 114), showed the crossover line to have very low ductility; whereas, the boiler material exhibited only slightly reduced ductility compared to the pretest pipe. As shown in Figure 122, the specimens were similar to conventional, flat, tensile specimens; however, they were longitudinal sections from the 1-inch (2.54-cm) pipe. Although the results from this type of specimen may not be useful for engineering design purposes, they are valid for comparison of relative properties or property changes such as was the intention of this study. The results of the room temperature and 2000°F (1095°C) tensile tests are summarized in Table XXXII. At both room temperature and 2000°F (1095°C) the strength of all the specimens is essentially the same except that the unexposed pretest material may be slightly stronger at both temperatures. The only significant deviation in properties is the relatively low room temperature ductility of the vapor crossover line compared to either the boiler or unexposed pretest material. The appearance of the tensile test specimens following fracture is shown in Figure 123. This reduced room temperature ductility confirms the validity of preliminary results on the ring sector tests from this loop and the High-Temperature Alkali Metal Valve Loop.[30] The results of evaluating specimens from both loops indicate a possible aging reaction for T-111 at 1900°F (1038°C).

(30) Harrison, R. W. and Holowach, J., Refractory Metal Valves for 1900°F Service in Alkali Metals Systems, NASA Contract NAS 3-8514, General Electric Report No. GESP-508, April 15, 1970.

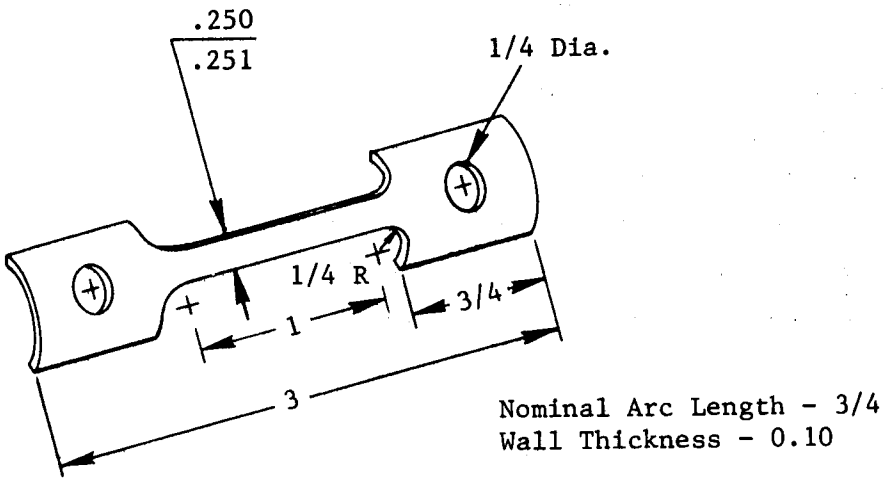


Figure 122. Tensile Specimens Used for Posttest Evaluation of 1-Inch (2.5-cm)-OD Pipe.

TABLE XXXII

TENSILE TEST RESULTS ON SPECIMENS OF T-111 PIPE[1]
EXPOSED FOR 10,000 HOURS IN THE T-111 RANKINE SYSTEM CORROSION TEST LOOP

Room Temperature Tests

Specimen	Exposure Temperature °F	Exposure Temperature °C	U.T.S. (ksi)	.02% Y.S. (ksi)	.2% Y.S. (ksi)	Elong. (%)
Unexposed	-	-	92.6	69.4	76.5	34.0
Boiler	2200	1204	90.4	61.9	70.5	32.0
Boiler	2200	1204	89.6	61.3	71.6	33.0
K Vapor Line	1900	1038	86.5	63.1	70.1	10.0
K Vapor Line	1900	1038	88.6	61.1	68.9	13.0

2000°F Tests[2]

Specimen	Exposure Temperature °F	Exposure Temperature °C	U.T.S. (ksi)	.02% Y.S. (ksi)	.2% Y.S. (ksi)	Elong. (%)
Unexposed	-	-	57.0	24.8	29.9	25.0
Boiler	2200	1204	51.6	23.1	27.4	28.0
Boiler	2200	1204	51.9	25.1	28.3	28.0
K Vapor Line	1900	1038	52.3	28.9	30.9	26.0
K Vapor Line	1900	1038	52.8	25.1	28.4	28.0

(1) 1-Inch OD x 0.1-Inch Wall (2.5-cm OD x 0.25-cm Wall)

(2) Tests conducted in a vacuum of $1.0 - 2.8 \times 10^{-6}$ torr ($1.3 - 3.7 \times 10^{-4}$ N/m^2)

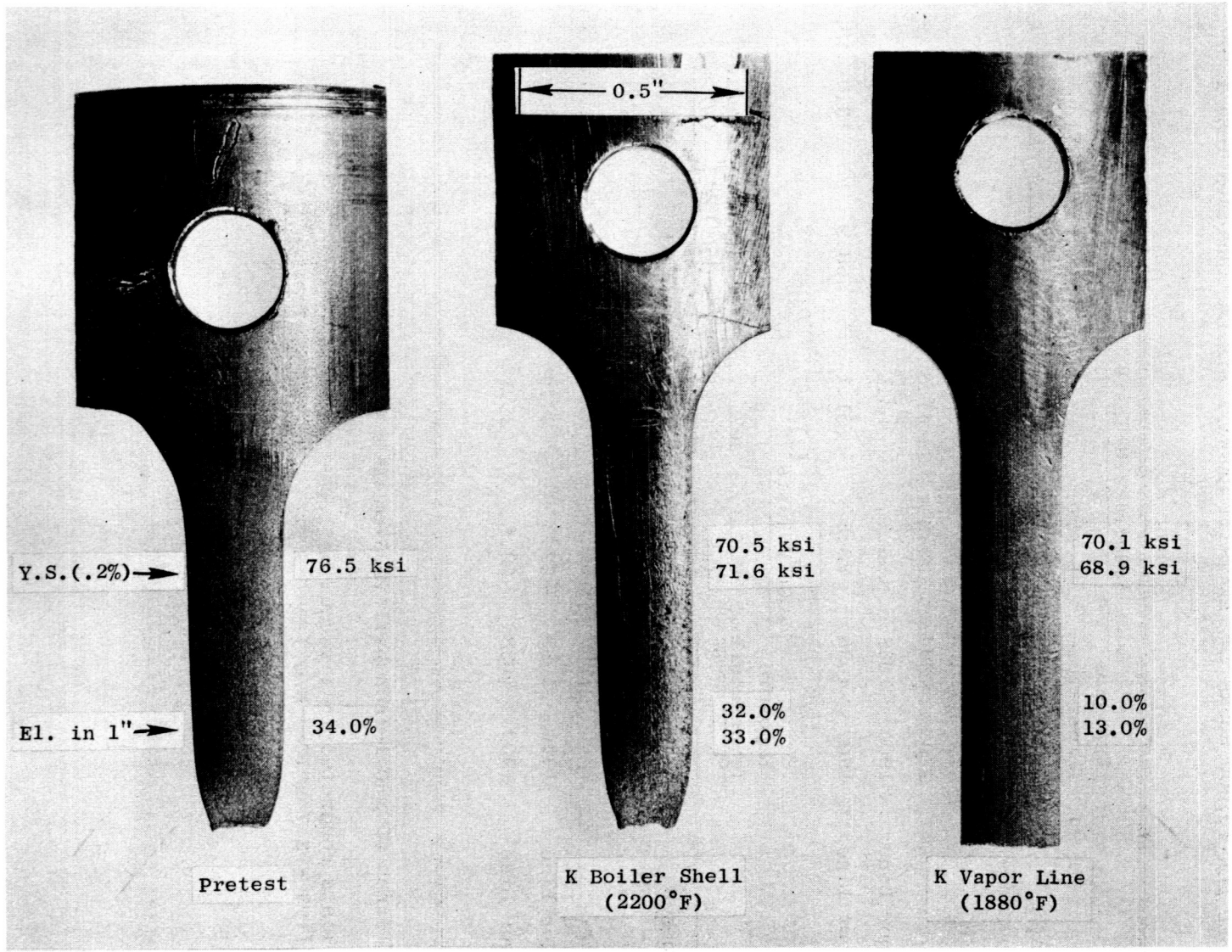


Figure 123. Fractured Tensile Test Specimens Cut From 1-Inch (2.5-cm) T-111 Pipe of the 10,000-Hour T-111 Corrosion Test Loop. Tensile Tests Performed at 80°F (27°C). (Orig. P70-10-16C)

XIII. SUMMARY AND CONCLUSIONS

The primary purpose of the T-111 Rankine System Corrosion Test Loop experiment was to determine the compatibility of advanced refractory alloys with the working fluids proposed for use in future space electric power systems. The containment material for the system, T-111 alloy, was in contact with liquid lithium and with potassium in both the liquid and the vapor phase. The candidate turbine alloy materials, Mo-TZC and Cb-132M, were subjected to a high-velocity, high-quality (nominally 88%), potassium environment. The principal results and conclusions are summarized below.

At the time of its construction, no tantalum alloy system of the size and complexity of the T-111 Corrosion Test Loop had been built and the successful fabrication of this system was in itself a significant accomplishment. This success was due in large measure to the results of NASA-developed technology at GE-NSP and other contractors which laid the ground work for the T-111 Loop program. The success of the fabrication effort was in large measure due to the high quality of the refractory alloy material. Considerable effort in the areas of specification preparation, procurement, and quality assurance was required to insure that material of the highest quality was used in building the system.

Despite the quality assurance efforts during the material procurement and fabrication phases of the program, a leak between the potassium and lithium circuits in the boiler did occur during the initial attempt to reach the test conditions. Following detection of the leak, a very detailed repair plan was developed and approved by the NASA Program Manager. The unqualified success of this most difficult leak isolation and repair procedure must be considered one of the highlights of the program.

Following repair of the boiler, the 10,000-hour test was initiated and successfully completed in an almost routine manner. The experience gained during the operation of the 5000-hour Cb-1Zr Rankine System Corrosion Test Loop was very useful in the achievement of the near-perfect operational record of the T-111 Corrosion Test Loop. Only four hours of total elapsed time were

lost during the 10,000-hour period, and these brief departures from the test conditions were caused by failures in the supporting equipment and by electrical storms. The problem which has historically "wiped out" most high-temperature refractory alloy tests has been contamination from either poor vacuum or contaminated inert gas environments. The very low pickups of oxygen and nitrogen by the T-111 alloy during the 10,000 hours of high-temperature operation demonstrated that complex refractory alloy systems can be tested for extended time periods with negligible contamination, if the proper techniques are utilized.

It should be noted that following completion of the test, considerable effort was expended in removing residual alkali metal from the test components prior to evaluation. Improper decontamination can negate the material evaluation of systems of this type as a result of corrosive reactions during the stripping process.

Extensive chemical and metallurgical evaluation of the principal loop components indicated that the structural materials selected for evaluation had excellent compatibility with the test environments. There is no doubt that the attention directed at the purity of the alkali metals and the cleanliness of the test system contributed substantially to the lack of significant attack of any of the test components. The Mo-TZC and Cb-132M turbine simulator materials experienced no significant change in dimensions, weight, or metallographic appearance.

The most significant observations resulting from the evaluation task were the migration of nitrogen in the lithium circuit and the migration of oxygen in the potassium circuit. More subtle indications of the transfer of these elements were noted in earlier tests but the high temperatures and extended test duration made these phenomena more prominent in this experiment. The nitrogen transfer from the hottest regions of the lithium circuit to the outer surface (lithium side) of the potassium containment tube in the boiler was most apparent in the high-heat-flux region of the boiler plug. This deposition of nitrogen from the lithium occurred as a result of the sharp temperature drop in the lithium in this region. The film of hafnium nitride, which had a maximum thickness of less than 0.001 inch (0.002 cm), detected

in this region had no detectable deleterious effect on the metallurgical reliability of the boiler tube.

Oxygen migration noted in the potassium circuit, particularly in various regions of the boiler, was considerably more complex to evaluate than the nitrogen mass transfer discussed above. The areas of large increase in oxygen concentration could be correlated with regions where the boiling process could result in high oxygen buildups in the residual liquid phase potassium. The extremely localized nature of the oxygen buildup and the shallow intergranular attack (0.010-inch, 0.025-cm maximum) noted in these areas suggests that boiler designers and materials technologists should work together to minimize this problem. Lengthening of the wet wall - dry wall transition region and minimization of the total oxygen inventory in the system (oxygen in the potassium and in the structural metals) should help to eliminate oxygen pickup as a significant compatibility problem for long-term (up to 5 years) operation. In addition, these results suggest that reductions in the getter element concentration of tantalum-base alloys (2 w/o Hf in T-111) could result in a deleterious effect on the alloy's corrosion resistance in potassium systems.

Some deterioration of the room temperature ductility of the T-111 alloy was noted after the long-term exposure, particularly in regions that operated at around 1900^{o}F (1038^{o}C). Although the ductility values measured in tensile test specimens of the loop pipe were 10 percent or greater, the substantial decrease in elongation values from pretest specimens suggests that studies of this phenomena would be worthwhile.

In summary, the structural materials and working fluids evaluated in this long-term test exhibited excellent compatibility and suitability for use in future space electric power systems.

XIV. PUBLISHED REPORTS

Quarterly Progress Reports	For Quarter Ending
Report No. 1 (NASA-CR-54477)	July 15, 1965
Report No. 2 (NASA-CR-54845)	October 15, 1965
Report No. 3 (NASA-CR-54911)	January 15, 1966
Report No. 4 (NASA-CR-72029)	April 15, 1966
Report No. 5 (NASA-CR-72057)	July 15, 1966
Report No. 6 (NASA-CR-72177)	October 15, 1966
Report No. 7 (NASA-CR-72230)	January 15, 1967
Report No. 8 (NASA-CR-72335)	April 15, 1967
Report No. 9 (NASA-CR-72336)	July 15, 1967
Report No. 10 (NASA-CR-72352)	October 15, 1967
Report No. 11 (NASA-CR-72383 also GESP-1)	January 15, 1968
Report No. 12 (NASA-CR-72452 also GESP-144)	April 15, 1968
Report No. 13 (NASA-CR-72483 also GESP-182)	July 15, 1968
Report No. 14 (NASA-CR-72505 also GESP-189)	October 15, 1968
Report No. 15 (NASA-CR-72527 also GESP-196)	January 15, 1969
Report No. 16 (NASA-CR-72560 also GESP-258)	April 15, 1969
Report No. 17 (NASA-CR-72592 also GESP-303)	July 15, 1969
Report No. 18 (NASA-CR-72620 also GESP-376)	October 15, 1969
Report No. 19 (NASA-CR-72662 also GESP-410)	January 15, 1970
Report No. 20 (NASA-CR-72739 also GESP-491)	April 15, 1970
Report No. 21 (NASA-CR-72782 also GESP-546)	July 15, 1970
Report No. 22 (NASA-CR-72818 also GESP-562)	October 15, 1970
Report No. 23 (NASA-CR-72853 also GESP-606)	January 15, 1971
Report No. 24 (NASA-CR-72985 also GESP-652)	April 15, 1971
Report No. 25 (No NASA or GESP Number)	July 15, 1971
Report No. 26 (No NASA or GESP Number)	October 15, 1971

Other Topical Reports on NASA Contract NAS 3-6474

"Capsule Tests of Advanced Tantalum Alloys in Flowing Lithium and Refluxing Potassium," G. P. Brandenburg and R. W. Harrison, GESP-694, January 15, 1972.

"Pumped Lithium Loop to Evaluate Advanced Refractory Metal Alloys and T-111 Fuel Element Cladding," G. P. Brandenburg, R. L. Davies, E. E. Hoffman, and J. P. Smith (To be published by NASA - Lewis Research Center).

"2500°F (1371°C) Lithium Thermal Convection Loop Test," G. P. Brandenburg, R. L. Davies, E. E. Hoffman, and J. P. Smith (To be published by NASA - Lewis Research Center).

☆U.S.Government Printing Office: 1976 — 660-085/22 Region 5-11

1. Report No.	2. Government Accession No.	3. Recipient's Catalog No.
NASA CR-134816 (Volume I)		

4. Title and Subtitle	5. Report Date
T-111 RANKINE SYSTEM CORROSION TEST LOOP	June 1975
	6. Performing Organization Code

7. Author(s)	8. Performing Organization Report No.
R. W. Harrison, E. E. Hoffman, and J. P. Smith	GESP-695
	10. Work Unit No.

9. Performing Organization Name and Address	11. Contract or Grant No.
General Electric Company Nuclear Systems Programs Cincinnati, Ohio 45215	NAS 3-6474
	13. Type of Report and Period Covered
12. Sponsoring Agency Name and Address	Contract Report
National Aeronautics and Space Administration Washington, D.C. 20546	14. Sponsoring Agency Code

15. Supplementary Notes

Final Report. Project Manager, Robert L. Davies, Materials and Structures Division, NASA Lewis Research Center, Cleveland, Ohio

16. Abstract

This report covers the results of a program whose objective was to determine the performance of refractory metal alloys in a two loop Rankine test system. The test system consisted of a circulating lithium circuit heated to 1230° C maximum transferring heat to a boiling potassium circuit with a 1170° C superheated vapor temperature. The results demonstrate the suitability of the selected refractory alloys to perform from a chemical compatibility standpoint.

MAR 1976
RECEIVED
NASA STI FACILITY
INPUT BRANCH

17. Key Words (Suggested by Author(s))	18. Distribution Statement
Liquid Metals Refractory Metals Power Systems	Unclassified-unlimited STAR Category 26 (rev.)

19. Security Classif. (of this report)	20. Security Classif. (of this page)	21. No. of Pages	22. Price*
Unclassified	Unclassified	278	

* For sale by the National Technical Information Service, Springfield, Virginia 22151